

---

# The role of CD18/CD11b on Dendritic cells and Generation of the CD18<sup>fl/fl</sup> mouse

Monika Bednarczyk



JOHANNES GUTENBERG  
UNIVERSITÄT MAINZ

---

Department of Dermatology

University Medical Center of the Johannes Gutenberg University Mainz

Germany

**This dissertation is submitted for the degree of Doctor rerum naturalium (Dr. rer. nat.)  
at the Faculty of Biology, Johannes Gutenberg University Mainz**

7. NOVEMBER 2020

JOHANNES GUTENBERG-UNIVERSITÄT MAINZ



## DECLARATION

This dissertation is the result of my own work and includes nothing, which is the outcome of work done in collaboration except where specifically indicated in the text. It has not been previously submitted, in part or whole, to any university or institution for any degree, diploma, or other qualification.

## ERKLÄRUNG

Ich erkläre, dass ich die vorgelegte Thesis selbständig, ohne unerlaubte fremde Hilfe und nur mit den Hilfen angefertigt habe, die ich in der Thesis angegeben habe. Alle Textstellen, die wörtlich oder sinngemäß aus veröffentlichten oder nicht veröffentlichten Schriften entnommen sind, und alle Angaben, die auf mündlichen Auskünften beruhen, sind als solche kenntlich gemacht. Bei den von mir durchgeführten Untersuchungen habe ich die Grundsätze guter wissenschaftlicher Praxis, wie sie in der Satzung der Johannes Gutenberg - Universität Mainz zur Sicherung guter wissenschaftlicher Praxis niedergelegt sind, eingehalten.

Signed: \_\_\_\_\_

Date: \_\_\_\_\_

Monika Bednarczyk, Msci Biotechnology (app. Molecular Biology)

Mainz



## SUMMARY / ABSTRACT

### **The role of CD18/CD11b on Dendritic cells and Generation of the CD18<sup>fl/fl</sup> mouse**

Monika Bednarczyk

$\beta$ 2 integrins are heterodimers composed of a constant  $\beta$ 2 (CD18) subunit, which is non-covalently bound to one of four different alpha subunits:  $\alpha$ L (CD11a),  $\alpha$ M (CD11b),  $\alpha$ X (CD11c) or  $\alpha$ D (CD11d). They mediate cell-cell and cell-matrix interactions, transendothelial migration, engulfment of opsonized pathogens, and cell signalling in leukocytes. In humans, lack of CD18 results in an impairment of immune functions, termed leukocyte-adhesion deficiency type 1 (LAD1), which manifests with recurrent infections and sporadic autoimmunity. The purpose of this project was to determine if and how  $\beta$ 2 integrins contribute to tumour development. Here we report that CD11b<sup>-/-</sup> mice inoculated with B16/OVA melanoma revealed a significantly reduced tumour progression, and a decreased tumour burden. The centre of the tumour mass was poorly infiltrated with F40/80<sup>+</sup>, Gr-1<sup>+</sup>, CD11c<sup>+</sup> and CD4/FoxP3<sup>+</sup> cells. The CD11b<sup>-/-</sup> DC characterized in addition with a reduced antigen uptake capacity. To further address the role of  $\beta$ 2 integrins on specific leukocytes in tumour microenvironment we generated a CD18flox mouse, based on the loxP-CD18-exon3-FRT-loxP construct, which enables a cell type-specific knock-down of CD18. Three independent conditional knock-outs were bred based on the Cre/loxP system: CD18 <sup>$\Delta$ CD11c</sup>, CD18 <sup>$\Delta$ Ly6G</sup> and CD18 <sup>$\Delta$ Foxp3</sup>. The CD18 <sup>$\Delta$ CD11c</sup> mouse revealed a specific deletion or reduction of  $\beta$ 2 integrins in BM-DC, as well as primary DC. Splenic CD18 <sup>$\Delta$ CD11c</sup> DC characterized with elevated IL-6, TNF- $\alpha$ , and IL-10 gene expression as well as synthesis and downregulation of SOCS2 and SOCS4 mRNA expression in response to MyD88-triggering TLR ligands. Despite the hyper-inducible signature of these CD18<sup>-/-</sup> DC we observed no genotype dependent difference in the T cell stimulatory capacity or tumour progression (B16/OVA melanoma) between CD18 <sup>$\Delta$ CD11c</sup> and CD18<sup>fl/fl</sup>. Research into the role of CD18 on other leukocyte subsets is already underway. Preliminary studies with CD18 <sup>$\Delta$ Ly6G</sup> and CD18 <sup>$\Delta$ Foxp3</sup> strains indicated a positive correlation between CD18 expression on Ly6G<sup>+</sup> or Foxp3<sup>+</sup> cells and tumour development. B16/OVA melanoma burden and growth were decreased in both knock-out strains. The CD18 <sup>$\Delta$ Foxp3</sup> mouse strain presented in addition with an autoimmune phenotype that manifested with psoriasis-like skin lesions, splenomegaly and lymphadenopathy. Future research will therefore focus on the role of CD18 on FoxP3<sup>+</sup> and Ly6G<sup>+</sup> leukocytes and on the mechanisms that drove the immunomodulation and reduced tumour growth.





# Contents

SUMMARY / ABSTRACT .....	v
LIST OF FIGURES.....	xv
LIST OF TABLES .....	xix
LIST OF ABBREVIATIONS AND ACRONYMS.....	xx
1. Introduction .....	1
1.1. Immune System .....	1
1.1.1. Ontogeny of the immune system.....	2
1.2. The biology of a dendritic cell (DC) .....	4
1.2.1. Development and subsets of DC .....	5
1.2.2. Processing and presentation of the antigen .....	6
1.2.3. Maturation and expression of surface receptors on DC .....	7
1.2.4. Tolerance induction and immune stimulation by DC .....	8
1.3. $\beta$ 2 Integrins .....	10
1.3.1. Structure of $\beta$ 2 integrins .....	11
1.3.1.1. $\beta$ 2 integrin alpha subunit.....	12
1.3.1.2. $\beta$ 2 integrin beta subunit.....	13
1.3.2. Interactions of $\beta$ 2 integrins with various ligands and their functions .....	14
1.3.2.1. Tissue distribution of $\beta$ 2 integrins .....	14
1.3.2.2. Ligand binding of $\beta$ 2 integrins.....	15
1.3.2.3. Function of $\beta$ 2 integrins .....	15
1.3.3. Clinical relevance of $\beta$ 2 integrins.....	17
1.3.3.1. The role of $\beta$ 2 integrins in cancer .....	17
1.3.3.2. The role of $\beta$ 2 integrins in autoimmune diseases.....	21
2. Results .....	27
2.1. Generation of the CD18 <sup>fl/fl</sup> mouse.....	27

2.1.1.	Recombination strategy for the generation of the CD18 <sup>fl/fl</sup> mouse .....	27
2.1.2.	Recombination of the BO44.2 vector with murine embryonic stem cells (JM8) 28	
2.1.3.	Selection of two recombinant ES-clones P1-9F and P3-10G .....	31
2.1.3.1.	Establishment of Southern Blot screening strategy .....	31
2.1.3.2.	Screening for the recombinant ES-clones .....	34
2.1.3.3.	Expansion of the heterozygous targeted clones .....	35
2.1.4.	Injection of the blastocyst with recombinant ES-clones .....	36
2.1.5.	Selection of chimeric offspring derived from the B6 Albino blastocyst recipient mouse 37	
2.1.6.	Deletion of the Neo-cassette from the agouti chimeric offspring via Flp-FRT recombination.....	39
2.1.7.	Breeding and screening of the homozygous CD18 <sup>fl/fl</sup> mice.....	41
2.1.8.	Sequencing of the CD18 <sup>fl/fl</sup> gene locus .....	42
2.2.	Breeding and characterisation of the new CD18 <sup>ΔCD11c</sup> mouse strain .....	44
2.2.1.	Breeding and screening strategy for the CD18 <sup>ΔCD11c</sup> .....	44
2.2.2.	Characterisation of the leukocyte progenitors in the bone marrow of the CD18 <sup>ΔCD11c</sup> mouse.....	45
2.2.3.	Characterisation of blood derived leukocytes from the CD18 <sup>ΔCD11c</sup> mouse .....	47
2.2.4.	Characterisation of the splenocytes derived from the CD18 <sup>ΔCD11c</sup> mouse.....	49
2.2.4.1.	Splenic T-lymphocytes derived from the CD18 <sup>ΔCD11c</sup> mouse .....	49
2.2.4.2.	Splenic B-lymphocytes derived from the CD18 <sup>ΔCD11c</sup> mouse .....	51
2.2.4.3.	Splenic macrophages derived from the CD18 <sup>ΔCD11c</sup> mouse.....	53
2.2.5.	Characterisation of Dendritic cells derived from the CD18 <sup>ΔCD11c</sup> mouse.....	55
2.2.5.1.	Analysis of bone-marrow derived DC from the CD18 <sup>ΔCD11c</sup> mouse .....	55
2.2.5.2.	Analysis of murine skin CD18 <sup>ΔCD11c</sup> DC.....	57
2.2.5.3.	Analysis of the murine lung CD18 <sup>ΔCD11c</sup> DC.....	59
2.2.5.4.	Analysis of the splenic CD18 <sup>ΔCD11c</sup> DC.....	61

2.2.5.5.	Cytokine secretion by stimulated splenic CD18 <sup>ΔCD11c</sup> DC .....	63
2.2.5.6.	Cytokine mRNA expression by CD18 <sup>ΔCD11c</sup> DC upon R848 stimulation ..	66
2.2.5.7.	SOCS protein mRNA expression by CD18 <sup>ΔCD11c</sup> splenic DC stimulated with R848	67
2.2.5.8.	In vitro T cell stimulatory capacity of the splenic CD18 <sup>ΔCD11c</sup> DC .....	69
2.2.5.9.	In vivo T cell stimulatory capacity of the CD18 <sup>ΔCD11c</sup> DC.....	75
2.2.6.	Tumour growth in CD18 <sup>ΔCD11c</sup> mice .....	80
2.3.	The role of CD11b for tumour development .....	81
2.3.1.	Tumour growth in CD11b <sup>-/-</sup> mice.....	81
2.3.1.1.	In vivo T cell proliferation assay in the CD11b <sup>-/-</sup> background .....	82
2.3.1.2.	B16-OVA melanoma growth in CD11b <sup>-/-</sup> mice .....	86
2.4.	The role of β2 integrins as mediators of intracellular uptake on dendritic cells .....	97
2.4.1.	The role of Mac-1 (CD18/CD11b) for uptake of complement-opsonized p(Cy5)	97
2.4.1.1.	Engulfment of p(Cy5) by CD11b <sup>-/-</sup> BM-DC.....	97
2.4.1.2.	Engulfment of p(Cy5) by CD11b <sup>-/-</sup> splenic DC .....	107
2.4.2.	Role of Mac-1 on DC for the uptake of Dextran.....	108
2.4.3.	Uptake of an antigen (Ovalbumin) by Mac-1 and it's intracellular processing	112
2.4.3.1.	Engagement of the OVA-AlexaFluor647 by CD11b <sup>-/-</sup> BM-DC and splenic DC	112
2.4.3.2.	Processing of the OVA-DQ by CD11b <sup>-/-</sup> BM-DC .....	114
3.	Discussion .....	117
3.1.	Biological role of β2 integrins .....	117
3.1.1.	β2 integrins .....	117
3.1.2.	Therapeutic usage of β2 integrins.....	118
3.2.	Leukocyte adhesion deficiency syndrome and models to study CD18 ablation .	119
3.2.1.	LAD syndromes.....	119

3.2.2.	Mouse models to study CD18 deficiency.....	120
3.3.	Conditional deletion of CD18 using a Cre-loxP strategy .....	122
3.4.	Targeting of CD18 in the murine embryonic stem cells by the means of homologous recombination yielded a CD18 floxed mouse line .....	123
3.5.	Deletion of CD18 specifically in murine DC (CD18 <sup>ΔCD11c</sup> ).....	125
3.6.	Ablation of CD18 specifically in CD11c <sup>+</sup> cells has no influence on maturation of other leukocytes.....	127
3.7.	CD18 <sup>ΔCD11c</sup> DC are characterized by elevated production of cytokines in response to stimulation.....	128
3.8.	β2 integrins may influence the cytokine production in concert with SOCS proteins	131
3.9.	Regulation of tumorigenesis by β2 integrin.....	135
3.10	CD11b modulates engulfment of complex polysaccharides and complement-opsinized polysaccharide coated particles.....	140
4.	Materials and Methods .....	146
4.1.	Materials and equipment .....	146
4.1.1.	Materials.....	146
4.1.2.	Buffers and solutions.....	147
4.1.3.	Antibodies .....	149
4.1.4.	Reagents and chemicals .....	151
4.1.5.	Cell culture .....	153
4.1.6.	B16/OVA Melanoma cell line.....	153
4.1.7.	Animals used for breeding and experiments .....	153
4.1.8.	Electrical equipment.....	155
4.2.	Materials and methods for generation of CD18 <sup>fl/fl</sup> mouse .....	157
4.2.1.	Amplification of the targeting vector BO44.2 .....	157
4.2.2.	Isolation of the genomic DNA .....	157
4.2.3.	Genomic Southern Blot.....	158

4.2.3.1. Buffers for genomic Southern Blot.....	158
4.2.3.2. DNA lysis, precipitation and digestion (gelatine 96-well plates: ES clones) for genomic Southern Blot .....	159
4.2.3.3. Gel preparation for genomic Southern Blot .....	160
4.2.3.4. Blotting .....	160
4.2.3.5. Southern Blot probe synthesis .....	161
4.2.3.6. Southern Blot probe labelling .....	162
4.2.3.7. Hybridisation.....	163
4.2.3.8. Detection of the Southern Blot Probe .....	163
4.2.4. Preparation of the Mouse Embryo Fibroblast (MEF) feeder cells .....	163
4.2.4.1. Thawing EFO .....	163
4.2.4.2. Expanding and splitting of the feeder cells .....	164
4.2.4.3. Treatment of active MEF with Mitomycin C (MMC) .....	164
4.2.4.4. Freezing of MMC-treated feeder cells .....	164
4.2.4.5. Plating of the mitotically inactive MEF feeder cells.....	164
4.2.5. Preparation of the Embryonic Stem cells (ES-cells) JM8.....	165
4.2.5.1. Thawing and splitting of ES-cells .....	165
4.2.5.2. Electroporation of the ES-cells .....	165
4.2.6. Picking of the ES cell colonies resistant to Neomycin.....	166
4.2.7. Coating of 96-well plates with gelatine.....	166
4.2.8. Splitting of the ES cells on 96-well plates (Feeder cell & gelatine coated).....	167
4.2.9. Freezing of the ES clones cultured on Feeder cells & gelatine.....	167
4.2.10. Expansion of positive clones .....	167
4.2.11. Blastocyst injection.....	168
4.2.12. CD18 <sup>fl/fl</sup> screening and breeding strategy .....	168
4.2.12.1. Screening of chimeras .....	168
4.2.12.2. Breeding of chimeras .....	169

4.2.13.	DNA sequencing of the CD18 <sup>fl/fl</sup> mice .....	172
4.2.14.	Breeding scheme of the CD18 <sup>ΔCD11c</sup> .....	172
4.2.15.	CD18 <sup>ΔCD11c</sup> mouse screening .....	174
4.3.	Cell biology methods.....	175
4.3.1.	Generation and analysis of Murine Bone Marrow-Derived Dendritic Cells (BMDC) .....	175
4.3.1.1.	Generation of BMDC .....	175
4.3.1.2.	BMDC activation assay.....	176
4.3.2.	Isolation and analysis of splenocytes .....	176
4.3.2.1.	Isolation of splenic dendritic cells.....	176
4.3.2.2.	Activation of splenic dendritic cells.....	177
4.3.2.3.	Isolation and analysis of splenic lymphocytes .....	177
4.3.3.	Isolation and analysis of murine blood and bone marrow cells .....	177
4.3.4.	Antigen uptake and processing analysis.....	178
4.3.5.	Preparation and staining of lung cells .....	178
4.3.6.	Preparation and staining of a single-cell suspensions from a murine skin.....	179
4.3.7.	<i>In vitro</i> T Cell Proliferation.....	179
4.3.8.	Cell apoptosis/necrosis detection .....	180
4.3.9.	Cytotoxicity test .....	180
4.4.	Nanoparticle experiments .....	181
4.4.1.	Adsorption of mouse native serum onto Dextran-Coated Colloidal Superparamagnetic Nanoparticles.....	181
4.4.2.	Cellular Binding and Uptake of Dextran-Coated Colloidal Superparamagnetic Nanoparticles.....	181
4.4.3.	Cellular Binding and Uptake of FITC-Dextran.....	181
4.4.4.	Flow Cytometric analysis of NP uptake.....	182
4.4.5.	Confocal Laser Scanning Microscopy (CLSM).....	182

4.4.6.	<i>In vitro</i> T cell-proliferation assays .....	182
4.5.	Immunological methods. ....	183
4.5.1.	Magnetic cell sorting .....	183
4.5.2.	Fluorescence activated cell sorting (FACS).....	183
4.5.3.	Cytokine measurement .....	184
4.5.4.	Immunohistochemical staining .....	184
4.6.	Real time quantitative PCR (qPCR) .....	186
4.7.	In vivo tumour model (B16-OVA Melanoma).....	188
4.8.	In vivo T Cell Proliferation .....	188
4.9.	Statistical analysis.....	189
	References .....	190
	Appendices .....	212
	Appendix A. BO44.2 Vector.....	212
	Appendix B. Karyotyping of recombinant ES. ....	221
	Appendix C. CD18 <sup>ΔCD11c</sup> BM-DC activation.....	222
	Appendix D. CD18 <sup>ΔCD11c</sup> splenic DC activation.....	223
	Appendix E. Analysis of the splenocytes from the CD11b <sup>-/-</sup> mice with B16-OVA Melanoma burden.....	225
	Appendix F. Uptake of OVA-AlexaFluor647 by CD11b <sup>-/-</sup> and WT BM-DC in mixed cultures. .....	226
	Appendix G. Ablation of CD18 in FoxP3 <sup>+</sup> and Ly6G <sup>+</sup> cells prevents tumour development .....	227
	Appendix H. CD18 <sup>ΔFoxp3</sup> phenotype.....	228
	Curriculum Vitae.....	<b>Fehler! Textmarke nicht definiert.</b>
	Publications .....	229
	List of presentations and conferences attended.....	230

## LIST OF FIGURES

Figure 1. Three phases of the initial response to a pathogen. ....	1
Figure 2. Cellular elements of the blood. ....	4
Figure 3. Dendritic cell development and subsets.....	6
Figure 4. Interaction of an APC with T lymphocytes. ....	8
Figure 5. T cell fate after activation via dendritic cell. ....	10
Figure 6. Representative members of integrins in vertebrates and their binding specificity... ..	11
Figure 7. Integrin structure.....	12
Figure 8. $\beta 2$ integrin activation states. ....	14
Figure 9. $\beta 2$ integrins: distribution, ligands and function. ....	17
Figure 10. Recombination strategy for the generation of CD18 <sup>fl/fl</sup> mouse.....	28
Figure 11. BO44.2 vector construct. ....	29
Figure 12. Restriction digest of the BO44.2 vector.....	30
Figure 13. Location of Southern Blot probes on the WT and targeted allele.....	32
Figure 14. Amplified Southern Blot probes for the detection of the recombined CD18 allele. .....	32
Figure 15. Southern Blot with probe overlapping CD18 exon 1 and exon 7.....	33
Figure 16. Detection of recombined ES-clones with Southern Blot.....	35
Figure 17. Southern Blot analysis of the expanded, recombined ES-clones.....	36
Figure 18. Scheme of the blastocyst injection with the recombined JM8 ES clones.....	37
Figure 19. Generation of the stable agouti Neo <sup>+</sup> chimeric offspring. ....	38
Figure 20. Neo-cassette-PCR screening of the chimeric offspring.....	39
Figure 21. PCR screening of the chimeric offspring after the Flp-FRT recombination. ....	40
Figure 22. PCR screening of the CD18 <sup>fl/fl</sup> mice. ....	42
Figure 23. DNA fragment for the sequencing of the recombined DNA fragment derived from the CD18 <sup>fl/fl</sup> mouse. ....	42
Figure 24 Analysis of the DNA sequence encompassing recombined CD18 exon3 locus.....	43

Figure 25. Breeding strategy for the CD18 <sup>ΔCD11c</sup> mice.....	44
Figure 26. PCR screening of the mice expressing CD11c-CRE.....	45
Figure 27. Gating strategy for the leukocytes derived from the bone marrow of the CD18 <sup>ΔCD11c</sup> . .....	46
Figure 28. Leukocyte composition in the bone marrow of the CD18 <sup>ΔCD11c</sup> mouse. ....	47
Figure 29. Leukocyte populations in the blood of the CD18 <sup>ΔCD11c</sup> mouse. ....	48
Figure 30. Splenic T lymphocyte population in the CD18 <sup>ΔCD11c</sup> mouse.....	50
Figure 31. Splenic B lymphocyte population in the CD18 <sup>ΔCD11c</sup> mouse.....	52
Figure 32. Splenic macrophage population in the CD18 <sup>ΔCD11c</sup> mouse.....	55
Figure 33. Analysis of the BM-DC population in the CD18 <sup>ΔCD11c</sup> mouse.....	57
Figure 34. Analysis of the skin DC population in the CD18 <sup>ΔCD11c</sup> mouse.....	58
Figure 35. Analysis of the lung DC population in the CD18 <sup>ΔCD11c</sup> mouse. ....	60
Figure 36. Analysis of the splenic DC population in the CD18 <sup>ΔCD11c</sup> mouse.....	62
Figure 37. Activation markers on unstimulated splenic DC population in the CD18 <sup>ΔCD11c</sup> mouse. .....	63
Figure 38. Cytokine secretion by splenic CD18 <sup>ΔCD11c</sup> upon TLR-ligand stimulation. ....	65
Figure 39. Dose dependent cytokine secretion by splenic CD18 <sup>ΔCD11c</sup> upon R848 stimulation. .....	66
Figure 40. Cytokine mRNA expression by CD18 <sup>ΔCD11c</sup> splenic DC upon R848 stimulation..	67
Figure 41. SOCS protein mRNA expression by CD18 <sup>ΔCD11c</sup> splenic DC upon R848 stimulation. .....	68
Figure 42. In vitro OT-II T-cell proliferation assay with CD18 <sup>ΔCD11c</sup> DC stimulated with CpG. .....	70
Figure 43. Cytokines produced in an in vitro OT-II T-cell proliferation assay with CD18 <sup>ΔCD11c</sup> DC stimulated with CpG.....	71
Figure 44. In vitro OT-II T-cell proliferation assay with CD18 <sup>ΔCD11c</sup> DC stimulated with R848. .....	71
Figure 45. Cytokines produced in an in vitro OT-II T-cell proliferation assay with CD18 <sup>ΔCD11c</sup> DC stimulated with R848.....	72

Figure 46. In vitro OT-I T-cell proliferation assay with CD18 <sup>ΔCD11c</sup> DC stimulated with R848. .....	73
Figure 47. Cytokines produced in an in vitro OT-I T cell proliferation assay with CD18 <sup>ΔCD11c</sup> DC stimulated with R848.....	74
Figure 48. Gating strategy for the in vivo OT-II T cell proliferation in CD18 <sup>ΔCD11c</sup> mice. ....	76
Figure 49. In vivo OT-II T cell proliferation in CD18 <sup>ΔCD11c</sup> mice. ....	77
Figure 50. In vivo OT-I T cell proliferation in CD18 <sup>ΔCD11c</sup> mice. ....	79
Figure 51. Analysis of tumour and lymphatic organs from CD18 <sup>ΔCD11c</sup> mice inoculated with B16-OVA melanoma.....	81
Figure 52. In vivo proliferation of OT2-Ly5.1 T-lymphocytes in CD11b <sup>-/-</sup> mice. ....	84
Figure 53. In vivo proliferation of OT1-Ly5.1 T-lymphocytes in CD11b <sup>-/-</sup> mice. ....	85
Figure 54. Tumour burden and growth in CD11b <sup>-/-</sup> mice. ....	87
Figure 55. Leukocytes infiltrating tumour mass and draining lymph nodes of the CD11b <sup>-/-</sup> . .	89
Figure 56. Immunohistological analysis of the B16-OVA melanoma infiltrating leukocytes in the CD11b <sup>-/-</sup> mice. ....	96
Figure 57. Gating strategy for the uptake of the p(Cy5) by the CD11b <sup>-/-</sup> BM-DC.....	98
Figure 58. Engulfment of the p(Cy5) by CD11b <sup>-/-</sup> BM-DC.....	99
Figure 59. Gating strategy for the uptake of p(Cy5) in mixed WT-CD11b <sup>-/-</sup> BM-DC cultures. .....	99
Figure 60. Engagement of p(Cy5) by BM-DC in mixed WT-CD11b <sup>-/-</sup> cultures. ....	100
Figure 61. Confocal microscopy of the p(Cy5) uptake by CD11b <sup>-/-</sup> BM-DC.....	102
Figure 62. Engulfment of the p(Cy5) by BM-DC blocked with α-CD11b Ab. ....	103
Figure 63. Gating strategy for analysis of the CD11b <sup>-/-</sup> BM-DC activation markers after treatment with p(Cy5). ....	104
Figure 64. Co-stimulatory molecule expression on the surface of the CD11b <sup>-/-</sup> BM-DC upon treatment with p(Cy5). ....	105
Figure 65. TNF-α secretion by CD11b <sup>-/-</sup> BM-DC exposed to the p(Cy5). ....	106
Figure 66. Gating strategy for the uptake of p(Cy5) by CD11b <sup>-/-</sup> splenic DC. ....	107

Figure 67. Uptake of p(Cy5) by CD11b <sup>-/-</sup> splenic DC. ....	108
Figure 68. Uptake of dextran by CD11b <sup>-/-</sup> BMDC.....	110
Figure 69. Uptake of dextran by CD11b <sup>-/-</sup> splenic DC.....	111
Figure 70. Uptake of OVA-AlexaFluor647 by CD11b <sup>-/-</sup> BM-DC. ....	113
Figure 71. Uptake of OVA-AlexaFluor647 by CD11b <sup>-/-</sup> splenic DC. ....	114
Figure 72. Uptake of OVA-DQ by CD11b <sup>-/-</sup> BM-DC.....	116
Figure 73. Cre-LoxP recombination scheme.....	122
Figure 74. TLR ligands and signalling.....	129
Figure 75. JAK/STAT signalling. ....	132
Figure 76. Model of the cross-talk between $\beta$ 2 integrin and SOCS or STAT molecules. ....	135
Figure 77. Main routes of cellular uptake of cargo. ....	141
Figure 78. Possible Mac-1 functions in the clathrin-dependent endocytosis.....	145
Figure 79. Southern Blot scheme. ....	160
Figure 80. Southern Blot probes overlapping exon 1 (A) and exon 7 (B) of the CD18 gene.162	
Figure 81 . Breeding strategy of the chimera mice acquired after blastocyst injection. ....	171
Figure 82. CD18 <sup><math>\Delta</math>CD11c</sup> breeding strategy. ....	174

## LIST OF TABLES

Table 1. The role of $\beta 2$ integrins in tumourigenesis. ....	20
Table 2. $\beta 2$ Integrins and their role in autoimmune diseases. ....	25
Table 3. CIS-SOCS protein family. ....	133
Table 4. Expendable materials used in the laboratory. ....	146
Table 5. Media used for the cell culture. ....	147
Table 6. List of the antibodies used in the laboratory. ....	149
Table 7. Reagents used in the laboratory. ....	151
Table 8. Mice strains used in the laboratory. ....	154
Table 9. Electrical equipment.....	155
Table 10. Buffers for the Southern blot.....	158
Table 11. Reaction mix for the ScaI digestion of the ES-clones.....	159
Table 12. Primers used for the synthesis of the Southern Blot probes (s-sense, as-antisense). .....	161
Table 13. Neo Cassette detection PCR protocol. ....	168
Table 14. CD18 homo- and heterozygote PCR screening protocol (s-sense, as-antisense)...	169
Table 15. PCR protocol for the detection of CD11c <sup>CRE</sup> genotype. ....	175
Table 16. List of antibodies used for the immunohistochemical staining of the frozen B16-OVA melanoma sections. ....	185
Table 17. Reverse transcription and qPCR reaction protocol. ....	187
Table 18. Primers used for the qPCR reactions (s-sense, as-antisense). ....	187

## LIST OF ABBREVIATIONS AND ACRONYMS

<b>1x</b>	<b>One fold</b>
<b>4x</b>	Four fold
<b>10x</b>	Ten fold
<b>20x</b>	Twenty fold
<b>100x</b>	Hundred fold
<b><math>\alpha</math>-</b>	anti
<b>Ab</b>	antibody
<b>APC</b>	antigen presenting cell
<b>Ag</b>	antigen
<b>BC</b>	B-cell (B-lymphocytes)
<b>BM-DC</b>	bone marrow-derived dendritic cell(s)
<b>BSA</b>	bovine serum albumin
<b>CD</b>	cluster of differentiation
<b>CDP</b>	Common DC precursor
<b>CFSE</b>	carboxylfluorescein diacetate succinimidyl ester
<b>cDC</b>	Conventional DC
<b>CIA</b>	Collagen induced arthritis
<b>CRISPR</b>	Clustered Regularly Interspaced Short Palindromic Repeats
<b>CTL</b>	cytotoxic lymphocyte
<b>DC</b>	dendritic cell
<b>dLN</b>	draining lymph node
<b>DMEM</b>	Dulbecco Mod's Eagle Medium
<b>DMSO</b>	Dimethylsulfoxide
<b>EAE</b>	Experimental autoimmune encephalomyelitis
<i>et al.</i>	et alii (and others)
<b>EDTA</b>	Ethylenediaminetetraacetic acid
<b>EF</b>	Embryonic fibroblasts (mouse)
<b>ES</b>	Mouse embryonic stem cells
<b>FACS</b>	fluorescent activated cell sorting
<b>FCS</b>	fetal calf serum
<b>FITC</b>	fluorescein isothiocyanate
<b>Flp</b>	flippase

<b>Flt3</b>	FMS-like tyrosine kinase 3
<b>FRT</b>	flippase recognition target
<b>GM-CSF</b>	granulocyte macrophage colony stimulating factor
<b>h</b>	hours
<b>HEPES</b>	(4-(2-hydroxyethyl)-1-piperazineethanesulfonic acid)
<b>i.d.</b>	intradermal
<b>i.p.</b>	intraperitoneal
<b>i.v.</b>	intravenous
<b>IgE</b>	immunoglobulin class E
<b>IgG</b>	immunoglobulin class G
<b>IL</b>	interleukin
<b>IFN-<math>\gamma</math></b>	interferon gamma
<b>IMDM</b>	Iscove's Modified Dulbecco's Medium
<b>IRF8</b>	IFN-regulatory factor 8
<b>KO</b>	Knockout
<b>LA-1</b>	Leukoadherin-1
<b>LC</b>	Langerhans cells
<b>LN</b>	lymph node
<b>LPS</b>	lipopolysaccharide
<b><math>\mu</math>g</b>	microgram
<b><math>\mu</math>l</b>	microliter
<b><math>\mu</math>m</b>	micrometer
<b>M</b>	molar
<b>MACS</b>	magnetic cell sorting
<b>MAPK</b>	mitogen-activated protein kinase
<b>M-CSF</b>	macrophage colony-stimulating factor
<b>mAb</b>	monoclonal antibody
<b>MDSC</b>	myeloid derived suppressor cell
<b>MEF</b>	Mouse embryonic fibroblasts
<b>MFI</b>	mean fluorescence intensity
<b>mg</b>	milligram
<b>MHC</b>	major histocompatibility complex
<b>min</b>	minute
<b>ml</b>	millilitre

<b>MR</b>	mannose receptor
<b>mM</b>	millimolar
<b>MMC</b>	Mitomycin
<b>MPS</b>	mononuclear phagocyte system
<b>n</b>	numbers
<b>NF-<math>\kappa</math>B</b>	nuclear factor 'kappa-light-chain-enhancer' of activated B-cells
<b>Ng</b>	Nanogram
<b>NK</b>	Natural killer
<b>nm</b>	nanometer
<b>NP</b>	Nanoparticle
<b>OVA</b>	ovalbumin
<b>o.n.</b>	overnight
<b>p</b>	p-value
<b>p.a.</b>	per analysis
<b>PAMP</b>	pathogen-associated molecular patterns
<b>pDC</b>	plasmacytoid DC
<b>PBS</b>	phosphate buffered saline
<b>PE</b>	phycoerythrin
<b>PFA</b>	paraformaldehyde
<b>pg</b>	pictogram
<b>qPCR</b>	Real time PCR
<b>rpm</b>	rounds per minute
<b>RT</b>	room temperature
<b>s.c.</b>	subcutaneous
<b>SEM</b>	standard error of the mean
<b>SIT</b>	Antigen-specific immunotherapy
<b>SLE</b>	Systemic lupus erythematosus
<b>SNP</b>	Single nucleotide polymorphism
<b>SOCS</b>	Suppressor of cytokine signalling
<b>SSC</b>	side scatter
<b>TC</b>	T cell (T-lymphocytes)
<b>TCR</b>	T cell receptor
<b>Th</b>	T helper cell
<b>Treg</b>	regulatory T cell

**TLR** toll like receptor

**vs.** *versus*

**WT** wild type



# 1. Introduction

## 1.1. Immune System

Immunology designates the study of the body's own defence against invading microorganisms, i.e. viruses, bacteria, fungi, parasites or malignant cells, as well as the establishment of tolerance towards endogenous and harmless environmental antigens. The immune response against a potential pathogen may be non-specific, involving innate/inherent immunity or specific, i.e. involving the adaptive immune system and production of antibodies. The body needs time in order to evoke a specific adaptive immune response during the primary pathogen encounter. This time gap is effectively managed by the inherent immune defence, which recognises evolutionarily conserved pathogen-associated molecular patterns (PAMPs) (Santoni et al., 2015) and initiates innate and subsequent adaptive immune response. The adaptive immune system, present only in vertebrates, develops over a lifetime and may create an immunological memory, which serves as a lifelong protective immunity against a specific pathogen (Kaufman, 2002). The interplay of both the innate and the adaptive immune system is therefore necessary for a successful immune defence (Fig.1). Pathogen recognition and immune effector functions are tightly regulated. Once the system is no longer able to self-regulate, i.e. loses tolerance towards self/non-harmful environmental antigens, it may contribute to conditions such as autoimmunity or allergy.

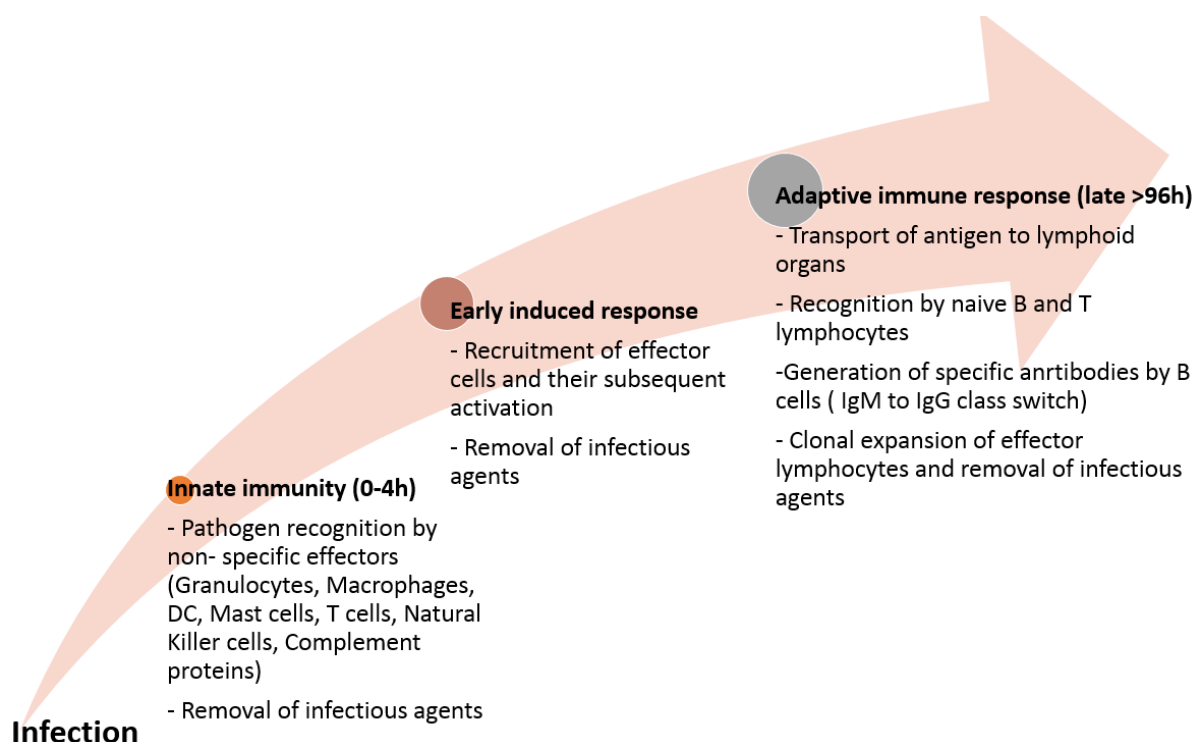


Figure 1. Three phases of the initial response to a pathogen.

### 1.1.1. Ontogeny of the immune system

Immune cells derive from leukocyte (white blood cell) precursors that originate from the bone marrow. The vast majority of leukocytes develops and differentiates at the site of origin, i.e. in the bone marrow, excluding T lymphocytes that develop in the thymus (J. W. Choi et al., 2017; Stutman, 1977; Vicente et al., 1998). Differentiated cells migrate to the periphery, where some reside within tissues and some remain in the bloodstream or within the lymphatic system that drains extracellular fluid. Pluripotent hematopoietic stem cells give rise to all the cellular elements of the blood, i.e. red and white blood cells. Leukocytes further develop into two main lineages: myeloid and lymphoid (Kondo, 2010).

Most cells of the innate immune system derive from the common myeloid progenitor. It gives rise to macrophages, granulocytes, myeloid dendritic cells and mast cells (as well as non-immune cells such as megakaryocytes and erythrocytes) (Weiskopf et al., 2016).

Macrophages derive from monocytes, which circulate in the blood stream for about 2 days before they enter the tissue and differentiate (J. Yang, Zhang, Yu, Yang, & Wang, 2014). Macrophages are long-lived tissue-resident cells, playing an important role in both innate and adaptive immunity (Davies, Jenkins, Allen, & Taylor, 2013). As a first line of defence (beside neutrophils) they engulf and kill invading pathogens and induce inflammation by secreting pro-inflammatory mediators that attract and activate other immune cells.

Granulocytes are relatively short-lived polymorphonuclear leukocytes, which can be divided into three subgroups: neutrophils, eosinophils and basophils. Neutrophils are the most abundant phagocytic cell type in the body, they account for about 60% of all the white blood cells. They internalize a variety of microorganisms or kill the pathogens extracellularly via excreted cytoplasmic granules that contain enzymes and antimicrobial substances. Moreover, they may bind microorganisms by releasing their own chromatin structures, the so called neutrophil extracellular trap (NET) (Kaplan & Radic, 2012; Palmblad, 1984). Eosinophils and basophils contain granules that harbour a variety of enzymes and toxic agents, which are effective in defence against parasites that are too large to be phagocytised (L. Huang & Appleton, 2016).

Mast cells differentiate in the tissue and protect against parasites as they are integrated within the internal surface barrier and secrete granules (rich in histamine and heparin that mediate inflammation) once they are activated. They orchestrate as well allergic responses since they contain high affinity receptors for the Fc fragment of IgE, an immunoglobulin that is secreted by plasma cells and physiologically binds parasites, but in the context of allergy binds non-

harmful environmental antigens and initiates inflammation (Krystel-Whittemore, Dileepan, & Wood, 2015).

Dendritic cells, as well as macrophages and neutrophils, belong to the group of active phagocytic cells of the immune system. They take up pathogens and extracellular matter via phagocytosis and receptor-mediated endocytosis (Savina & Amigorena, 2007). They process the invading microorganisms and are able to present the microorganism-derived antigens to T lymphocytes, which are effector cells that eradicate recognised pathogens/infected cells. Thus, dendritic cells, as antigen presenting cells (APCs) and phagocytes relate to both adaptive and innate immunity (They & Amigorena, 2001).

Common lymphoid progenitors give rise to lymphocytes that belong to the adaptive immune system as well as to natural killer cells that are part of the innate immune system. The later recognise virus-infected and malignant cells with a variety of surface receptors. An NK-cell distinguishes a healthy cell from an abnormal one by a net input of the activating and inhibitory signals derived for the receptors that inspect the cell (Vivier, Tomasello, Baratin, Walzer, & Ugolini, 2008). An overall balance between the inhibitory and activating receptors that bind ligands on the surface of an inspected cell, regulates the action of the NK-cell. A virus-infected cell, a cancer cell or a cell that misses MHC-I will be exposed to IFN- $\gamma$ , granzymes and perforins secreted by the NK-cell and thus will be eradicated (Orange & Ballas, 2006).

Lymphocytes, on the contrary, act in an antigen-specific manner. There are two types of lymphocytes, namely B lymphocytes (B cells) and T lymphocytes (T cells), each playing different roles. Naïve lymphocytes circulate in the body in an inactive state, and first upon antigen encounter become fully functional. B cells differentiate to plasma cells upon antigen binding to the B cell receptor (BCR) and activation by the T helper cell, subsequently they produce antibodies that target the same antigen that bound the BCR (Treanor, 2012). The antigen-recognizing T cell receptor (TCR), is similar to the BCR, nevertheless it has got an altered structure and recognition properties (L. Chen & Flies, 2013; Cooper & Alder, 2006). When a T cell encounters an antigen it proliferates and differentiates towards one of the effector T cell subset. T cells recognize oligopeptide presented via MHC by an APC (signal 1) in the context of co-stimulatory molecules (signal 2); only then T cell activation occurs. Soluble mediators released by an APC (signal 3) determine the mode and degree of T cell polarization. There are three main effector T cell classes: cytotoxic, helper and regulatory T cell. CD8<sup>+</sup> cytotoxic T cells destroy pathogen-infected or mutated cells, whereas CD4<sup>+</sup> helper T cells provide additional signals in order to activate B-cells, stimulate antibody secretion and

produce cytokines and chemokines that attract and activate other effector cells. Helper T cells are sub-divided into further groups (Th1, Th2, Th17, Th9 or Th22), all being specific for a certain mode of immune action, playing protective as well as pathogenic functions (Raphael, Nalawade, Eagar, & Forsthuber, 2015). Regulatory T cells, on the other hand, suppress other lymphocytes and control the immune response. During original exposure to an antigen, a fraction of memory lymphocyte arises. They reside within lymphatic organs (central memory T cells) or in the periphery (resident memory T cells) for a prolonged time and expand immediately as effector memory T cells once the same pathogen crosses the barrier, therefore upon subsequent exposure to a pathogen immune system can eliminate an invader more effectively (McHeyzer-Williams, Okitsu, Wang, & McHeyzer-Williams, 2011) (Chang, Wherry, & Goldrath, 2014).

A close interplay of all mentioned immune cell types normally provides an effective protection against pathogens and is important for the removal of damaged tissue and mutated/neoplastic cells. Development of the bone marrow-derived leukocytes is depicted in the figure below (Fig.2).

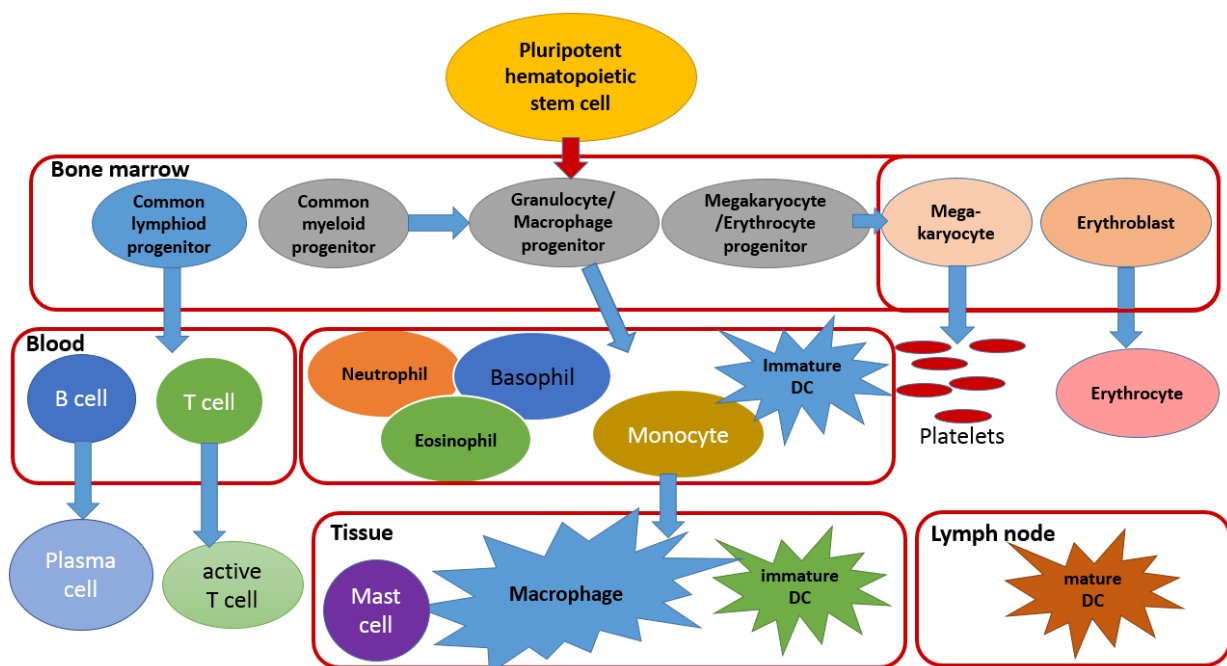


Figure 2. Cellular elements of the blood.

## 1.2. The biology of a dendritic cell (DC)

Myeloid DC specialise in recognition of pathogens and cancer cells. Being an interface between innate and adaptive immune system DC clear the system of the pathogens via phagocytosis and orchestrate an adaptive immune response conducted by effector T lymphocytes.

### 1.2.1. Development and subsets of DC

Dendritic cells belong to the mononuclear phagocyte system (MPS) along with monocytes and macrophages. The characteristics of these cell types are overlapping. They may, however, be distinguished according to their location, ontogeny, function and phenotype (Guilliams et al., 2014). Murine dendritic cells are defined by the expression of CD11c and MHC-II (Steinman, Kaplan, Witmer, & Cohn, 1979). According to further surface marker expression DC can be further divided into subsets. Guilliams and colleagues introduced a two-level nomenclature for the murine DC subsets. At the first level, describing the ontogeny of the cell, common DC precursors in the bone marrow give rise to both conventional and plasmacytoid DC (with pre-cDC and pre-pDC stage). At the 2<sup>nd</sup> level, DC can be sub-divided into three subsets according to their markers and function (two conventional and one plasmacytoid DC subset has been distinguished). Conventional DC (cDC) are divided into cDC1 (CD8 $\alpha$ <sup>+</sup> CD103<sup>+</sup>) and cDC2 (CD11b<sup>+</sup> CD172a<sup>+</sup>), plasmacytoid DC (CD123<sup>+</sup> BDCA<sup>+</sup>) remained as one subset of interferon producing cells that can influence T cell fate. In addition following markers, including chemokine- and Fc- receptors, can be used in the DC subset specification: F4/80, Clec9a, CD24, CD64 (Fc $\gamma$ RI), XC chemokine receptor 1 (XCR1), or CX3 chemokine receptor 1 (CX3CR1). Apart from the classification described above there are many other suggestions how to subset DC, however these are not discussed here. Pre-cDC develop in the bone marrow and migrate to tissues where they finally differentiate to cDC, whereas pDC differentiate in the bone marrow (Onai et al., 2007).

Development of all DC populations is dependent on the FMS-like tyrosine kinase 3 ligand (FLT3L) (McKenna et al., 2000). Subsequent differentiation into a particular subset is determined by expression of distinct transcription factors. Development of cDC1 depends on the expression of IFN-regulatory factor 8 (IRF8) (Schiavoni et al., 2002), DNA-binding protein inhibitor ID2 (Ginhoux et al., 2009), basic leucine zipper transcriptional factor ATF-like 3 (BATF3) (Hildner et al., 2008), nuclear factor interleukin (IL)-3-regulated protein (NFIL3)(Kashiwada, Pham, Pewe, Harty, & Rothman, 2011), and/or Sec22b (Alloatti et al., 2017). Differentiation towards cDC2 is guided by RELB (L. Wu et al., 1998), PU.1 (Guerriero, Langmuir, Spain, & Scott, 2000), recombining binding protein suppressor of hairless (RBPJ) (Caton, Smith-Raska, & Reizis, 2007), and IRF4 (Schlitzer et al., 2013), whereas plasmacytoid DC development is driven by E2-2 (H. S. Ghosh, Cisse, Bunin, Lewis, & Reizis, 2010) and Zeb2 (Scott et al., 2016). E2-2 and Zeb2 repress ID2, needed for the cDC1 differentiation.

Dendritic cells residing in the tissues express characteristic surface markers depending on whether they have a cDC1 or cDC2 signature. Conventional DC1 express CD8a<sup>+</sup> in the spleen, CD207<sup>+</sup> in the dermis, CD103<sup>+</sup>CD11b<sup>-</sup> in the intestine and CD103<sup>+</sup> in the lung, whereas cDC2 are CD4<sup>+</sup> in the spleen, CD207<sup>+</sup>CD11b<sup>+</sup> in the dermis, CD103<sup>+</sup>CD11b<sup>+</sup> in the intestine and CD11b<sup>+</sup> in the lung, as summarized in Figure 3 (K. Liu & Nussenzweig, 2010).

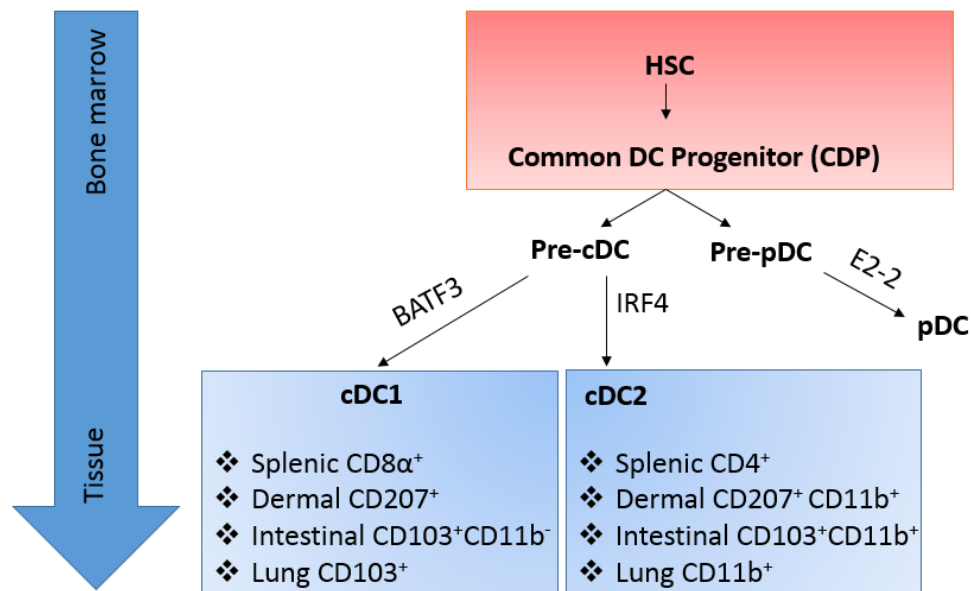


Figure 3. Dendritic cell development and subsets.

## 1.2.2. Processing and presentation of the antigen

All cDC have a characteristic morphology possessing a finger-like projections (dendrites) that facilitate peripheral patrolling for pathogens and efficient presentation of antigens via the MHC molecules to naïve T lymphocytes (Steinman & Witmer, 1978). Dendritic cells constantly sample the environment, and process engulfed material intracellularly. Exogenous material may be internalized via receptor mediated endocytosis, pinocytosis, macropinocytosis or phagocytosis. The route of uptake may as well influence the antigen presentation route (Kamphorst, Guermonprez, Dudziak, & Nussenzweig, 2010).

Murine cDC1 internalize antigens from the surrounding and present them on the MHC-II, just like other DC cell subsets, however they are not as efficient as the cDC2 (Rizzitelli, Hawkins, Todd, Hodgkin, & Shortman, 2006). Conventional DC1 are rather specialized in cross-presentation of exogenous antigens via MHC-I to CD8<sup>+</sup> T cells (Gutierrez-Martinez et al., 2015). They present in particular dead-cell-derived antigens (engulfed by Clec9a or the scavenger receptor CD36), viral antigens (Bedoui et al., 2009) and tumour-specific antigens (Schiavoni, Mattei, & Gabriele, 2013). Most peptides presented on MHC-I, derive from proteasome-degraded proteins that were synthesised in the cell and are transported by TAPs

(transporter associated with antigen processing) to the endoplasmic reticulum, where they are loaded onto MHC-I with the help of chaperons. Subsequently, MHC-I are trafficked through the Golgi apparatus to the plasma membrane, so that the antigen can be presented to T lymphocytes (Hewitt, 2003). This special feature of CD8<sup>+</sup> DC to cross-present engulfed material in the context of MHC-I, rather than MHC-II, is an essential element of the immune response against infected cells as well as tumour cells. Furthermore, splenic CD8<sup>+</sup> DC1 and cDC1 outside of the spleen sense pathogen-associated molecular patterns (PAMPs) through toll-like receptors (TLRs, apart from TLR-7) (Edwards et al., 2003) and secrete cytokines in response to it. Stimulation through TLR-9, 11 or 13 (that recognise foreign DNA, flagellin or ribosomal RNA, respectively) leads to secretion of IL-12p40 (O. Schulz et al., 2000). Stimulation of TLR-3, recognising dsRNA, is crucial for the secretion of IFN- $\beta$  and hence for the stimulation of the immune response in mice (Hochrein et al., 2001).

Conventional DC2 (always expressing CD11b) also detect pathogens within the cytoplasm via a range of receptors including RIG-1 (recognising ssRNA) and some inflammasome components (NLRX1, caspase1). Moreover, they express C-type lectins, NOD-like receptors as well as TLRs: TLR-7 exclusively, but no TLR-3 or TLR-12 (Luber et al., 2010). Therefore, they can sense both pathogen-associated molecular patterns (PAMPs) and damage associated molecular patterns (DAMPs) derived from altered/neoplastic cells. TLR ligands trigger splenic DC to secrete pro-inflammatory cytokines, like IL-6, TNF- $\alpha$ , as well as low levels of IL-10. In peripheral tissues activated CD11b<sup>+</sup> DC secrete IL-6, IL-23, TGF- $\beta$  and IL-1. cDC2 are in general specialized in priming of CD4<sup>+</sup> T cells (Dudziak et al., 2007). Endosomes of the cDC2 are rich in MHC-II molecules and so once the pathogen is engulfed and digested, the pathogen-derived peptides can bind to MHC-II and be presented on the cell surface. In a non-activated DC (in the absence of danger signals), MHC-II gets ubiquitinated and is degraded in the lysosome, whereas in the activated DC ubiquitination is repressed and the endosome with a peptide-loaded-MHC-II fuses with the plasma membrane (ten Broeke, Wubbolts, & Stoorvogel, 2013).

### 1.2.3. Maturation and expression of surface receptors on DC

During antigen uptake and processing in presence of danger signals or cytokines DC matures and increases the expression of the surface co-stimulatory molecules, like CD80, CD86, CD40 as well as MHC-II. Activated DC transiently increases phagocytosis and macropinocytosis rate to sample the environment more thoroughly before it orchestrates immune response and

stimulates other cell types (indirectly with cytokines and directly over the immunological synapse: lymphocyte priming). Furthermore, upon maturation DC increase their migratory potential to move from the periphery to the lymph node, where they can present the antigen to the lymphocytes and initiate immune response (West et al., 2004). The interaction between DC and T cell is presented in Figure 4. Within the centre of immunological synapse (IS), a space where cells interact with each other, a processed peptide is presented to the T cell via T- cell receptor (TCR) and its co-receptors (CD4 or CD8)(Acuto, 2003). The interaction between an APC and a lymphocyte is stabilized by adhesion molecules, such as ICAM-1 and LFA-1(Anderson & Siahhaan, 2003), forming the outer area of the IS. In this context co-stimulatory molecules on the DC, CD80 and CD86, provide a stimulatory signal for T cell activation via binding to the CD28 on T cells. The final stimulus comes for the interaction of CD40 on DC with CD40L (also known as CD154) on T cell and thus cells stimulate one another (Somoza & Lanier, 1995).

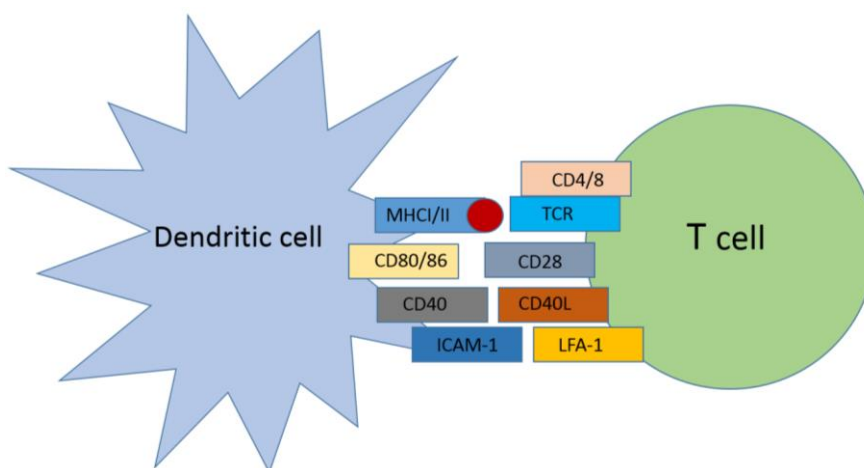


Figure 4. Interaction of an APC with T lymphocytes.

#### 1.2.4. Tolerance induction and immune stimulation by DC

Activated DC that carry an antigen can evoke an immune response specific against that antigen. The type of antigen, its uptake route and environmental context influence the mode of immune stimulation (Kamphorst et al., 2010). Exogenous antigens may be cross-presented in the context of MHC-I, which leads to activation of naïve CD8<sup>+</sup> T cells. These CD8<sup>+</sup> T cells differentiate then towards cytotoxic effector cells (CTLs), which recognise and kill infected or neoplastic cells via secretion of granzymes, perforins, or FasL binding (inducing apoptosis) (Halle, Halle, & Forster, 2017). Intra- and extracellular pathogens as well as toxins presented on MHC-II activate CD4<sup>+</sup> effector T cells. Naïve CD4<sup>+</sup> T cell may then differentiate toward distinct

pathways, thus generating various T helper cell subsets, like Th1, Th2, Th9, Th17 or Treg (Hoefig & Heissmeyer, 2018).

IFN- $\gamma$  and IL-12 stimulate STAT1 and STAT4, respectively, which in turn induce *Tbet* expression and subsequently Th1 signature genes (Y. Zhang, Zhang, Gu, & Sun, 2014). A Th1-biased immune response is generated against intracellular pathogens and is essential for the induction of CTL (W. S. Kim, Shin, & Shin, 2018).

Th2 differentiation, on the other hand, is driven by IL-4 and downstream activation of STAT6 and *GATA3* expression. Polarized Th2 lymphocytes secrete mainly IL-4, IL-5, IL-13 and contribute to elimination of helminths. An armed T helper cell can as well activate B cell to induce humoral immune response. An antigen-specific Th2 cell binds the peptide presented on the MHC-II on B cell and conveys signalling that results in production of specific antibodies. Apart from fighting of pathogens, Th2 lymphocyte play as well an essential role in the pathomechanism of allergic disease and atopy (Lorentsen et al., 2018).

Th17 polarized T cells fight of bacteria and fungi found within epithelial barriers in the gastrointestinal tract, respiratory tract and in the skin (H. Y. Kim et al., 2018; Y. Li et al., 2018). They are as well known to contribute to the autoimmune diseases, such as psoriasis (Bian et al., 2018; Hirota et al., 2018). Th17 reactions are dependent on IL-6, TGF- $\beta$  and IL-23 stimulation, upon which they activate Stat3 and ROR $\gamma$ t (Tanaka et al., 2011). The hallmark of the Th17 lymphocyte is secretion of IL-17.

In response to IL-2 and TGF- $\beta$ , T cell activate Stat5 and Smad2/3, which in turn up-regulate transcription of FoxP3, a signature of regulatory T lymphocytes (Tregs). Treg suppress effector T cell by secretion of IL-10 and TGF- $\beta$  and therefore regulate the course of inflammation (M. Liang, Liwen, Yun, Yanbo, & Jianping, 2018). Tolerogenic dendritic cells (tolDC) and macrophages, may as well produce IL-10 under certain conditions and promote immune tolerance (Comi, Amodio, & Gregori, 2018).

Depending on the context of antigen presentation (MHC-I or MHC-II), cytokine milieu and type of pathogen, T cells become profiled toward a specific immunologic signature (Halle et al., 2017). The figure below (Fig.5), based on a review article (Hoefig & Heissmeyer, 2018), summarizes possible fates of a T lymphocytes influenced by an APC.

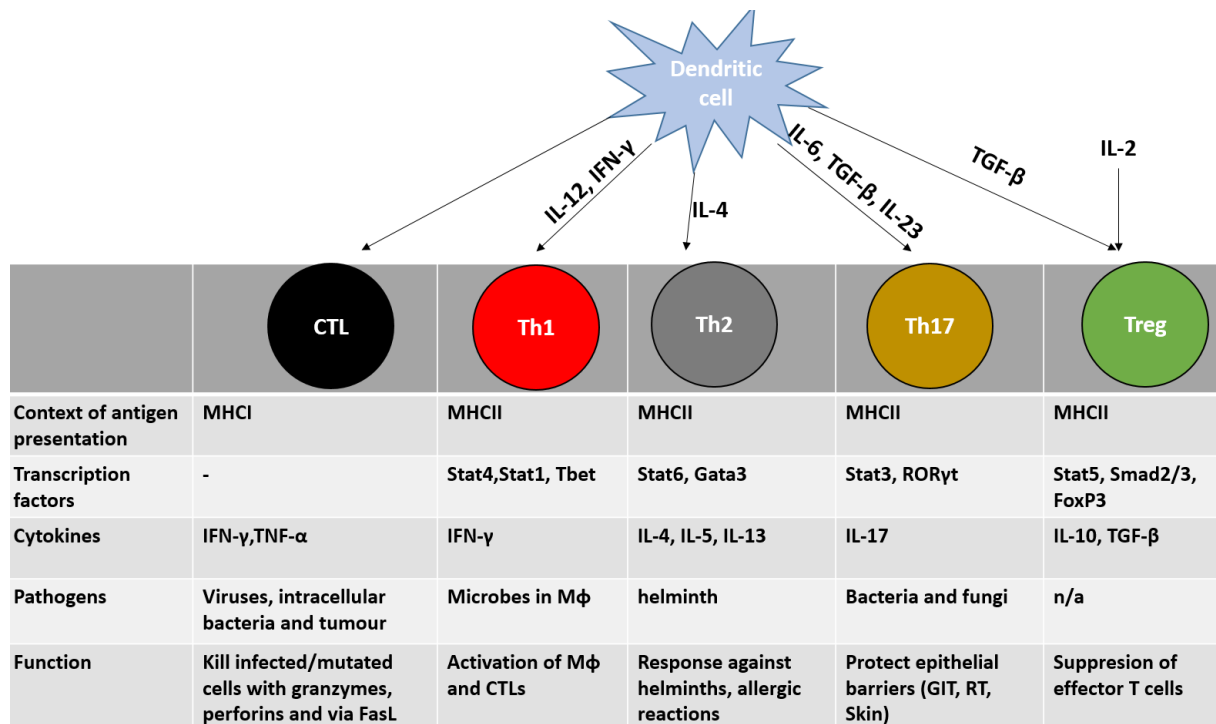


Figure 5. T cell fate after activation via dendritic cell.

### 1.3. β2 Integrins

Integrins are evolutionary conserved heterodimeric transmembrane receptors that allow cell-cell or cell-matrix interactions (Johnson, Lu, Denessiouk, Heino, & Gullberg, 2009). They maintain the communication between the cytoskeleton and extracellular matrix. Upon binding to a ligand they transduce a signal that modulates cell cycle, cytoskeletal re-arrangement and expression of other surface receptors. Beta1, β2 and αV containing heterodimers compose three largest groups of integrins and are vastly distributed among tissues. In the field of immunology, integrins expressed on the leukocytes are particularly interesting since they influence the course of an immune response. The following integrins act as leukocyte-specific receptors: all β2, β1α4, β1α9 and β7αE (Mitroulis et al., 2015).

Integrins are heterodimers that constitute of two non-covalently bound subunits, alpha and beta. Both subunits are anchored in the plasma membrane and bind divalent cations, but only the alpha subunit determines the ligand specificity (Hynes, 2002). There are 24 αβ heterodimers in vertebrates, assembled of 18α and 8β subunits (Takada, Ye, & Simon, 2007). Eight heterodimers recognise a RGD peptide sequence (Arg-Gly-Asp), present for example in collagen and laminin. Another eight integrins, including all four β2 integrins, recognise a GFOGR triple-helical sequence, found specifically within collagen, and nine integrins contain

an  $\alpha$ -I domain. (Barczyk, Carracedo, & Gullberg, 2010). Thus integrins may be classified according to a specific ligand they bind. Apart from ligands that are characteristic for a certain subgroup, integrins bind a variety of other ligands both soluble and cell bound, which are in detail discussed in chapter 1.3.2.

The representative members of integrins in vertebrates and their ligand specifications are summarized in the Figure 6 below.

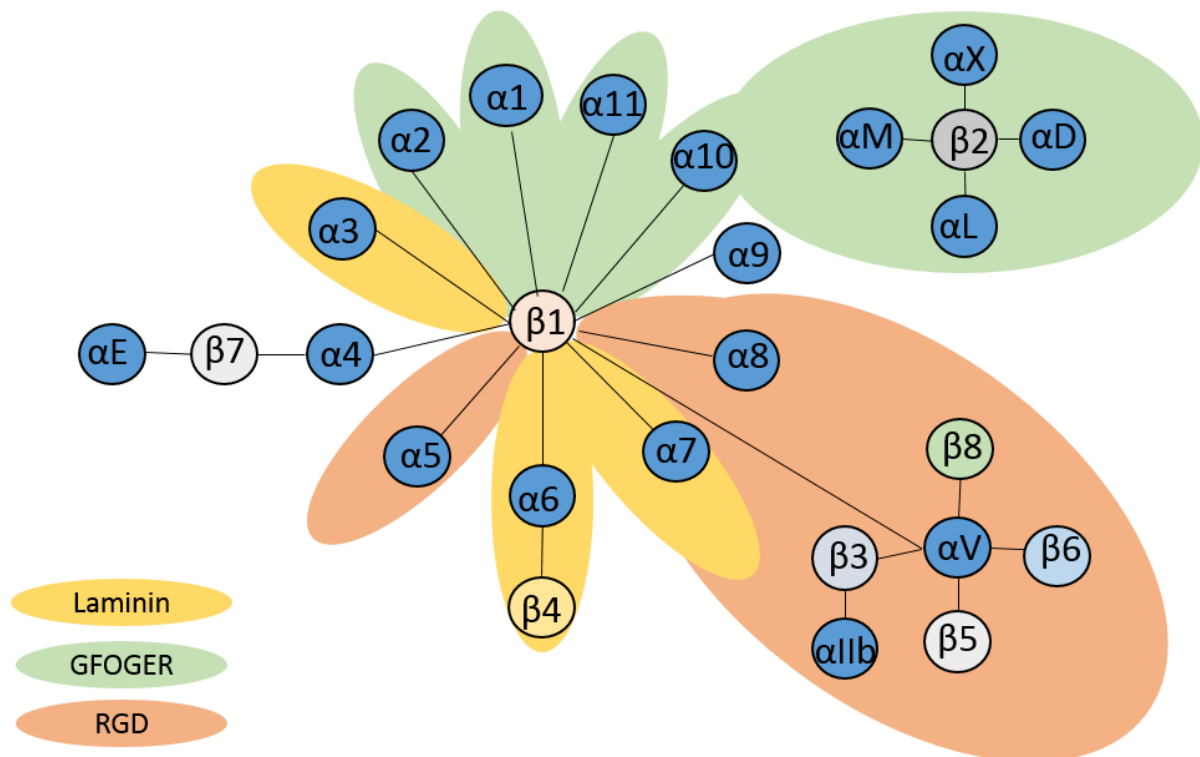


Figure 6. Representative members of integrins in vertebrates and their binding specificity.

### 1.3.1. Structure of $\beta$ 2 integrins

$\beta$ 2 integrins are heterodimers composed of a constant  $\beta$ 2 (CD18) subunit, which is non-covalently bound to one of 4 different alpha subunits:  $\alpha$ L (CD11a),  $\alpha$ M (CD11b),  $\alpha$ X (CD11c) or  $\alpha$ D (CD11d). Subunits dimerize intracellularly before they get integrated in the membrane, i.e. there are no free subunits expressed on the cell surface (M. J. Humphries, 2000). The abundance of alpha subunit limits therefore the amount of integrin presented on the cell surface, as the CD18 subunit is present in excess in the cell (Santala & Heino, 1991). The structure of a  $\beta$ 2 integrin is presented in Figure 7 below.

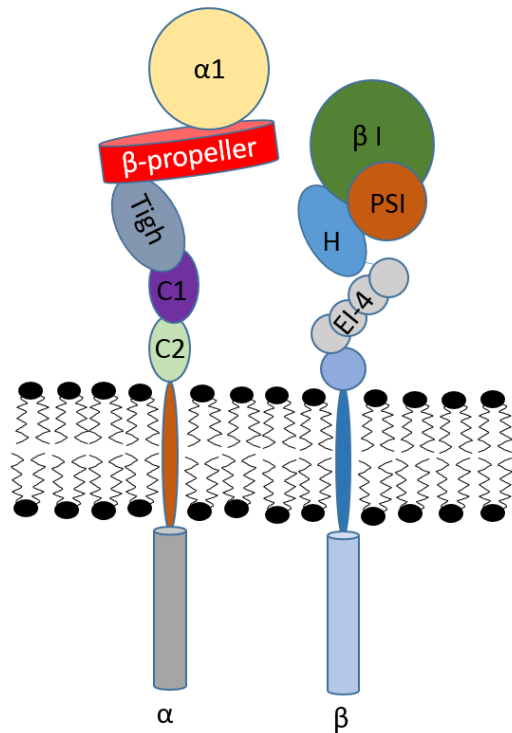


Figure 7. Integrin structure.

### 1.3.1.1. $\beta 2$ integrin alpha subunit

The alpha subunit defines the ligand specificity of the  $\beta 2$  integrin. The head of any alpha subunit is composed of seven-bladed beta-propeller motif connected to the calf-1 and calf-2 over a thigh. Calcium-binding EF-hand domains found within last three propeller blades modulate allosterically ligand binding on the other pole of the propeller upon recruitment of a cation (M. J. Humphries, Symonds, & Mould, 2003). Between the 2<sup>nd</sup> and 3<sup>rd</sup> blade of the beta-propeller a 200 amino acid I domain (also known as A domain) is inserted and enables the integrin to bind collagen with its  $\alpha C$  helix (Chouhan et al., 2014). The  $\alpha I$  domain, expanding the cleft between the beta-propeller and the  $\beta I$  domain of the beta-subunit, provides therefore a binding surface that allows interaction with much bigger ligands and over more residues. Binding of  $Mg^{++}$  to the metal-ion-dependent-adhesion-site (MIDAS) motif of the  $\alpha I$ -domain bridges binding of the integrin to collagen or ICAM over their negative glutamate-rich residues (K. Zhang & Chen, 2012). A C-terminal glutamate residue of the  $\alpha 1$  domain itself is as well an intrinsic ligand for the MIDAS on the  $\beta 1$  domain of the integrin  $\beta$ -subunit, assuring its conformational change upon ligand binding. A crystal structure of a metastable  $\alpha X \beta 2$  revealed that in a high affinity open form,  $\alpha I \alpha 7$  helix unwinds and extends away from the  $\alpha I$  domain, forming an intrinsic ligand between the  $\beta$ -propeller and the  $\beta I$  domain (M. Sen, Yuki, & Springer, 2013). Blockade

of the interaction between  $\alpha 1$  and  $\beta 1$  domain disrupts signalling (Shimaoka, Salas, Yang, Weitz-Schmidt, & Springer, 2003). As reported for CD11c/CD18, the  $\beta A$  domain of the beta subunit conveys outside-in signalling generated by intrinsic ligand in  $\alpha A$ -containing integrins (M. Sen et al., 2013). The cytoplasmic tail of the alpha subunit is not yet well studied.

### 1.3.1.2. $\beta 2$ integrin beta subunit

Beta subunit of the  $\beta 2$  integrin is connected to the cytoskeleton and conveys intracellular signalling. It contains eight extracellular domains: four integrin-epidermal growth factor (EGF)-like domains (EI-4), hybrid, plexin-semaphorin-integrin (PSI), a  $\beta$ -tail and a  $\beta I$  domain. The  $\beta I$  domain contains, like the  $\alpha I$  domain on the  $\alpha$ -subunit, a metal ion dependent adhesion site (MIDAS) that binds  $Mg^{++}$  and thus bridges binding to aspartate residues within the ligand or to the glutamate residues within the  $\alpha I$  domain. It acts as an allosteric regulator of  $\alpha I$ -ligand binding (Shimaoka, Xiao, et al., 2003). Moreover, the intrinsic binding of Glu310 ( $\alpha L$ ) to the MIDAS on the activated  $\beta I$  domain leads to transmission of an activated state from the beta over to alpha subunit and is required for the overall  $\alpha M\beta 2$  activation (Luo, Carman, & Springer, 2007; W. Yang, Shimaoka, Salas, Takagi, & Springer, 2004). Adjacent to the MIDAS motif is the ADMIDAS, a negative regulator, which inhibits activation of the integrin at high  $Ca^{++}$  concentrations and stabilizes its closed conformation (Zhu et al., 2008). As shown for the beta subunit of the beta3 integrin it may as well play a role in the activation of the integrin, as the  $Mn^{++}$  ions compete with  $Ca^{++}$  for the binding to ADMIDAS and lead to the activation of the subunit (J. Chen, Salas, & Springer, 2003). A ligand bound  $\beta 1$  domain contains additionally a ligand-associated metal binding site (LIMBS) recruiting  $Ca^{++}$  (Xiao, Takagi, Collier, Wang, & Springer, 2004). LIMBS stabilizes the metal ion at MIDAS of the beta chain of beta3 integrin (Rui et al., 2014).

As depicted in Figure 8 there are three conformational states of  $\beta 2$  integrins: the bent with closed headpiece (A), the extended with closed headpiece (B) and the extended with open headpiece (C), which are corresponding to the low-, intermediate- and high-affinity states, respectively. Divalent cations and inside-out signalling are both factors that primarily influence the activation of the integrin and thus its affinity toward a particular ligand.

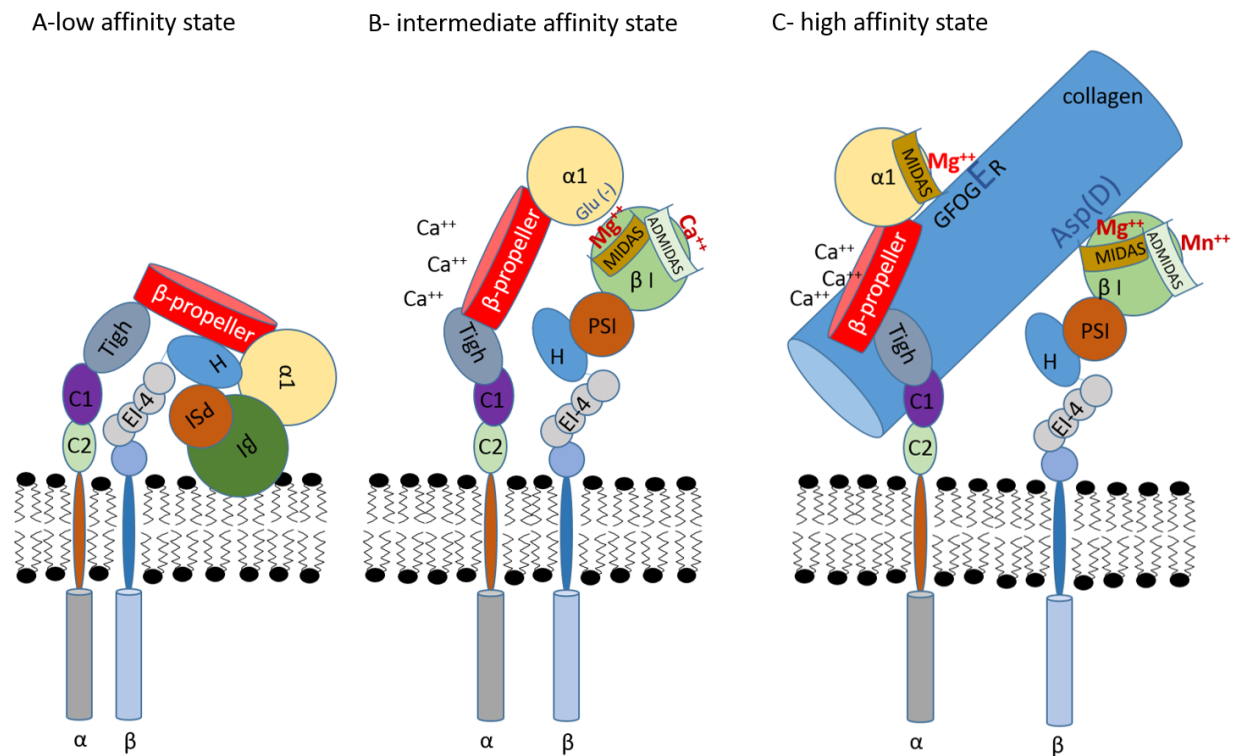


Figure 8.  $\beta_2$  integrin activation states.

### 1.3.2. Interactions of $\beta_2$ integrins with various ligands and their functions

Distribution of  $\beta_2$  integrins on leukocytes and their ligand specificity determines their functions. Most leukocytes circulate in the blood and upon encounter of inflamed endothelia migrate toward the tissue, where they serve as barrier guardians and fight invading pathogens.  $\beta_2$  integrins play an essential role in innate immune reactions as they mediate endothelium-binding of leukocytes and orchestrate binding of extracellular matrix and complement-opsonised pathogens. Furthermore, as a part of the adaptive immune system reactions they modulate lymphocyte proliferation and differentiation.

#### 1.3.2.1. Tissue distribution of $\beta_2$ integrins

$\beta_2$  integrins are distributed exclusively on leukocytes. CD11a/CD18 (LFA-1) is most abundant on lymphocytes (Y. X. Liu et al., 2015), whereas CD11b/CD18 (MAC-1) is mostly expressed on myeloid cells, predominantly neutrophils (W. D. Huang et al., 2009). In addition, it has been reported that CD11b is as well present on the surface of NK cells, some mast cells and lymphocytes (B cell, CD8<sup>+</sup> and  $\gamma\delta$  T cells) (Fiorentini et al., 2001; Ghosn, Yang, Tung, Herzenberg, & Herzenberg, 2008; Graff & Jutila, 2007; Rosenkranz et al., 1998). CD11c/CD18,

like CD11b, is mostly expressed on myeloid cell lineages and predominates on DC. Similarly to CD11b, CD11c is as well present on some NK cell and lymphocytes (Karnell et al., 2017; W. Li et al., 2013; Vinay & Kwon, 2010). CD11d is expressed in mouse on a small fraction of leukocytes, being most abundant on myeloid cell lineages, like macrophages, and is upregulated upon inflammation, whereas in human blood cells it is in addition highly expressed on NK cells, B cells, and  $\gamma\delta$ T cells (Aziz et al., 2017; Siegers, Barreira, Postovit, & Dekaban, 2017). Tissue distribution of  $\beta 2$  integrin is summarized in Figure 9.

### *1.3.2.2. Ligand binding of $\beta 2$ integrins*

In  $\beta 2$  integrin alpha subunit is the leading, ligand binding determinant. CD11a engages intercellular adhesion molecules 1-5 (ICAMs), junctional adhesion molecule 1 (JAM1) and endothelial cell-specific molecule-1 (ESM-1) (Bechard et al., 2001; Kummer & Ebnet, 2018; Walling & Kim, 2018). CD11b binds numerous, both soluble and cellular, ligands. Cell bound ligands include ICAM1-4, VCAM-1, JAM-3, Thy-1, RAGE, DC-SIGN and CD40L (Jin et al., 2013; Kummer & Ebnet, 2018; N. Li et al., 2018; Schubert et al., 2011; Yakubenko, Yadav, & Ugarova, 2006). The list of CD11b-binding soluble ligands is quite extensive, including C3b, fibrin(ogen), Factor Xa, platelet Ib, heparin, polysaccharides, ssDNA, dsRNA, apoptotic bodies, some acute phase proteins, HMGB1 and denatured proteins among many others (Hyun, Lefort, & Kim, 2009; Podolnikova, Podolnikov, Haas, Lishko, & Ugarova, 2015). Moreover, CD11b binds apoptotic bodies and recruits some matrix proteins, like fibronectin, fibrinogen, vitronectin, Cyr61 and plasminogen.

CD11c ligands overlap partially with the CD11b-ligands, CD11c also binds ICAM1, ICAM4, Thy-1 and vascular cell adhesion protein 1(VCAM-1) found on the cell surface. CD11c- soluble ligands include iC3b, heparin, polysaccharides, and negatively charged denatured proteins (J. Choi, Leyton, & Nham, 2005; J. D. Humphries, Byron, & Humphries, 2006).  $\beta 2$  integrin specific ligands are listed in Figure 9.

### *1.3.2.3. Function of $\beta 2$ integrins*

CD18 deficiency in humans, also known as leukocytes adhesion deficiency 1 (LAD1) syndrome, demonstrates with life-threatening, recurrent bacterial or fungal infections of soft tissue. Likewise, CD18<sup>-/-</sup> mice characterize with neutrophilia and development of spontaneous bacterial infections (Scharffetter-Kochanek et al., 1998). Interestingly, deletion of any of the alpha subunit alone does not lead to induction of spontaneous infections in mice. CD11a<sup>-/-</sup> mice have mild neutrophilia, and thus have problems to clear of bacterial infections (S. Ghosh,

Chackerian, Parker, Ballantyne, & Behar, 2006; Shaw et al., 2004). CD11a deficient mice fail as well to reject immunogenic tumours and respond weakly to alloantigens, because apart from adhesion to endothelium, CD11a modulates adhesion of lymphocytes to antigen presenting cells, formation of the immunological synapse and subsequent TCR signalling amplification, as well as adhesion to target cells for killing (Walling & Kim, 2018) (Shier et al., 1996).

CD11b<sup>-/-</sup> mice are characterised by a diminished neutrophil activation during inflammation and defective T cell proliferation in response to bacterial infection, however, they do not develop spontaneous infections and are not impaired in tumour response (H. Wu et al., 2004). Interestingly, Mac-1 deficient mice present with a better tumour growth control as they modulate VEGF secretion by polymorphonuclear neutrophils cells and thus CD11b ablation slows neovascularisation down (Soloviev et al., 2014). In the context of innate immune response, CD11b is a crucial  $\beta 2$  integrin involved in phagocytosis of serum coated pathogens and phagocytosis of apoptotic bodies, at the same time it negatively regulates TLR-triggered immune response being protective against sepsis (Coxon et al., 1996; Han et al., 2010; Le Cabec, Carreno, Moisand, Bordier, & Maridonneau-Parini, 2002). Despite some immunological deficiencies, CD11b null mice are prone to develop autoimmune diseases, as CD11b was shown to be crucial for the establishment of peripheral tolerance (Ehrichtiou et al., 2007; Garbers & Rose-John, 2017). Furthermore, Mac-1 deficient mice were shown to be protected from thrombosis as Mac-1 engagement of platelet GPIIb/IIIa is important in formation of thrombus in responses to injury (Y. Wang et al., 2017). Mac-1 is therefore involved in many processes important for immunological tolerance, innate as well as adaptive immune responses and blood homeostasis.

CD11c null mouse, as well as CD11a<sup>-/-</sup>, presented with an aggravated form of Lyme carditis upon infection with the spirochete *Borrelia burgdorferi*, which was most likely caused by an increased macrophage infiltration (Guerau-de-Arellano, Alroy, Bullard, & Huber, 2005; H. Wu et al., 2004). Thus, CD11c seem to be crucial for the clearance of some bacterial infection. It was indeed reported that CD11c is important for the adherence of neutrophils and monocytes to stimulated endothelium cells, and for the phagocytosis of complement coated material (Lu et al., 2016).

CD11d<sup>-/-</sup> mice present with reduced CD3 and CD28 lymphocyte marker expression, and a disrupted ratio of CD4<sup>+</sup> to CD8<sup>+</sup> T cells, possibly caused by lack of CD11d expression in the thymus that resulted in an inaccurate T cell development. On a functional level, CD11d deficient

mice failed to convey an immune response against staphylococcal enterotoxin (H. Wu et al., 2004).

Even though, all four  $\beta 2$  integrins specialize in particular functions, there are processes to which all of them contribute, such as adhesion to inflamed endothelium and migration of the leukocytes. Since deficiency of any alpha subunit phenotypically did not resemble ablation of the CD18 beta chain, most likely some  $\beta 2$  integrins can compensate for the lack of others (Engelhardt, 2008; Gower et al., 2011; Lo, Van Seventer, Levin, & Wright, 1989; Walling & Kim, 2018). Figure 9 summarizes leukocyte expression, ligand-specificity and function of individual  $\beta 2$  integrins.

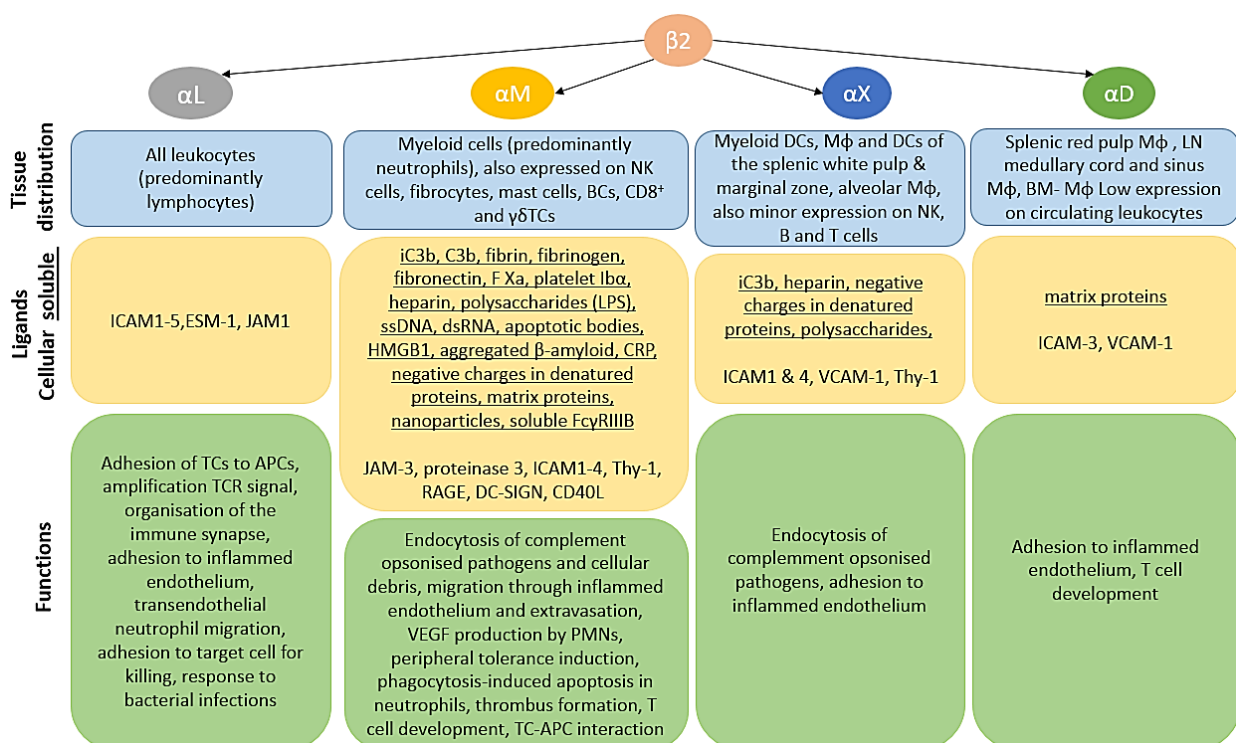


Figure 9.  $\beta 2$  integrins: distribution, ligands and function.

### 1.3.3. Clinical relevance of $\beta 2$ integrins

#### 1.3.3.1. The role of $\beta 2$ integrins in cancer

Even though tumorigenesis susceptibility has not been described in patients suffering from leukocyte adhesion deficiency (LAD) syndrome, there is a body of literature showing that individual  $\beta 2$  integrins play a role in cancer development. Several studies have shown that expression of  $\beta 2$  integrins or its absence serves either in favour or against tumour development.

Integrins mediate interaction of leukocytes with another cells, such as distinct WBCs, endothelium or tumour cells, and with extracellular matrix. Their adhesive properties have been controversially described in the context of tumour growth control. In case of CD11a/CD18 it has been shown that on one hand, it is an essential modulator of the immunological synapse between a NK cell or T lymphocyte and a cancer cell. Hence it is responsible for both adhesion and targeted release of the cytotoxic granules that kill the tumour cell (Anikeeva et al., 2005; M. Zhang, March, Lane, & Long, 2014). On the other hand, the same adhesion process may be of a disadvantage as it has been reported that LFA-1 and Mac-1 mediate adhesion of polymorphonuclear neutrophils (PMNs) to both epithelium and ICAM-1-expressing melanoma cells, allowing a tandem migration of tumour cells and their extravasation (Fu et al., 2011; S. Liang, Slattery, & Dong, 2005). Thus, binding of an integrin to its ligand expressed on the tumour cell may lead both to eradication of the tumour or to its metastasis.

Integrin-mediated migration of leukocytes, especially CD18/CD11b, is a process that, interestingly, has mostly been described as supportive for the tumour growth. Immunohistochemical analysis of the human gastric tumour tissues revealed, that most tumour infiltrating CD11b<sup>+</sup> cell were as well CD11c<sup>+</sup> and that high infiltration of these cells positively correlated with tumour size, venous invasion, lymph node metastasis, general metastasis stage and FoxP3<sup>+</sup> cell infiltration. Patients with high CD11b<sup>+</sup> cell tumour- infiltration had therefore a poorer surgical outcome (Okita et al., 2014). It remains unclear, however, whether CD11b or CD11c expression merely is a marker for immunosuppressive myeloid cells within the tumour microenvironment or whether these molecules are functionally relevant in this context. Following the topic, Zhang and colleagues (Q. Q. Zhang et al., 2015) published that CD11b deficiency in mice led to a reduced infiltration of spontaneous intestinal adenoma with myeloid cells, which resulted with inactivated Wnt/ $\beta$ -catenin pathway and suppression of tumour growth. Knock-out or blockage of CD11b has as well been shown to suppress melanoma growth in mice, thus suggesting a functional relevance of CD11b for tumour progression. The authors reported further that in the CD11b<sup>-/-</sup> mice, leukocytes enriched only in the area around melanoma and that macrophages treated with a gadolinium chloride (a potent macrophage inhibitor that suppresses CD11b expression) increased expression of pro-inflammatory cytokines and in consequence stimulated CD4<sup>+</sup> T cell to secretion of IL-17, which suppresses tumour. Impairment of leukocyte migration resulting from blockage or ablation of integrins has as well been shown to correlate with an improved outcome of the tumour irradiation. A systemic application of CD11b monoclonal antibodies or partial ablation of CD18

(CD18hypomorphism) increased the antitumor response after radiation in mice, as the myeloid cells could not migrate to the site to restore the vasculature (Ahn et al., 2010).

A study conveyed by Soloviev and colleagues in the field of tumour angiogenesis has shown that not only migration but as well VEGF secretion is orchestrated by integrins and influences tumour fate. As reported, CD11b, but not CD11a, deficiency in mice led to a decrease in the tumour neovascularisation in both B16F10 melanoma and RM1 prostate cancer model in mice. A reason for this, as authors described, is an impaired infiltration of tumour tissue with PMNs and macrophages, which secrete VEGF needed for vessel development. In addition, the CD11b<sup>-/-</sup> PMNs presented themselves with a markedly reduced degranulation and VEGF secretion upon TNF- $\alpha$  stimulation (Hamalainen, Solovieva, Vehmas, Leino-Arjas, & Hirvonen, 2014).

Apart from leukocyte adhesion, migration, and vascularisation it was noted that  $\beta$ 2 integrin mechanistically influence endocytosis and subsequent immune signalling involved in immune response against a cancer. Spriell and colleagues published data showing that Mac-1 is essential for Fc-receptor engagement in order to convey an antibody mediated anti-tumour response in a murine melanoma model. CD11b<sup>-/-</sup> mice were less protected upon antibody application and developed significantly more lung metastasis (van Spriell, van Ojik, Bakker, Jansen, & van de Winkel, 2003). Thus, endocytosis of the tumour derived debris and an immunological response to it are both regulated by  $\beta$ 2 integrin.

The expression of  $\beta$ 2 integrins has a different relevance when a leukocyte itself becomes a cancer cell, like in chronic lymphatic leukemia (CLL). In CLL the overall CD18 expression in comparison to the healthy cell is lower and an impaired CD18 variant (glutamate to lysin E630K change) has recently been described to positively correlate with disease susceptibility (Goldin et al., 2016). Furthermore, in CLL the adhesion of the cell over LFA-1 is disturbed as the inside-out signalling involving Rap1 GTPase is defective and hence clonal mature B cells retain in the blood being almost completely non-functional (Hartmann et al., 2009; Till et al., 2008). In contrast to CLL that characterises with a decreased expression of the  $\beta$ 2 integrin, some tumour cell lines, like epithelial ovarian cancer (EOC), can express Mac-1 de novo (Saed et al., 2018). However, the consequences of it for the tumour fate have not yet been elucidated.

Taken together, there is obviously a link between different  $\beta$ 2 integrins and tumour development of hematopoietic and non-hematopoietic origin. The role of  $\beta$ 2 integrin in various malignancies is summarized in Table 1. In general, leukocytic tumour infiltration, mediated by LFA-1 and Mac-1, appears to be supporting growth of an established tumour that already

communicates with an environment in order to induce tolerance. Even though  $\beta 2$  integrins are required for the humoral response against the tumour, at the same time their pro-tolerogenic behaviour may facilitate the immunoevasion of a cancer. An in depth understanding of the  $\beta 2$  integrin role in the tumour microenvironment may allow development of new therapeutic strategies.

Table 1. The role of  $\beta 2$  integrins in tumorigenesis.

Integrin subunit	Cell type	Species	Tumour model	Details	Reference
CD18	S100A8+ cells (myeloid cells)	m	Lewis lung carcinoma (LLC) and MC38 colon adenocarcinoma	Tumours growing in CD18 hypomorphic, but not CD11b deficient mice were more sensitive to irradiation in comparison to the WT	(Ahn et al., 2010)
	B cell	h	Chronic lymphatic leukemia (CLL)	An impaired CD18 variant (E630K) positively correlates with CLL susceptibility	(Goldin et al., 2016)
CD11a	NK, TC	h	n/a	Establishment of an intercellular synapse with cancer cell and targeted granules release relay on LFA-1	(Anikeeva et al., 2005; M. Zhang et al., 2014)
	B cell	h	Chronic lymphatic leukemia (CLL)	Impaired CLL cell motility and accumulation in the blood due to defective Rap-1 GTPase signaling	(Hartmann et al., 2009; Till et al., 2008)
CD11a CD11b	PMN	m	Melanoma	ICAM-1 expressing melanoma cells bind PMNs via LFA-1 and Mac-1 and thus are carried across the vasculature to form metastasis	(S. Liang et al., 2005)
CD11b	PMN	m	B16F10 Melanoma, RM1 prostate cancer	PMNs fail to infiltrate tumour tissue and secrete VEGF needed for the neovascularisation	(Hamalainen et al., 2014)
		m	spontaneous intestinal adenoma	CD11b <sup>-/-</sup> myeloid cells fail to infiltrate tumour mass, which results in suppression of tumour growth and inactivation of Wnt/ $\beta$ -catenin pathway in the tumour	(Q. Q. Zhang et al., 2015)
		m	Squamous cell carcinoma xenografts	Systemic application of CD11b monoclonal antibodies increased the antitumor response after radiation	(Ahn et al., 2010)
		h	Gastric cancer	Strong CD11b <sup>+</sup> cell infiltration positively correlated with tumour size, venous invasion, lymph node	(Okita et al., 2014)

				metastasis, general metastasis stage and FoxP3 <sup>+</sup> cell infiltration	
		h	epithelial ovarian cancer (EOC)	Novel expression of CD11b on epithelial ovarian cancer (EOC) cell lines	(Saed et al., 2018)
		m	Melanoma	Mac-1 is essential for the antibody-mediated antitumor response	(van Spriël et al., 2003)
CD11c	APC	h	Gastric cancer	CD11c <sup>+</sup> cell tumour infiltration positively correlated with tumour size.	(Okita et al., 2014)
CD11d	Mφ	m		CD11b upregulation leads to an excessive adhesion at the inflammation site and chronification of inflammation.	(Aziz et al., 2017)

### 1.3.3.2. *The role of $\beta$ 2 integrins in autoimmune diseases*

A growing body of research suggests that  $\beta$ 2 integrins play an important role in tolerance induction and suppression of inflammation. Integrin-dependent migration of leukocytes towards inflamed tissue, ligand binding and the following signalling modulate the immune response. Decades ago, it has already been noted that LAD-1 patients with complete absence of  $\beta$ 2 integrins suffer not only from bacterial infections, but as well from renal or intestinal autoimmune diseases, and some of them presented with type 1 diabetes (T1D) or autoimmune cytopenia after haematopoietic stem cell transplantation (HSCT) (D'Agata, Paradis, Chad, Bonny, & Seidman, 1996; De Rose et al., 2018; Uzel, Kleiner, Kuhns, & Holland, 2001). Likewise, a mouse model of LAD-1, a CD18<sup>-/-</sup> mouse, demonstrated with chronic dermatitis and splenomegaly, which indicates a circulating systemic inflammation (Scharffetter-Kochanek et al., 1998; Wilson et al., 1993).

In case of the LFA-1, the evidence so far suggests that CD11a expressed on T cells can exert both pro- and anti-inflammatory effects. Apart from the crucial role in transmigration, CD11a stabilizes the connection of the T cell to APC and thus strengthens TCR- signalling acting pro-inflammatory (Van Seventer, Shimizu, Horgan, & Shaw, 1990; Varga et al., 2010). A Transfer of encephalitogenic CD11a<sup>-/-</sup> T cells to WT mice reduced the severity of the EAE, which means that T cell needs CD11a to get primed and to mediate an inflammatory response (Dugger, Zinn, Weaver, Bullard, & Barnum, 2009). On the contrary, a CD11a-deficient mouse presented with a reduced Treg fraction in the CNS, which facilitated disease development and increased its severity (Gultner et al., 2010). Indeed, the expression of CD18 was found to be crucial for the

development of the regulatory T cell in the mouse (Marski, Kandula, Turner, & Abraham, 2005). Thus, a transfer of encephalogenic WT T cells to CD11a knockout mice led unsurprisingly to a fatal course of the EAE (Dugger et al., 2009).

Apart from EAE, CD11a has been studied in the context of other autoimmune manifestations. An elevated expression of CD11a on T cell was shown to positively correlate with the activity of systemic sclerosis, systemic lupus erythematosus (SLE), rheumatoid arthritis (RA) and autoimmune thrombocytopenia (Y. X. Liu et al., 2015; Singh, Colmegna, He, Weyand, & Goronzy, 2008; Y. Wang et al., 2014; Watts et al., 2005; Zhao et al., 2010). Moreover, a blockade of CD11a with Efalizumab was used in treatment of psoriasis as it suppresses T cell responsiveness (Guttman-Yassky et al., 2008). Unfortunately, the drug had to be withdrawn from the market since it caused reactivation of the JC virus and subsequent progressive multifocal leukoencephalopathy (PML) in patients.

In contrast to CD11a, which mostly exerts its pro- and anti-inflammatory effects on lymphoid cells, CD11b was described to act predominantly on the myeloid cell lineage with few exemptions. In general, CD11b was shown to maintain peripheral tolerance. It suppressed IL-6 secretion and subsequent Th17 differentiation in the model of orally induced tolerance in mouse (Ehirchiou et al., 2007; Stevanin et al., 2017). Furthermore, CD11b maintained autoreactive B cell tolerance via negative BCR signalling and a CD11b<sup>+</sup> B cells could in addition suppress TCR signalling in murine experimental autoimmune hepatitis (Ding et al., 2013; X. Liu et al., 2015).

Meta-analysis of ITGAM (CD11b) gene polymorphisms, which place CD11b in an inactive state, revealed a significant correlation to development of SLE and RA in various ethnical communities (Fan et al., 2011; Lee & Bae, 2015). There are three common CD11b SNPs that translate into miss-sense mutations (P1146S, R77H, A858V) and are responsible for SLE pathogenesis and its common complication: lupus nephritis (Fagerholm, MacPherson, James, Sevier-Guy, & Lau, 2013; Toller-Kawahisa et al., 2014). In murine collagen induced arthritis (CIA) model, deletion of CD11b induced early disease onset and increased the severity of CIA via excessive IL-6 secretion and subsequent Th17 polarization of lymphocytes. Moreover, CIA severity in CD11b<sup>-/-</sup> mice could be rescued with an adoptive WT DC transfer (Stevanin et al., 2017). The role of CD11b on dendritic cells has further been examined in an EAE model. It was shown that WT mice injected i.v. with an autoantigen peptide of myelin oligodendrocyte glycoprotein (MOG) prior to immunization developed a less severe form of EAE as compared to CD11b<sup>-/-</sup>. Here CD11b<sup>+</sup>CD11c<sup>+</sup> dendritic cells of the immunized mice accumulated in the

CNS and presented *ex vivo* with a tolerogenic signature secreting IL-10 and TGF- $\beta$ . Furthermore, adoptive transfer of those DC led to reduced EAE pathology (H. Li et al., 2008). Interestingly, CD11b expressed on T lymphocytes presented an opposing effect as compared to CD11b expressing APC in the pathogenesis of EAE. It was reported that WT T cells were required for the complete EAE manifestation, as transfer of antigen restimulated T cells derived from CD11b<sup>-/-</sup> mouse produced significantly reduced EAE symptoms (Bullard et al., 2005). Hence, CD11b may exert opposing immunological effects depending on the leukocyte subset it is expressed on.

Mac-1 may furthermore support the inflammatory process by interacting with human Fc receptor, amplifying its signalling, as well as by facilitating migration of the leukocytes to the site of inflammation. It has long been established that CD11b physically interacts with human Fc $\gamma$  receptors (Fc $\gamma$ IIA, Fc $\gamma$ IIIB) expressed by neutrophils, thereby strengthening Fc receptor mediated calcium signalling, reactive oxygen species production, antibody-mediated phagocytosis and release of pro-inflammatory cytokines (Galon et al., 1996; Kindzelskii, Yang, Nabel, Todd, & Petty, 2000; Krauss et al., 1994; Ortiz-Stern & Rosales, 2003; Sehgal, Zhang, Todd, Boxer, & Petty, 1993; Stockl et al., 1995). In a humanized SLE model, where mice express human Fc $\gamma$ RIIA, CD11b deficiency protected the mice from lupus nephritis that normally develops as a consequence of injection with human SLE sera (Rosetti et al., 2012). Murine Fc $\gamma$ RIII and Fc $\gamma$ RIV (corresponding to human Fc $\gamma$ RIIIB and Fc $\gamma$ RIIA), on the other hand, do not require Mac-1 to regulate the FcR function (T. Tang et al., 1997). Nevertheless, murine Fc $\gamma$ R engagement with IgG opsonized particles led to an activation and accumulation of Mac-1 in the phagocytic cup, which affected the phagocytosis efficiency (Jongstra-Bilen, Harrison, & Grinstein, 2003).

Another way CD11b contributes to inflammation is via control of leukocyte migration. In the late '90s, flow cytometric studies on psoriatic lesions revealed an increased accumulation of CD11b<sup>+</sup> cells (van Pelt, Kuijpers, van de Kerkhof, & de Jong, 1998). Furthermore, expression of CD11b on granulocytes and monocytes derived from patients suffering from pustular psoriasis was significantly elevated in comparison to cells derived from psoriasis vulgaris patients or healthy donors (Sjogren, Ljunghusen, Baas, Coble, & Stendahl, 1999). Consequently, Cao and colleagues suggested that lesional activity of CD11b<sup>+</sup> cells (i.e. their MPO secretion level) may as well be used as a severity score scheme alongside with psoriasis area and severity index (PASI), since it correlated with blood myeloperoxidase (MPO) activity (a biomarker for systemic inflammation) (Cao et al., 2013). A similar finding was obtained in another autoimmune blistering skin disease Bullous pemphigoid (BP), which is mediated by

autoantibodies reactive to hemidesmosomes of basal keratinocytes (an IgG-mediated inflammation model). Here, CD11b<sup>+</sup> cell accumulated in the skin at early time points of the inflammation process. The development of the disease in mice injected with a hemidesmosome antigen (BP180) was significantly decreased in the Mac-1 deficient mice as compared with WT controls, since CD11b<sup>-/-</sup> neutrophils could not infiltrate the tissue (Z. Liu, Zhao, Li, Diaz, & Mayadas, 2006).

Taken together, CD11b seems to act as a double edged sword in the pathogenesis of autoimmunity. On one hand it allows the cell to migrate and start up the inflammation, on the other hand it exerts a control over the immune response and induces tolerance. The control over immune response is presumably managed via regulation of antigen presentation (Varga et al., 2007). Tolerogenic function of CD11b has recently been addressed in a therapeutic context. A newly developed drug, Leukadherin-1 (LA-1), which activates CD11b was shown to suppresses the SLE progression in mice (Faridi et al., 2017)

There is not much evidence for a direct role of the CD11c or CD11d alone in any autoimmune disease model. Sharing many similarities with Mac-1, CD11c is involved in cell migration, phagocytosis and cytokine production, all of which are essential for a proper immune reaction. It has been noted that iC3b binding site on the CD11c was required for the induction of the delayed type hypersensitivity (Sadhu et al., 2007) and that cholesterol accumulation in CD11c<sup>+</sup> cells leads to lymphocyte stimulation and production of autoantibodies (Ito et al., 2016). Induction of tolerance was, however, no yet discussed as a direct, CD11c-dependent process. Given that, it seems that CD11c on its own exerts a rather pro-inflammatory function. Likewise, in case of CD11d it was reported that pro-inflammatory macrophages and white adipose tissue upregulate the expression of the CD11d and therefore contribute to chronification of the inflammation (Thomas, Dunn, Oort, Grino, & Adams, 2011) (Aziz et al., 2017). It has been noted in addition that activation of CD11d leads to an increased IL-1 $\beta$  expression (Miyazaki et al., 2014), which indicates that CD11d expression may contribute to the systemic inflammation or inflammasome activation (Dinarello, 2011).

To sum up, all four  $\beta$ 2 integrins contribute to inflammation. CD11a and CD11b have been extensively studied in various autoimmune models like EAE, SLE or CIA and contribute to the inflammatory bursts in various ways (supporting cell migration, autoantigen uptake, subsequent signalling and antigen presentation to T lymphocytes). Among all  $\beta$ 2 integrins, only CD11b was assigned an important role in the control of inflammation and induction of tolerance. CD11c and CD11d were less well explored in an autoimmune setting so far. The role of individual  $\beta$ 2 integrins in the different autoimmune diseases is summarized in Table 2. A more

in depth analysis of the mechanisms underlying the pathology in autoimmunity involving integrins may lead to development of new alternative therapies for auto-inflammation.

*Table 2.  $\beta 2$  Integrins and their role in autoimmune diseases.*

<b>Integrin subunit</b>	<b>Cell type</b>	<b>Species</b>	<b>Disease/state of immune system</b>	<b>Details</b>	<b>Reference</b>
CD18		h	LAD	LAD patients suffer from intestinal colitis, periodontitis, Type1 Diabetes, autoimmune cytopenia	(D'Agata et al., 1996; De Rose et al., 2018; Hajishengallis & Moutsopoulos, 2016; Uzel et al., 2001)
		m	LAD	chronic dermatitis and splenomegaly	(Scharffetter-Kochanek et al., 1998; Wilson et al., 1993)
CD11a	TC	m	EAE	Pro and anti-inflammatory function	(Dugger et al., 2009; Gultner et al., 2010)
	TC	h	Systemic sclerosis	Overexpression positively correlates with disease activity	(Y. Wang et al., 2014)
	TC	h	Psoriasis	Blockade with Efalizumab induces T cell hyporesponsiveness and reduces psoriasis severity	(Guttman-Yassky et al., 2008)
	TC	h	Autoimmune thrombocytopenia	High expression positively correlates with autoimmune thrombocytopenia pathogenesis	(Y. X. Liu et al., 2015)
	TC	h	SLE	High expression positively correlates with SLE severity	(Zhao et al., 2010)
	TC	h	RA	High expression positively correlates with RA pathogenesis	(Singh et al., 2008)
		m		Expression is essential for CIA development	(Watts et al., 2005)
CD11b	DC	m	RA	Controls balance between Th17 and Treg via IL-6	(Stevanin et al., 2017)
	APC	m	Peripheral tolerance	Plays central role in establishment of orally induced peripheral tolerance via IL-6 secretion control and Th17 suppression	(Ehreichiou et al., 2007)
		h	RA, SLE	Polymorphisms are associated with SLE and RA	(Fagerholm et al., 2013; Fan et al., 2011; Lee & Bae, 2015)
		m	SLE	Activation suppresses autoimmunity	(Faridi et al., 2017)
	DC	m	EAE	CD11b <sup>+</sup> DC of MOG immunized mice accumulate in CNS and	(H. Li et al., 2008)

				present with a tolerogenic signature (IL-10 and TGF- $\beta$ secretion)	
	TC	m		Encephalogenic T cells from a CD11b <sup>+</sup> mouse are required for the EAE development	(Bullard et al., 2005)
	BC	m	Experimental autoimmune hepatitis	CD11b expressing BC suppress T cell response by TCR signalling downregulation	(X. Liu et al., 2015)
		h	Psoriasis	Frequency of CD11b <sup>+</sup> cells in the lesion correlates with MPO activity. CD11b expression is elevated on granulocytes and macrophages in pustular psoriasis.	(Cao et al., 2013; Sjogren et al., 1999; van Pelt et al., 1998)
	Neutrophil	m	Bullous pemphigoid	CD11b is required for the initial skin infiltration by neutrophils and inflammation development in anti-BP180 Ab injected mice	(Z. Liu et al., 2006)
CD11c	DC	m	Autoantibody production	Cholesterol accumulation in CD11c <sup>+</sup> cell contributes to autoimmune processes	(Ito et al., 2016)
CD11d		m/h	Obesity	CD11b expression is elevated in the white adipose tissue of obese mouse or humans	(Thomas et al., 2011)

## 2. Results

### 2.1. Generation of the CD18<sup>fl/fl</sup> mouse

#### 2.1.1. Recombination strategy for the generation of the CD18<sup>fl/fl</sup> mouse

Generation of the CD18<sup>fl/fl</sup> mouse involved two rounds of recombination. First homologous recombination took place on the level of an embryonic stem cell, in an *in vitro* cell culture. Therefore, embryonic stem cells (JM8) were electroporated with a linearized BO44.2 vector bearing a targeting construct based on the LoxP-FRT-neo-FRT-loxP cassette. This cassette targeted the murine CD18 gene and flanked exon 3 with loxP sites in order to achieve a conditionally inactive CD18 allele. The targeting vector recombined with the ES-cell CD18 gene locus via the vectors arms of homology (a short arm on the 5' site and a long arm on the 3' site), and thus a recombined ES-cell with an integrated targeting construct was generated and subsequently injected into a blastocyst of a recipient B6-Albino mouse. Since the targeting construct carried a Neomycin resistance gene, which was used both for the positive ES-clone selection and screening of mice generated from chimeric germline, the Neo-positive chimeric offspring was further crossed with a FLP deleter mouse in order to achieve a site-directed recombination, in which the recombinase flippase (Flp) cut between two short flippase (Flp) recognition targets (FRT) and excised the Neomycin resistance gene.

As a consequence of homologous ES-recombination and subsequent Flp-mediated recombination, a mouse with a floxed CD18 gene 3-(loxP-CD18 exon FRT-loxP) was generated. The recombination strategy is depicted in Figure 10. As such, the mouse resembled a WT phenotype and only once it's crossed with a Cre recombinase expressing mouse, a cell specific knock-out is obtained. Cre recombinase-mediated recombination, analogous to FRT-FLP recombination, is a site directed recombination, in which the DNA fragment between the loxP site is excised in cell type specific manner.

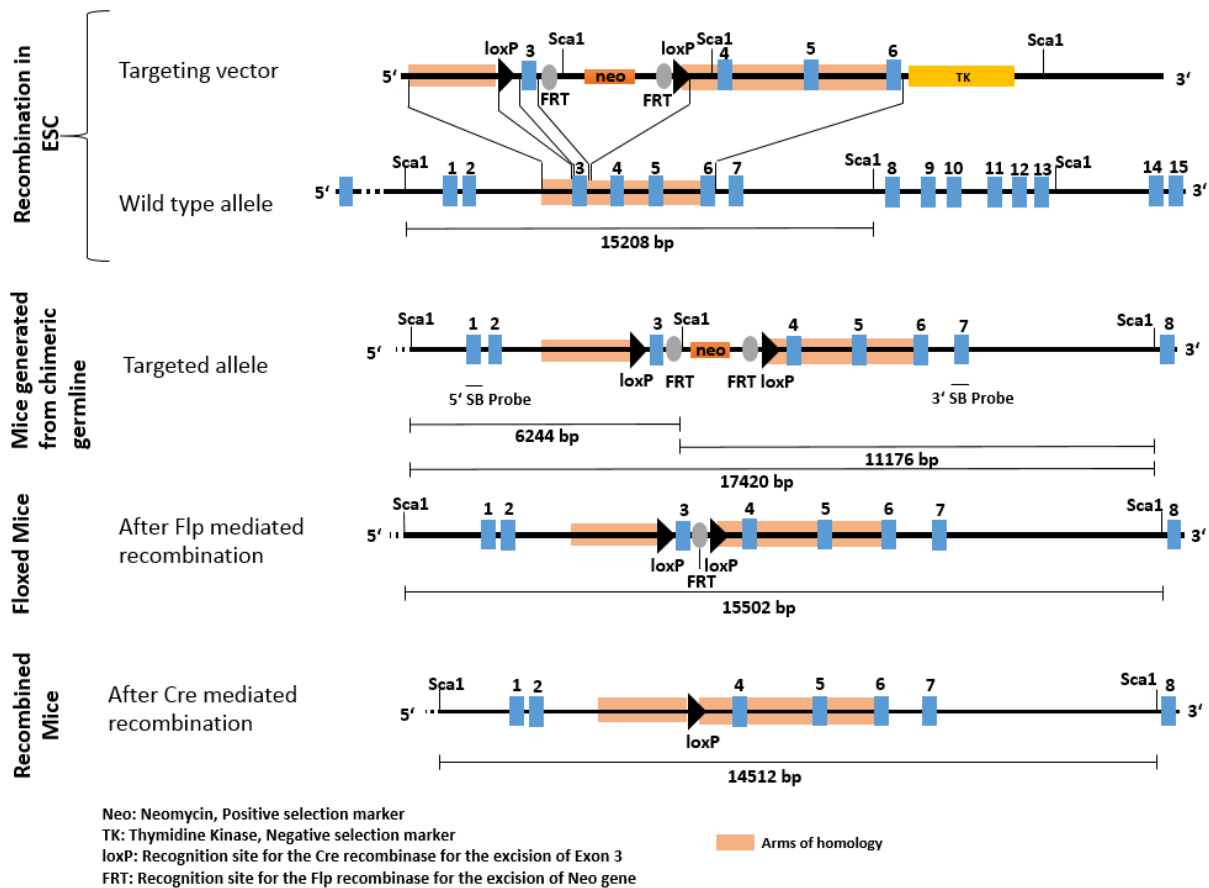


Figure 10. Recombination strategy for the generation of CD18<sup>fl/fl</sup> mouse.

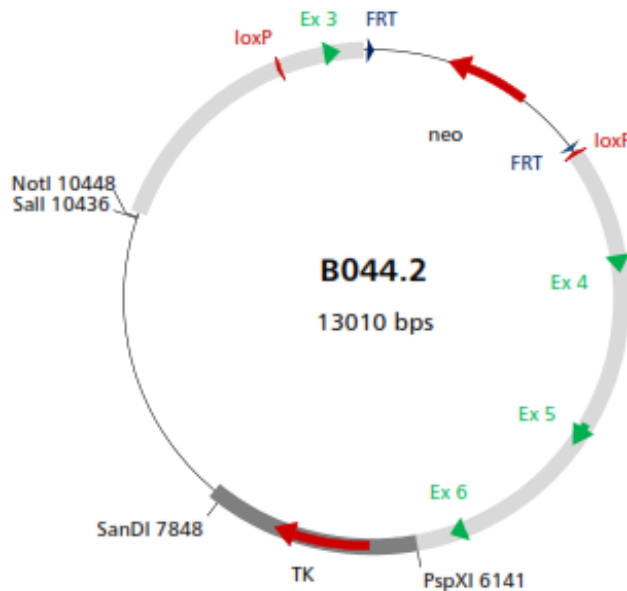
Targeting vector encoded CD18 exon 3 flanked by loxP sites and long arms of homology, over which it recombined with the WT embryonic stem cell DNA. The floxing cassette contained as well a Neomycin resistance gene that facilitated selection of the recombined embryonic stem cells. After Flp mediated recombination, the Neomycin cassette was excised from the genome, and subsequent Cre mediated recombination deleted CD18 exon 3, leading to a complete CD18 deletion in the specific cell type (determined by the Cre-recombinase expression).

### 2.1.2. Recombination of the BO44.2 vector with murine embryonic stem cells (JM8)

The BO44.2 vector, targeting the CD18 exon 3 with a loxP-FRT-neo-FRT-loxP construct, was customized by PolyGene Transgenetics (Rümlang, Switzerland). It is a 13.010bp plasmid. The targeting construct is flanked by 5' short and 3' long arm of homology, the latter containing CD18 exon 4, 5 and 6 sequence. The plasmid vector design along with its restriction digest products (adopted from the PolyGene Transgenetics vector report) is shown in Figure 11 below. Although the vector harbours a TK- counter selection cassette in addition to the Neo-cassette,

the former was not used here to yield resistant clones. Recombined embryonic stem cell clones were selected only upon G418 resistance. Appendix A contains detailed sequence data of the plasmid along with customer vector information.

A



B

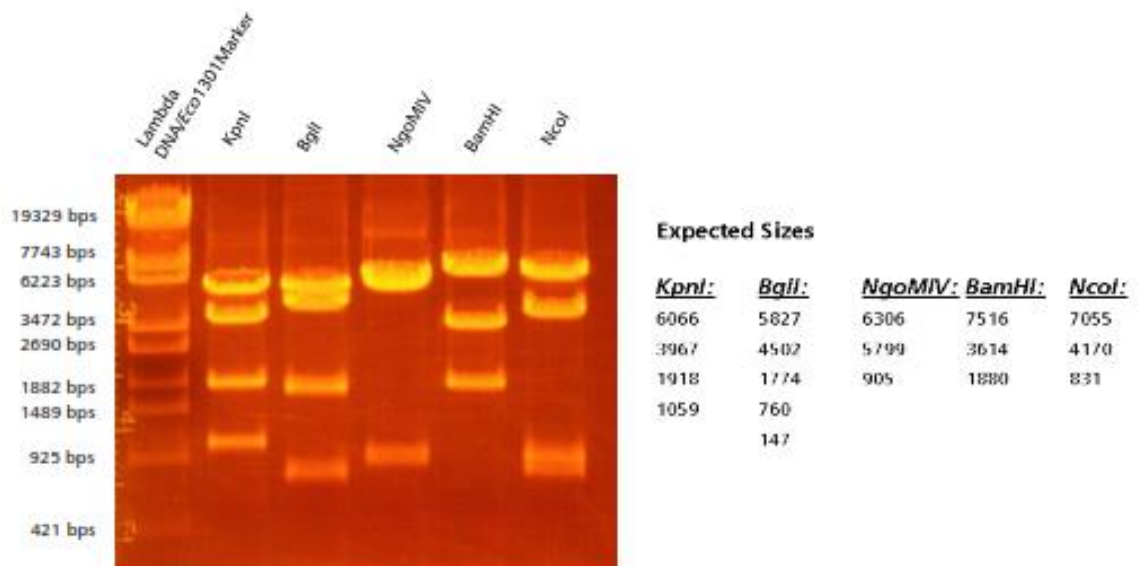


Figure 11. B044.2 vector construct.

A 13.010bp long vector was customized by Polygene. It contained CD18 exon 3-6 and long arms of homology. Exon 3 along with the Neo-cassette found between two FLP sites were flanked by loxP sites. NotI and SalI restriction sites were cloned in to linearize the vector prior

to electroporation (A). Restriction digests of the vector, carried out at Polygene, confirm the integrity of the product (B). Both figures are adopted from Polygene.

The BO44.2 plasmid was successfully amplified with SURE competent cells (Agilent technologies) and purified with QIAprep®Spin Midiprep Kit. Subsequently, the integrity of the isolated plasmid was controlled with restriction digests using *Not1+Sal1*, *BamHI* and *KpN1* (Fig.12). Restriction digests yielded products of expected sizes. A *Not1/Sal1* double-digest produced a 13kb linearized fragment due to the close proximity of both restriction sites. *BamHI* produced a 7.516bp, 3.614bp and 1.880 bp fragment. *Kpn1* yielded a 6.066bp, 3.967bp, 1.918bp and 1.059bp fragment. In case of both *BamHI* and *KpN1* digests there was a weak 13kb band of undigested plasmid visible, most likely a coiled form in case of *KpN1*, and both coiled and super-coiled form in case of *BamHI*. The undigested plasmid yielded two bands on the gel, which resembled a relaxed and a coiled form of the plasmid. The relaxed plasmid form tends to run higher than at the expected size and the coiled form migrates further than the expected size as it is more compact than when linearized.

The *Not1+Sal1* double-digested BO44.2 was extracted from the gel (QIAquick® Gel Extraction Kit) and the integrity was evaluated by an agarose gel electrophoresis (Fig.12). Twenty five micrograms of the gel-purified vector DNA were dissolved in 200µl of PBS and used for the electroporation of embryonic stem cells (clone JM8).

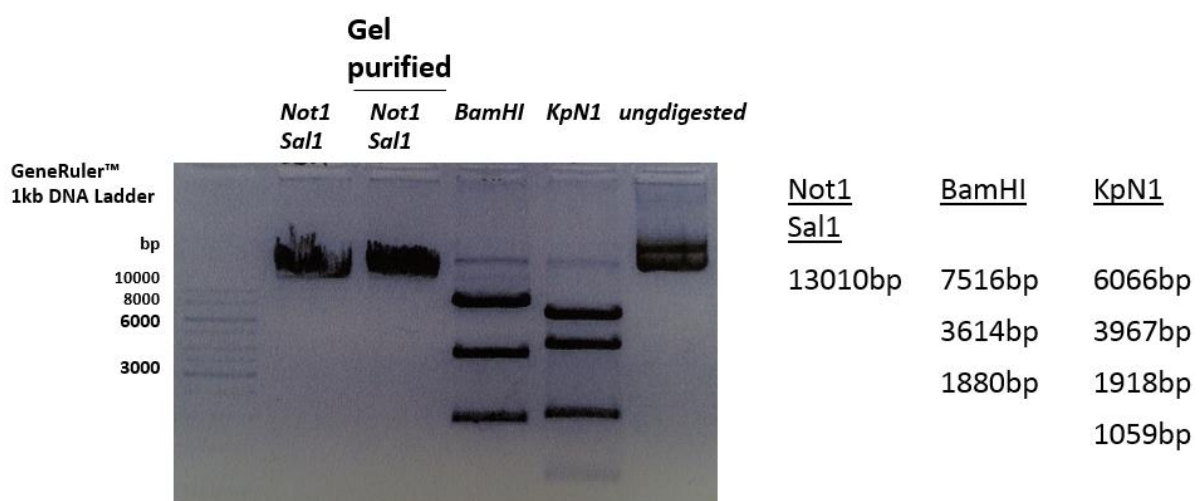


Figure 12. Restriction digest of the BO44.2 vector.

*Not1/Sal1* digest produced a 13kb linearized fragment. *BamHI* produced a 7516bp, 3614bp and 1880 bp fragment. *Kpn1* yielded a 6066bp, 3967bp, 1918bp and 1059bp fragment. A weak 13kb

*band of an undigested plasmid was visible in BamHI and KpnI digests. Undigested plasmid was seen in its coiled and supercoiled form.*

### 2.1.3. Selection of two recombinant ES-clones P1-9F and P3-10G

Embryonic stem cells (JM8) were electroporated with linearized BO44.2 vector and cultured further in media containing a G418 antibiotic to select embryonic cells that integrated vector DNA containing G418 resistance gene. Subsequently, grown colonies were picked and expanded individually. The recombined clones were screened using a Southern Blot method.

#### 2.1.3.1. Establishment of Southern Blot screening strategy

Southern Blot is a molecular biology method that allows detection of a specific DNA sequence using a radio-labelled probe that may hybridise with it. Since it is highly specific and less error prone than a PCR, it was applied to screen for recombinant ES clones.

The loxP-FRT-neo-FRT-loxP cassette introduced an extra ScaI restriction site into genomic DNA, which was used to distinguish between the WT and a recombined ES-cell. The WT ES-cell carried a ScaI restriction site upstream CD18 exon 1 and between the 13<sup>th</sup> and 14<sup>th</sup> exon, whereas a recombined ES-cell genome carried an extra ScaI restriction site between FRT and Neo-cassette, i.e. between the 3<sup>rd</sup> and 4<sup>th</sup> exon. Thus, a ScaI restriction digest produced a single 15.208bp DNA fragment in case of the WT and two DNA fragments, 6.244bp and 11.176bp in length, in case of the recombined ES-cell. In order to detect these restriction digest products two Southern Blot probes were designed, one hybridising within the CD18 exon 1 region and another one hybridising within the CD18 exon 7 region (Fig.13). A probe overlapping the exon sequence had an increased specificity. Both probes were PCR-amplified using WT genomic DNA as a template (Fig.14), gel-purified and used for the synthesis of the <sup>32</sup>P-labelled probes. For every Southern Blot hybridisation a fresh probe was amplified with <sup>32</sup>P-dCTP, using 30ng of the gel-purified probe WT DNA as a template (TAKARA Ladderman Labelling Kit).

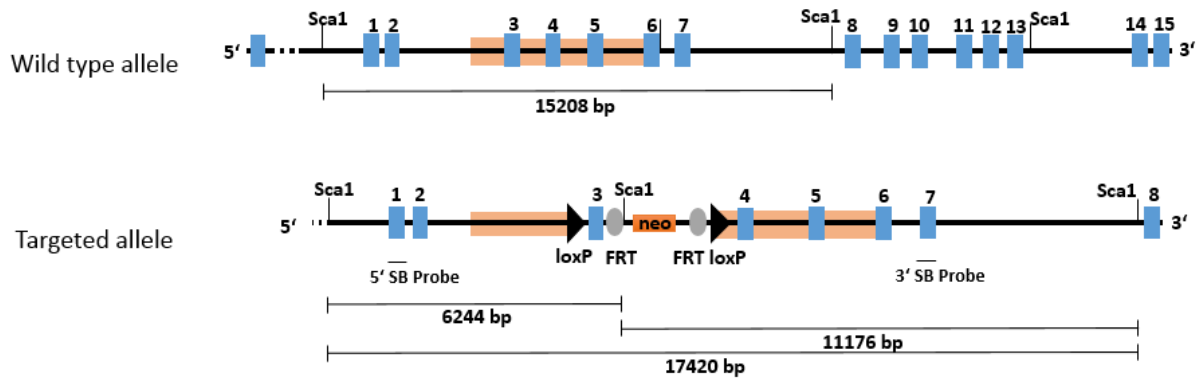


Figure 13. Location of Southern Blot probes on the WT and targeted allele.

One Southern Blot probe, overlapping CD18 exon1 bound to a 6244bp DNA fragment derived form a Sca-1 restriction digest. Second probe, overlapping CD18 exon7 bound to a 11176bp DNA fragment derived from a Sca-1 restriction digest. Both probes bound a 15208bp fragment produced after Sca1 digestion of the genomic DNA.

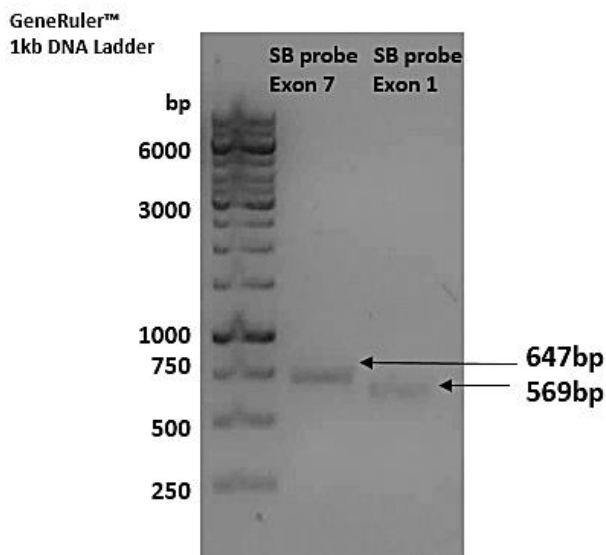


Figure 14. Amplified Southern Blot probes for the detection of the recombined CD18 allele.

Southern Blot probe overlapping CD18 exon7 was 647bp long and was amplified using the following set of primers: 5'ACACATGACAGCTGGGAAGA-3'and 5'-GTCACCAACAGCGAACAGTT '3. Southern Blot probe overlapping CD18 exon1 was 569bp long and was amplified using the following set of primers: 5'-CAGTCCCATCTCCACTCAG-3' and 5'-GGCACTCTTTGAAGCACCAA '3.

The Southern Blot was established first using a WT genomic DNA digested with Sca1. Digested DNA fragments were separated on a 0.8% agarose gel (Fig.15 upper panel) and transferred onto a Hybond N+ Membrane. The membrane-bound DNA was subsequently hybridised with radioactively labelled probes and exposed to Kodak MS Biomax film (Fig.15 lower panel). The localisation of the band present on the developed film was compared with the agarose gel picture to estimate the size of the DNA fragment, to which the probe hybridised to. Both designed probes (overlapping exon 1 and exon 7) hybridised to the 15kb DNA fragment derived from the Sca1 digest of the WT genomic DNA and hence both could be used for the Southern Blot screening. Screening of the complete recombinant ES-clone was carried out using a probe overlapping CD18 exon 1 only (5' Southern Blot probe).

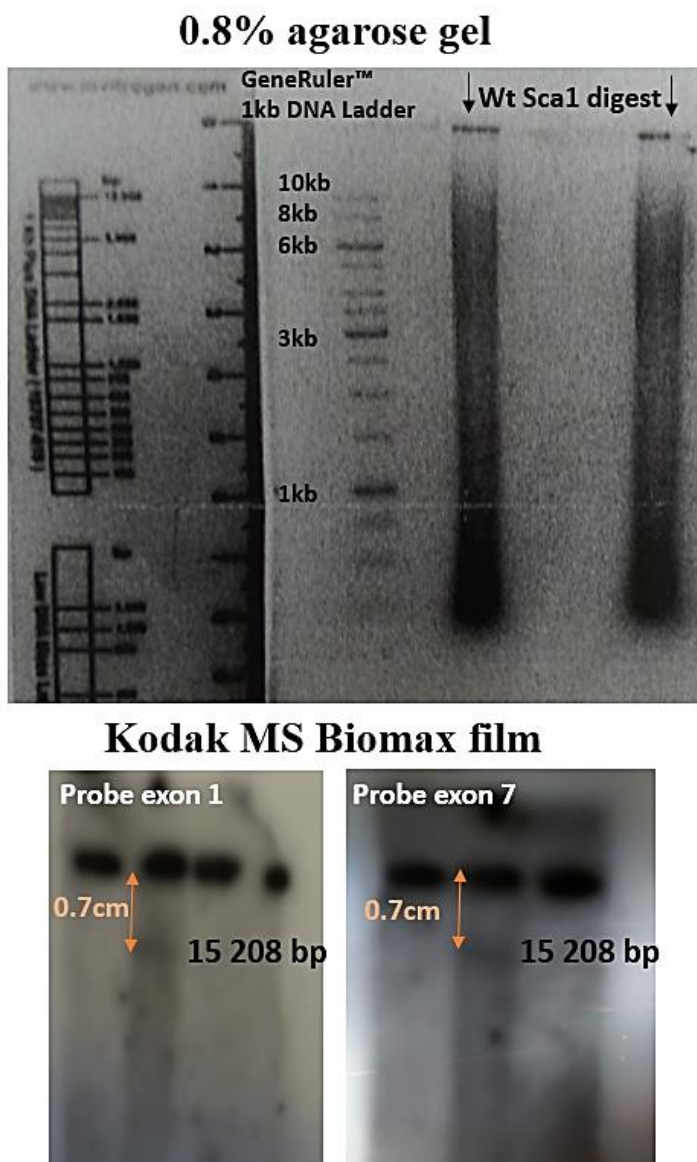


Figure 15. Southern Blot with probe overlapping CD18 exon 1 and exon 7.

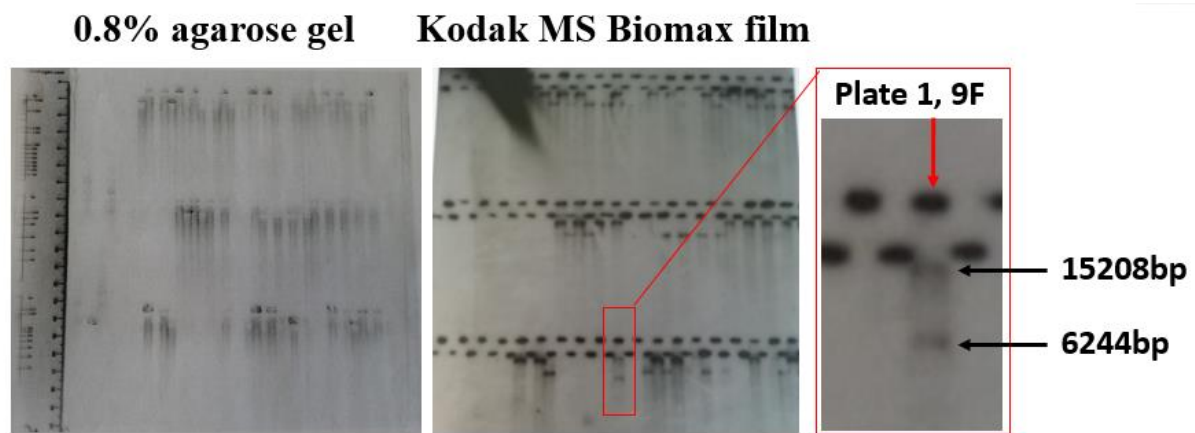
*Both Southern Blot probes were tested with WT genomic DNA prior to embryonic stem cell screening. ScaI digest of the WT genomic DNA run on a 0.8% agarose gel is presented in the upper panel, next to the 1kb DNA ladder is a centimetre ruler used to determine the position of the probe on the film. Kodak films with both probes bound to the WT 15kb fragment are shown in the lower panel.*

### *2.1.3.2. Screening for the recombinant ES-clones*

Once ES-cells transfected with linearized BO44.2 formed colonies, these were cherry-picked and expanded individually in 96-well format. As soon as clones were confluent, half of the cells was further cultured on gelatine coated 96-well plates and the remaining half was further expanded on the feeder cell layer under G418 selection and subsequently frozen at pluripotent state at -80°C in triplicates. This pluripotent ES-clone stock served as a source of recombinant ES-clones that would be expanded for the blastocyst injection. ES-clones cultured on the gelatine coated plates were used as a source of DNA for the Southern Blot screening. In this way the isolated DNA was not contaminated with non-recombinant feeder cell DNA. These ES-clones were cultured to their maximal confluency to ensure sufficient DNA amounts and frozen at -20°C prior to screening. Gelatine cultured ES-cells lost their pluripotency, due to the lack of the feeder cell layer. However, pluripotency was not required for the detection of the recombined genomic DNA.

Over 900 ES-clones were screened with the established Southern Blot strategy using the probe overlapping CD18 exon 1. For this, one 96-well gelatine plate was thawed at a time, cells were lysed and the DNA was digested with *ScaI*. All 96 restriction digests were run in parallel on an agarose gel and DNA was transferred onto a Hybond N+ Membrane, which was then hybridised with the <sup>32</sup>P-labelled probe. A single 15kb band indicated the presence of the WT allele, whereas a 6.2kb band indicated the presence of the targeted allele. Two ES clones (P1-9F and P3-10G, names encoding plate number and coordinates) presented with both bands, a 15kb for the WT and a 6.2 kb band for the targeted allele (Fig. 16). They were therefore recognized as heterozygous targeted clones, i.e. recombined ES-clones, where linearized targeting vector integrated by homologous recombination into one of the WT CD18 alleles.

A



B

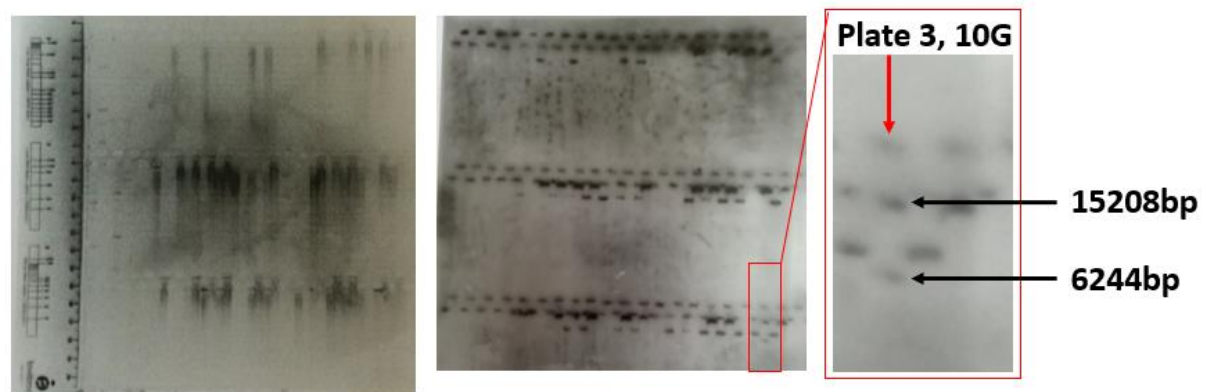


Figure 16. Detection of recombined ES-clones with Southern Blot.

Out of over 900 clones, 2 clones recombined. Clones used for the screening were cultured separately on the gelatine 96-well plates; one plate was screened at a time and clones carried the name that encrypted the number of the plate and location on the plate. Clones 1-9F (A) and 3-10G (B) presented with both 15kb band for the WT DNA and a 6kb recombined product. Agarose gel pictures (right) show *ScaI* DNA digest. Kodak film (right) shows, where the Southern Blot probe bound on the membrane with transferred DNA digest.

### 2.1.3.3. Expansion of the heterozygous targeted clones

The two identified, recombinant clones (P1-9F and P3-10G) were further expanded from the stock kept at  $-80^{\circ}\text{C}$ . Clones grown in the adjacent wells were expanded along with the recombinant clones, to ensure that the positive clone would not be lost in case of falsely determined clone location on the plate. Cells were cultured on a feeder cell layer to prevent the loss of pluripotency and were expanded from 96-well to a 10cm dish format. A minimum of  $10^7$  ES cells per clone was generated in the culture and stored in liquid nitrogen ( $10^6$  cells

/vial) for subsequent blastocyst injection. Both clones were re-screened with Southern Blot after expansion (Fig. 17).

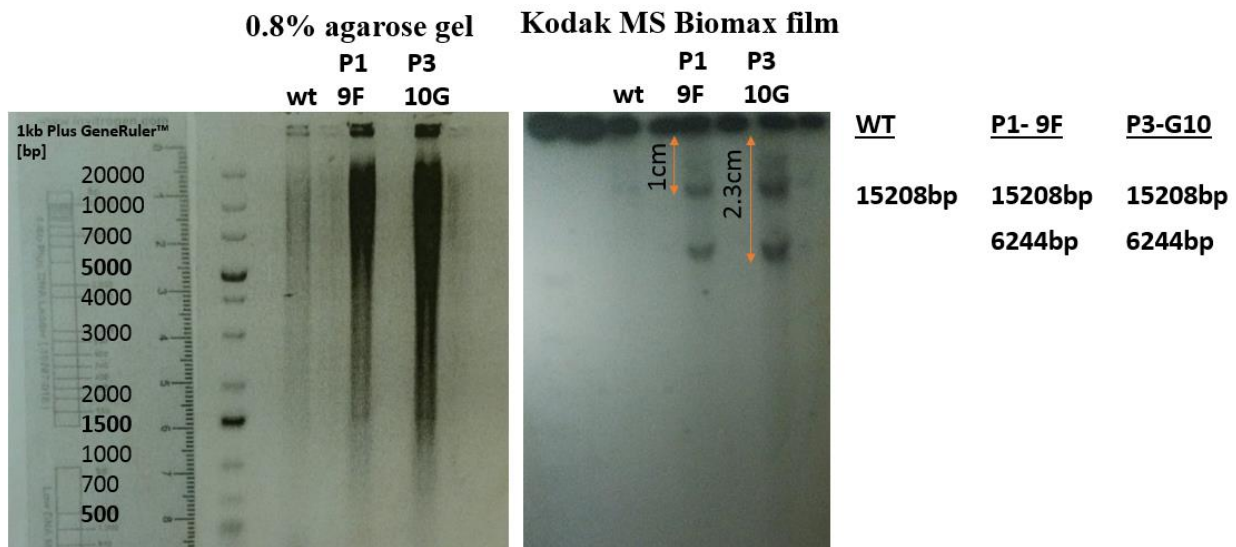


Figure 17. Southern Blot analysis of the expanded, recombined ES-clones.

Both positive clones, 1-9F and 3-10G, were expanded from the stock and rescreened with Southern Blot (probe for CD18 exon 1). Agarose gel picture (left) presents *ScaI* digest of the recombined clones and a WT genomic DNA control. Kodak film (right) shows, where the Southern Blot probe bound on the membrane with transferred DNA digest.

#### 2.1.4. Injection of the blastocyst with recombinant ES-clones

The expanded clones P1-9F and P3-G10 were used for the blastocyst injections, which were carried out at Polygene Transgenetics in Rümlang (Switzerland) and at the Transgenic Facility Mainz (TFM). Prior to injections both clones were tested for mycoplasma infections (intracellular parasite), to prevent that infected clones would be introduced into a blastocyst. In addition, the recombinant ES clones were karyotyped at Polygene Transgenetics. Karyotypes were assessed for both clones, each 10 cells (Appendix B). One hundred percent of the nuclei showed the expected karyotype of 40 chromosomes. Therefore, both clones were highly suitable for the generation of chimeric mice. At both transgenic facilities, approved and expanded clones were injected into blastocysts, which were subsequently transferred into the uterus of a recipient B6 Albino female mouse in order to generate chimeric offspring (Fig.18).

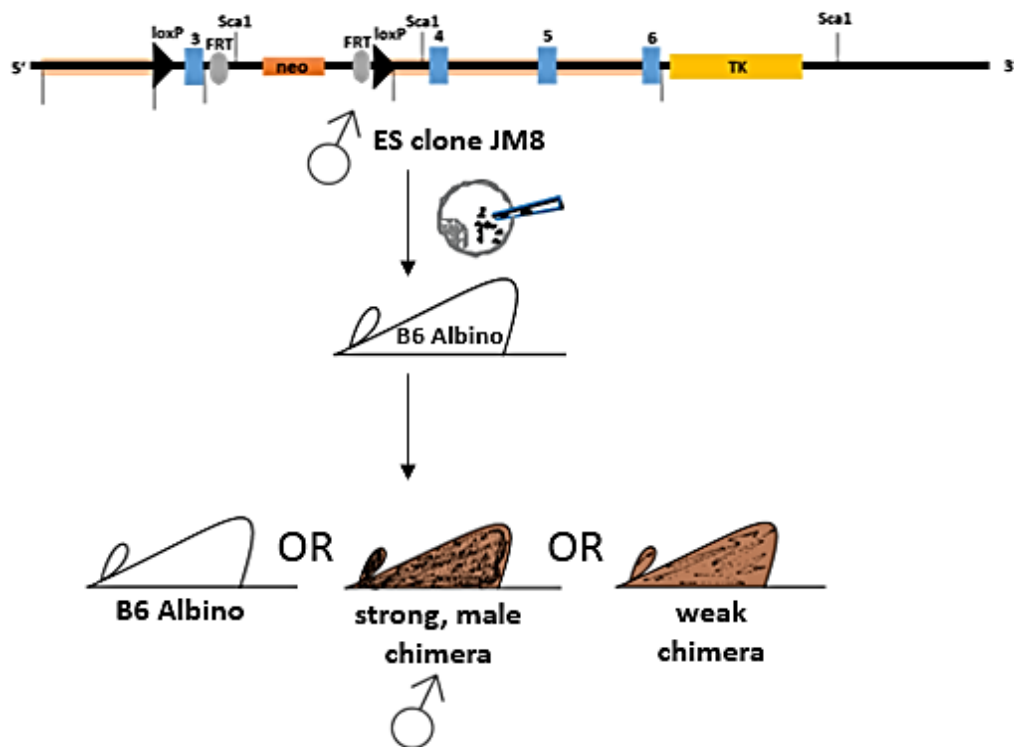


Figure 18. Scheme of the blastocyst injection with the recombined JM8 ES clones.

Blastocyst of the Albino recipient mouse was injected with the recombined ES-clones and re-applied to the uterus of the mouse. The genetic contribution of the ES was assessed according to the coat colour of the mice. Strong chimeras were agouti, and WT mice remained albino.

### 2.1.5. Selection of chimeric offspring derived from the B6 Albino blastocyst recipient mouse

Chimeric litter mice derived from the B6 Albino mouse injected with a recombined-ES-cell-blastocyst were initially selected according to the coat colour. Since the JM8 ES cells were derived from a mouse with a black coat and were introduced into a blastocyst with albino background one could evaluate the genomic contribution of the ES cells according to the coat colour of the litter mice. The offspring with albino coat would not be genetically changed by the ES, whereas agouti mice would be the expected chimeric knock-in mice. The chimera strength differed between the siblings, one could distinguish a higher and a lower genetic contribution to the coat colour. The gender discrimination was another important factor used to judge the chimeras' strength, as the JM8 ES cells were of male origin, the most chimeric offspring was automatically male too. Only strong male chimers (with the darkest coat shade) were selected for further breeding.



*First male offspring derived from the blastocyst recipient mice were selected upon the coat colour and crossed back over one generation to the B6 Albino background. Strongest chimeras (agouti, see picture above) were screened subsequently for the Neo-cassette to reconfirm the genotype.*

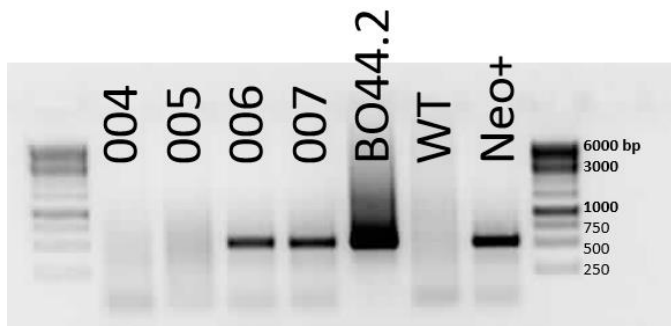


*Figure 20. Neo-cassette-PCR screening of the chimeric offspring.*

*Samples derived from offspring of B6-Albino females and agouti male born to ES-injected blastocyst recipient mouse. A 542bp fragment was amplified with a primer pair that bound Neo-cassette DNA sequence (5'-CAAGCTCTTCAGCAATATCACGGG-3' and 5'-CCTGTCCGGTGCCCTGAATGAACT-3'). Mice 006 and 007, bred in the Transgenic Facility in Mainz, were positive for the Neo-cassette and thus chimeric. Vector DNA, WT DNA and DNA derived from the Neo<sup>+</sup> mouse from Polygene were used as controls.*

### 2.1.6. Deletion of the Neo-cassette from the agouti chimeric offspring via Flp-FRT recombination

The Neo-cassette is regularly flanked by flippase (FLP) recognition target (FRT) sites to enable its removal by means of FLP recombination. Flp-FRT recombination is an analogue to the Cre-lox recombination. An enzyme, flippase (Flp), deletes the DNA fragment between the short FRT sites.

Therefore, as depicted in Figure 21, the Neo<sup>+</sup> CD18<sup>wt/fl</sup> chimeras were crossed with Flp deleter mice (B6 background) and the offspring was either WT or Neo<sup>-</sup> CD18<sup>wt/fl</sup>. The Neo negative chimeras were screened by PCR, which enabled detection of both WT and recombined CD18 allele. Use of the primer combination B2-3 yielded two PCR products in case of the chimeric Flp-FRT recombined genomic DNA: a 233bp fragment for the WT allele and a 487bp fragment for the recombined allele. The BO44.2 plasmid DNA measured 2413bp and the DNA fragment containing the Neo-cassette that was excised by flippase was 1926bp long (Fig.21, blue Table).

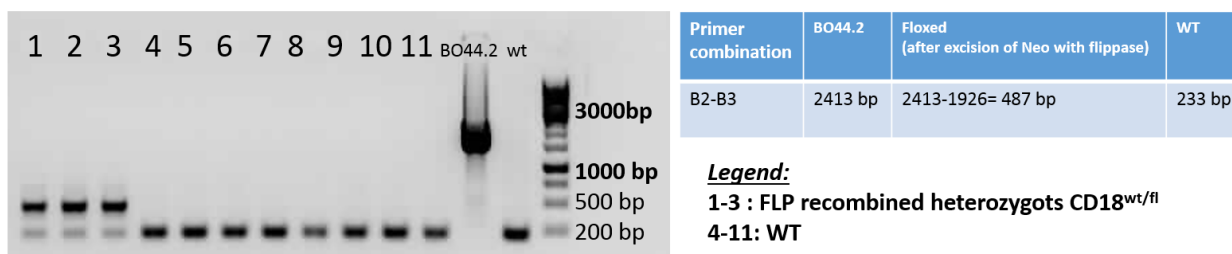
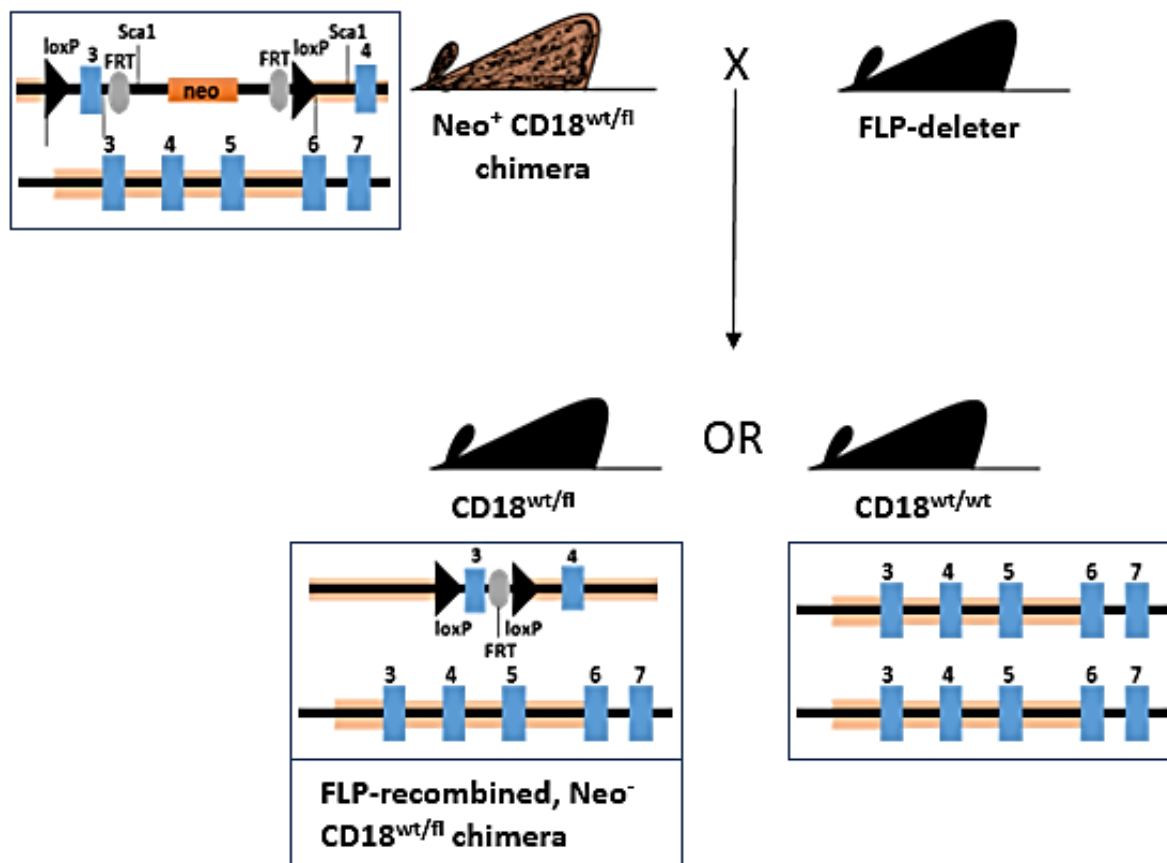


Figure 21. PCR screening of the chimeric offspring after the Flp-FRT recombination.

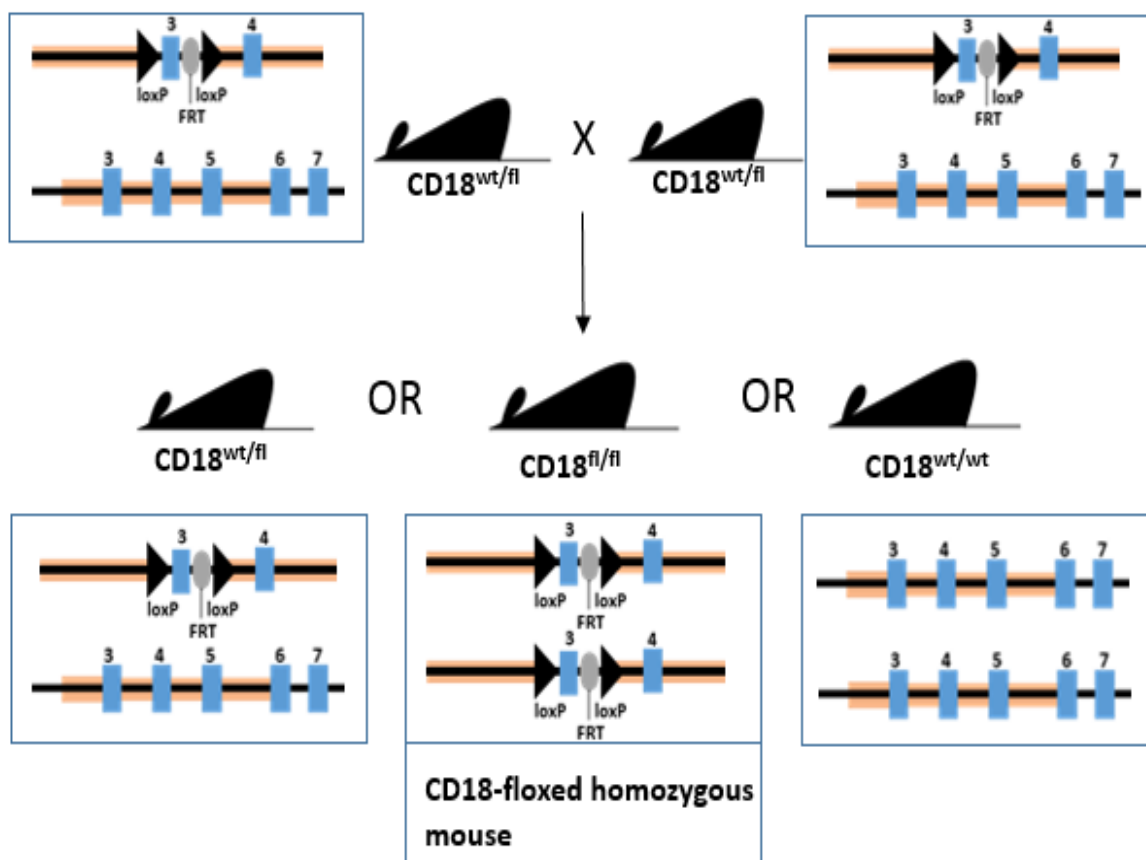
Agouti chimeras that tested positive for the Neo-cassette were crossed with Flp deleter mouse to delete Neo-cassette from the genome. The offspring was screened with a primer pair that detected both WT and recombined allele [B2(s): 5'-GTGACACTTTACTTGCGACCA-3'B3 (as):5'-TGCCAATAAAGAATTCAGAGCC-3']. The Flp-FRT recombined mice presented with both bands, one for the WT (233bp) and one for recombined allele (487bp).

### 2.1.7. Breeding and screening of the homozygous CD18<sup>fl/fl</sup> mice

Heterozygous CD18<sup>wt/fl</sup> x Flp-FRT recombined offspring was further crossed and the resulting generation was either WT, heterozygous or homozygous for the recombined CD18 allele (Fig.22A, breeding scheme). The mouse genomic DNA (tail biopsies) was analysed by PCR using B2-3 primer combination, which allowed detection of both the WT (233bp) and the floxed CD18 allele (487bp) (Fig.22B, gel photo). The homozygous CD18<sup>fl/fl</sup> knock-in mice were founders of a stable floxed mouse line, which was subsequently crossed with CRE-recombinase expressing mice to generate offspring with a cell type specific knock-out. The CD18<sup>fl/fl</sup> strain showed no apparent phenotype.

CD18<sup>fl/fl</sup> mice generated from the founders bred at Polygene (Rümlang, Switzerland) were used for further crossing with mice expressing CRE in a cell type-specific manner, whereas mice that were generated at the transgenic facility in Mainz were Flp-FRT recombined and CD18<sup>fl/fl</sup> Neo<sup>-</sup> males were used for semen cryopreservation.

A



**B**

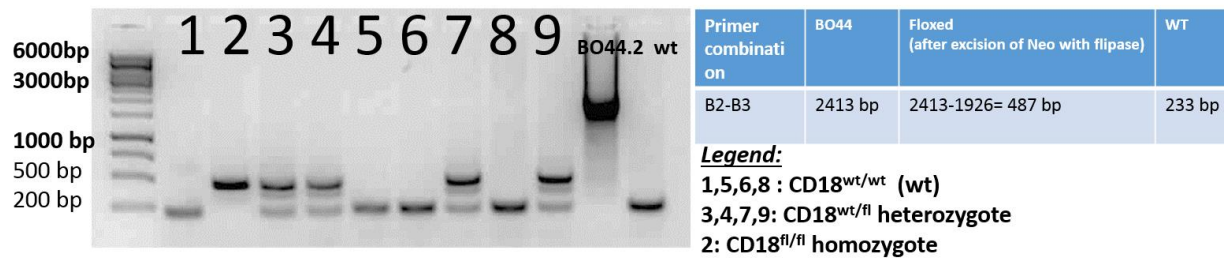


Figure 22. PCR screening of the CD18<sup>fl/fl</sup> mice.

The CD18<sup>fl/fl</sup> mouse generation derived from crossing of the heterozygous offspring after Flp-FRT recombination, i.e. after deletion of the Neo-cassette from the genome. The PCR strategy allowed detection of both WT and recombined CD18 allele. Using primer pair B2-3 [ B2(s): 5'-GTGACACTTTACTTGCGACCA-3' B3(as): 5'-TGCCAATAAAGAATTTTCAGAGCC-3'] a single 487bp product was amplified in case of the CD18<sup>fl/fl</sup> homozygote, a single 233bp product in case of the WT and both products were detected in case of the heterozygote.

2.1.8. Sequencing of the CD18<sup>fl/fl</sup> gene locus

In order to assess the sequence of the floxed CD18 exon3 locus, genomic DNA was isolated from a tail biopsy of a CD18<sup>fl/fl</sup> mouse and amplified with primers that bound the genomic DNA outside of the loxP-exon3-loxP construct. Prior to sequencing the PCR product was gel purified and its integrity was evaluated via gel electrophoresis (Fig.23). Sequence analysis revealed that this 1.367bp fragment encompassed CD18-Exon3 along with the overlapping loxP sites and one FRT site. Correct sequences of both loxP sites along with Exon 3 were detected. One FRT site remained after the Flp-FRT recombination between Exon 3 and the downstream LoxP site. No sequence alterations were found within the sequenced fragment (Fig.24).

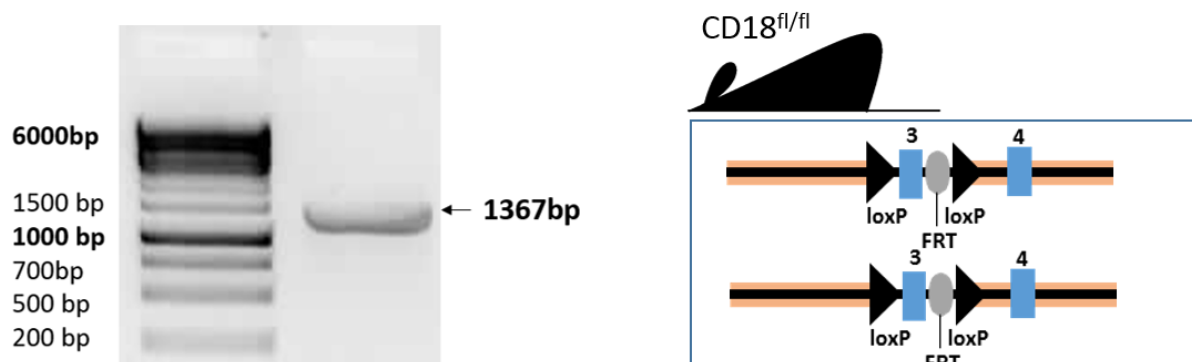


Figure 23. DNA fragment for the sequencing of the recombined DNA fragment derived from the CD18<sup>fl/fl</sup> mouse.

DNA fragment (1367bp) containing Exon3 flanked by loxP sites was amplified using the following primer pair: A1: 'GACCCCTAGATCTTCCCTGC', B4: 'ATAGAACCACCAACCTCGCA'.

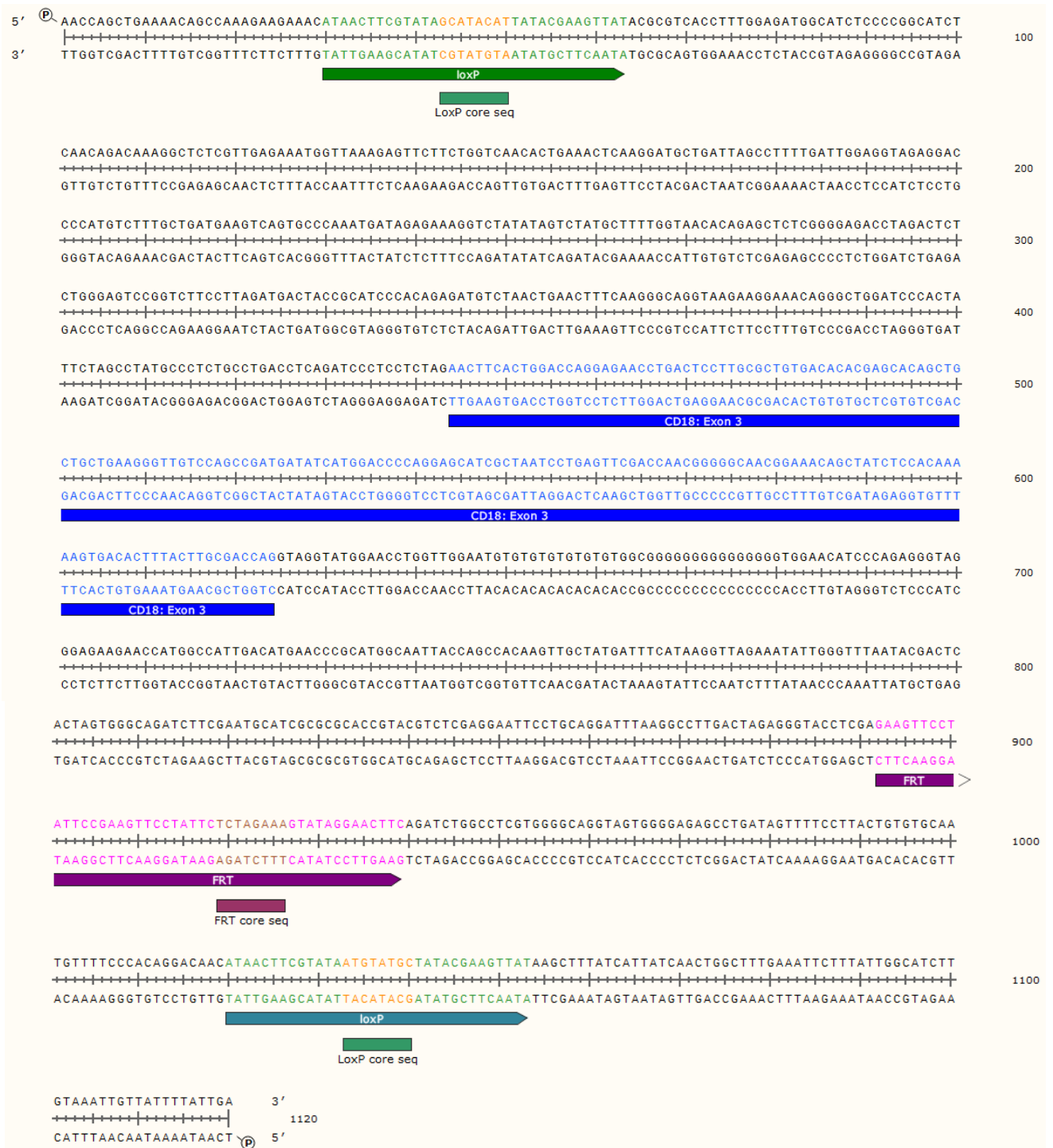


Figure 24 Analysis of the DNA sequence encompassing recombined CD18 exon3 locus. This 1367bp DNA fragment was amplified using a primer pair (A1: 'GACCCCTAGATCTTCCCTGC', B4: 'ATAGAACCACCAACCTCGCA') that bound

outside of both loxP sites (green) and thus the DNA fragment contained the complete CD18 Exon3 (blue) along with loxP sites and the remaining FRT site (violet).

## 2.2. Breeding and characterisation of the new CD18<sup>ΔCD11c</sup> mouse strain

### 2.2.1. Breeding and screening strategy for the CD18<sup>ΔCD11c</sup>

In order to generate a DC-specific CD18 knock-out, the Flp-FRT recombined CD18<sup>fl/fl</sup> mice were crossed with CD11c<sup>CRE</sup> mice (Caton et al., 2007), kindly supplied by Prof. Clausen. CD11c<sup>CRE</sup> mice are BAC transgenics, in which Cre recombinase replaced CD11c exon I in the entire *Itgam* (CD11c) gene (the 5' end of the adjacent *Itgam* gene is missing to prevent its overexpression). The resulting CD18<sup>w<sup>t</sup>/fl</sup> CD11c<sup>CRE</sup> offspring was crossed back to CD18<sup>fl/fl</sup> background and thus within the next generation CD18<sup>fl/fl</sup> CD11c<sup>CRE</sup> (i.e. CD18<sup>ΔCD11c</sup>) mice were acquired (a detailed breeding summary is depicted in the 'Materials and Method' section: Breeding of the CD18<sup>ΔCD11c</sup>). To establish the CD18<sup>ΔCD11c</sup> breeding, CD18<sup>fl/fl</sup> CD11c<sup>CRE</sup> males were paired with CD18<sup>fl/fl</sup> females (Fig.25). To maintain a BAC transgene stability, the CD11c<sup>CRE</sup> was always carried by males as shown in the breeding scheme below.

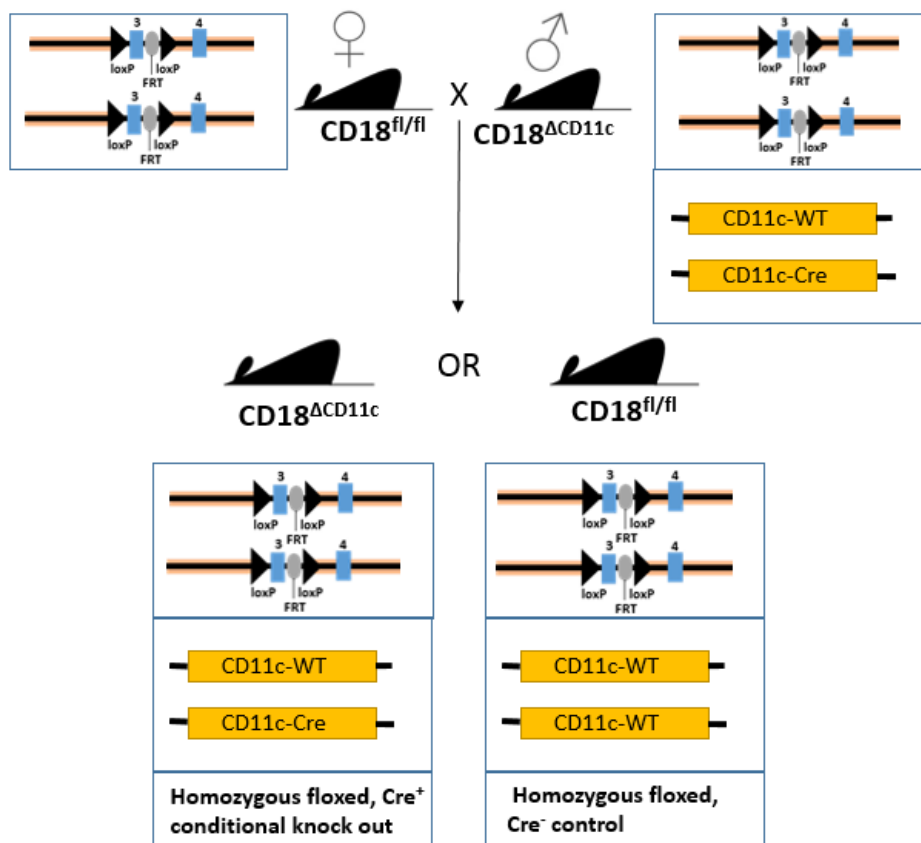


Figure 25. Breeding strategy for the CD18<sup>ΔCD11c</sup> mice.

The  $CD18^{\Delta CD11c}$  male was crossed with the  $CD18^{fl/fl}$  female and thus the offspring was always homozygous for the floxed construct and only 50% of the offspring would carry the BAC transgene:  $CD11c$ -CRE. The remaining 50% of the mice were  $CD18^{fl/fl}$  and were used as control mice for the generated DC-specific  $CD18$  knock-outs.

The offspring derived from a  $CD18^{\Delta CD11c}$  x  $CD18^{fl/fl}$  breeding pair was  $CD18^{\Delta CD11c}$  in 50% and the remaining 50% was  $CD18^{fl/fl}$ . The PCR screening was carried out as described before. Since all mice were homozygous for the floxed allele, the offspring was screened for the presence of the CRE-recombinase only. The  $CD11c^{CRE}$  recombinase was detected using a double PCR reaction, in which two products were amplified at the same time, namely: a 313bp fragment for the CRE-recombinase and a 510bp fragment for actin, as an internal positive DNA quality control (Fig.26).

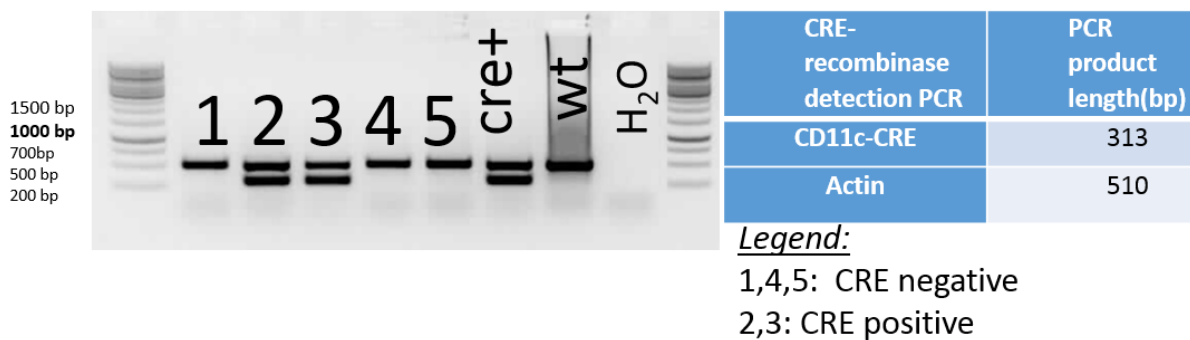


Figure 26. PCR screening of the mice expressing  $CD11c$ -CRE.

$CD18^{\Delta CD11c}$  x  $CD18^{fl/fl}$  offspring was homozygous for the floxed construct and in 50% heterozygous for the  $CD11c$ -CRE, thus the litter mice had to be screened for  $CD11c$ -CRE recombinase. Using a double PCR reaction, two PCR products were amplified: a 313bp fragment for the CRE-recombinase and a 510bp fragment for the Actin, which served as a quality control for the isolated DNA. Positive mice had both bands and negative had only Actin-band.

## 2.2.2. Characterisation of the leukocyte progenitors in the bone marrow of the $CD18^{\Delta CD11c}$ mouse

In order to analyse leukocyte subsets, first the bone marrow of  $CD18^{\Delta CD11c}$  and the corresponding  $CD18^{fl/fl}$  control mice was isolated (from the femur and tibia), depleted of erythrocytes and stained with fluorescently labelled antibodies. Four main leukocyte subsets were distinguished, i.e. T lymphocytes' progenitor ( $CD3^+$ ), B lymphocytes ( $CD19^+$ ), granulocytes ( $CD11b^+Ly6G^+Ly6C^{low}$ ) and monocytes ( $CD11b^+Ly6G^+Ly6C^{high}$ ) (Fig.27). The

bone marrow from both control and knock-out mice contained about 1.2-1.5% of CD3<sup>+</sup> lymphocytes, 20% of CD19<sup>+</sup> lymphocytes, about 24% of granulocyte progenitors and 5% of monocyte progenitors (Fig.28). Thus, the beta-2 integrin knock-out in the CD11c<sup>+</sup> cells had no influence on the composition of the analysed leukocytes in the bone marrow.

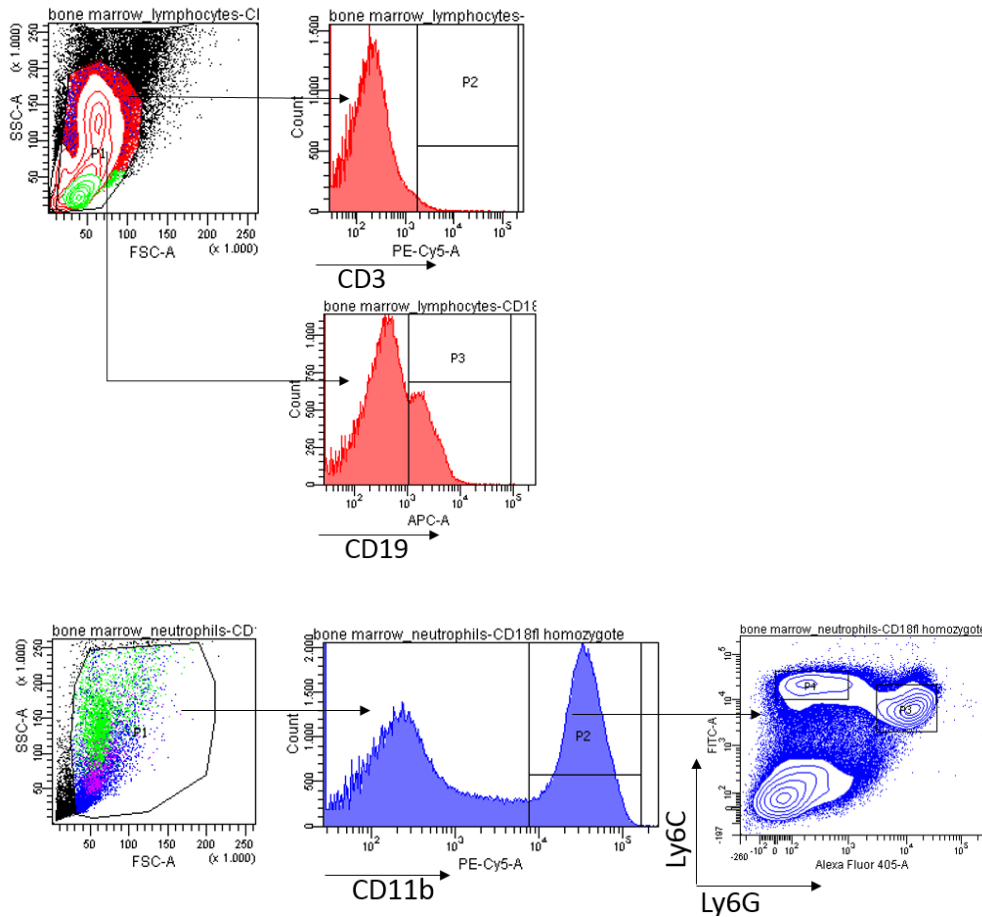


Figure 27. Gating strategy for the leukocytes derived from the bone marrow of the CD18<sup>ΔCD11c</sup>. T and B lymphocytes were identified as CD3 or CD19 positive fractions of the erythrocyte-depleted bone marrow leukocytes. Granulocytes and monocytes were pre-gated as CD11b positive fraction and then discriminated using anti-Ly6G and Ly6C antibodies. Classical monocytes were recognised as CD11b<sup>+</sup>Ly6G<sup>-</sup>Ly6C<sup>high</sup>, whereas granulocytes as CD11b<sup>+</sup>Ly6G<sup>+</sup>Ly6C<sup>low</sup>.

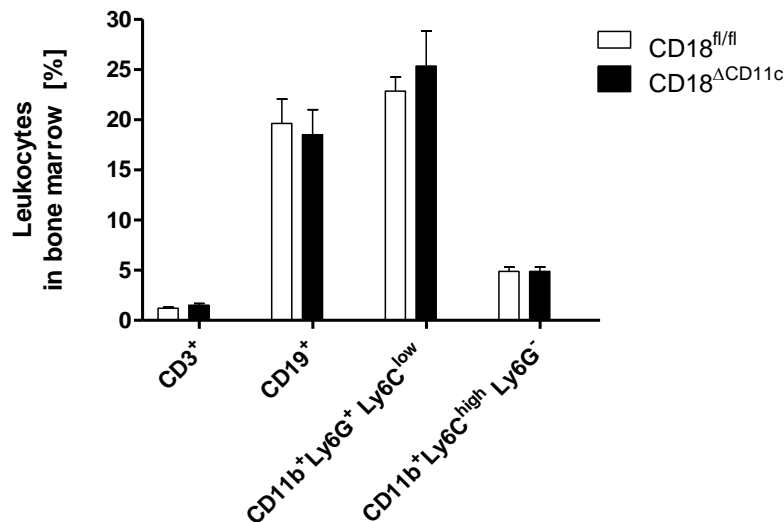


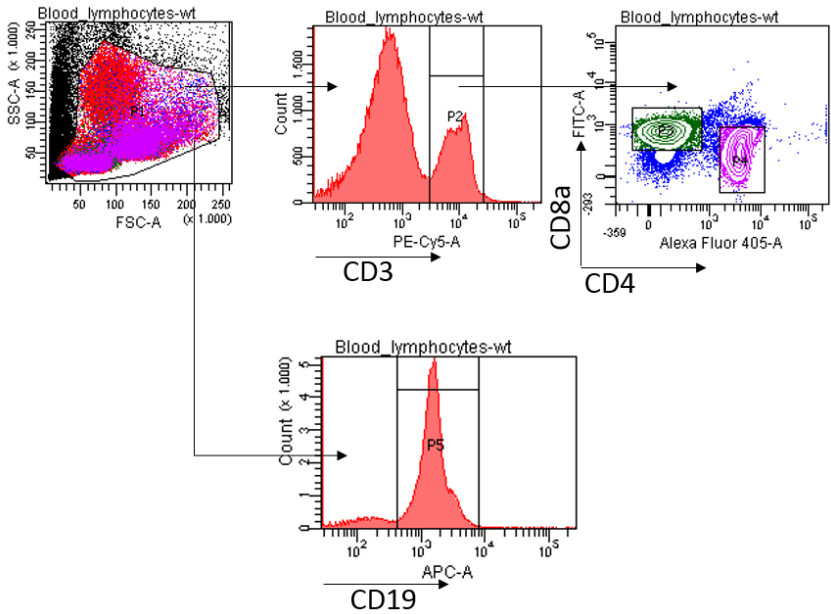
Figure 28. Leukocyte composition in the bone marrow of the CD18<sup>ΔCD11c</sup> mouse.

Bone marrow was extracted from the femur and tibia of the CD18<sup>ΔCD11c</sup> and CD18<sup>fl/fl</sup> mouse. Cell suspension was erythrocyte-depleted and stained with antibodies against murine CD3 (for T lymphocytes), CD19 (for B lymphocytes), CD11b, Ly6G and Ly6C. Classical monocytes were determined as CD11b<sup>+</sup>Ly6G<sup>-</sup>Ly6C<sup>high</sup>. Granulocytes were identified as CD11b<sup>+</sup>Ly6G<sup>+</sup>Ly6C<sup>low</sup>. Fractions of leukocyte subtypes are presented as percentage of the whole bone marrow leukocyte population. Depicted bars represent mean with SEM (n=4).

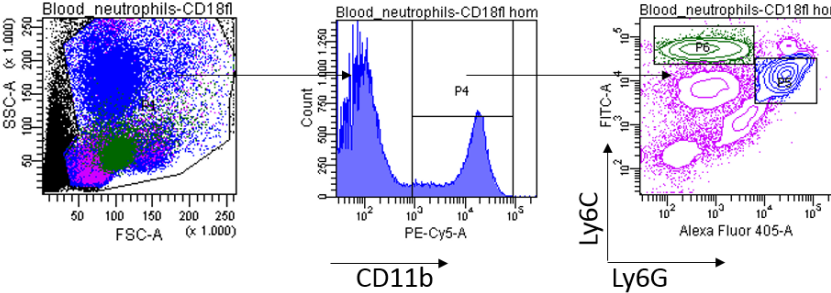
### 2.2.3. Characterisation of blood derived leukocytes from the CD18<sup>ΔCD11c</sup> mouse

Next, blood of the CD18<sup>ΔCD11c</sup>, CD18<sup>fl/fl</sup> and C57BL/6 was isolated, depleted of erythrocytes and the following cell subsets were distinguished: T lymphocytes (CD4<sup>+</sup> and CD8a<sup>+</sup> subpopulations of the CD3<sup>+</sup> cells), B lymphocytes (CD19<sup>+</sup>) (Fig.29 A), classical monocytes (CD11b<sup>+</sup>Ly6G<sup>-</sup>Ly6C<sup>high</sup>) and granulocytes (CD11b<sup>+</sup>Ly6G<sup>+</sup>Ly6C<sup>low</sup>) (Fig.29 B). No genotype specific differences were observed in the analysed populations (Fig. 29 C).

A



B



C

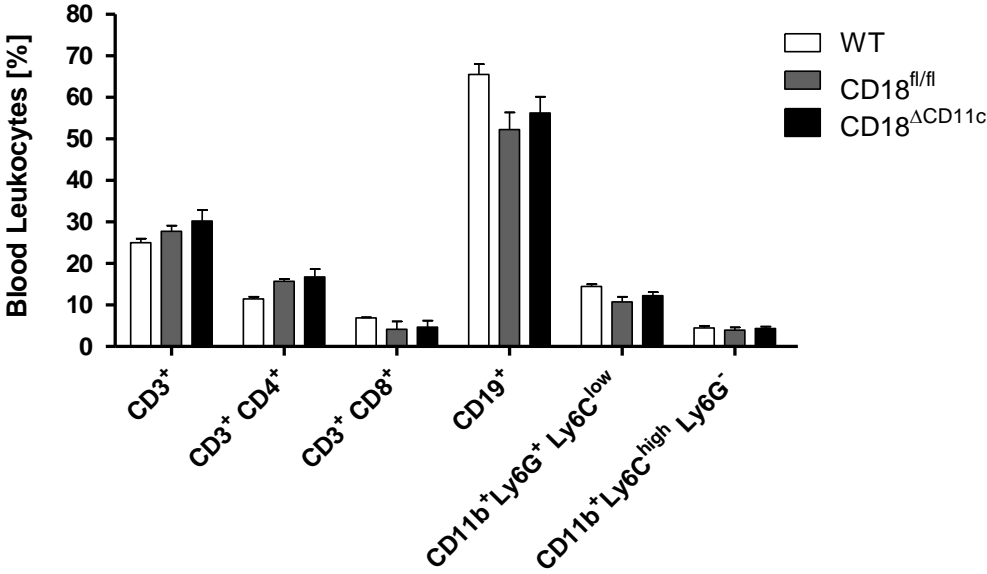


Figure 29. Leukocyte populations in the blood of the CD18<sup>ΔCD11c</sup> mouse.

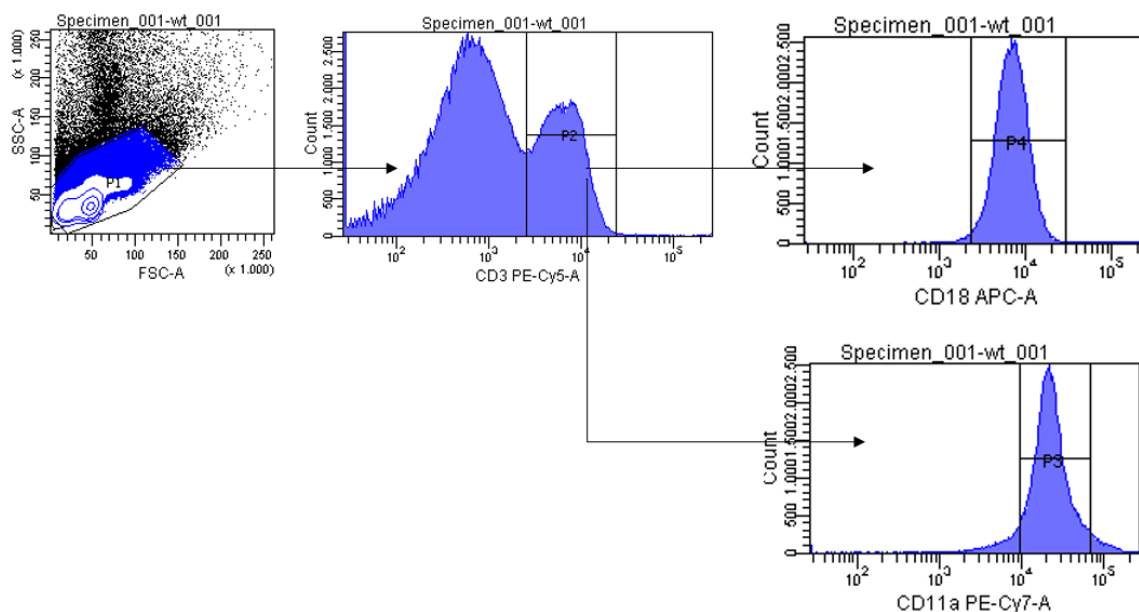
*Erythrocyte-depleted blood from WT C57BL/6, CD18<sup>fl/fl</sup> and CD18<sup>ΔCD11c</sup> was used to analyse following leukocyte populations: T lymphocytes (CD3<sup>+</sup> and CD4<sup>+</sup>/CD8<sup>+</sup> subpopulations), B lymphocytes (CD19<sup>+</sup>), monocytes (CD11b<sup>+</sup>Ly6G<sup>-</sup>Ly6C<sup>high</sup>) and granulocytes (CD11b<sup>+</sup>Ly6G<sup>+</sup>Ly6C<sup>low</sup>). Fractions of leukocyte subtypes are presented as percentage of the whole blood leukocyte population (C). Depicted bars represent mean with SEM (n=4 for CD18<sup>fl/fl</sup> and CD18<sup>ΔCD11c</sup>; n=2 for WT C57BL/6).*

## 2.2.4. Characterisation of the splenocytes derived from the CD18<sup>ΔCD11c</sup> mouse

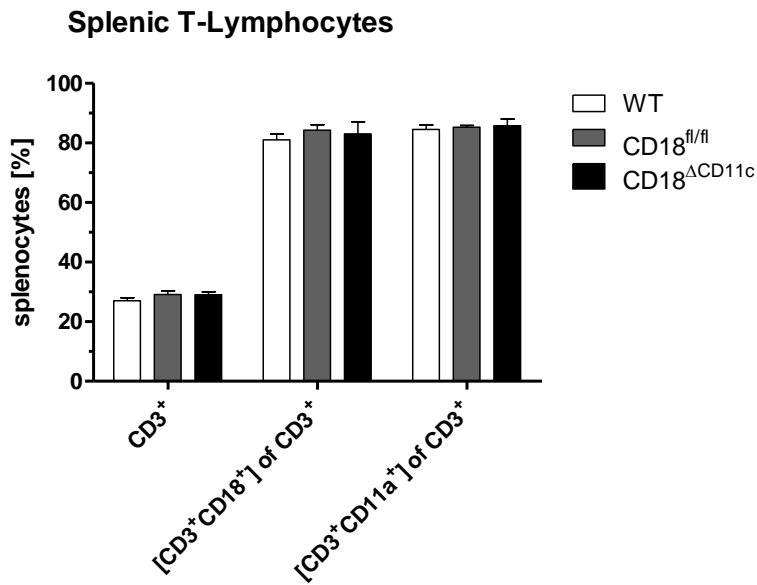
### 2.2.4.1. Splenic T-lymphocytes derived from the CD18<sup>ΔCD11c</sup> mouse

Initial analysis of splenic immune cells involved analysis of CD3<sup>+</sup> population and expression of both CD18 and CD11a on the surface of the T lymphocytes (Fig. 30A). The CD3<sup>+</sup> population made in all mice strains around 27-29% of the splenic leukocytes. Over 80% of these T lymphocytes expressed both CD18 and CD11a, in all mouse strains (Fig. 30B). T lymphocytes were then classified as CD4<sup>+</sup> or CD8<sup>+</sup> and further markers were identified on these subpopulations, namely CD25 and FoxP3. The CD4<sup>+</sup> T lymphocytes made around 13% of the WT- C57BL/6, 17% of the CD18<sup>fl/fl</sup> and 18% of the CD18<sup>ΔCD11c</sup> splenic population. About 10-12% was FoxP3<sup>+</sup>CD4<sup>+</sup>, about 7% was CD25<sup>+</sup>CD4<sup>+</sup> and 7% was CD25<sup>+</sup>FoxP3<sup>+</sup>CD4<sup>+</sup>, equally distributed in all strains. Around 8-9% of the splenocytes were CD3<sup>+</sup>CD8<sup>+</sup> double positive, and only a small fraction was CD25<sup>+</sup>CD8<sup>+</sup> (below 1% in all strains) (Fig. 30C)

A



**B**



**C**

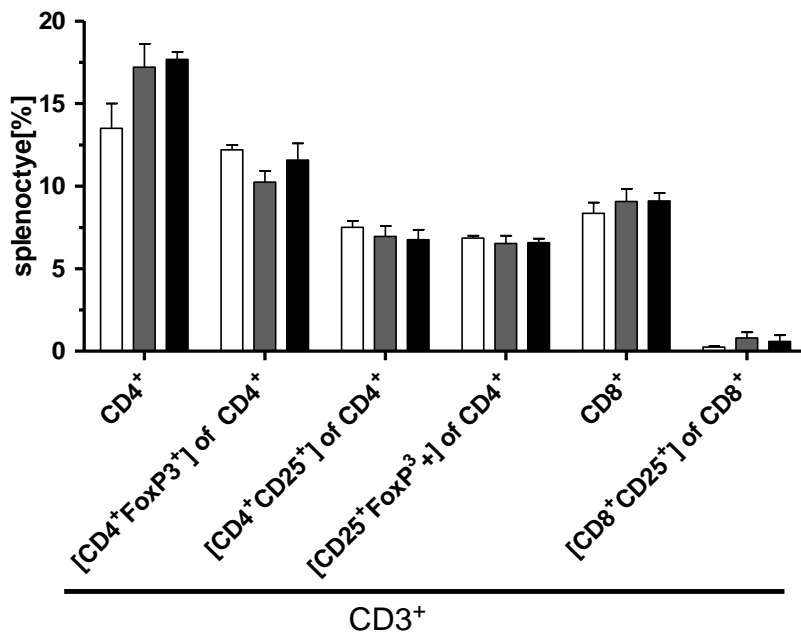


Figure 30. Splenic T lymphocyte population in the CD18<sup>ΔCD11c</sup> mouse.

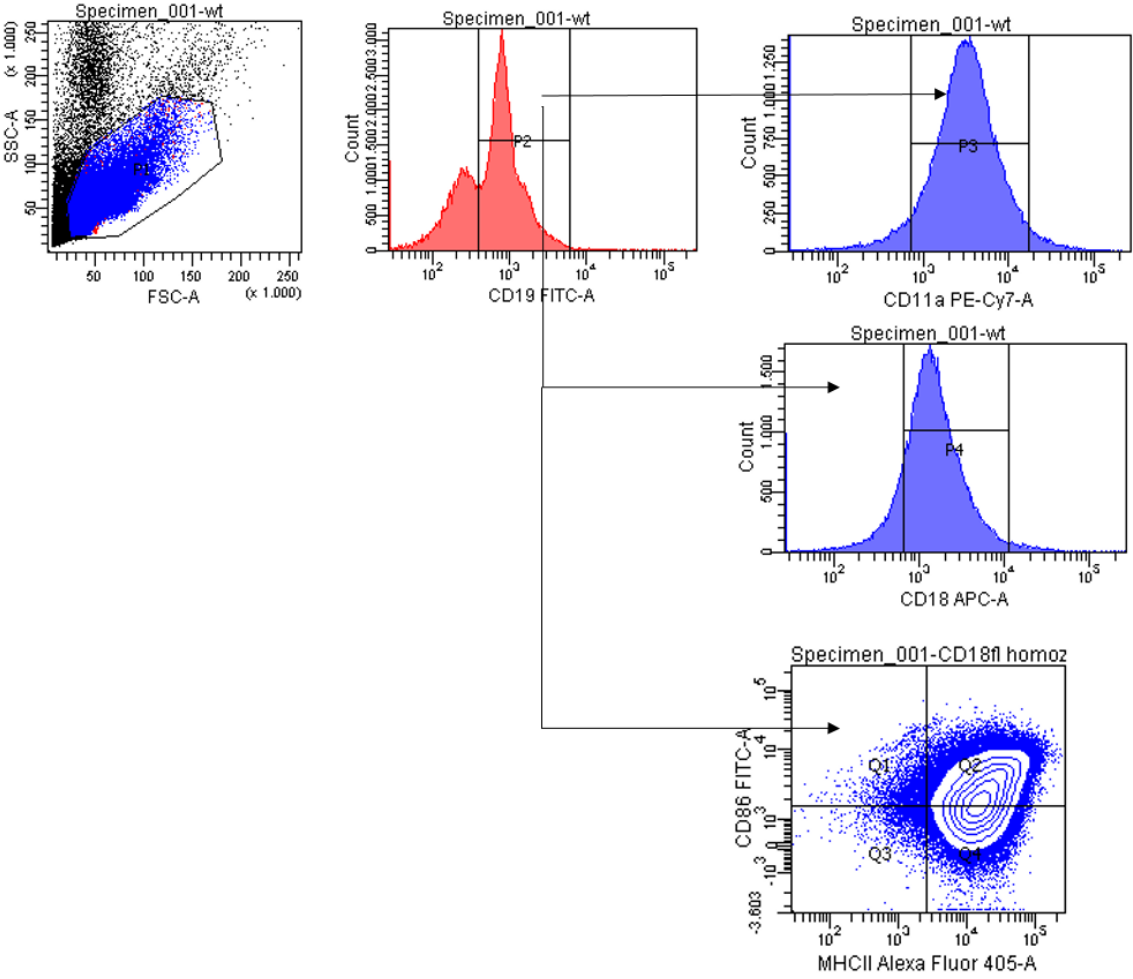
Erythrocyte-depleted splenic leukocyte populations from WT C57BL/6, CD18<sup>fl/fl</sup> and CD18<sup>ΔCD11c</sup> were initially stained with anti-CD3 and  $\beta 2$  integrin's markers: anti-CD11a and anti-CD18 (A, B). CD3<sup>+</sup> lymphocytes were further subdivided into CD4<sup>+</sup> and CD8<sup>+</sup>. The CD3<sup>+</sup>CD4<sup>+</sup> population was subsequently analysed for the expression of Foxp3 and CD25 (single and double positive populations). The CD3<sup>+</sup>CD8<sup>+</sup> population was analysed only for the CD25 expression (C). Fractions of T lymphocyte subtypes are presented as percentage of the

whole CD3<sup>+</sup> population. Depicted bars represent mean with SEM (n=4 for CD18<sup>fl/fl</sup> and CD18<sup>ΔCD11c</sup>; n=2 for WT C57BL/6).

#### 2.2.4.2. Splenic B-lymphocytes derived from the CD18<sup>ΔCD11c</sup> mouse

For the analysis of the splenic B lymphocyte population of CD18<sup>ΔCD11c</sup> mice, spleens from WT C57BL/6, CD18<sup>fl/fl</sup> and CD18<sup>ΔCD11c</sup> mice were isolated, erythrocyte-depleted and expression of the following markers was evaluated: CD19, CD18, CD11a, MHC-II and CD86 (Fig. 31A). The CD19<sup>+</sup> fraction reached about 59% of the WT C57BL/6, 52% of the CD18<sup>fl/fl</sup> and 49% of the CD18<sup>ΔCD11c</sup> splenic leukocytes. In order to analyse the expression of β2 integrin on the splenic B cell surface, the CD19<sup>+</sup> fraction was gated for CD18 and CD11a. The double positive cell populations (CD19<sup>+</sup>CD18<sup>+</sup> and CD19<sup>+</sup>CD11a<sup>+</sup>) resembled the total CD19<sup>+</sup> fraction percentagewise and thus both control and CD18<sup>ΔCD11c</sup> derived B cells expressed CD18 and CD11a in the same manner ( over 90% of the B cells expressed the investigated markers). Furthermore, co-stimulatory molecules expression was investigated. C57BL/6 derived splenocytes presented with a slightly lower fraction of triple positive population (CD19<sup>+</sup>CD86<sup>+</sup>MHC-II<sup>+</sup>), reaching 39% of the splenocyte population, whereas both CD18<sup>fl/fl</sup> and CD18<sup>ΔCD11c</sup> derived B lymphocytes equally expressed both markers (about 51% triple positive among the splenocyte population). Thus, the complete B cells population was positive for CD86 and MHC-II in case of the CD18<sup>fl/fl</sup> control and CD18<sup>ΔCD11c</sup> knock-out mice (Fig. 31B).

A



B

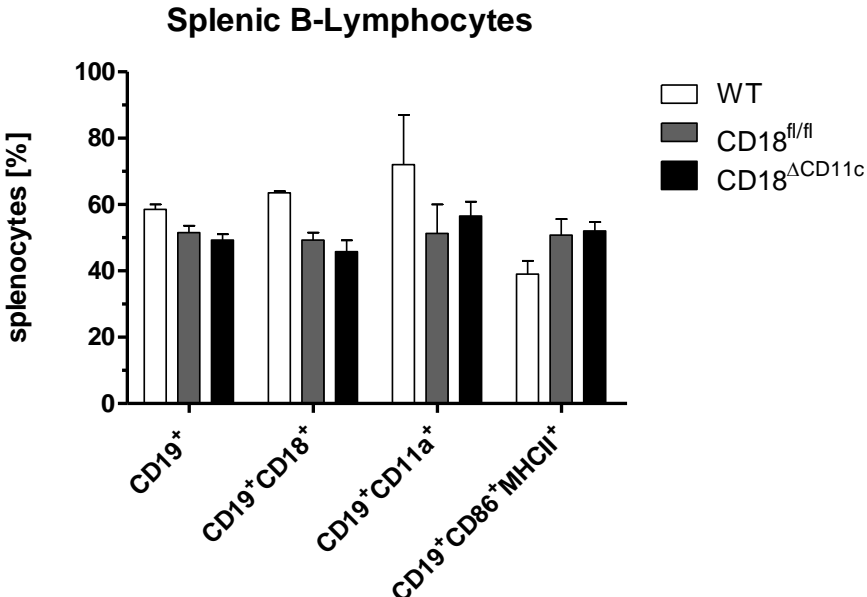


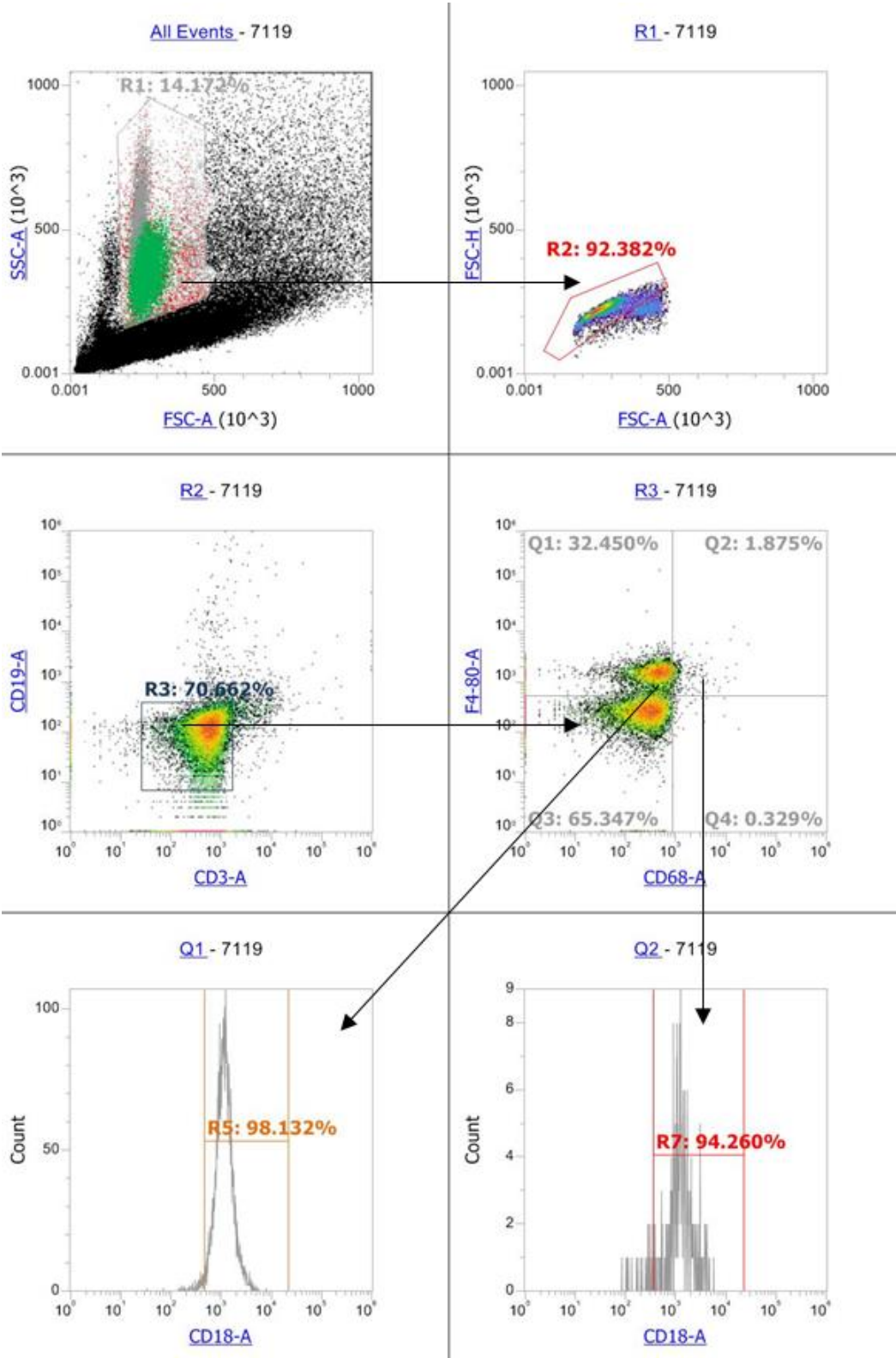
Figure 31. Splenic B lymphocyte population in the CD18<sup>ΔCD11c</sup> mouse.

*Erythrocyte-depleted splenic leukocyte population from WT C57BL/6, CD18<sup>fl/fl</sup> and CD18<sup>ΔCD11c</sup> was initially stained with anti-CD19 and beta-2 integrin's markers: anti-CD11a and anti-CD18, further cells were sub-gated for CD86 and MHC-II (A). Both single CD19<sup>+</sup> and double positive CD19<sup>+</sup>CD18/ CD19<sup>+</sup>CD11a<sup>+</sup> were analysed as percentage of the whole splenocyte population (B). CD19<sup>+</sup> lymphocytes were further analysed for their activation markers: CD86 and MHC-II. Depicted bars represent mean with SEM (n=4 for CD18<sup>fl/fl</sup> and CD18<sup>ΔCD11c</sup>; n=2 for WT C57BL/6).*

#### **2.2.4.3. Splenic macrophages derived from the CD18<sup>ΔCD11c</sup> mouse**

In order to analyse splenic macrophages derived from the CD18<sup>ΔCD11c</sup> mouse, spleens of the CD18<sup>fl/fl</sup> and CD18<sup>ΔCD11c</sup> were isolated and depleted of CD90.2<sup>+</sup> and CD19<sup>+</sup> cells using magnetic bead sorting (Milteyni Biotec). Depletion of CD90.2<sup>+</sup> and CD19<sup>+</sup> cells (i.e. T and B lymphocytes) enriched the DC/macrophage fraction and facilitated the analysis. The analysis involved expression of CD18 and CD11b on the surface of F4/80<sup>+</sup>CD68<sup>-</sup> and F4/80<sup>+</sup>CD68<sup>+</sup> cell population. A CD3<sup>-</sup>CD19<sup>-</sup> double negative population was divided into F4/80<sup>+</sup>CD68<sup>-</sup> and F4/80<sup>+</sup>CD68<sup>+</sup>. These two populations were subsequently analysed for the expression of the CD18 and CD11b (Fig. 32A). The F4/80<sup>+</sup>CD68<sup>+</sup> double positive population was equally positive for the expression of both CD18 and CD11b in both control and KO samples, reaching around 95% of CD18<sup>+</sup> and around 85% of CD11b<sup>+</sup>. The F4/80<sup>+</sup>CD68<sup>-</sup> population expressed both markers almost equally (~98%) in case of the CD18<sup>fl/fl</sup> and CD18<sup>ΔCD11c</sup> samples (Fig. 32B, C).

A



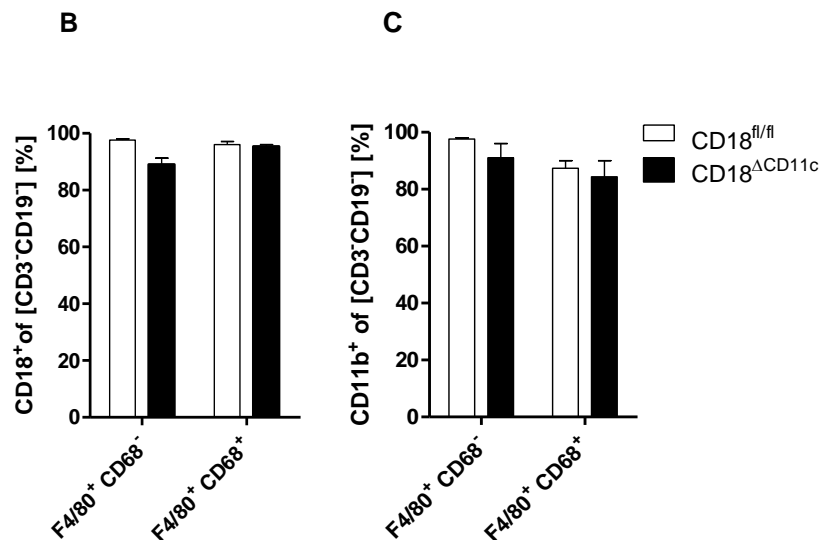


Figure 32. Splenic macrophage population in the CD18<sup>ΔCD11c</sup> mouse.

Erythrocyte-depleted splenic leukocyte populations from CD18<sup>fl/fl</sup> and CD18<sup>ΔCD11c</sup> were initially enriched in DC and Macrophages by sorting CD19<sup>+</sup> and CD90.2<sup>+</sup> cells out. Subsequently a double negative CD3<sup>-</sup>CD19<sup>-</sup> subset was double gated for F4/80 and CD68 (A). Both F4/80<sup>+</sup>CD68<sup>+</sup> and F4/80<sup>+</sup>CD68<sup>-</sup> populations were analysed for the expression of CD18 (B) and CD11b (C). Depicted bars represent mean values with SEM (n=3).

## 2.2.5. Characterisation of Dendritic cells derived from the CD18<sup>ΔCD11c</sup> mouse

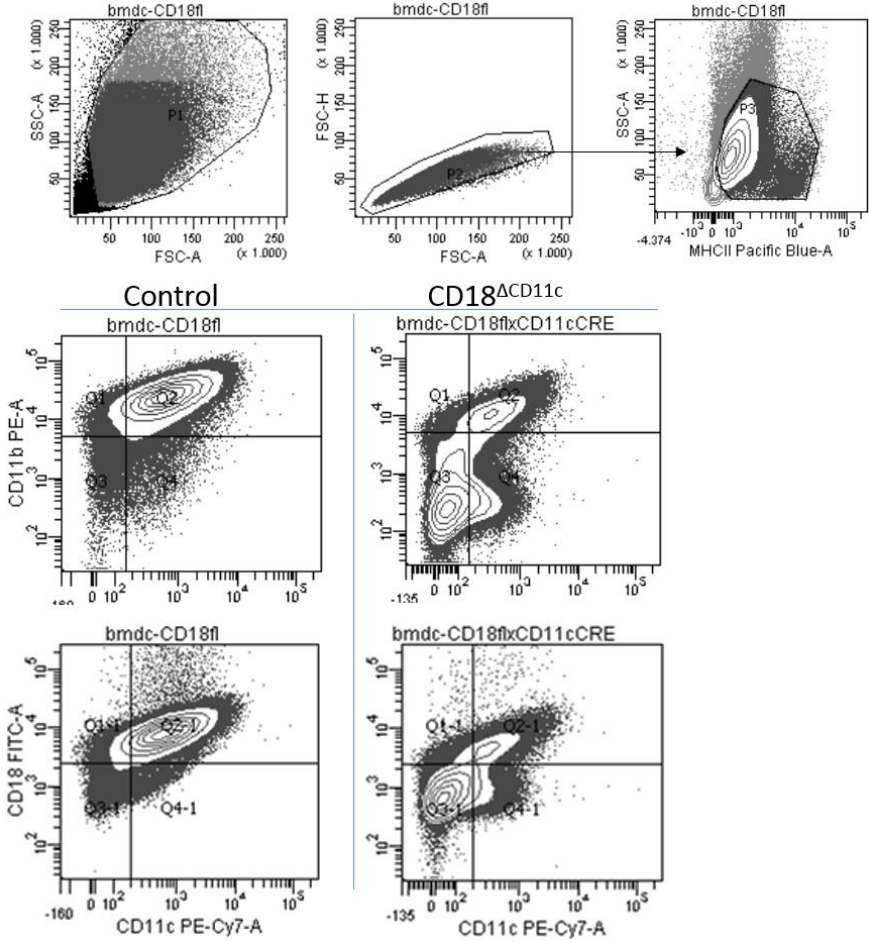
Both *in vitro* cultured, bone-marrow derived DC (BM-DC) and tissue isolated DC were analysed for the expression of β2 integrins. BMDC were cultured with GM-CSF (4ng/ml) and harvested on day 7 of the *in vitro* culture. Tissue derived dendritic cells were isolated from the skin (ear), lung and the spleen.

### 2.2.5.1. Analysis of bone-marrow derived DC from the CD18<sup>ΔCD11c</sup> mouse

BM-DC were analysed in both CD18<sup>fl/fl</sup> and CD18<sup>ΔCD11c</sup> cultures for their expression of CD18, CD11c and CD11b. The starting population was preselected as MHC-II<sup>+</sup> and subsequently double positive CD11c<sup>+</sup>CD11b<sup>+</sup> and CD11c<sup>+</sup>CD18<sup>+</sup> subsets were analysed (Fig. 33A). In bone marrow cells derived from CD18<sup>ΔCD11c</sup> and CD18<sup>fl/fl</sup> mice the MHC-II<sup>+</sup> fraction constituted about 72-73% of the starting population. From these, the CD11c<sup>+</sup>CD11b<sup>+</sup> double positive population constituted 81% in the CD18<sup>fl/fl</sup> control group and 27% in the CD18<sup>ΔCD11c</sup> group. The CD11c<sup>+</sup>CD18<sup>+</sup> double positive fraction constituted 76% of the MHC-II<sup>+</sup> population

derived from the control group and only 18.5% of the knock-out group (Fig. 33B). Initial analysis of the expression of co-stimulatory molecules upon CpG stimulation suggested a reduced response to TLR ligand in the CD18<sup>ΔCD11c</sup> BM-DC as compared with the CD18<sup>fl/fl</sup> control (Appendix C.)

**A**



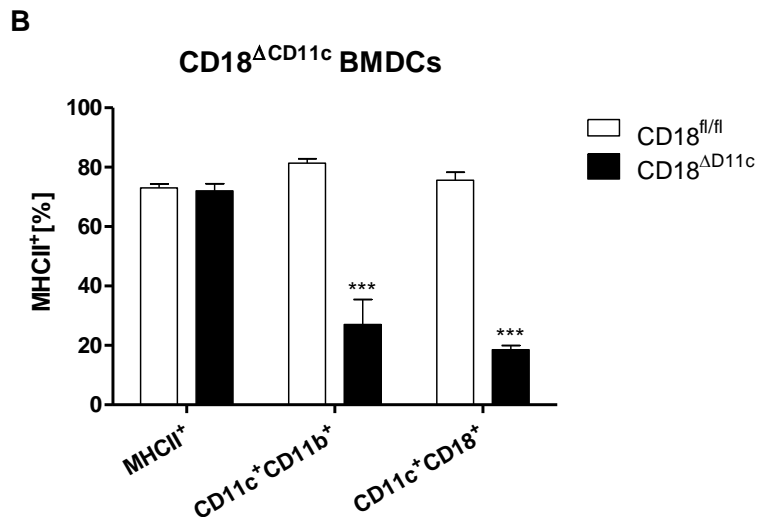


Figure 33. Analysis of the BM-DC population in the CD18<sup>ΔCD11c</sup> mouse.

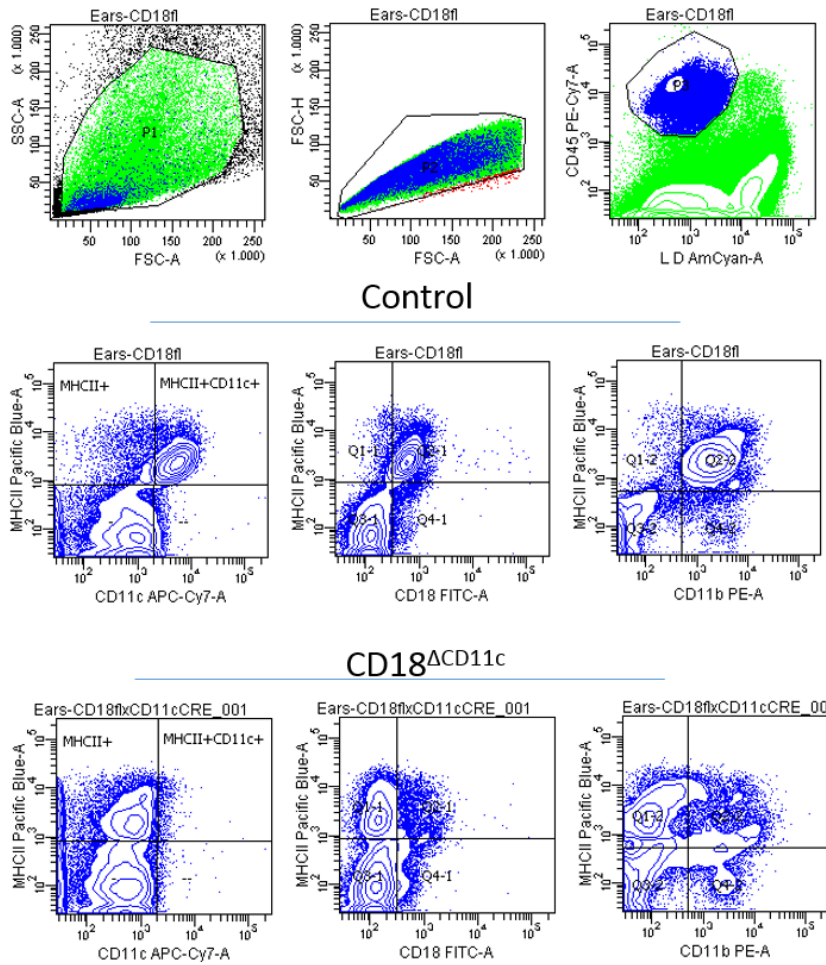
Erythrocyte-depleted bone-marrow cells from CD18<sup>fl/fl</sup> and CD18<sup>ΔCD11c</sup> were cultured for 7 days with GM-CSF and subsequently analysed for the expression of the  $\beta$ 2 integrins (CD18, CD11c and CD11b). The MHC-II<sup>+</sup> population was sub-gated for double positive CD11c<sup>+</sup>CD11b<sup>+</sup> and CD11c<sup>+</sup>CD18<sup>+</sup> subset (A). The expression of the  $\beta$ 2 integrins was evaluated as percentage of double positive within the MHC-II<sup>+</sup> population (B). Depicted bars represent mean with SEM (n=4).

#### 2.2.5.2. Analysis of murine skin CD18<sup>ΔCD11c</sup> DC

Ear skin from CD18<sup>ΔCD11c</sup> and CD18<sup>fl/fl</sup> was digested with a solution containing Collagenase IV, Dispase, Hyaluronidase and DNase. The viable (LD<sup>-</sup>) leukocyte population (CD45<sup>+</sup>) was further analysed for the expression of MHC-II and  $\beta$ 2 integrins (CD18, CD11c, CD11b). Leukocyte populations were analysed as double positive for MHC-II and CD18/CD11b out of CD45<sup>+</sup>LD<sup>-</sup>MHC-II<sup>+</sup> triple positive (Fig. 34A). The expression of CD11c was reduced to 12%, of CD18 to 30% and of CD11b to 36% in samples derived from the CD18<sup>ΔCD11c</sup>. CD11c, CD18

and CD11b were expressed respectively on 71%, 90% and 94% of the MHC-II<sup>+</sup> cells in the CD18<sup>fl/fl</sup> control samples (Fig. 34B).

**A**



**B**

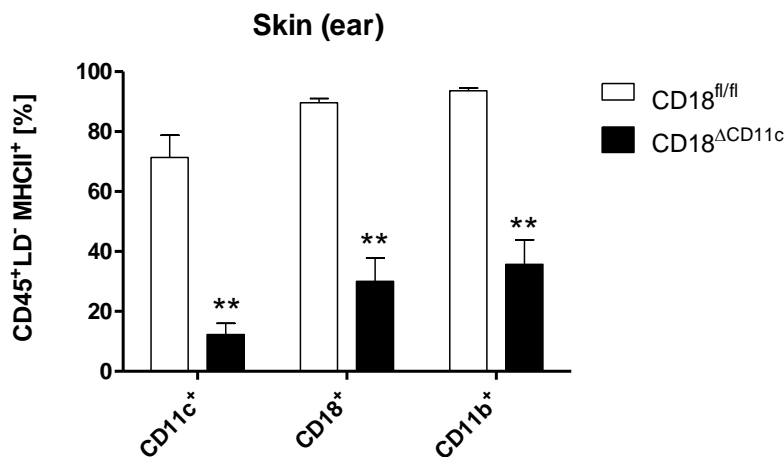


Figure 34. Analysis of the skin DC population in the CD18<sup>ΔCD11c</sup> mouse.

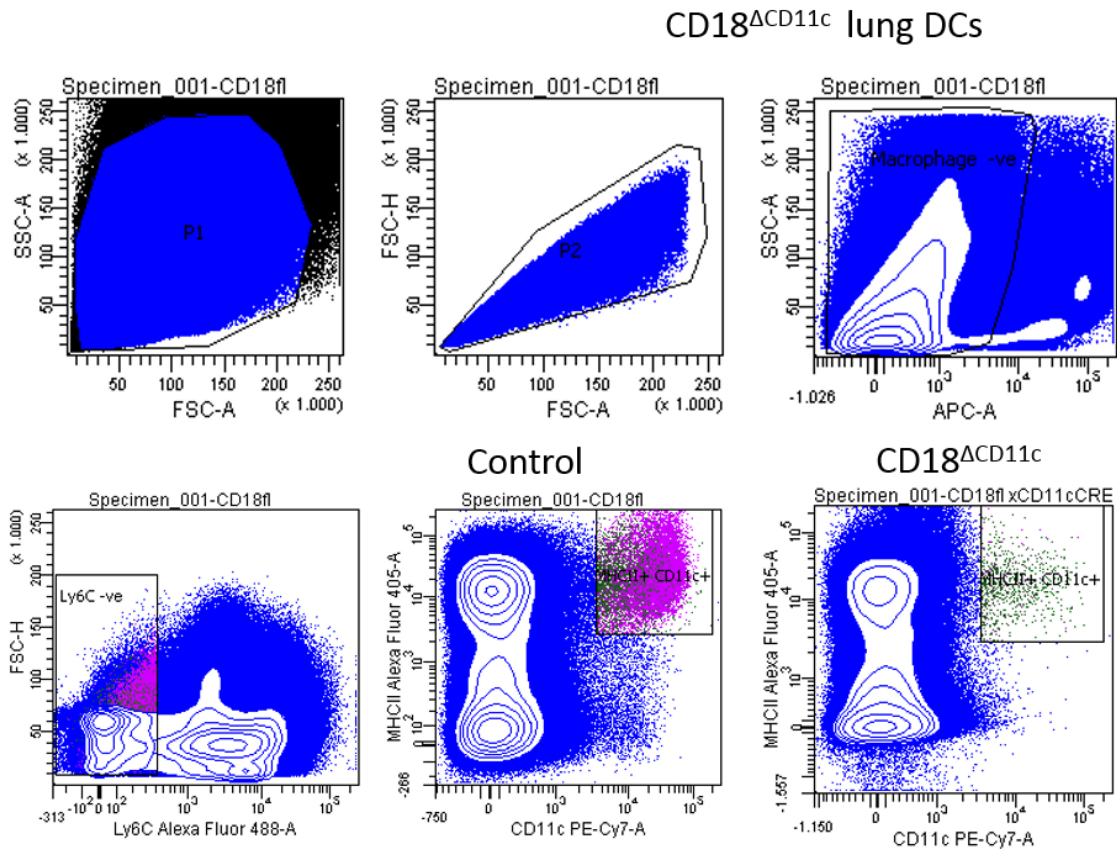
The CD45<sup>+</sup> leukocyte population from the skin cell suspension of CD18<sup>fl/fl</sup> and CD18<sup>ΔCD11c</sup> background were analysed for the expression of the following markers: MHC-II, CD18, CD11c

and CD11b. The MHC-II<sup>+</sup> population was explicitly analysed for the expression of CD11c, CD18 and CD11b separately (A). The expression of the  $\beta$ 2 integrin was evaluated as percentage of positives within the MHC-II<sup>+</sup> population (B). Depicted bars represent mean values with SEM (n=3). LD stand for fixable viability dye- only viable cells (LD-) were analysed.

### 2.2.5.3. Analysis of the murine lung CD18 <sup>$\Delta$ CD11c</sup> DC

Lungs of the CD18 <sup>$\Delta$ CD11c</sup> and CD18<sup>fl/fl</sup> mice were prepared and digested in solution containing Collagenase Type IA. Autofluorescent macrophage population was gated out during the flow cytometric analysis using a free detection channel (APC channel in this case). Further, the Ly6C (monocyte) negative population was sub-gated for MHC-II<sup>+</sup>CD11c<sup>+</sup> (Fig. 35A). The MHC-II<sup>+</sup>CD11c<sup>+</sup> double positive population constituted 4.3% of the macrophage/monocyte negative lung cell population in the CD18<sup>fl/fl</sup> control, whereas it was almost completely missing in the CD18 <sup>$\Delta$ CD11c</sup> knock-out (0.4%) (Fig. 35B).

A



B

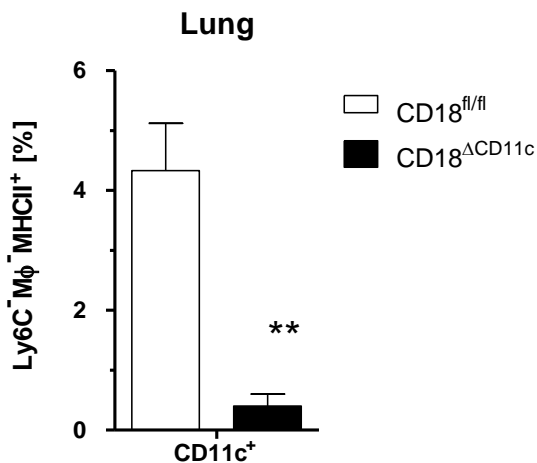


Figure 35. Analysis of the lung DC population in the CD18<sup>ΔCD11c</sup> mouse.

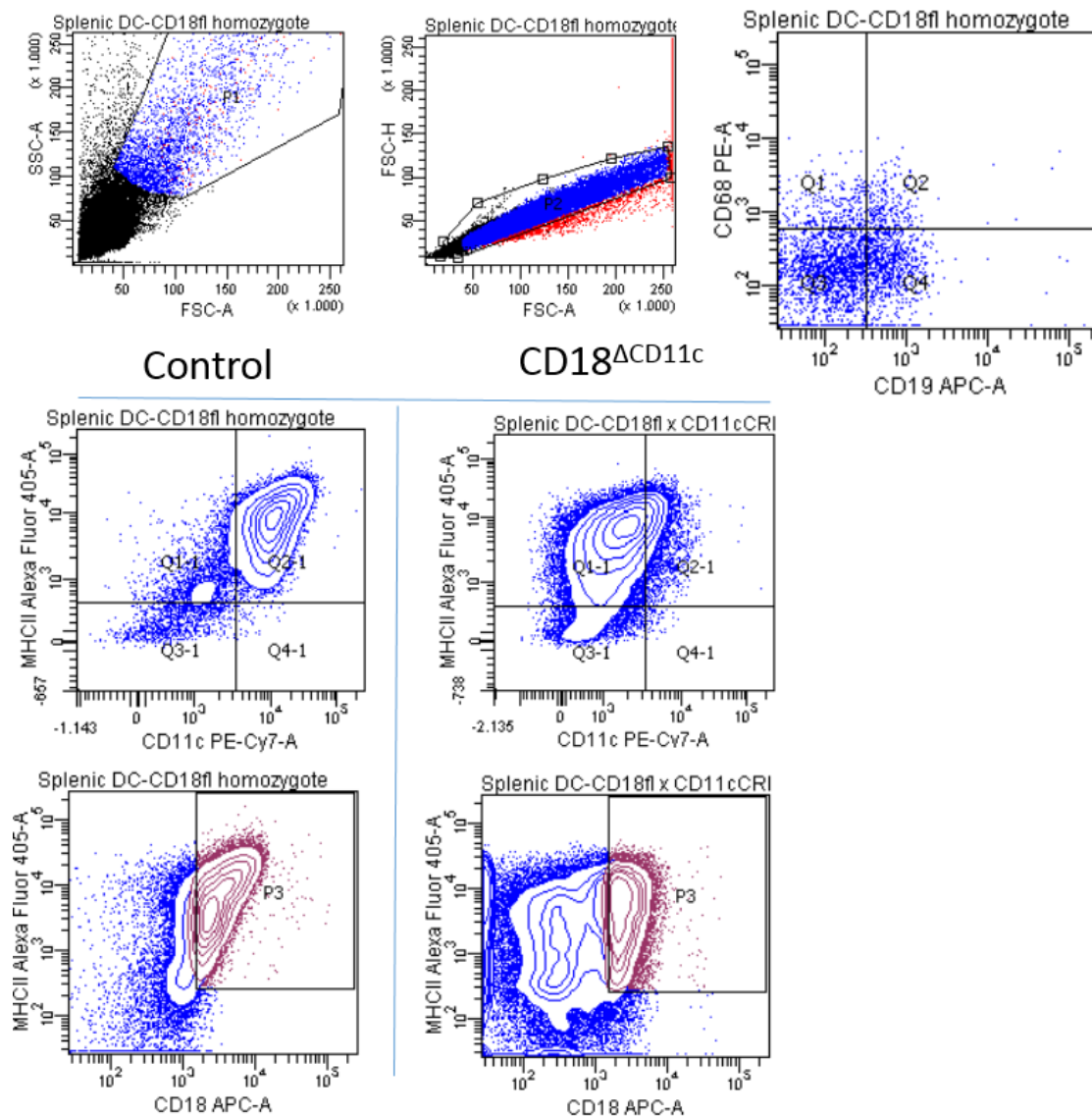
Digested lung cells from CD18<sup>fl/fl</sup> and CD18<sup>ΔCD11c</sup> mice were first gated on macrophage/monocyte negative population, i.e. APC channel (free channel for autofluorescent Macrophages) and Ly6C<sup>-</sup>. Subsequently the Mφ<sup>-</sup>/Ly6C<sup>-</sup> population was presented as double positive MHC-II<sup>+</sup>CD11c<sup>+</sup> (A). The MHC-II<sup>+</sup> population was explicitly analysed for the

expression of CD11c and was evaluated as percentage of positives within the MHC-II<sup>+</sup> population. Depicted bars represent mean with SEM (n=3).

#### 2.2.5.4. Analysis of the splenic CD18<sup>ΔCD11c</sup> DC

Spleens derived from CD18<sup>ΔCD11c</sup> and CD18<sup>fl/fl</sup> were prepared and the DC-population was enriched using the Pan Dendritic Cell Isolation Kit (Miltenyi Biotec). The isolated CD68<sup>-</sup>CD19<sup>-</sup> double negative population was analysed for the expression of MHC-II, CD11c and CD18 (Fig. 36A). Expression of CD11c and CD18 was presented as frequency of the CD68<sup>-</sup>CD19<sup>-</sup>MHC-II<sup>+</sup> cells. In the CD18<sup>ΔCD11c</sup> population the expression of CD18<sup>+</sup> cells dropped down to 13% and the expression of CD11c to 7%. In the CD18<sup>fl/fl</sup> control group both markers were expressed on 84-87% of the analysed CD68<sup>-</sup>CD19<sup>-</sup>MHC-II<sup>+</sup> population (Fig. 36B, C).

**A**



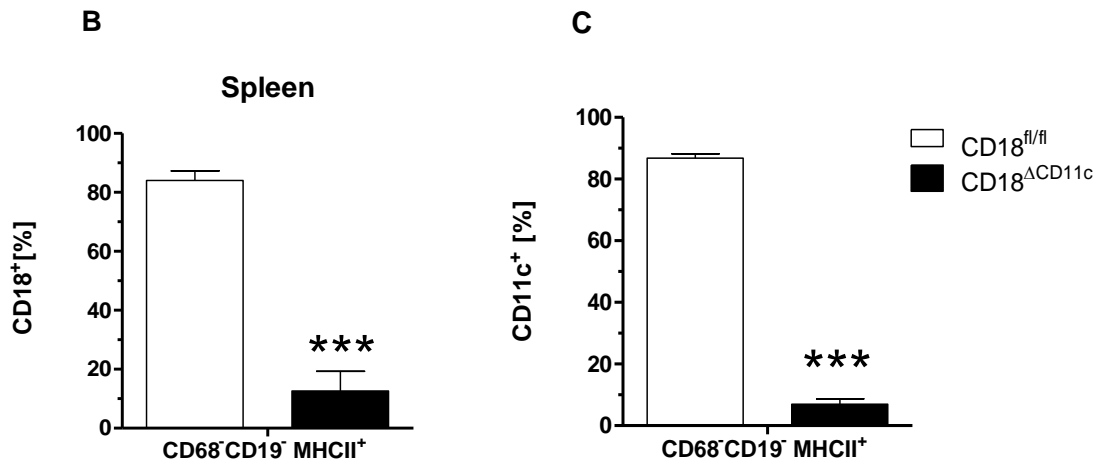


Figure 36. Analysis of the splenic DC population in the CD18<sup>ΔCD11c</sup> mouse.

The splenic cell-population was enriched in DC using the Pan Dendritic Cell Kit (Miltenyi Biotec). The CD68<sup>+</sup>CD19<sup>-</sup> double negative population was gated for the MHC-II and then further sub-gated for CD18 and CD11c (A). CD11c and CD18 positive fractions were evaluated as percentage of the mother population (B, C). Depicted bars represent mean values with SEM (n=3).

Splenic DC were further analysed for the expression of co-stimulatory molecules directly after isolation. The level of the MHC-II, CD80, CD86 and CD40 expression on the cell surface was assessed as mean fluorescence intensity (MFI) of the fluorescently labelled marker-specific antibody bound to the cell (Fig. 37A). There were no significant differences in the abundance of CD80, CD86 and CD40 between CD18<sup>fl/fl</sup> and CD18<sup>ΔCD11c</sup>, however expression of the MHC-II was slightly decreased in the knock-out reaching the MFI of 5827, whereas the control reached the MFI of 8186 (Fig. 37B-E).

The expression of the co-stimulatory molecules upon overnight TLR-ligand stimulation (Poly I:C, R848, LPS and CpG) was comparable in case of both CD18<sup>fl/fl</sup> control and CD18<sup>ΔCD11c</sup> mice, except for MHC-II, showing in both unstimulated and stimulated samples of CD18<sup>ΔCD11c</sup> mice a slightly lower expression level ( Appendix D).

A

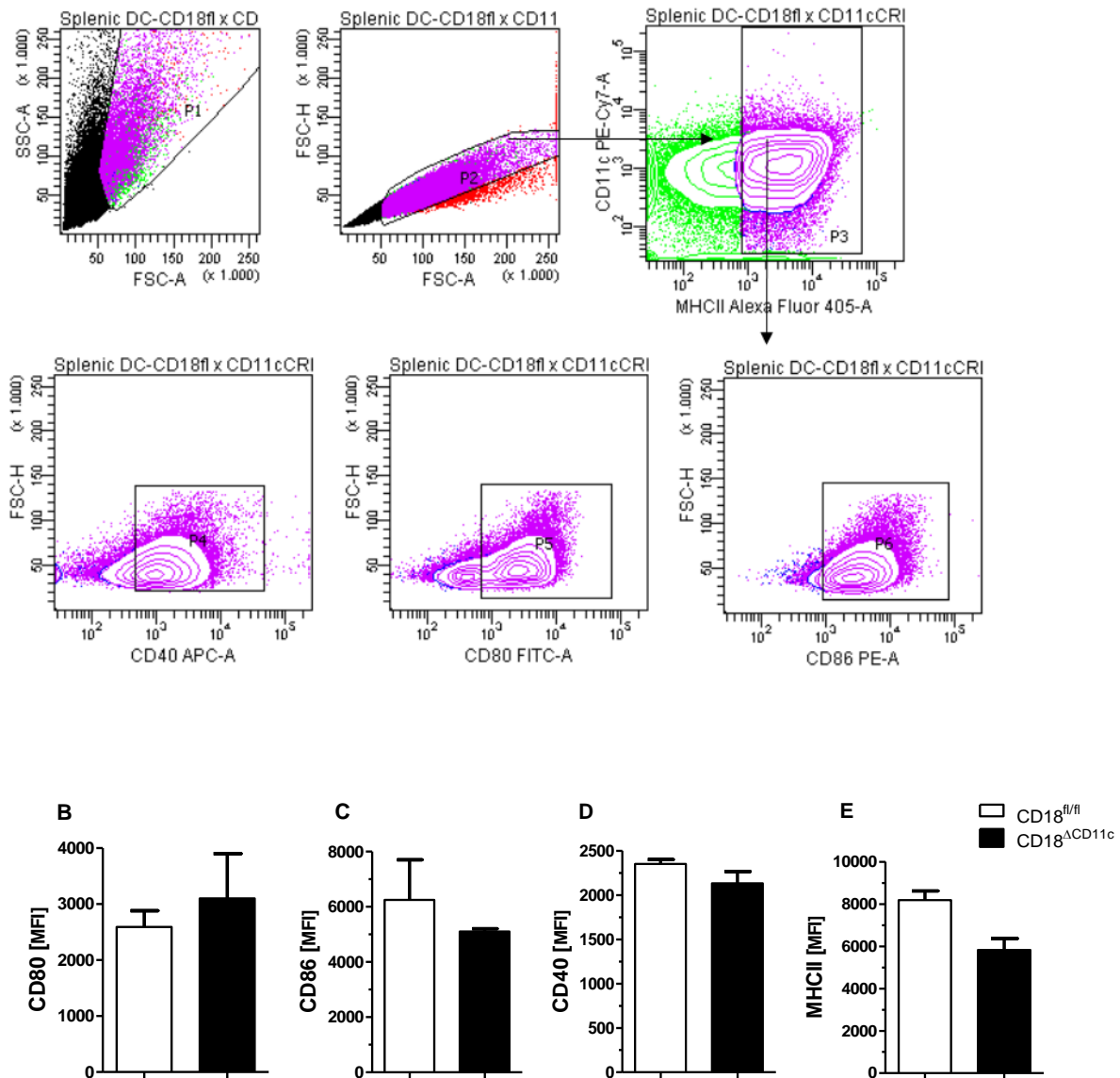


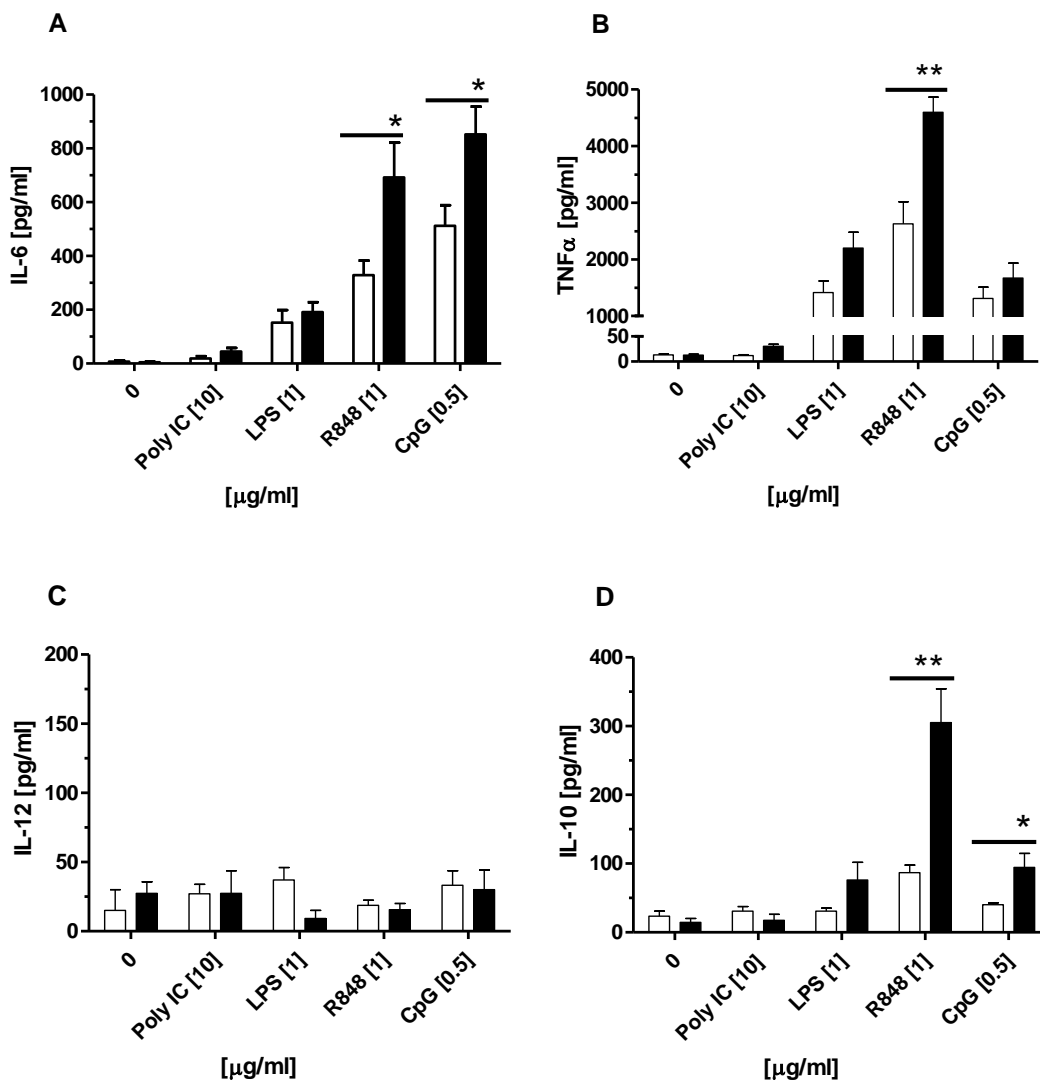
Figure 37. Activation markers on unstimulated splenic DC population in the CD18<sup>ACD11c</sup> mouse.

The splenic cell-population was enriched in DC using the Pan Dendritic Cell Kit (Miltenyi Biotec). Cells were gated for the MHC-II (E) and out of MHC-II<sup>+</sup> further sub-gated for CD80 (A), CD86 (B) and CD40(C). Gating strategy is presented in A. Expression of the activation markers was evaluated as mean fluorescent intensity (MFI). Depicted bars represent mean with SEM (n=2).

#### 2.2.5.5. Cytokine secretion by stimulated splenic CD18<sup>ACD11c</sup> DC

To investigate the cytokine release pattern of CD18<sup>ACD11c</sup> DC after overnight stimulation with different TLR ligands, spleens from CD18<sup>ACD11c</sup> and CD18<sup>fl/fl</sup> were isolated and the DC

fractions were enriched using the Pan Dendritic Cells Kit (Milteyi Biotec). Cells were stimulated overnight with Poly I:C, LPS, R848 or CpG and subsequently supernatants were collected for further analysis. Using a CBA the following cytokines were measured in the culture supernatants: IL-6, TNF- $\alpha$ , IL-12, IL-10, and IL-1 $\beta$  (Fig.38). Poly I:C stimulation induced similar, moderate cytokine secretion in both groups. LPS stimulated CD18 $\Delta$ CD11c splenic DC showed a tendency to express higher levels of TNF- $\alpha$ , IL-10, and IL-1 $\beta$ . Likewise, incubation of DC with CpG led to a significantly higher secretion of IL-6 and IL-10 in the CD18 $\Delta$ CD11c DC. R848 proved to be the most potent stimulator and induced a significantly elevated secretion of IL-6, IL-10 and TNF- $\alpha$  and IL-12. R848 induced cytokine secretion in a dose dependent manner, reaching the maximal stimulation at 10ng/ml in case of TNF- $\alpha$  and IL-12 and at 100ng/ml in case of IL-10 and IL-6 (Fig. 39).



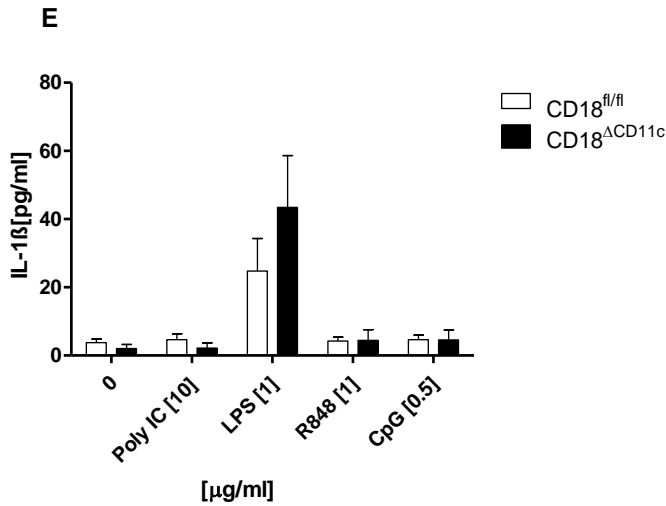
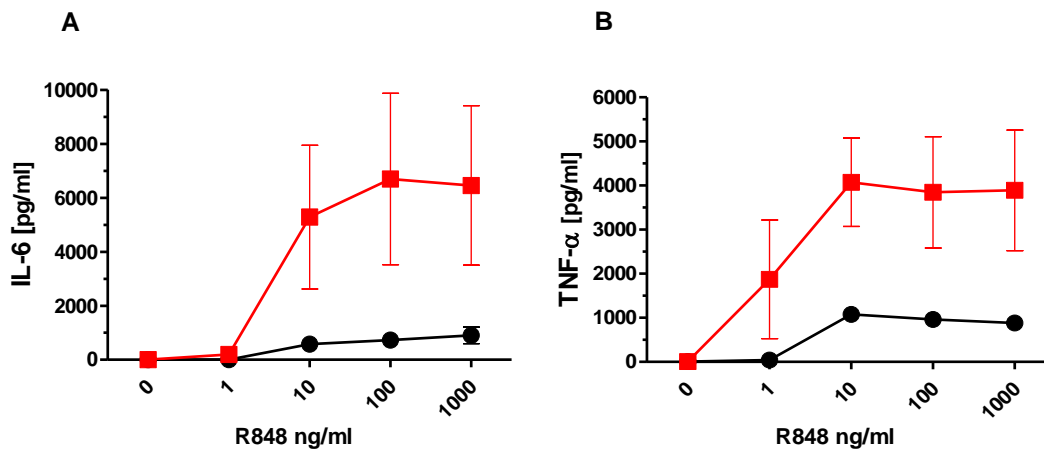


Figure 38. Cytokine secretion by splenic CD18<sup>ΔCD11c</sup> upon TLR-ligand stimulation.

Splenic DC population (enriched using Miltenyi Pan Dendritic Cell Kit) was stimulated overnight with PolyI:C (10μg/ml), LPS (1μg/ml), R848 (1μg/ml) and CpG (0.5μg/ml). Cytokine secretion (IL-6-A, TNF-α-B, IL-12-C, IL-10-D, and IL-1β-E) was measured in the supernatants using a cytometric bead array (BD Pharminogen). Depicted bars represent mean with SEM (n=5, with exception for IL-12: n=2-5).



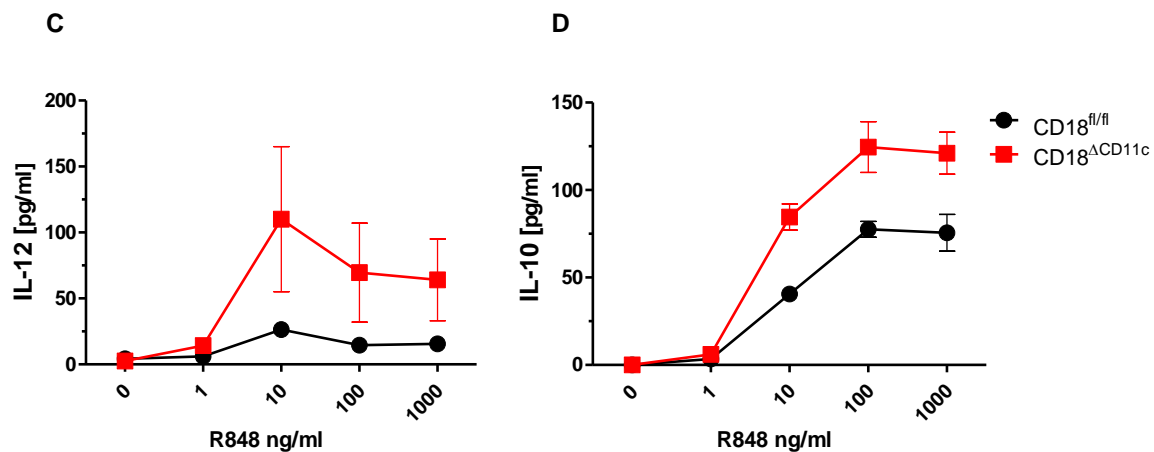


Figure 39. Dose dependent cytokine secretion by splenic CD18<sup>ACD11c</sup> upon R848 stimulation.

Splenic DC population was enriched using the Pan Dendritic Cell Kit (Milteyi). Cells were stimulated overnight with increasing concentrations of R848 (1<10<100<1000 ng/ml) and cytokines (IL-6-A, TNFa-B, IL-12-C, IL-10-D) were then measured in the supernatants using cytometric bead array (BD Pharminogen). Curves represent mean values with SEM (n=2).

#### 2.2.5.6. Cytokine mRNA expression by CD18<sup>ACD11c</sup> DC upon R848 stimulation

To analyse whether the elevated cytokine production in stimulated CD18<sup>ACD11c</sup> DC as compared to CD18<sup>fl/fl</sup> DC was due to transcriptional upregulation, splenic dendritic cells (isolated with the Pan Dendritic Cell Kit, Miltenyi Biotec) from CD18<sup>fl/fl</sup> and CD18<sup>ACD11c</sup> mice were stimulated with R848 (1µg/ml) and RNA was extracted after 1h and 4h of incubation. The extracted RNA was reverse-transcribed to cDNA and cytokine mRNA expression levels were analysed using real time quantitative PCR (qPCR) approach. The expression of cytokine-encoding mRNA was normalized to expression levels of ubiquitin C (UBC) as a housekeeping gene. The analysis revealed that expression of IL-6 mRNA was elevated in the CD18<sup>ACD11c</sup> DC already 1h after stimulation and at 4h time-point as compared with the control DC population (Fig. 40A). Expression of TNF-α mRNA was twice as high in the CD18<sup>ACD11c</sup> DC after 1h of stimulation and then dropped down to the level of the CD18<sup>fl/fl</sup> control at 4h time point (Fig. 40B), whereas IL-10 mRNA expression was even in both, the CD18<sup>fl/fl</sup> and CD18<sup>ACD11c</sup> group (Fig. 40C). Therefore, CD18 plays a role in the transcriptional regulation of the pro-inflammatory cytokines IL-6 and TNF-α in the stimulated DC.

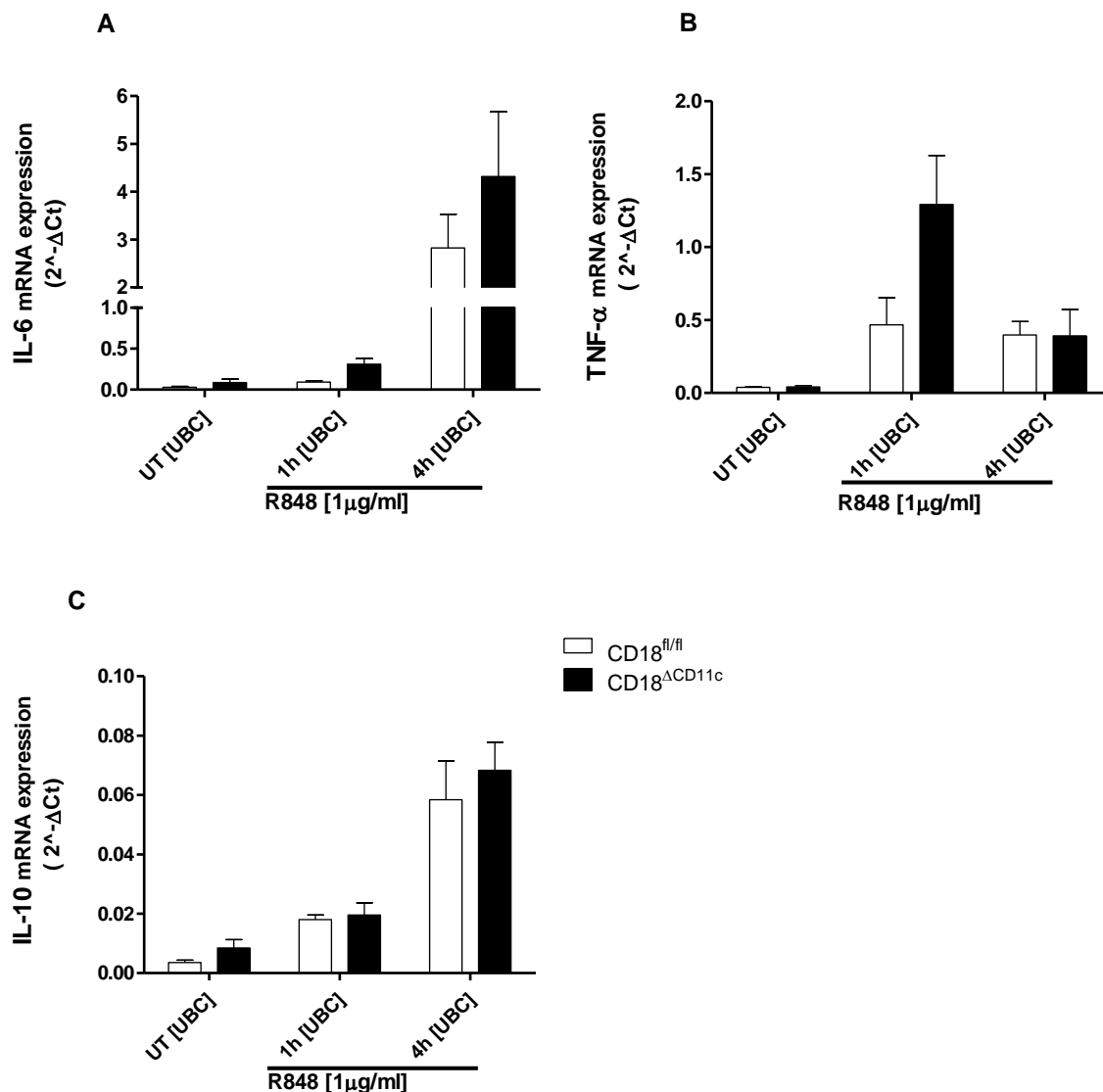


Figure 40. Cytokine mRNA expression by CD18<sup>ΔCD11c</sup> splenic DC upon R848 stimulation.

Splenic dendritic cells (isolated using Pan Dendritic Cell Kit, Miltenyi Biotec) were left unstimulated (UT), or were stimulated for 1h and 4h with R848 (1μg/ml), subsequently RNA was isolated and reverse-transcribed into cDNA. Expression of cytokine mRNA was evaluated using the qPCR approach. Following cytokines were analysed: IL-6(A), TNF-α (B), IL-10(C). Bars represent mean with SEM of the expression normalized to the housekeeping gene (UBC) (n=3-4).

#### 2.2.5.7. SOCS protein mRNA expression by CD18<sup>ΔCD11c</sup> splenic DC stimulated with R848

R848 stimulated splenic CD18<sup>ΔCD11c</sup> DC were analysed for the expression of suppressor of cytokine signalling proteins (SOCS) mRNA species. SOCS proteins are negative regulators of

the cytokine signalling and since CD18<sup>ΔCD11c</sup> DC presented with a higher cytokine secretion we speculated that CD18 may play a role in cytokine regulation via SOCS proteins. Expression of SOCS2 mRNA in the CD18<sup>ΔCD11c</sup> and CD18<sup>fl/fl</sup> samples increased constantly over the time of stimulation. However, the expression in CD18<sup>ΔCD11c</sup> DC was much lower (1.4-fold of the UBC) at 4h time point in comparison to the CD18<sup>fl/fl</sup> control (4-fold of UBC) (Fig. 41A). Expression of SOCS4 mRNA in the CD18<sup>ΔCD11c</sup> sample underwent a biphasic change, being strongly increased early after stimulation (12-fold of UBC after 1h), and dropped drastically 4h after stimulation (0.07-fold of the UBC) as compared with CD18<sup>fl/fl</sup> DC samples. Similarly to SOCS2, SOCS4 mRNA expression in the CD18<sup>fl/fl</sup> control sample gradually increased over time from a 0.3-fold after 1h to 2.5-fold of UBC expression after 4h (Fig. 41B). Consequently, after 4h of stimulation CD18<sup>ΔCD11c</sup> cells expressed less SOCS2 and SOCS4 mRNA as compared with the CD18<sup>fl/fl</sup> DC.

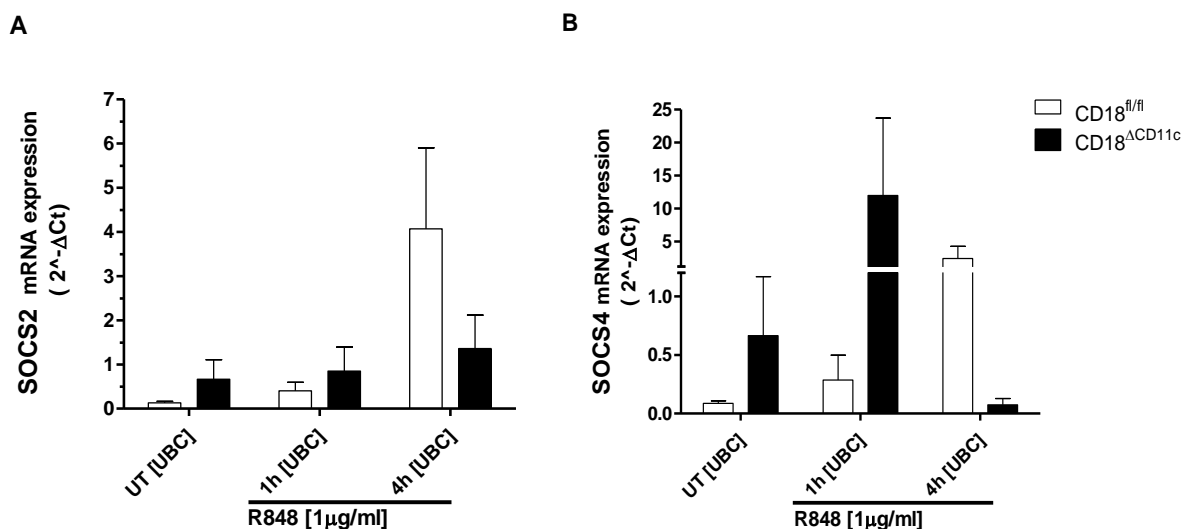


Figure 41. SOCS protein mRNA expression by CD18<sup>ΔCD11c</sup> splenic DC upon R848 stimulation. Splenic dendritic cells (isolated using Pan Dendritic Cell Kit, Miltenyi Biotec) were left unstimulated (UT), or were stimulated for 1h and 4h with R848 (1μg/ml), subsequently RNA was isolated and reverse-transcribed into cDNA. Expression of SOCS2 (A) (n=3-4) and SOCS4 (B) (n=2-4) mRNA was evaluated using the qPCR approach. Bars represent mean with SEM of the SOCS expression normalized to the housekeeping gene (UBC).

### 2.2.5.8. *In vitro* T cell stimulatory capacity of the splenic CD18<sup>ΔCD11c</sup> DC

In order to assess the T cell priming capacity of the CD18-deficient DC, spleens from CD18<sup>ΔCD11c</sup> as well as CD18<sup>fl/fl</sup> control mice were prepared and DC were acquired. T cells were added to serially diluted DC pre-treated with an adjuvant and an antigen. After several days of co-incubation tritium-labelled thymidine (3H-TdR) was added to the cultures to evaluate proliferation of the T lymphocytes. In addition, fractions of the co-culture supernatants were collected every day for the analysis of the cytokine production.

#### 2.2.5.8.1. *In vitro* proliferation of OT-II CD4 T-lymphocytes primed with CpG or R848 stimulated CD18<sup>ΔCD11c</sup> DC

To examine the CD4<sup>+</sup> T-cell stimulatory capacity of the CD18<sup>ΔCD11c</sup> DC, CD4<sup>+</sup> T cells were isolated from OT-II mice and co-incubated with serial dilutions of splenic DC. DC were stimulated with an adjuvant (CpG or R848) and an antigen (OVA-peptide). Supernatants were collected every day and analysed for the cytokine content (TNF- $\alpha$ , IL-2, IL-10, IFN- $\gamma$ ). Independent of the DC-activating agent (CpG or R848) CD18<sup>ΔCD11c</sup> DC induced comparable proliferation of the CD4<sup>+</sup> lymphocytes as the control CD18<sup>fl/fl</sup> DC (Fig. 42 and Fig. 44). In the cultures with OVA-CpG stimulated CD18<sup>ΔCD11c</sup> DC, secretion of TNF- $\alpha$ , IL-2, IL-10, and of IFN- $\gamma$  was elevated in comparison to the control co-cultures containing CD18<sup>fl/fl</sup> DC (Fig. 43). TNF- $\alpha$  secretion was elevated throughout the entire co-culture time, whereas IL-2, IL-10, and IFN- $\gamma$  in the last days of incubation. In the co-cultures containing OVA-R848 stimulated CD18<sup>ΔCD11c</sup> DC, secretion of TNF- $\alpha$  and IFN- $\gamma$  were elevated as compared with the control group, however levels of IL-2 and IL-10 secretion remained the same in both knock-out and control group (Fig. 45). Thus, *in vitro* co-cultures containing CD18<sup>ΔCD11c</sup> DC pre-treated with an antigen and TLR-ligand, CpG or R848, presented with an elevated cytokine secretion. This, however, had no functional consequences for the T lymphocyte proliferation.

**In vitro T cell (OT-II) proliferation assay with splenic CD18<sup>ΔCD11c</sup>DCs**

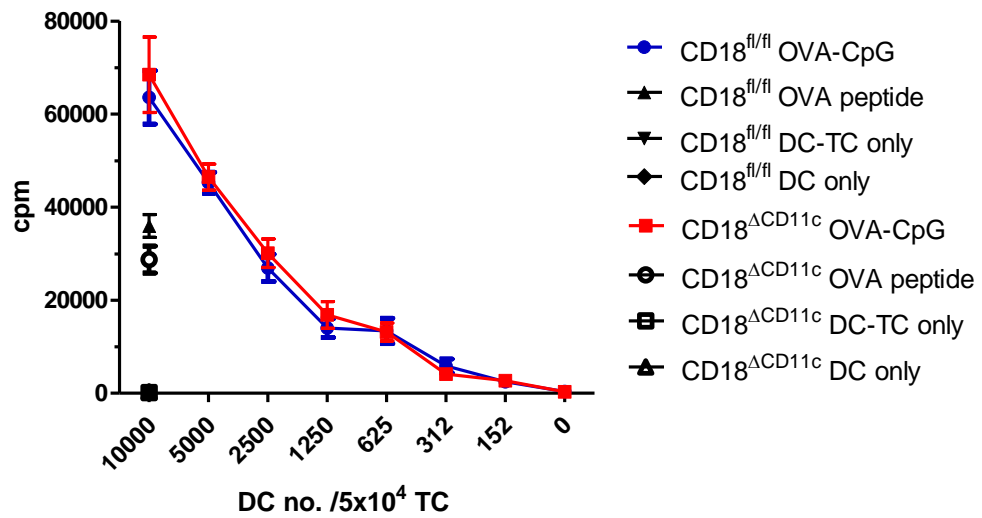
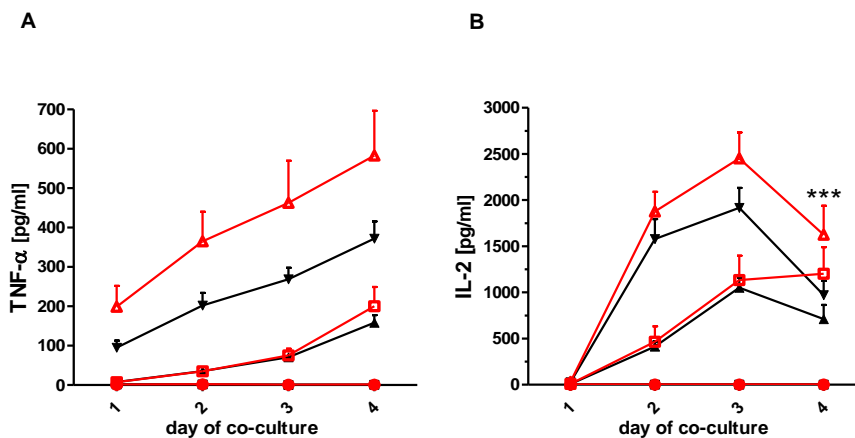


Figure 42. In vitro OT-II T-cell proliferation assay with CD18<sup>ΔCD11c</sup> DC stimulated with CpG.

CD4<sup>+</sup> T cells were co-incubated with DC-serial dilutions in presence of OVA peptide (100ng/ml) and CpG (100ng/ml) and after 4 days of culture tritium-labelled thymidine (<sup>3</sup>H-TdR) was added, cells were harvested the next day and DNA-incorporation of the <sup>3</sup>H-TdR was assessed with beta-counter. Co-cultures without adjuvant and antigen, as well as DC only were used as controls. Depicted curves represent mean values with SEM (n=6 for CD18<sup>fl/fl</sup> / n=5 for CD18<sup>ΔCD11c</sup>).



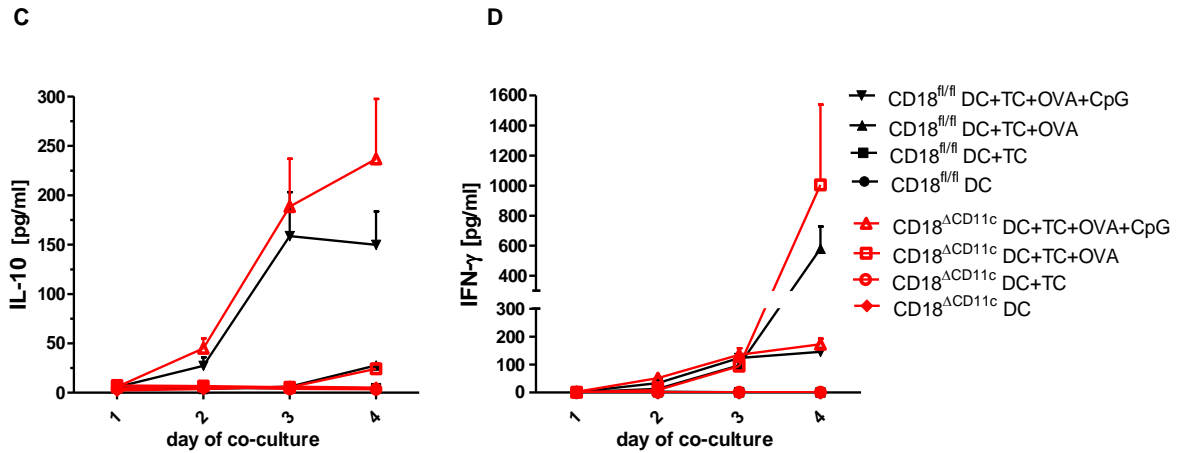


Figure 43. Cytokines produced in an *in vitro* OT-II T-cell proliferation assay with CD18<sup>ΔCD11c</sup> DC stimulated with CpG.

CD4<sup>+</sup> T cells were co-incubated with DC-serial dilutions in presence of OVA peptide (100ng/ml) and CpG (100ng/ml). Supernatants were collected every day of the co-culture and release of TNF-α(A), IL-2(B), IL-10(C), and IFN-γ(D) was analysed. Co-cultures without adjuvant and antigen, as well as DC only were used as controls. Depicted curves represent mean values with SEM (n=6 for CD18<sup>fl/fl</sup> / n=5 for CD18<sup>ΔCD11c</sup>).

**In vitro T cell (OT-II) proliferation with R848 stimulated splenic CD18<sup>ΔCD11c</sup> DCs**

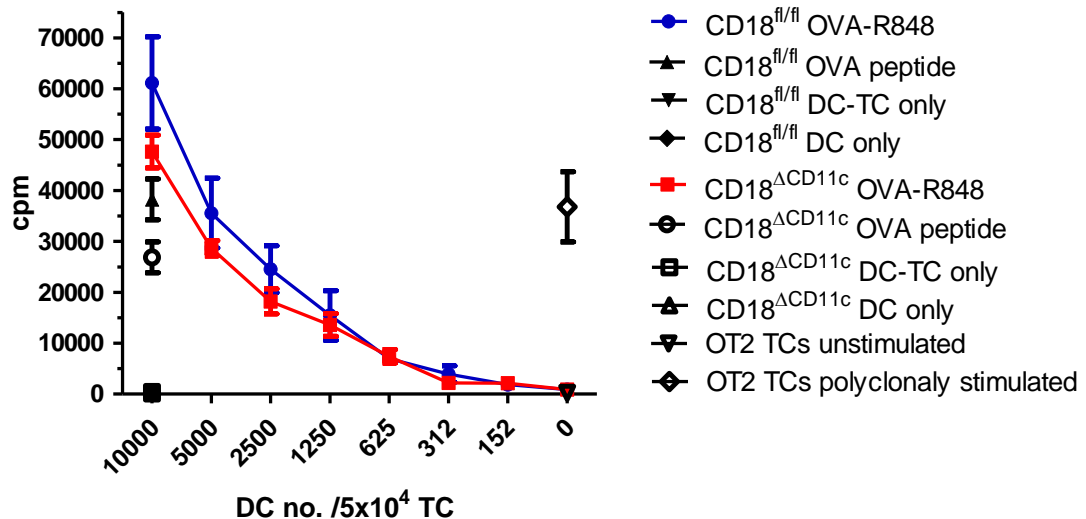


Figure 44. *In vitro* OT-II T-cell proliferation assay with CD18<sup>ΔCD11c</sup> DC stimulated with R848.

CD4<sup>+</sup> T cells were co-incubated with DC-serial dilutions in presence of OVA peptide (100ng/ml) and R848 (100ng/ml) and after 3 days of culture tritium-labelled thymidine (<sup>3</sup>H-TdR) was added, cells were harvested the next day and DNA-incorporation of the <sup>3</sup>H-TdR was

assessed with beta-counter. Co-cultures without adjuvant and antigen, as well as DC only were used as controls. Depicted curves represent mean values with SEM (n=4).

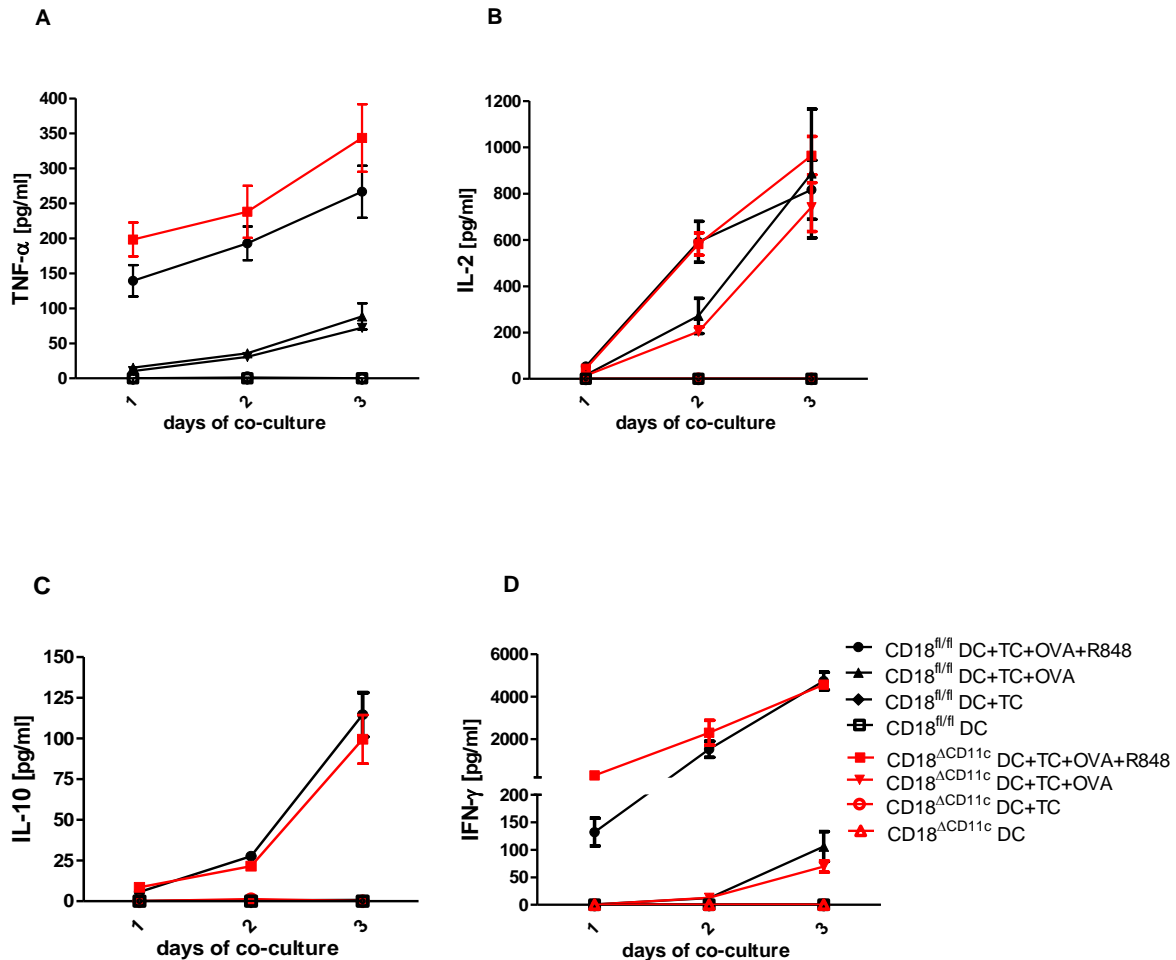


Figure 45. Cytokines produced in an *in vitro* OT-II T-cell proliferation assay with CD18<sup>ΔCD11c</sup> DC stimulated with R848.

CD4<sup>+</sup> T cells were co-incubated with DC-serial dilutions in presence of OVA peptide (100ng/ml) and R848 (100ng/ml). Supernatants were collected every day of the co-culture and release of TNF-α(A), IL-2(B), IL-10(C), and IFN-γ(D) was analysed. Co-cultures without adjuvant and antigen, as well as DC only were used as controls. Depicted curves represent mean values with SEM (n=4).

2.2.5.8.2. *In vitro* proliferation of OT-I CD8 T-lymphocytes primed with R848 stimulated CD18<sup>ΔCD11c</sup> DC

To examine the CD8<sup>+</sup> T-cell stimulatory capacity of CD18<sup>ΔCD11c</sup> DC, CD8<sup>+</sup> T cells were isolated from an OT-I mouse and co-incubated with serial dilutions of DC derived from

CD18<sup>ΔCD11c</sup> or CD18<sup>fl/fl</sup> mouse. Co-cultures were carried out in the presence of a DC-activating agent (R848) and an antigen (SIINFEKL). Supernatants were collected on two consecutive days of the co-culture and analysed for cytokine content (TNF- $\alpha$ , IL-2, IFN- $\gamma$ ). CD18<sup>ΔCD11c</sup> DC induced similar proliferation of the CD8<sup>+</sup> lymphocytes as the control CD18<sup>fl/fl</sup> DC (Fig. 46). A slightly reduced proliferation of the T cell in cultures with highest DC concentration may be due to overstimulation and subsequent exhaustion of T cells.

On the first day of culture cytokine release did not differ between the groups. On the second day CD18<sup>ΔCD11c</sup> cultures stimulated with SIINFEKL showed a somewhat higher secretion of TNF- $\alpha$ , IL-2, and IFN- $\gamma$ . In the cultures containing fully stimulated CD18<sup>ΔCD11c</sup> DC (SIINFEKL+R848), overall cytokine levels were similar as in the control group (Fig. 47).

***In vitro* T Lymphocyte (OT-I) proliferation with R848stimulated splenic CD18<sup>ΔCD11c</sup> DCs**

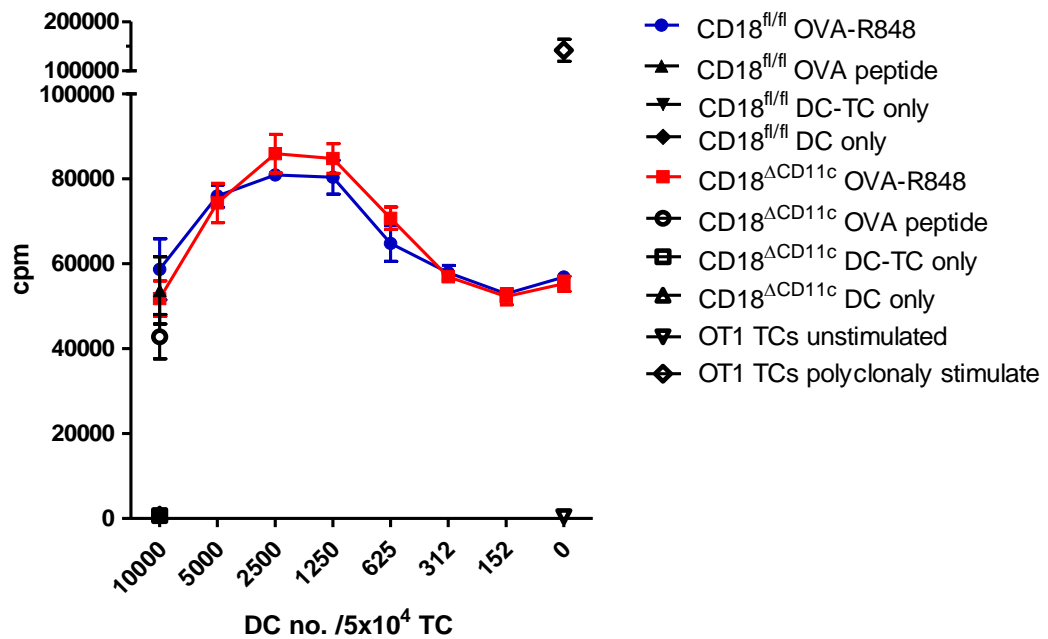


Figure 46. *In vitro* OT-I T-cell proliferation assay with CD18<sup>ΔCD11c</sup> DC stimulated with R848. CD8<sup>+</sup> T cells were co-incubated with serial dilutions of DC in presence of SIINFEKL (100ng/ml) and R848 (100ng/ml) and after 3 days of culture tritium-labelled thymidine (<sup>3</sup>H-TdR) was added, cells were harvested the next day and DNA-incorporation of the <sup>3</sup>H-TdR was assessed with beta-counter. Co-cultures without adjuvant and antigen, as well as DC only were used as controls. Depicted curves represent mean values with SEM (n=4).

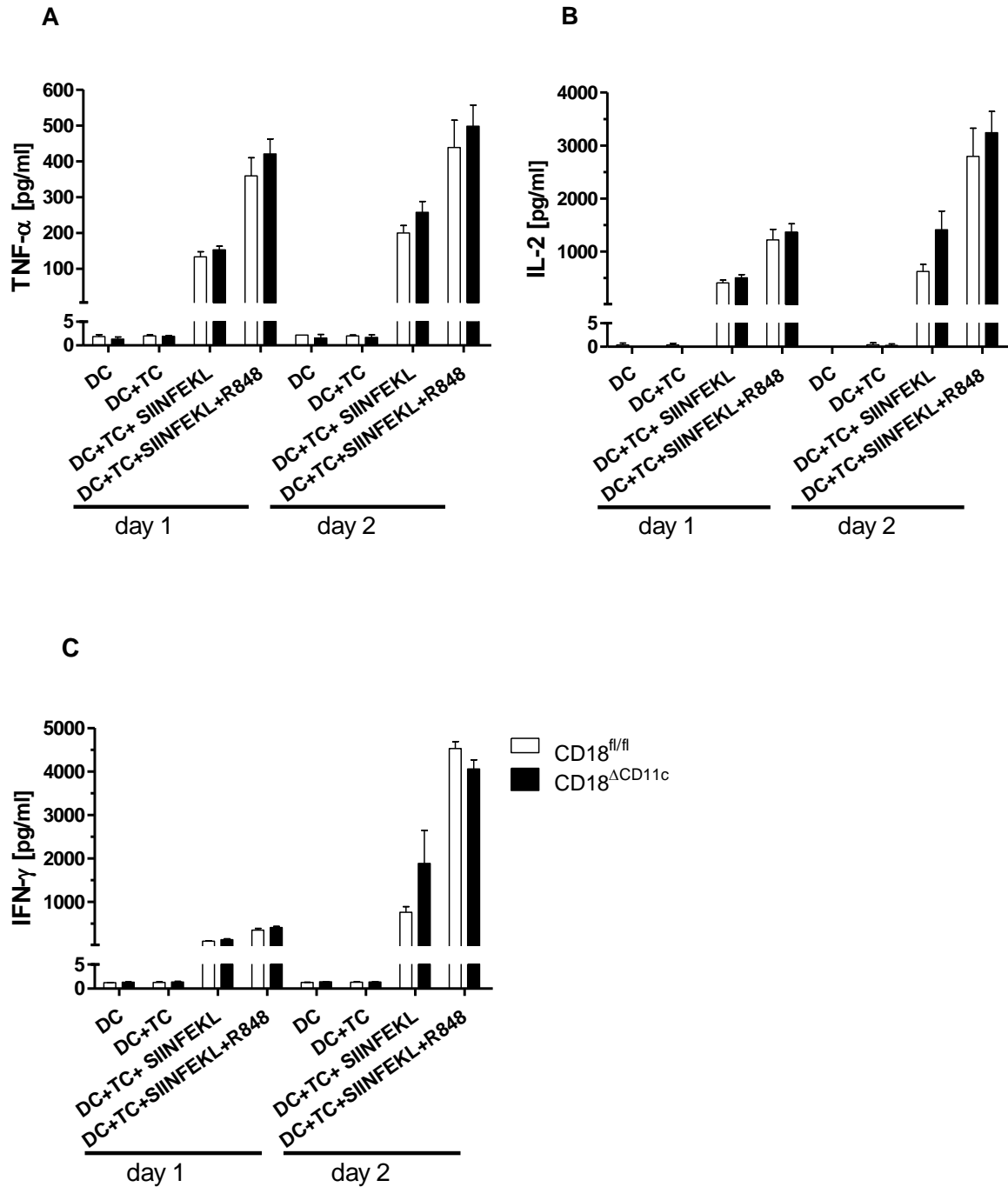


Figure 47. Cytokines produced in an in vitro OT-I T cell proliferation assay with CD18<sup>ΔCD11c</sup> DC stimulated with R848.

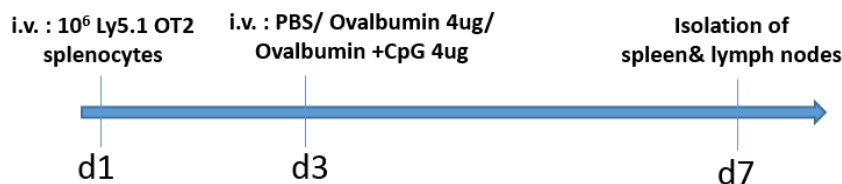
CD8<sup>+</sup> T cells were co-incubated with DC-serial dilutions in presence of SIINFEKL (100ng/ml) and R848 (100ng/ml). Supernatants were collected on two consecutive days of the co-culture and release of TNF- $\alpha$  (A), IL-2 (B), and IFN- $\gamma$ (C) was analysed. Co-cultures without adjuvant and antigen, as well as DC only were used as controls. Depicted bars represent mean values with SEM (n=4).

### 2.2.5.9. *In vivo* T cell stimulatory capacity of the CD18<sup>ΔCD11c</sup> DC

To investigate the T cell stimulatory capacity of CD18<sup>ΔCD11c</sup> DC *in vivo*, CFSE labelled splenocytes derived from the OT-I or OT-II x Ly5.1 mice were injected intravenously into CD18<sup>ΔCD11c</sup> and CD18<sup>fl/fl</sup> mice and their proliferation was analysed after subsequent administration of adjuvant and antigen.

#### 2.2.5.9.1. *In vivo* OT-II T-cell proliferation in the CD18<sup>ΔCD11c</sup> mice

To assess proliferation of CD4<sup>+</sup> T lymphocytes *in vivo* in the CD18<sup>ΔCD11c</sup> background, splenocytes derived from OT-II x Ly5.1 mice were labelled *in vitro* with CFSE and injected intravenously in parallel into CD18<sup>ΔCD11c</sup> and CD18<sup>fl/fl</sup> mice. Four days after injection of OVA and CpG, CD45.1<sup>+</sup> T lymphocytes were retrieved from the spleen and their proliferation was assessed as CFSE dilution of the CD3<sup>+</sup>CD4<sup>+</sup> cell population (Fig. 48). In the PBS control group only a background amount of about 10% cells underwent one division, which was non-specific in both groups (Fig. 49A). In the OVA injected CD18<sup>ΔCD11c</sup> group more T cells underwent first and second division as compared to the CD18<sup>fl/fl</sup> control group (Fig. 49B), whereas in the fully stimulated OVA+CpG group no differences were observed between CD18<sup>ΔCD11c</sup> and CD18<sup>fl/fl</sup> mice with regard to T cell proliferation (Fig. 49C).



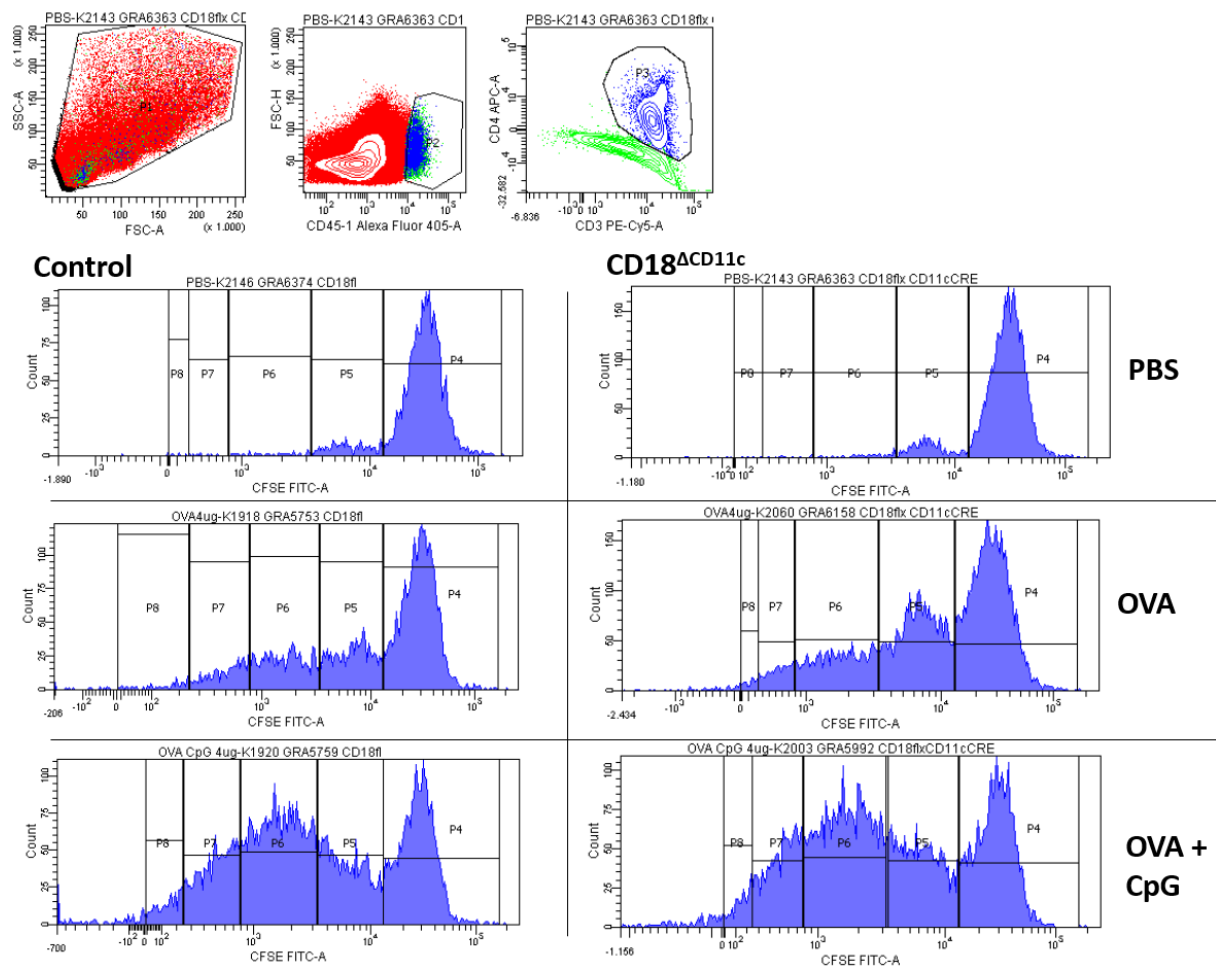


Figure 48. Gating strategy for the *in vivo* OT-II T cell proliferation in  $CD18^{\Delta CD11c}$  mice.

$CD18^{\Delta CD11c}$  and  $CD18^{fl/fl}$  mice were injected with CFSE labelled splenocytes, after subsequent OVA and CpG injections splenocytes were retrieved and *ex vivo* analysed using flow cytometry.  $CD45.1^+$  population was sub-gated for  $CD3^+CD4^+$  lymphocytes and the intracellular CFSE content was analysed on a histogram. Mother population (with highest CFSE content) was gated according to the PBS group and daughter populations with divided lymphocytes were gated, where CFSE signal weakened down.

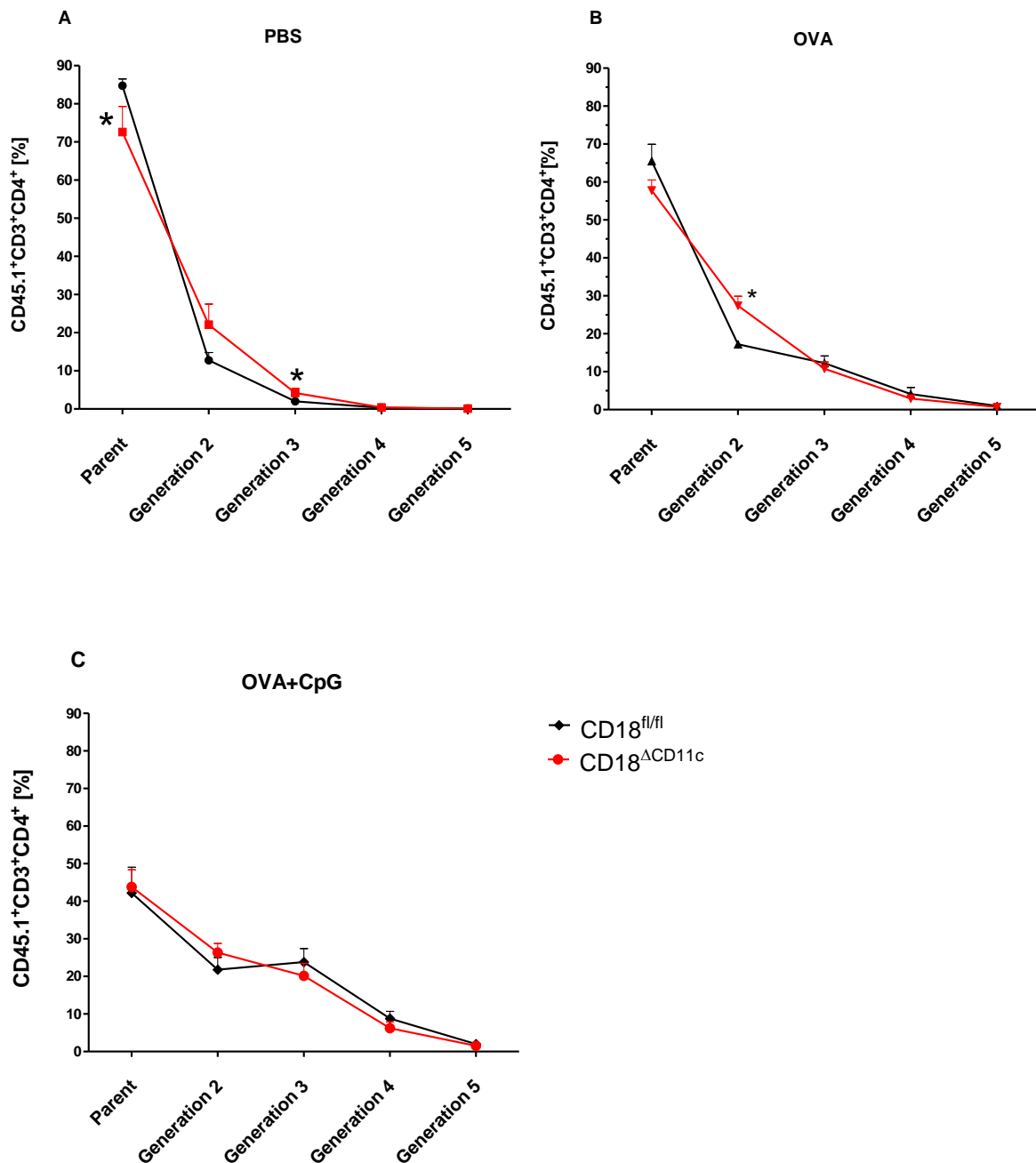


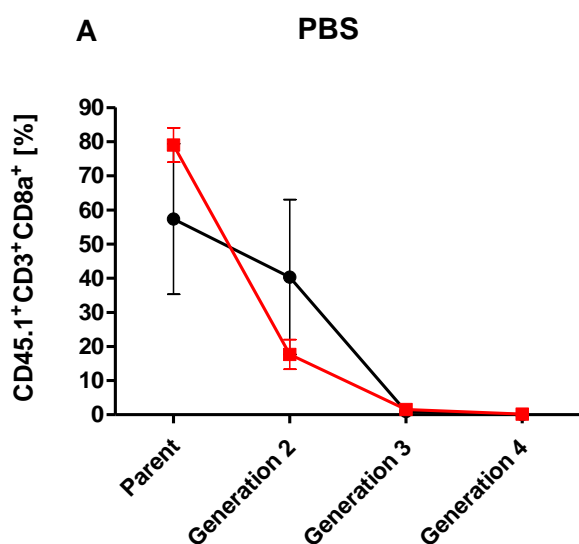
Figure 49. In vivo OT-II T cell proliferation in CD18<sup>ΔCD11c</sup> mice.

CD18<sup>ΔCD11c</sup> and CD18<sup>fl/fl</sup> mice were injected with CFSE labelled splenocytes, and after subsequent OVA and CpG injections splenocytes were retrieved and ex vivo analysed using flow cytometry. The CD45.1<sup>+</sup> population was sub-gated for CD3<sup>+</sup>CD4<sup>+</sup> lymphocytes and the intracellular CFSE content was analysed. The T lymphocyte parent population (non-divided) and subsequent daughter populations that underwent divisions are presented as fractions (%) of total CD45.1<sup>+</sup>CD3<sup>+</sup>CD4<sup>+</sup> T cell population. Three groups were analysed: PBS control group (A), OVA group (B) and fully stimulated OVA+CpG group (C). Lines represent mean with SEM

( $CD18^{fl/fl}$ :  $n=4$  in control groups/ $n=5$  in OVA/CpG group;  $CD18^{\Delta CD11c}$ :  $n=5$  in control groups/ $n=6$  in OVA/CpG group).

2.2.5.9.2. *In vivo* OT-I T-cell proliferation in the  $CD18^{\Delta CD11c}$  mice

To assess proliferation of  $CD8a^+$  T lymphocytes *in vivo* in the  $CD18^{\Delta CD11c}$  background, splenocytes from the OT-I x Ly5.1 mice were injected intravenously into  $CD18^{\Delta CD11c}$  and  $CD18^{fl/fl}$  mice. Four days after SIINFEKL and CpG injections,  $CD45.1^+$  T lymphocytes were retrieved from the spleen and their proliferation was assessed as CFSE dilution of the  $CD3^+CD8^+$  cell population. As observed for the  $CD4^+$  OT-II T cells, no differences in OT-I T cell proliferation were noted between  $CD18^{\Delta CD11c}$  and  $CD18^{fl/fl}$  background in any of the analysed group (Fig. 50).



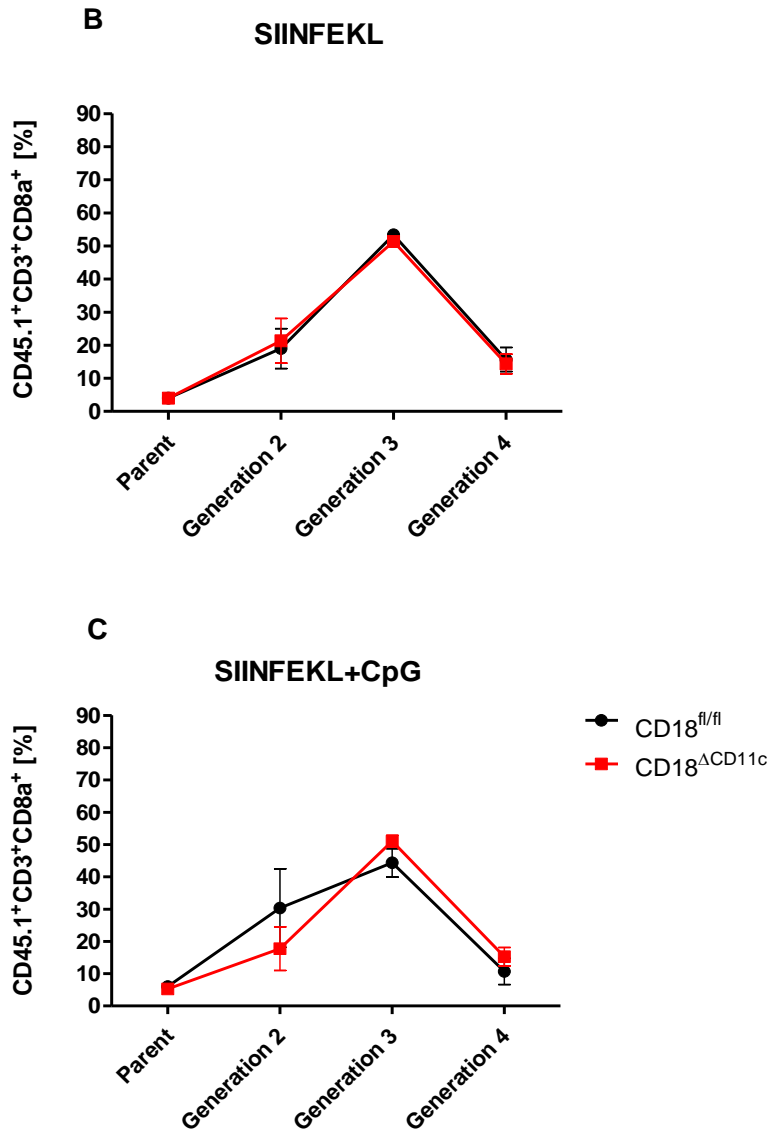


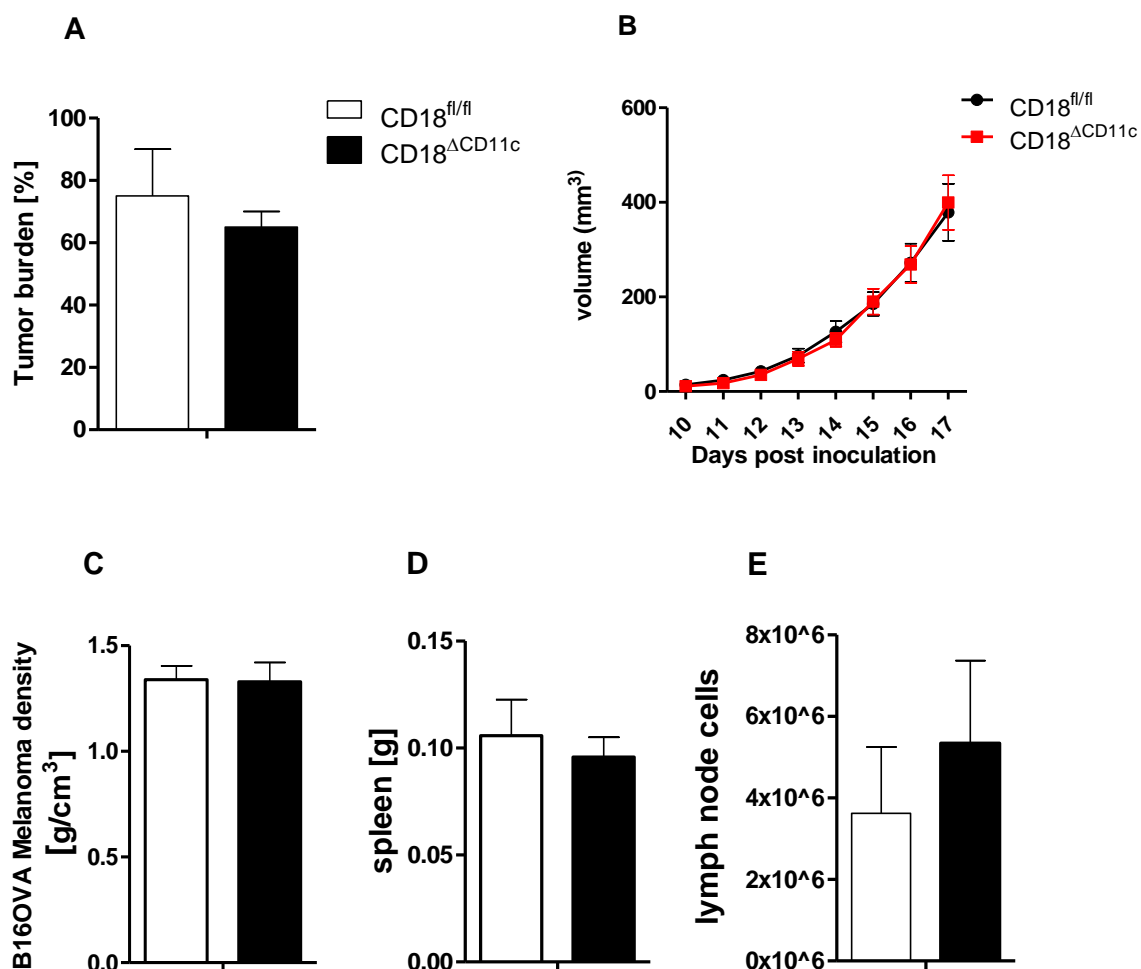
Figure 50. *In vivo* OT-I T cell proliferation in CD18<sup>ΔCD11c</sup> mice.

CD18<sup>ΔCD11c</sup> and CD18<sup>fl/fl</sup> mice were injected with CFSE labelled splenocytes (day 1), and after subsequent SIINFEKL and CpG (day 3) injections splenocytes were retrieved and *ex vivo* analysed using flow cytometry (day 7). The CD45.1<sup>+</sup> population was sub-gated for CD3<sup>+</sup>CD8a<sup>+</sup> lymphocytes and the intracellular CFSE content was analysed. The T lymphocyte parent population (non-divided) and subsequent daughter populations that underwent divisions are presented as fractions (%) of total CD45.1<sup>+</sup>CD3<sup>+</sup>CD8a<sup>+</sup> T cell population. Three groups were analysed: PBS control group (A), SIINFEKL group (B) and fully stimulated SIINFEKL+CpG group (C). Lines represent mean with SEM (n=3).

### 2.2.6. Tumour growth in CD18<sup>ΔCD11c</sup> mice

To analyse the role of  $\beta$ 2 integrins on DC for tumour development, CD18<sup>ΔCD11c</sup> and CD18<sup>fl/fl</sup> were inoculated subcutaneously with B16-OVA melanoma cells. Tumour growth measurements as well as *ex vivo* analysis of lymphatic organs were performed.

CD18<sup>ΔCD11c</sup> mice showed an insignificantly lower frequency of tumour development after inoculation with B16/OVA melanoma cells (Fig. 51A). The growth rate and densities were, nevertheless, virtually the same in both groups (Fig. 51B, C). The spleen mass was comparable in both groups (Fig. 51D). Despite a higher draining lymph node cell count in case of the tumour-burdened CD18<sup>ΔCD11c</sup> mice, lymphocytes showed less proliferation after *in vitro* restimulation (Fig. 51E, F).



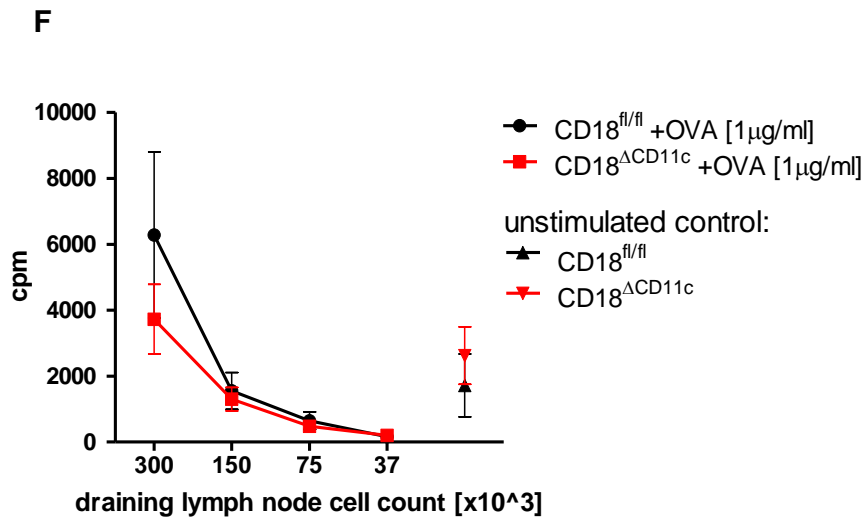


Figure 51. Analysis of tumour and lymphatic organs from CD18<sup>ΔCD11c</sup> mice inoculated with B16-OVA melanoma.

Twenty mice of CD18<sup>fl/fl</sup> and CD18<sup>ΔCD11c</sup> genotype were inoculated subcutaneously with B16-OVA melanoma and subsequently tumour growth (B), tumour density (C), spleen weight (D), draining lymph node cell count (E) and draining lymph node cell ex vivo stimulatory capacity (F) were analysed in mice that developed tumour (A). Bars and curves represent mean values with SEM (A: n=20, B/C/D/E: n>11, F: n=7).

## 2.3. The role of CD11b for tumour development

To study the role of CD11b for tumour development, CD11b<sup>-/-</sup> and WT mice were inoculated subcutaneously with B16-OVA melanoma and subsequently analysed with regard to tumour growth, the composition and activation state of immune cells within the tumour mass and draining lymph node. Tumour growth was measured every consecutive day with a calliper (starting around day 10 after injection) and after it reached a size of 700-800 mm<sup>3</sup> mice were sacrificed for subsequent analysis.

### 2.3.1. Tumour growth in CD11b<sup>-/-</sup> mice

In initial experiments potential effects of Mac-1 and β2 integrins on the *in vivo* T cell stimulatory capacity were tested.

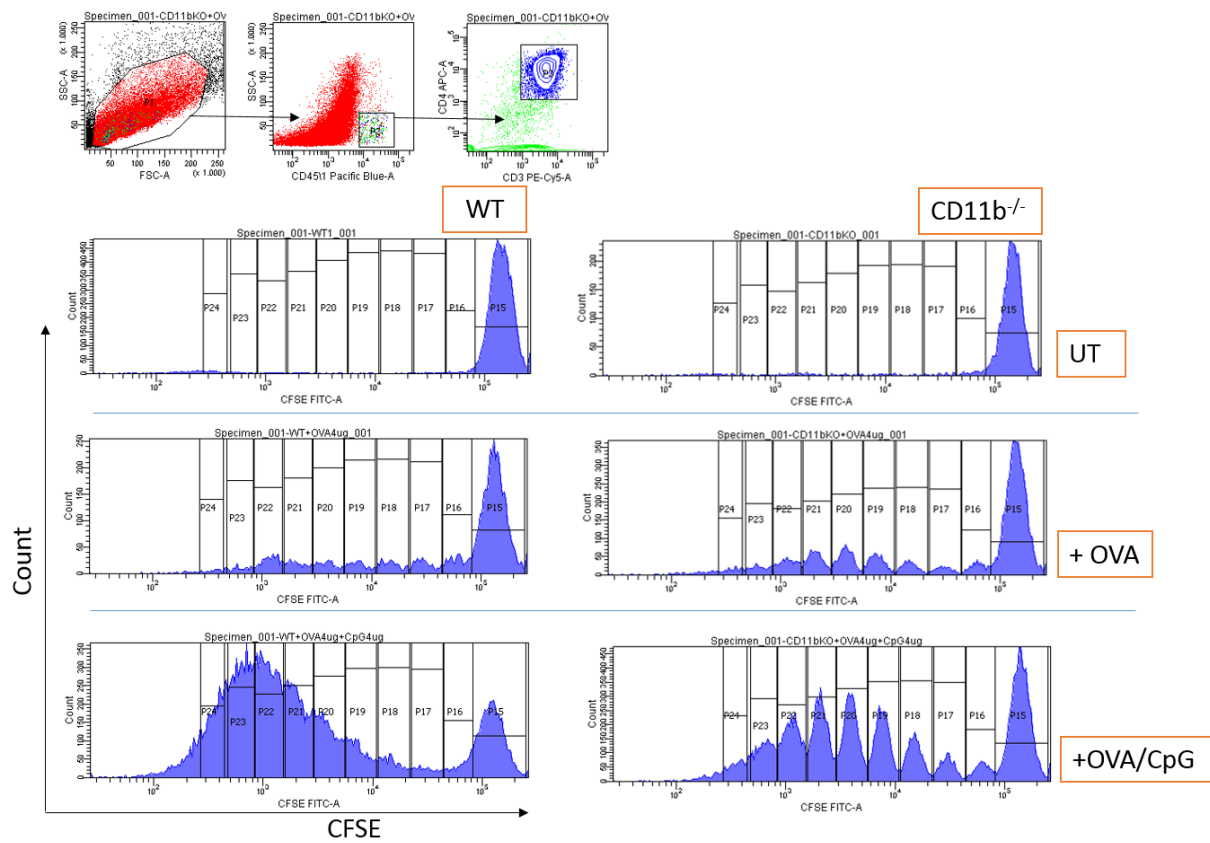
### 2.3.1.1. *In vivo T cell proliferation assay in the CD11b<sup>-/-</sup> background*

To assess the T cell stimulatory capacity of antigen presenting cells in CD11b<sup>-/-</sup> mice splenocytes from Ly5.1/OT2 or Ly5.1/OT1 mice were labelled with CFSE *in vitro* and then injected intravenously into WT and CD11b<sup>-/-</sup> recipient mice. Subsequently, the recipients were immunized with an antigen (OVA grey peptide or SIINFEKL) and an adjuvant (CpG). After several days spleens were isolated and the proliferation of T-lymphocytes was evaluated as CFSE fluoresce intensity of divided T cells via flow cytometry (Fig. 52A).

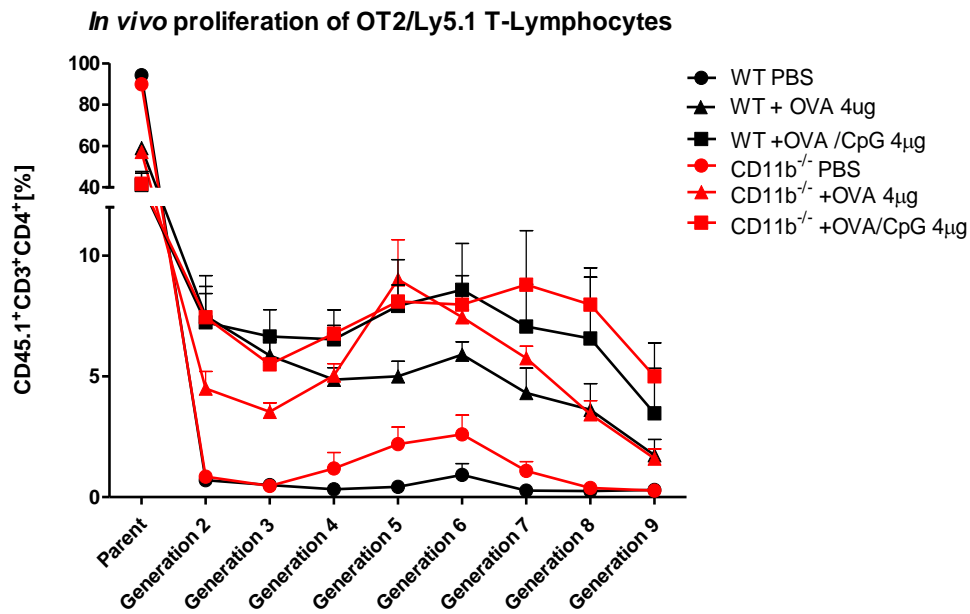
Ly5.1/OT2 T lymphocytes isolated from CD11b<sup>-/-</sup> mice immunized with OVA-ODN and CpG displayed enhanced proliferation as reflected by a larger fraction of T cells in the late generations in comparison to T cells derived from accordingly treated WT mice. Sixth till ninth generation of the divided T cells was on average 20% greater in the CD11b<sup>-/-</sup> compared with WT. In unstimulated and antigen stimulated mice T cells proliferated slightly better in CD11b<sup>-/-</sup> recipient mice in the middle, 5<sup>th</sup> till 7<sup>th</sup>, generations (Fig. 52B). Altogether CD4<sup>+</sup> TC were enriched in later generation in the CD11b<sup>-/-</sup>, i.e. they proliferated more frequently than in the WT group.

*Ex vivo* restimulated splenocytes from CD11b<sup>-/-</sup> mouse proliferated slightly higher than the WT, especially in case of splenocytes derived from an unstimulated and OVA-stimulated *in vivo* OT-2/Ly5.1 culture. Even the basal proliferation in an *ex vivo* culture of splenocytes derived from the PBS treated *in vivo* group (without a stimulus) was noted higher in the splenocytes derived from the CD11b<sup>-/-</sup> background (Fig. 52C). This means that CD11b<sup>-/-</sup> mice provided a milieu, in which T lymphocytes were more potently stimulated by CD11b<sup>-/-</sup> antigen presenting cells.

A



B



C

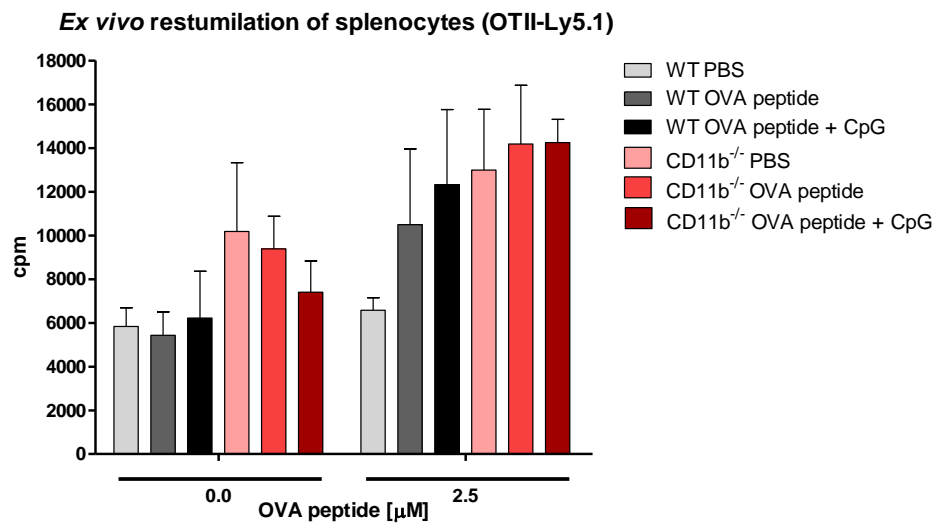


Figure 52. *In vivo* proliferation of OT2-Ly5.1 T-lymphocytes in CD11b<sup>-/-</sup> mice.

Splenocytes from OT2-Ly5.1 mice were injected intravenously into WT and CD11b<sup>-/-</sup> mice. Following subsequent injection of an antigen and adjuvant (OVA grey peptide and CpG) mice were sacrificed and splenic T cells were analysed. CD45.1<sup>+</sup> Cell population was sub-gated for CD3<sup>+</sup>CD4<sup>+</sup> and these double positives were analysed for the CFSE content (A). Proliferation was measured as the percentage of T cells in the specific generations derived from the divided parent T cell population (B), curves represent mean values with SEM (n=6). Splenocytes derived from the experiment were additionally re-stimulated *ex vivo* with an antigen (C), bars represent mean values with SEM (n=4).

*In vivo* proliferation of CD8<sup>+</sup> T cells (OT1/Ly5.1) was comparable in both WT and CD11b<sup>-/-</sup> mice (Fig. 53A). The *ex vivo* SIINFEKL-restimulated splenocyte proliferation in antigen+adjuvant stimulated *in vivo* cultures was slightly higher in cultures derived from CD11b<sup>-/-</sup> mice. Proliferation of the untreated *ex vivo* cultured splenocytes from the PBS and SIINFEKL *in vivo* groups was insignificantly higher in the CD11b<sup>-/-</sup> background (Fig. 53B). Interestingly, *ex vivo* SIINFEKL stimulated splenocytes from the fully activated (SIINFEKL+ CpG) *in vivo* WT group secreted more INF- $\gamma$ , IL-17 and IL-10 in the course of the culture (Fig. 53C-E).

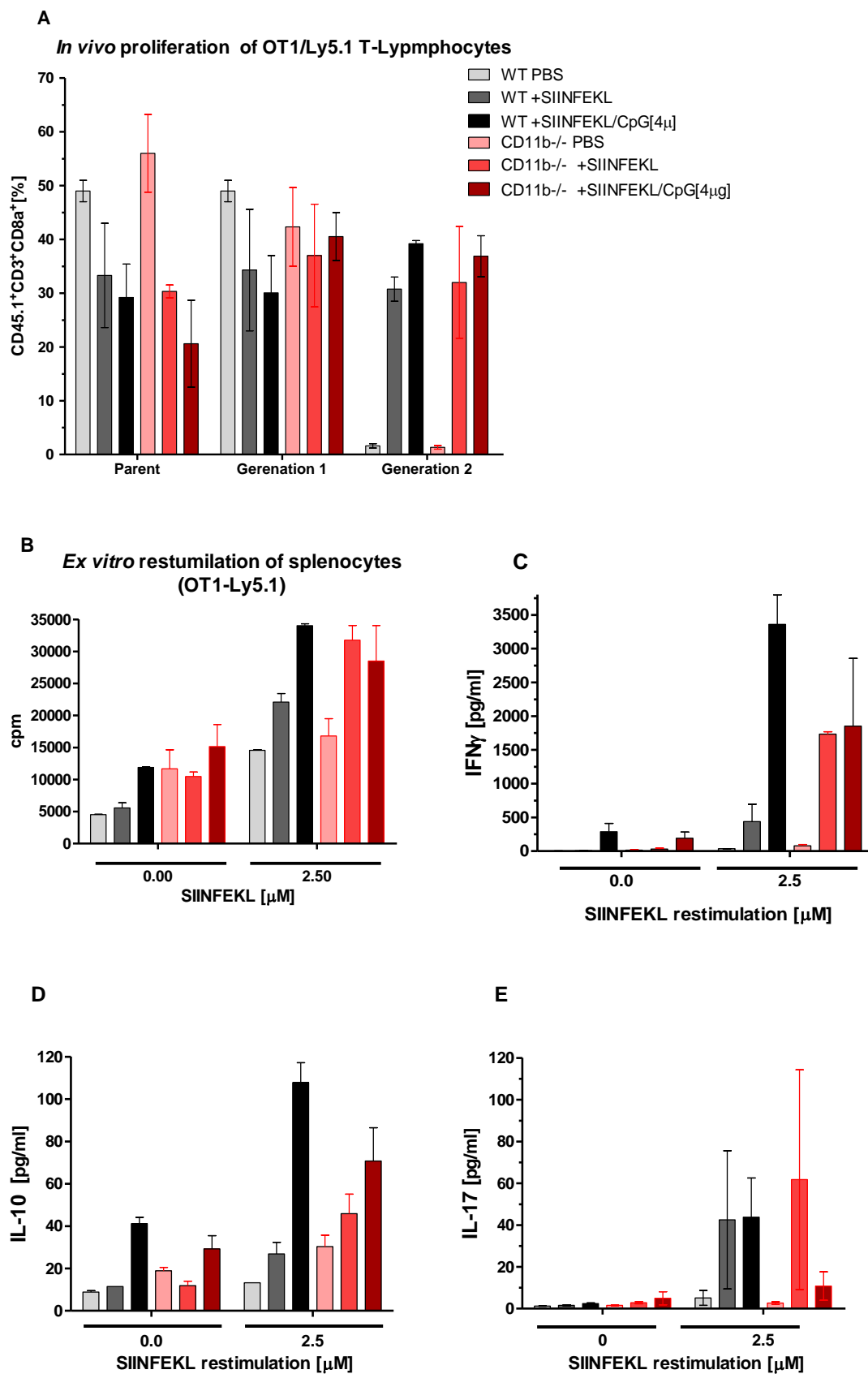


Figure 53. *In vivo* proliferation of OT1-Ly5.1 T-lymphocytes in *CD11b*<sup>-/-</sup> mice.

*Splenocytes from OT1-Ly5.1 mice were injected intravenously into WT and CD11b<sup>-/-</sup> mice. Following subsequent injection of antigen and adjuvant (SIINFEKL and CpG) mice were sacrificed and splenic T cell were analysed. CD45.1<sup>+</sup> Cell population was sub-gated for CD3<sup>+</sup>CD8<sup>+</sup> and these double positives were analysed for the CFSE content. Proliferation was measured as the percentage of T cells in the specific generations derived from the divided parent T cell population (A), bars represent mean values with SEM (n=2 for WT, n=3 for CD11b<sup>-/-</sup>). Splenocytes derived from the experiment were additionally restimulated ex vivo with an antigen (B) and the IFN- $\gamma$ (C), IL-10(D) and IL-17(E) concentrations were measured in the cultures. Bars represent mean values with SEM (n=4).*

### 2.3.1.2. B16-OVA melanoma growth in CD11b<sup>-/-</sup> mice

In subsequent *in vivo* B16-OVA melanoma experiments 35 WT and 30 CD11b<sup>-/-</sup> mice were inoculated with tumour. Analysis covered tumour burden, tumour growth, the composition of leukocytes infiltrating tumour along with the adjacent skin as well as draining lymph node leukocytes and splenocytes.

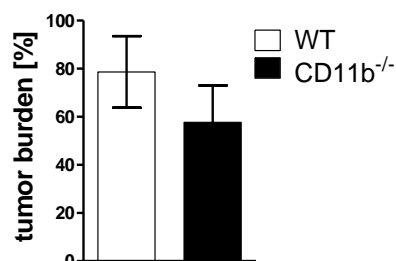
Among CD11b<sup>-/-</sup> mice inoculated with B16-OVA melanoma cells only 57% developed tumour, whereas WT mice presented with a higher tumour development frequency of 79% (Fig. 54A). Moreover, tumour growth was significantly attenuated in the CD11b<sup>-/-</sup> mice. During the first 5 days of tumour measurements tumour growth was reduced in the CD11b<sup>-/-</sup> mice by 37% on average (Fig. 54B). When normalized to the primary tumour mass, tumour volume in WT multiplied at a much faster rate in comparison to the CD11b<sup>-/-</sup>. Already on day 6 the tumour mass in the WT multiplied on average 1.5 fold more than in the CD11b<sup>-/-</sup> and the difference increased over time (Fig. 54C).

FACS analysis of leukocytes retrieved from the tumour mass (Fig. 55A) and the adjacent skin revealed no differences in the composition of infiltrating cells, same frequencies of CD3<sup>+</sup>, F4/80<sup>+</sup> and CD11c<sup>+</sup> cells were detected in samples derived from both WT and CD11b<sup>-/-</sup> mice (Fig. 55B,C). FACS analysis of draining lymph node cells (Fig. 55E) revealed an insignificant decrease in the fractions of CD11c<sup>+</sup> and CD3<sup>+</sup> cells in CD11b<sup>-/-</sup> mice, while the proportions of CD4<sup>+</sup> and CD8<sup>+</sup> T cells were equal in mice of either genotype (Fig. 55D).

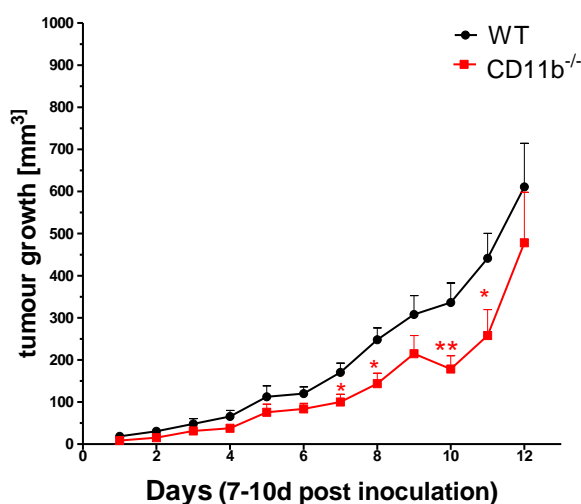
The composition of splenic leukocytes retrieved from the mice inoculated with B16/OVA did not show genotype-dependent differences in both tumour bearing mice as well as mice that did not develop melanoma with regard to the frequencies of CD11c<sup>+</sup> DC, F4/80<sup>+</sup> macrophages, CD19<sup>+</sup> B cells and T cell subsets (CD4, CD8, CD25 and FoxP3). However, activated T cells

(CD25<sup>+</sup>) were in both groups slightly elevated in the tumour bearing mice in comparison to those that did not develop tumour (Appendix E).

**A**



**B**



**C**

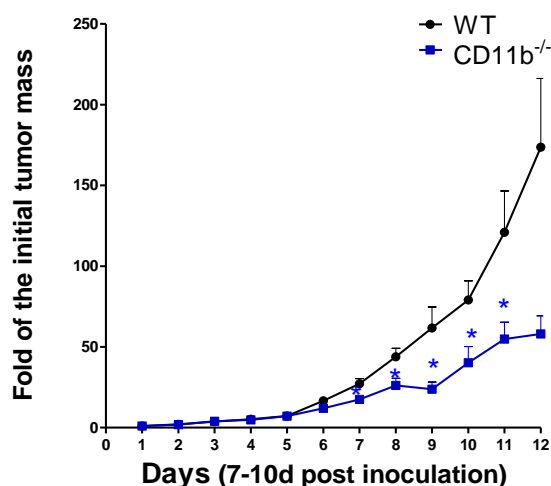
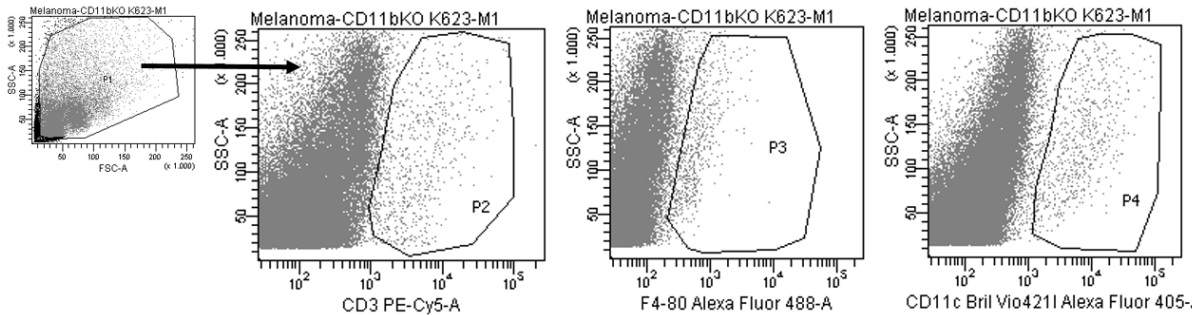


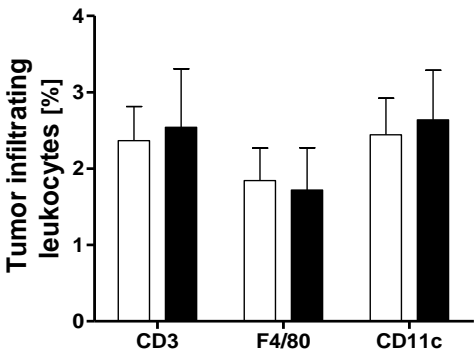
Figure 54. Tumour burden and growth in CD11b<sup>-/-</sup> mice.

In the course of 3 *in vivo* experiments 35 WT and 30 CD11b<sup>-/-</sup> mice were inoculated with B16-OVA melanoma. Tumour burden (percentage of mice that developed tumour, graph A) and tumour growth (B, C) were analysed. Tumour growth was measured as width\*length\*depth\*3.14/6 and plotted as mm<sup>3</sup> (B), as well as normalized to the initial tumour mass (C). Bars and curves represent mean with SEM.

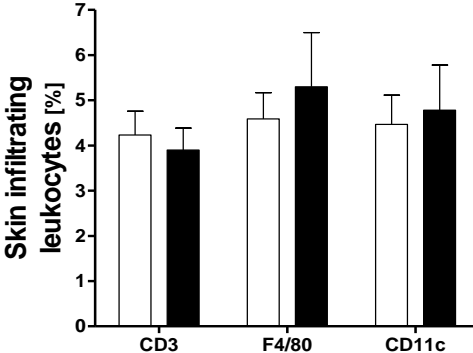
A



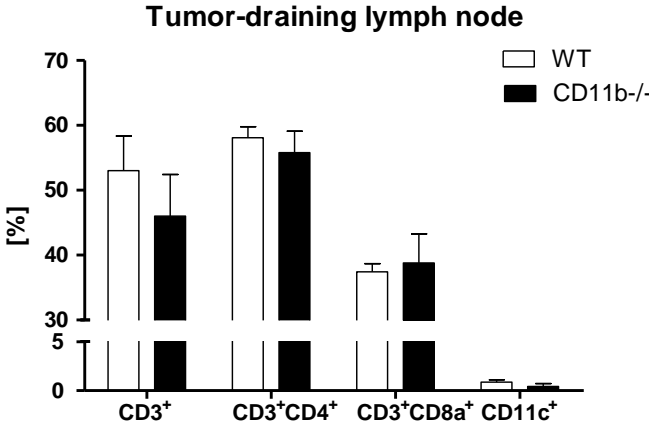
B



C



D



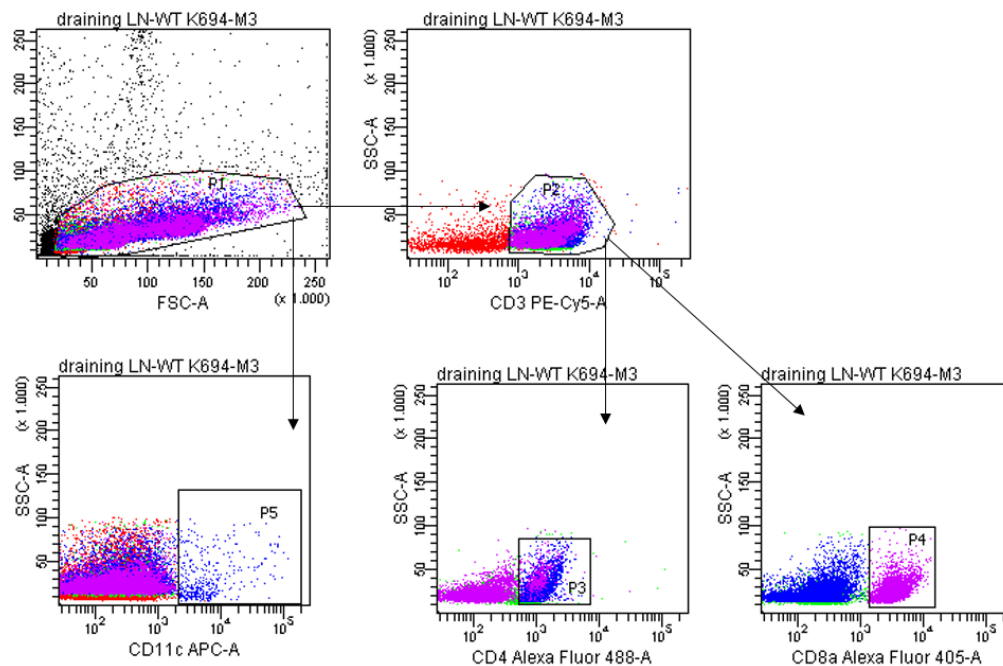
**E**

Figure 55. Leukocytes infiltrating tumour mass and draining lymph nodes of the  $CD11b^{-/-}$ .

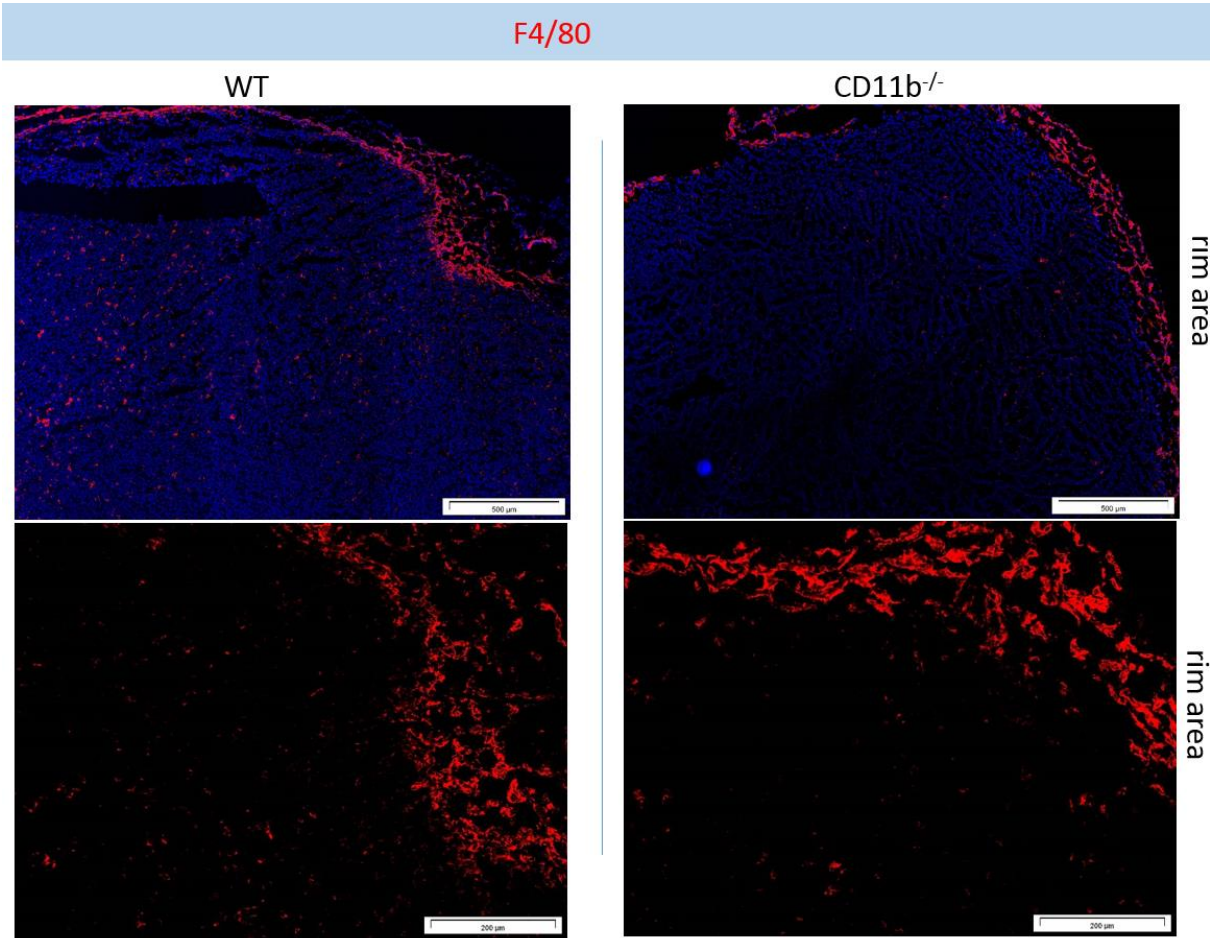
Tumour tissue as well as the adjacent skin and draining lymph nodes were FACS-analysed in the  $CD11b^{-/-}$  and WT mice with B16-OVA melanoma burden. Tissue was isolated after tumour reached a maximum of  $800\text{mm}^3$  or ulcerated. Tumour mass (B) and the adjacent skin (C) were gated for  $CD3^+$ ,  $F4/80^+$  and  $CD11c^+$  cells (A), whereas draining lymph node was analysed for  $CD3^+$  cells, distinguishing  $CD4^+$  and  $CD8^+$  subtypes as well as  $CD11c^+$  cells (D,E). Bars represent mean with SEM ( $n=9$  for WT,  $n=5$  for  $CD11b^{-/-}$ ).

Immunohistological analysis of cryopreserved melanoma revealed an increased infiltration of  $F4/80^+$  macrophages,  $CD11c^+$  dendritic cells (Fig. 56A-D) and  $Gr-1^+$  granulocytes (Fig. 56E) towards the tumour mass in the WT. Macrophages, DC and granulocytes within the tumour of the  $CD11b^{-/-}$  mice tended to remain at the tumour margin.

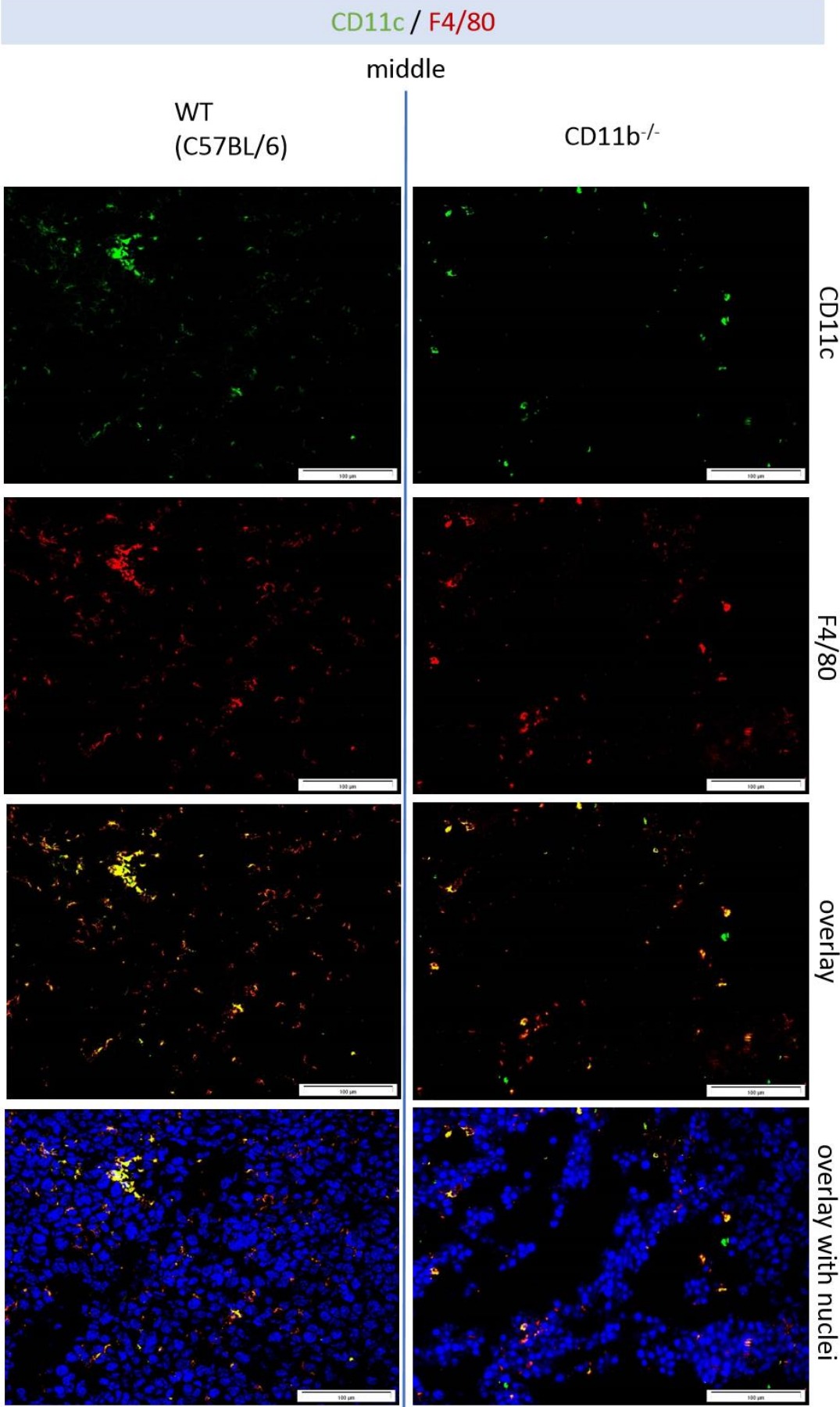
Hardly any  $CD4^+FoxP3^+$  cells were detected in tumour from the  $CD11b^{-/-}$  mouse, whereas multiple regulatory T cells were found within melanoma that developed in WT mouse (Fig. 56F).

The rim area of the tumour derived from  $CD11b^{-/-}$  mouse predisposed to a poor vasculature in comparison to WT. No differences in vascularisation were observed in the central tumour mass (Fig. 56G).

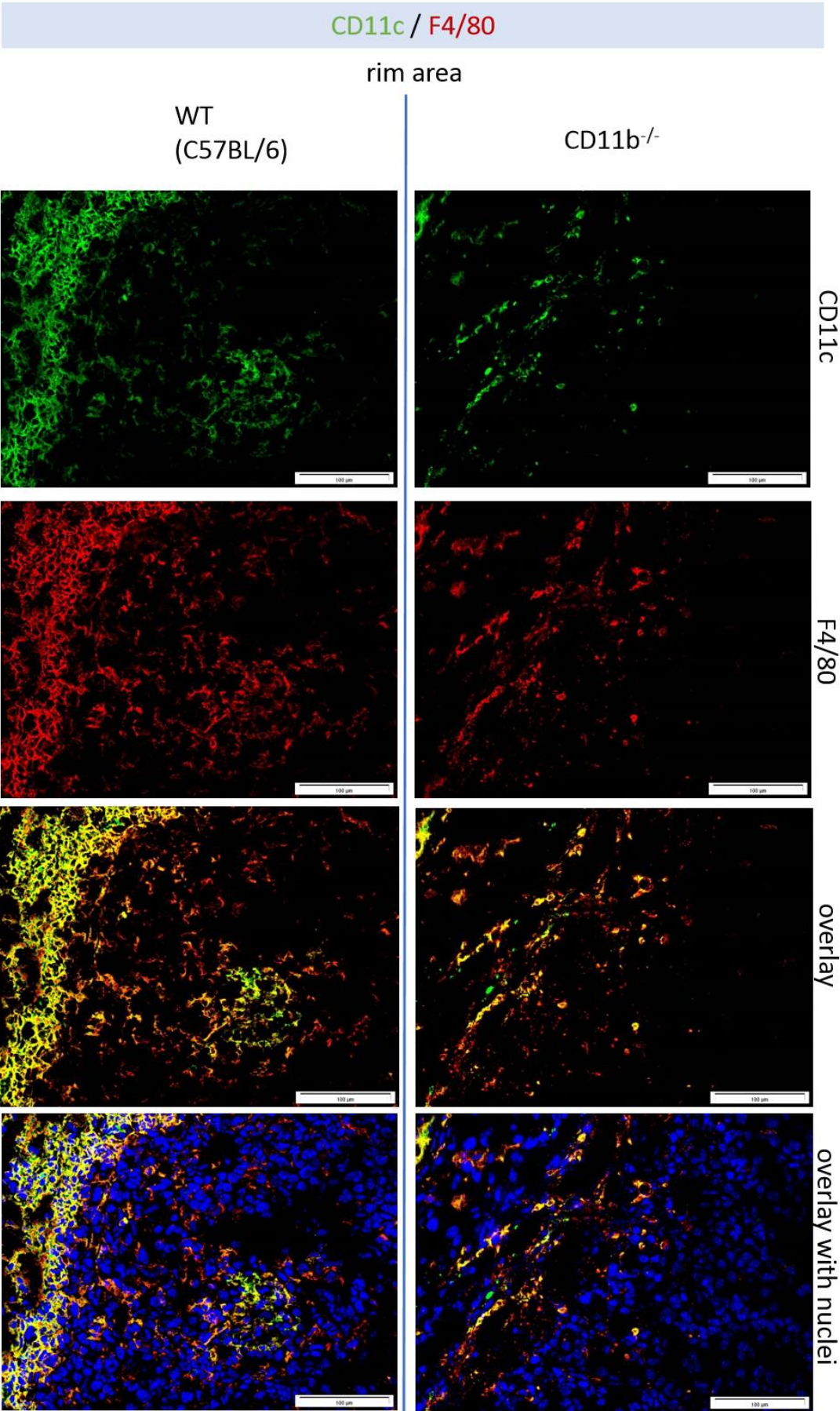
A



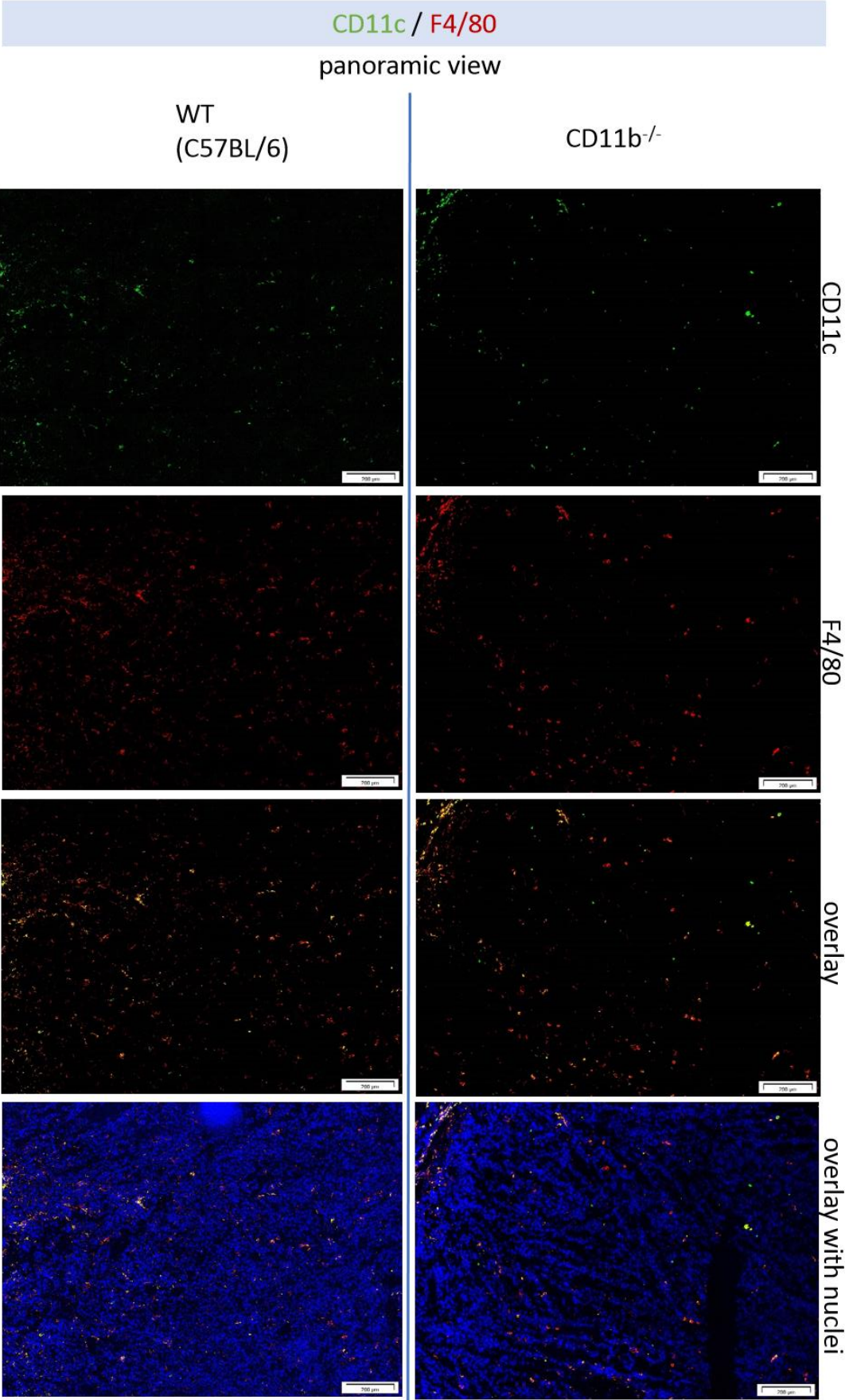
B



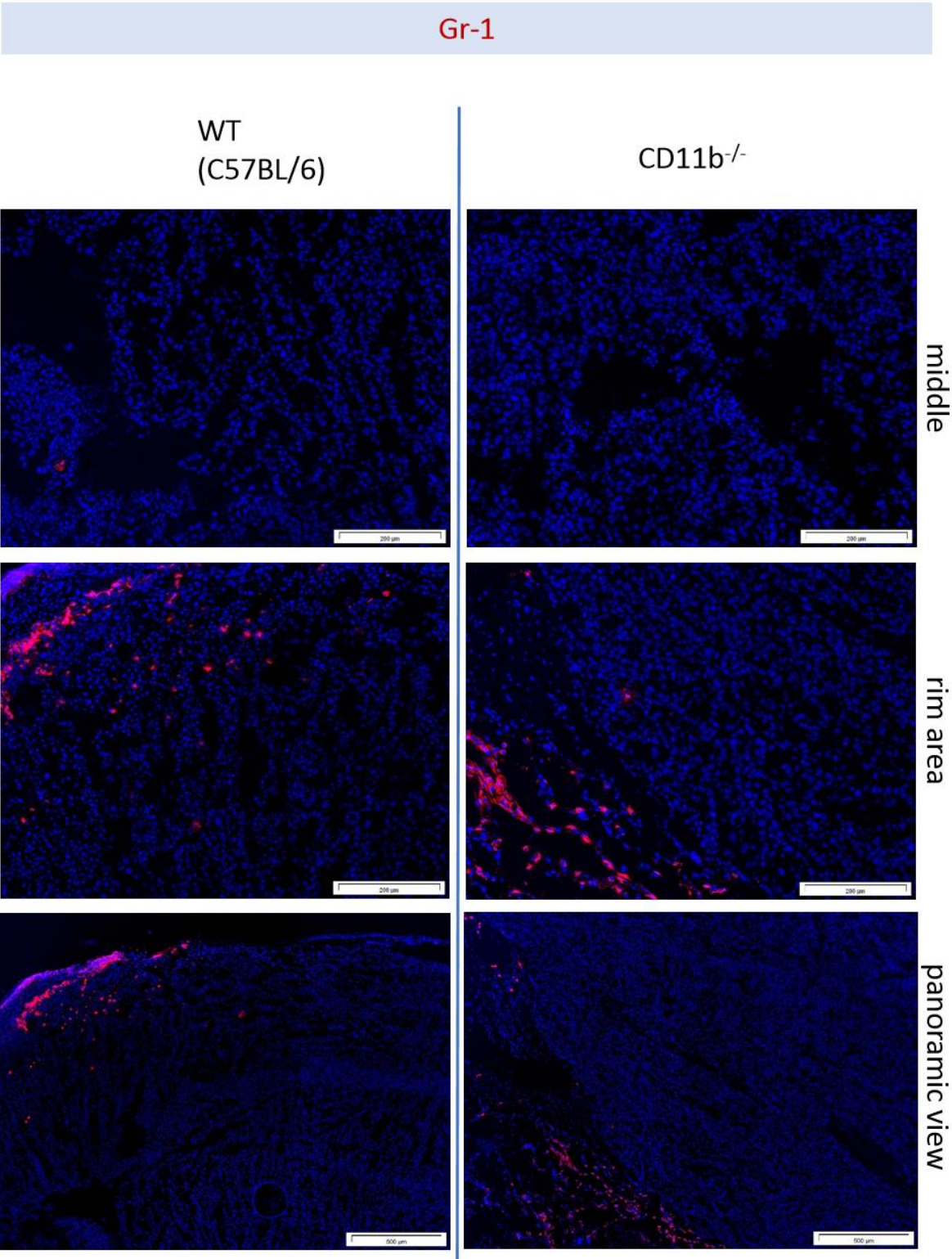
C



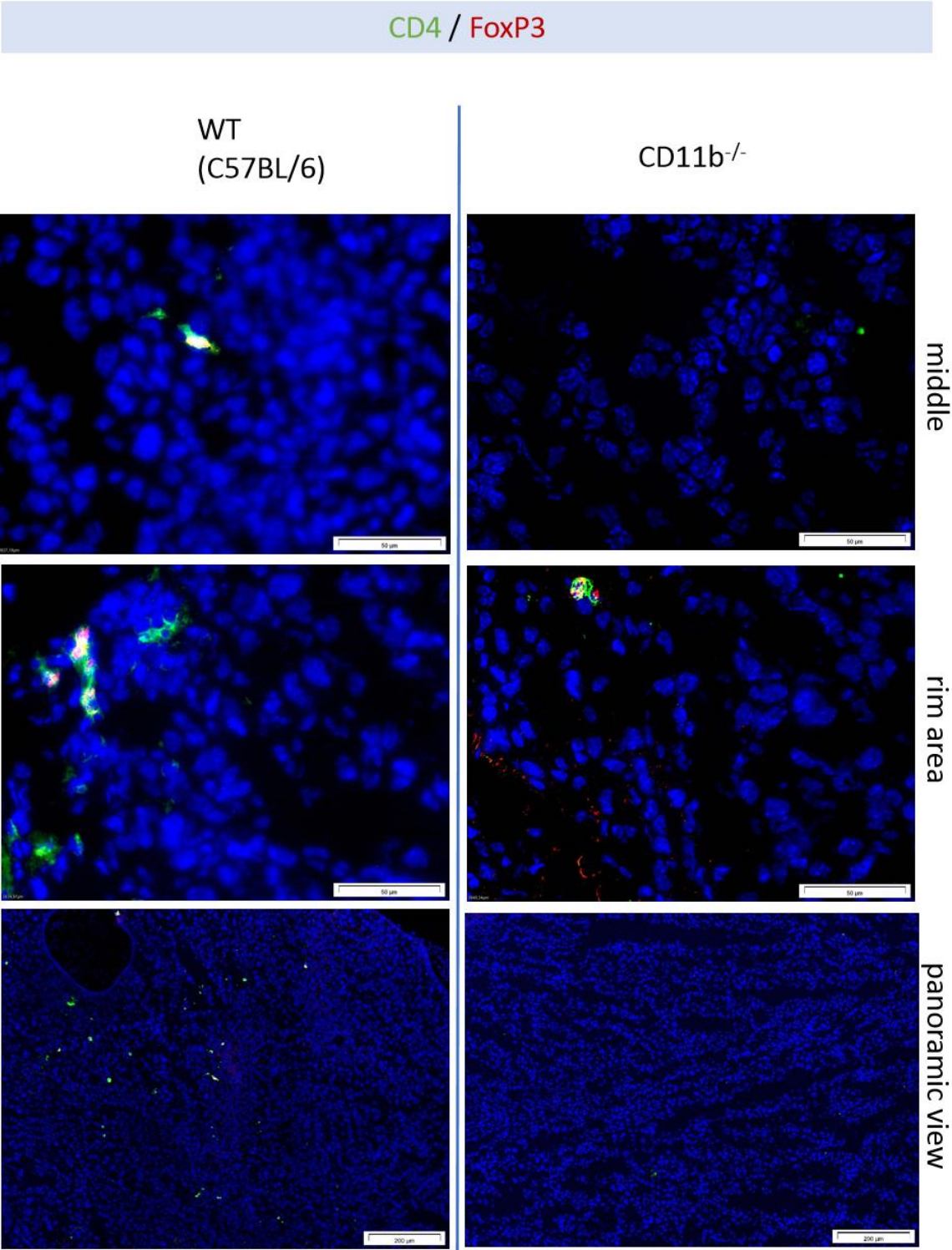
D



E



F



G

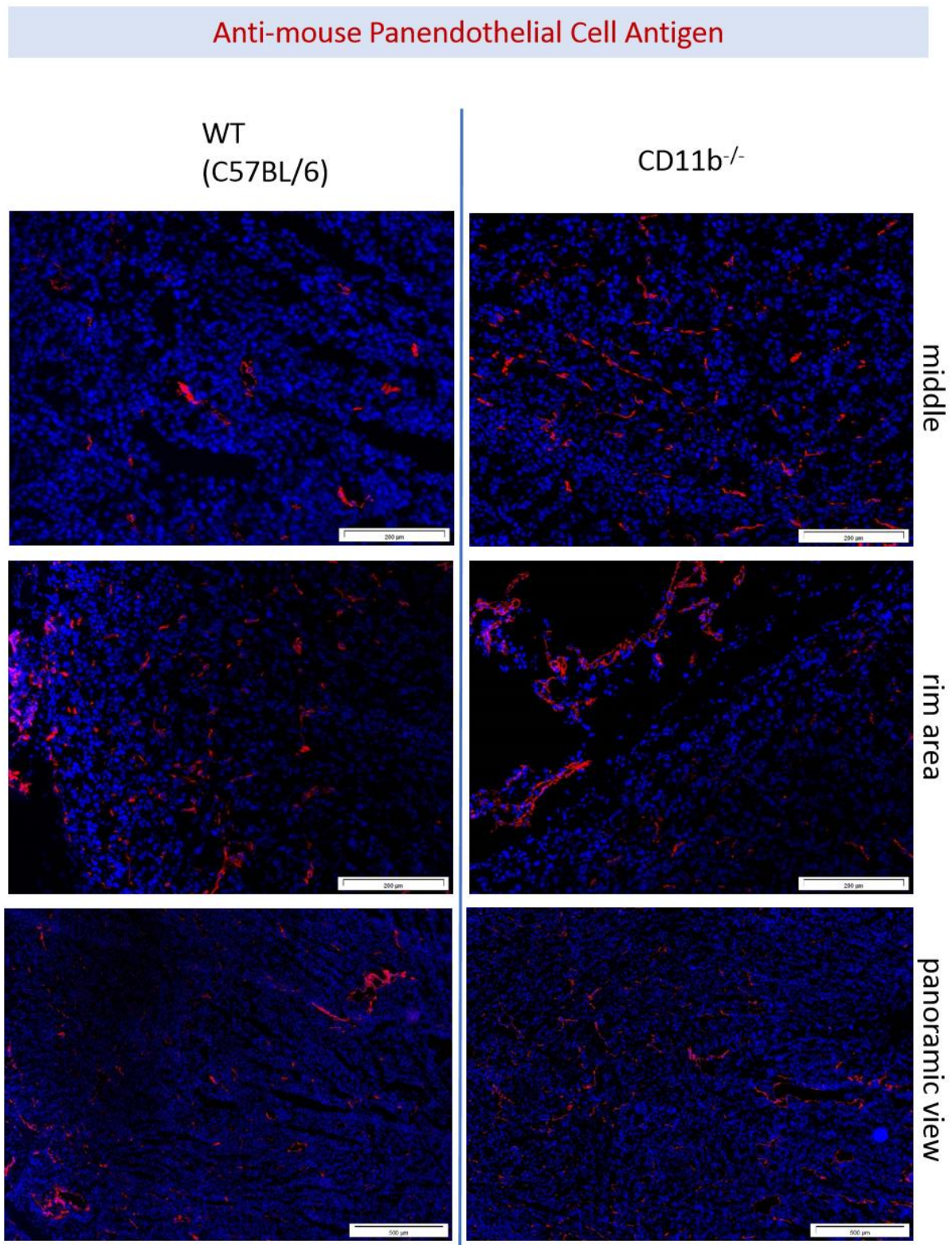


Figure 56. Immunohistological analysis of the B16-OVA melanoma infiltrating leukocytes in the CD11b<sup>-/-</sup> mice.

Cryopreserved tumours from WT and CD11b<sup>-/-</sup> mice were used to prepare slides that were subsequently stained with antibodies against F4/80 (A), F4/80 and CD11c (B, C, D), Gr-1(E),

*CD4 and FoxP3 (F) and pan-endothelial cell antigen (G). Pictures represent middle and rim area of the tumour as well as a central, zoomed out panoramic view. Nuclei were counterstained with DAPI (Vector Laboratories, Ltd). Stained sections were visualized using a fluorescence microscope (Olympus IX81).*

## **2.4. The role of $\beta$ 2 integrins as mediators of intracellular uptake on dendritic cells**

### **2.4.1. The role of Mac-1 (CD18/CD11b) for uptake of complement-opsonized p(Cy5)**

#### **2.4.1.1. Engulfment of p(Cy5) by $CD11b^{-/-}$ BM-DC**

In order to analyse the role of Mac-1 for the uptake of dextran-coated superparamagnetic iron oxide nanoparticles that were functionalized with Cy5 by Miltenyi Biotec (Germany), BM-DC generated from WT and  $CD11b^{-/-}$  mice were co-incubated with p(Cy5) in the presence or absence of murine native serum. At two time points (0.5 and 4h), and two temperatures (4°C and 37°C), binding of this type of NP by BM-DC was examined by flow cytometry (Fig. 57). Incubation at 37°C leads to an active engulfment of external material involving cytoskeletal activity, whereas incubation at 4°C may lead only to cell-surface binding.

In the BM-DC cultures at 37°C, under a serum free condition as well as in the presence of FCS, p(Cy5) beads were engulfed to comparable extend by WT and  $CD11b^{-/-}$  BM-DC. However, once p(Cy5) were pre-incubated with native murine serum about 40% more WT BM-DC engulfed the beads after half an hour and 53% more after four hours as compared with the  $CD11b^{-/-}$  BM-DC. No significant difference was observed in uptake of p(Cy5) opsonised with heat-inactivated (HI) serum or at 4°C (Fig. 58). Since uptake of the beads by  $CD11b^{-/-}$  BM-DC was significantly decreased in the serum condition as compared to the HI-serum in the early time point, CD11b seem to play an important role in engagement of the complement opsonised nanomaterial.

The same tendency as in the native-serum-conditioned cultures was observed in all groups (Medium, Serum and HI Serum) in the mixed culture condition (WT and knock-out BM-DC cultured together with beads) (Fig. 59). After half an hour of incubation there was a significant drop of the uptake by the knock-out (in the serum group by about 45% and in the HI-serum by about 53%). At 4h time point, the uptake was significantly reduced by about 38% in all groups in the knock-out DC. The positive influence of serum on the uptake was most prominent in the

early incubation time compared to the HI-serum (29% vs 19% in the WT and 16% vs 10% in the CD11b<sup>-/-</sup>) and it became minute after 4 h of incubation (Fig.60).

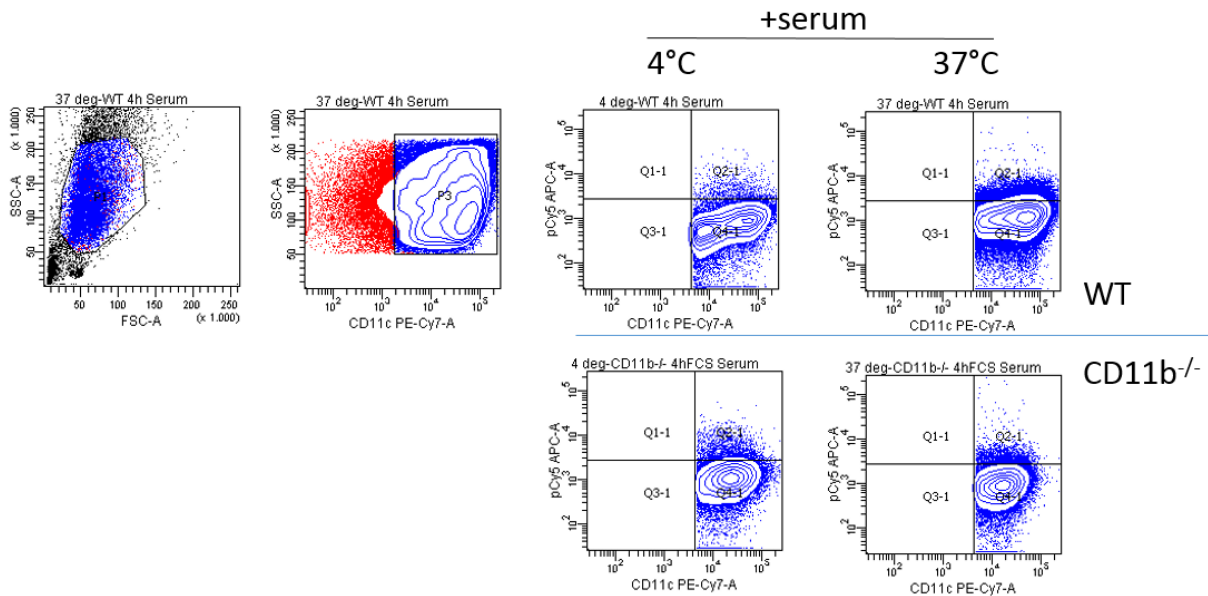
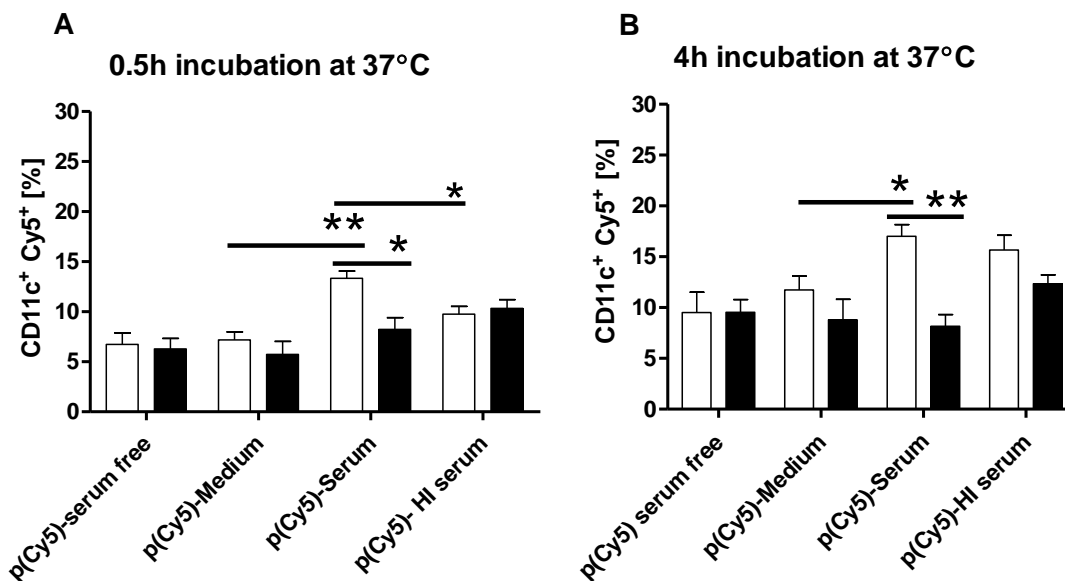


Figure 57. Gating strategy for the uptake of the p(Cy5) by the CD11b<sup>-/-</sup> BM-DC.

BM-DC from a WT and CD11b<sup>-/-</sup> mice were cultured with p(Cy5) in presence or absence of native mouse serum. After 30 min and 4h of incubation cells were washed and stained with an antibody against CD11c. CD11c<sup>+</sup> BM-DC population was sub-gated for the p(Cy5) (APC channel) and double positive population, i.e. BM-DC that bound/engulfed p(Cy5), was analysed.



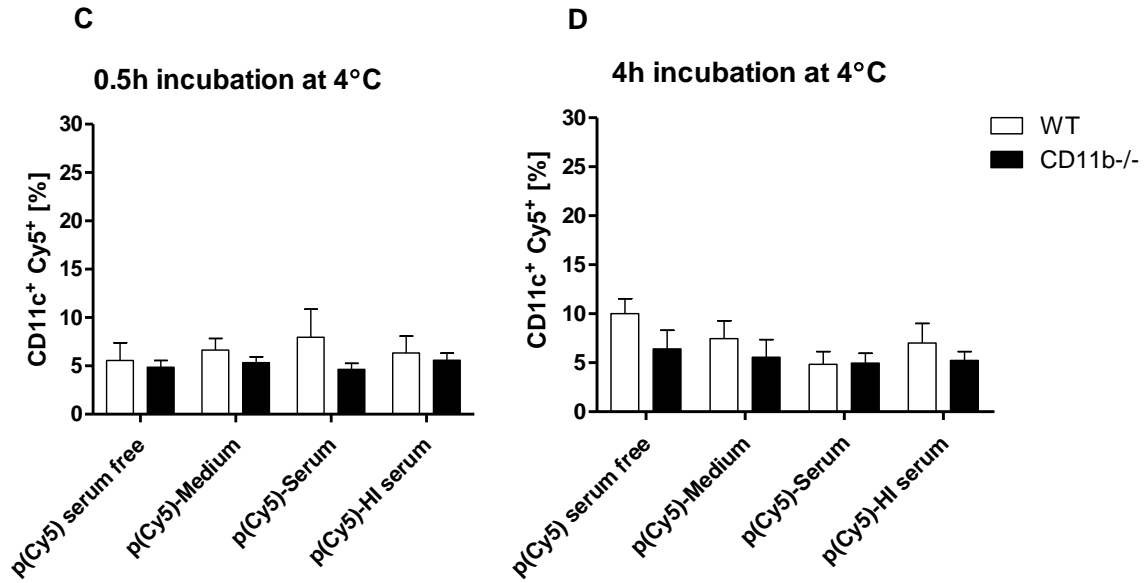


Figure 58. Engulfment of the p(Cy5) by CD11b<sup>-/-</sup> BM-DC.

BM-DC from a WT and CD11b<sup>-/-</sup> mice were cultured with p(Cy5) opsonized with native mouse serum or HI native mouse serum as well as in serum(FCS)-free medium and standard medium conditioned with FCS. After 30 min (A, C) and 4h (B, D) of incubation at 37°C or 4°C cells were washed and stained with an antibody against CD11c. CD11c<sup>+</sup> BM-DC population was sub-gated for the p(Cy5) and uptake was evaluated as percentage of the CD11c<sup>+</sup> DC positive for the p(Cy5). Depicted bars represent mean values with SEM (n=3-5).

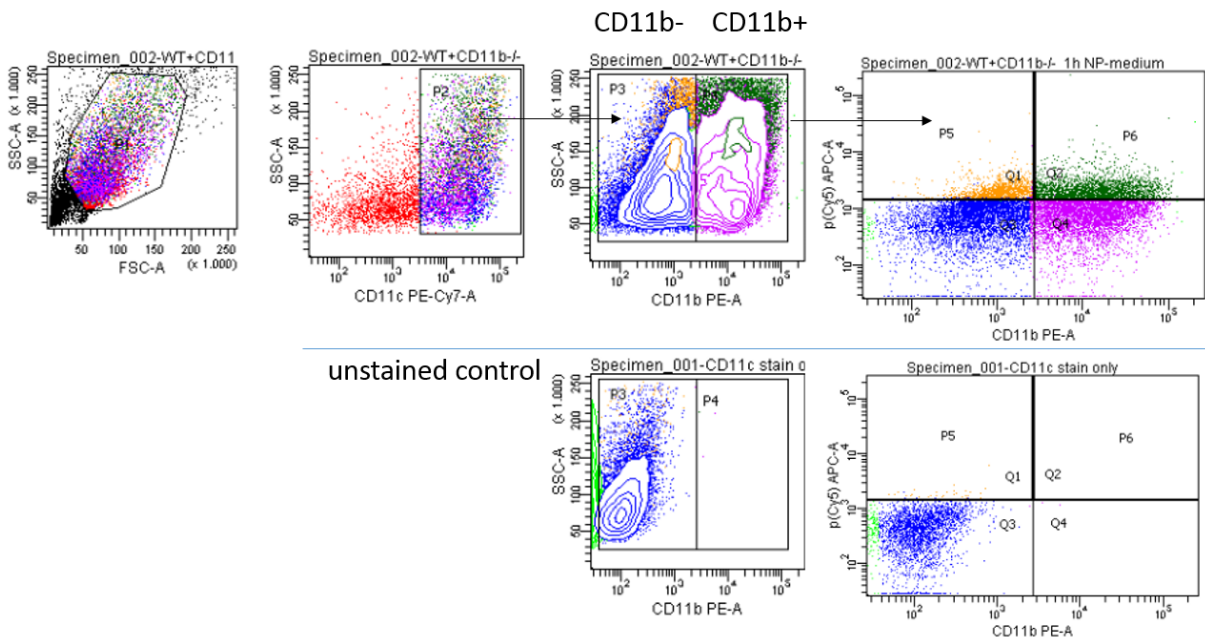


Figure 59. Gating strategy for the uptake of p(Cy5) in mixed WT-CD11b<sup>-/-</sup> BM-DC cultures.

*BM-DC from a WT and CD11b<sup>-/-</sup> mice were cultured together (as mixed culture) with p(Cy5) opsonized with native mouse serum or HI native mouse serum as well as in standard culture medium containing FCS. After 30 min and 4h of incubation cells were washed and stained with an antibody against CD11c. CD11c<sup>+</sup> BM-DC population was sub-gated for CD11b positive and negative populations and both populations further gated against the p(Cy5) on one plot.*

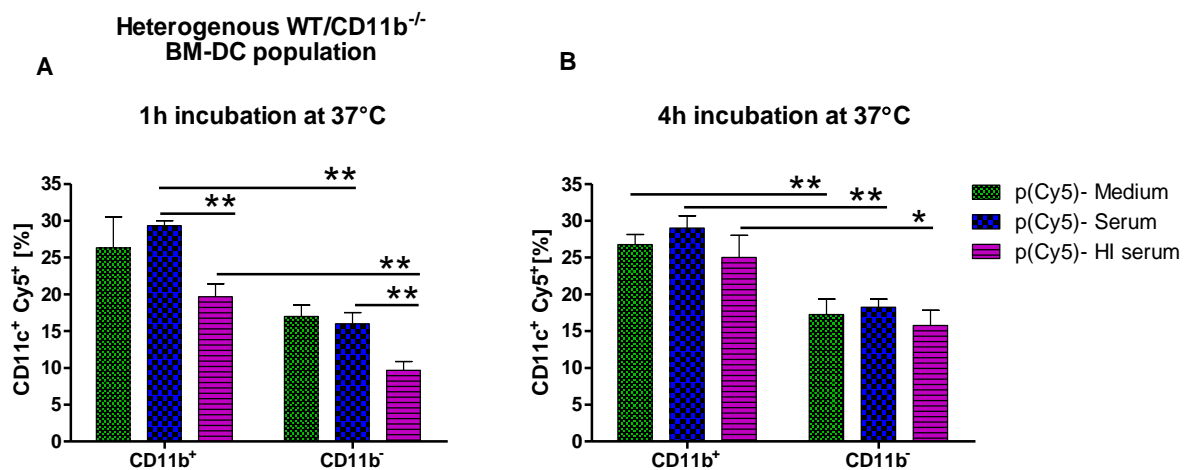
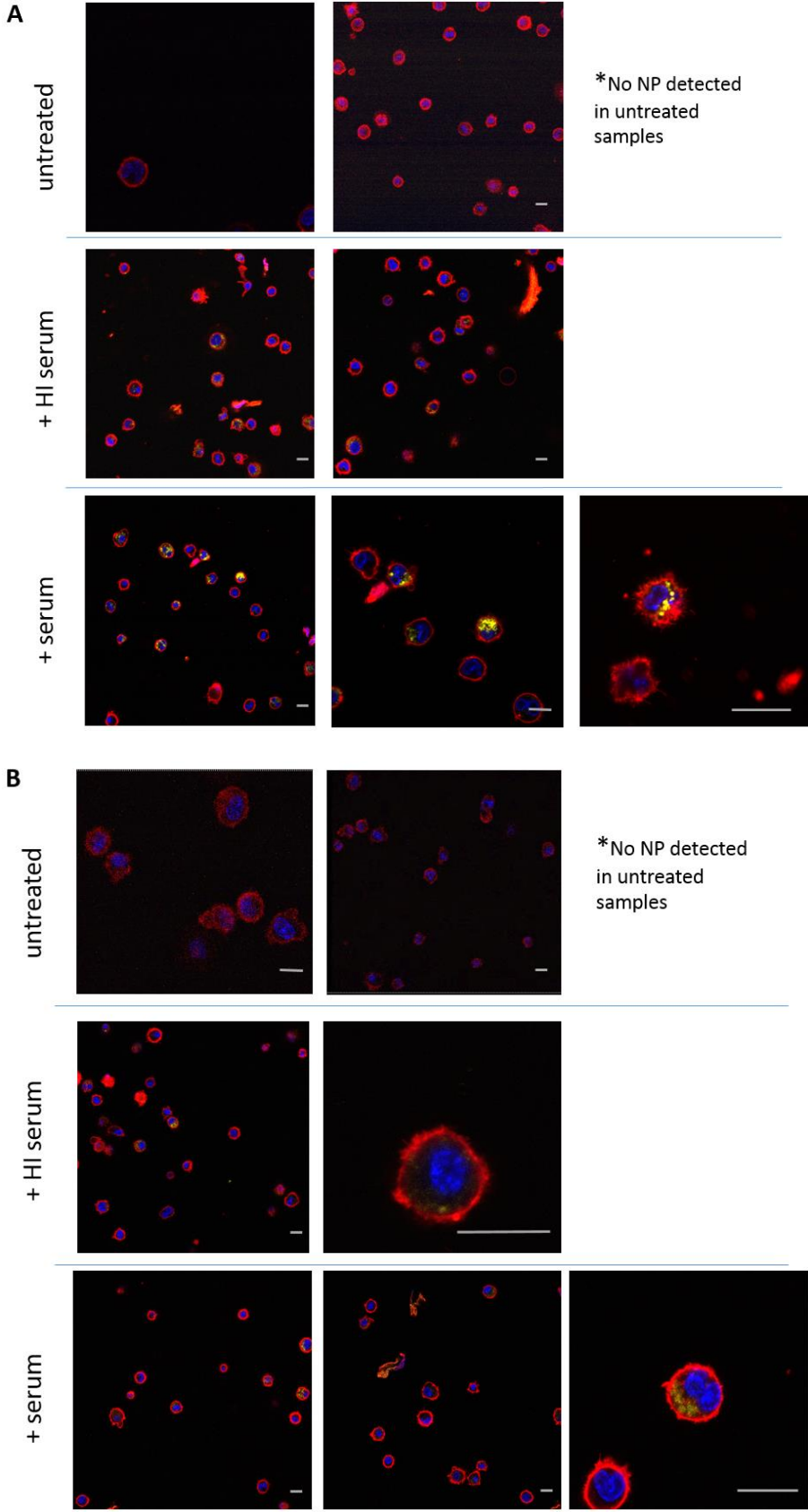


Figure 60. Engagement of p(Cy5) by BM-DC in mixed WT-CD11b<sup>-/-</sup> cultures.

*BM-DC from a WT and CD11b<sup>-/-</sup> mice were cultured together heterogeneously with p(Cy5) in presence or absence of native mouse serum as well as in HI-native serum conditioned medium. After 1h and 4h of incubation at 37°C cell were washed and stained with an antibody against CD11c and CD11b. CD11c<sup>+</sup> BM-DC population was sub-gated for CD11b against p(Cy5) and uptake was evaluated as percentage of the CD11c<sup>+/+</sup>/CD11b<sup>+/+</sup> or CD11c<sup>+/+</sup>/CD11b<sup>-/-</sup> DC positive for the p(Cy5). Depicted bars represent mean values with SEM (n=3).*

To assess cellular uptake of p(Cy5), confocal microscopy was performed and the uptake per cell was quantitated as mean fluorescent intensity of p(Cy5) in the cell. WT BM-DC on average engulfed twice as much p(Cy5) in comparison to CD11b<sup>-/-</sup> BM-DC once beads were pre-coated with native mouse serum (average MFI per cell: 21.143 in WT, 9.635 in CD11b<sup>-/-</sup>), whereas no qualitative differences were detected in the HI- serum group and no uptake was noted in case of non-treated p(Cy5) beads (Fig. 61).



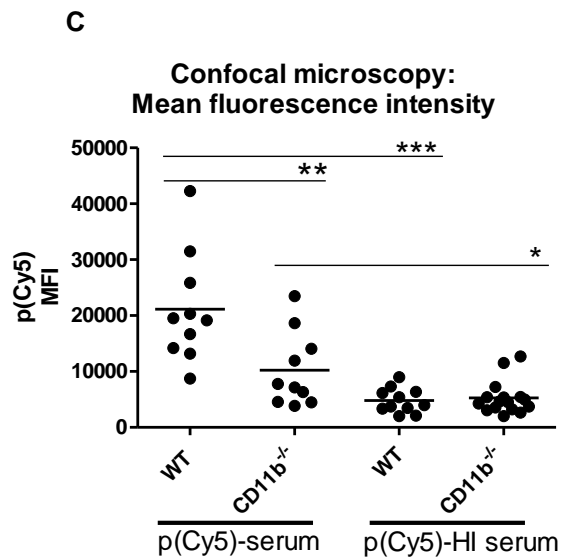


Figure 61. Confocal microscopy of the p(Cy5) uptake by CD11b<sup>-/-</sup> BM-DC.

BM-DC derived from C57BL/6(A) or B6.129S4-Itgam<sup>tm1Myd/J</sup> mice(B) were added NPs (7μl NPs+ 63μl medium/ native serum or HI native serum, 30min pre-incubation at 37°C) and cultured for 4h in the 24-well plate. Subsequently cells were transferred onto 8-chamber slides and nuclei were stained with Hoechst 33342, the plasma membrane was counter-stained with CellMaskOrange. Samples were analysed by TCS SP5 Confocal Microscope equipped with 40x/1.3oil objective (The Microscopy Core Facility of the IMB, Mainz, Germany). The scale bar in the corner of the pictures (A-WT, B-CD11b<sup>-/-</sup>) represents 20μm. Standard medium condition is described as untreated. The mean fluorescent intensity of p(Cy5) per cell is depicted in the graph (C) as mean with SEM (n=10).

The decrease in the uptake capacity observed for CD11b<sup>-/-</sup> BM-DC could be mimicked using a blocking α-CD11b Ab (10μg/ml) (Fig. 62). For this, BM-DC were blocked with an α-CD11b Ab or the corresponding isotype control Ab (IgG2b) prior to exposure to p(Cy5) pre-treated with native serum. After 4h of incubation with p(Cy5), BM-DC blocked with α-CD11b Ab presented with a reduced recruitment of the beads coated with native-serum and HI-native serum in comparison to WT and isotype Ab (IgG2b) pre-treated BM-DC. The blocking antibody reduced the uptake of the beads to comparable extend in all groups, whereas in case of CD11b<sup>-/-</sup> BM-DC an effect of serum was still detectable, as the uptake of p(Cy5) pre-incubated with native serum was higher than in the medium or after HI-serum pre-treatment.

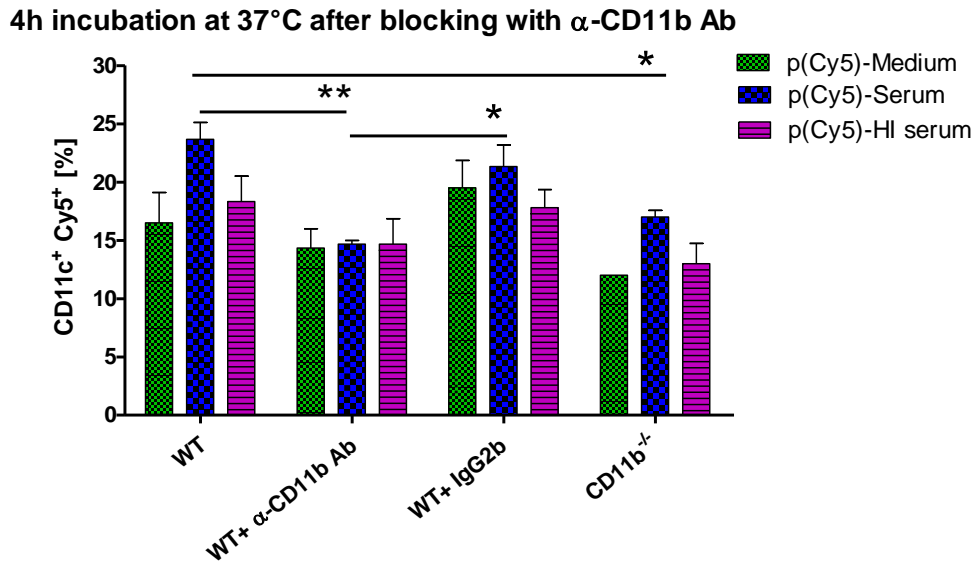


Figure 62. Engulfment of the p(Cy5) by BM-DC blocked with  $\alpha$ -CD11b Ab.

BM-DC from a WT and CD11b<sup>-/-</sup> mice were cultured with p(Cy5) in presence or absence of native mouse serum as well as in HI-native serum conditioned medium. WT BM-DC were additionally pre-treated with  $\alpha$ -CD11b Ab or a corresponding Ab isotype control (IgG2b). After 4h of incubation at 37°C cells were washed and stained with an antibody against CD11c. The uptake was evaluated as percentage of the CD11c positive for the p(Cy5). Depicted bars represent mean values with SEM (n=3).

To assess the potential of the p(Cy5) to activate BM-DC, cells were analysed for the expression of activation markers on the cell surface (CD80, CD86, CD40 and MHC-II), as well as the secretion of TNF- $\alpha$  after co-culture of BM-DC with differentially pre-treated beads.

Expression of the activation markers was quantitated as the mean fluorescent intensity of the according fluorochrome-coupled marker-specific Ab (Fig. 63). BM-DC were exposed to standard medium, native or HI-native serum opsonized beads. Serum alone, LPS-treated and untreated cells were used as controls. The overall expression of CD80 and MHC-II was diminished in the CD11b<sup>-/-</sup> cells irrespective of the treatment. Expression of the CD80, CD86 and CD40 did not change upon incubation with beads (regardless of the pre-treatment) in both WT and CD11b<sup>-/-</sup> BM-DC, whereas the expression of the MHC-II showed a tendency to be slightly elevated in the WT once cells were stimulated with any of the component, including native serum alone. The MFI of MHC-II expression in the CD11b<sup>-/-</sup> BM-DC remained on the level of the untreated sample in case of any applied treatment (Fig. 64).

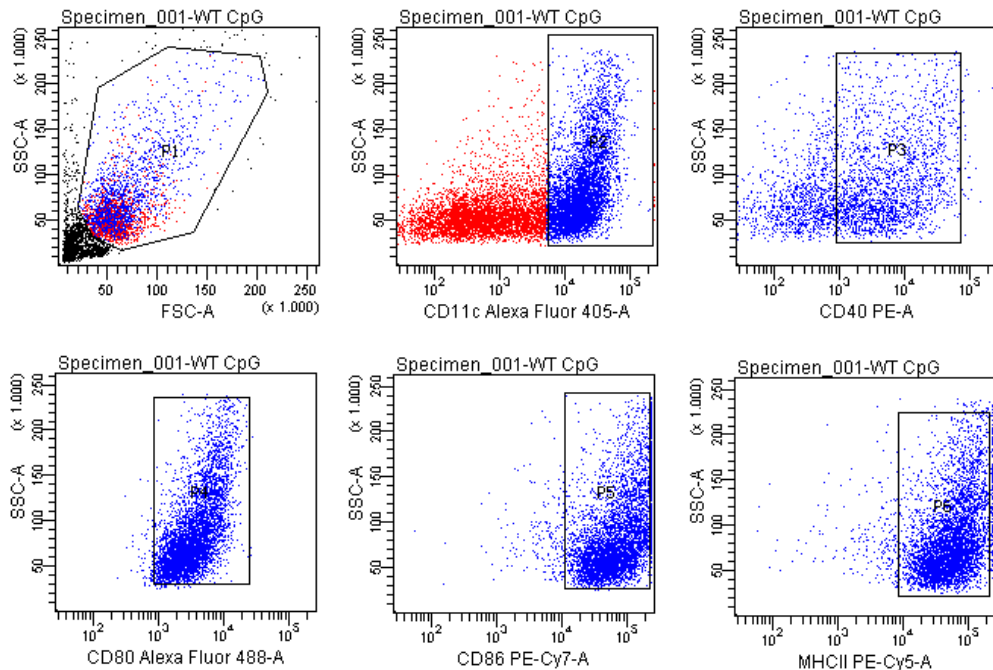


Figure 63. Gating strategy for analysis of the  $CD11b^{-/-}$  BM-DC activation markers after treatment with p(Cy5).

WT and  $CD11b^{-/-}$  BM-DC were pre-treated with standard medium, native or HI-serum pre-incubated beads (serum alone and LPS were used as controls). Cells were subsequently stained against CD11c, CD80, CD86, CD40 and MHC-II. The entire population was first gated for CD11c and then sub-gated for the mentioned activation markers. Mean fluorescence intensity was evaluated for every marker separately.

Another parameter to evaluate the activation state of BM-DC is the secretion of cytokines. Thus, the secretion of TNF- $\alpha$ , a signalling protein moderating systemic inflammation, was assessed after incubation with pre-treated p(Cy5) beads at various time-points (0.5h, 1h, 4h and 12h of co-incubation). The differences in the TNF- $\alpha$  culture concentration were most pronounced at early (half an hour and 1h) time points. Secretion of TNF- $\alpha$  was on average 35% higher in the  $CD11b^{-/-}$  culture when compared to the WT (~ 132 pg/ml in the WT and 202 pg/ml in the  $CD11b^{-/-}$ ) (Fig. 65A, B). After four hours of incubation  $CD11b^{-/-}$  DC secreted on average 22% more TNF- $\alpha$  than the WT BM-DC, whereas after 12h no difference was apparent in the standard medium condition (Fig. 65B, D).

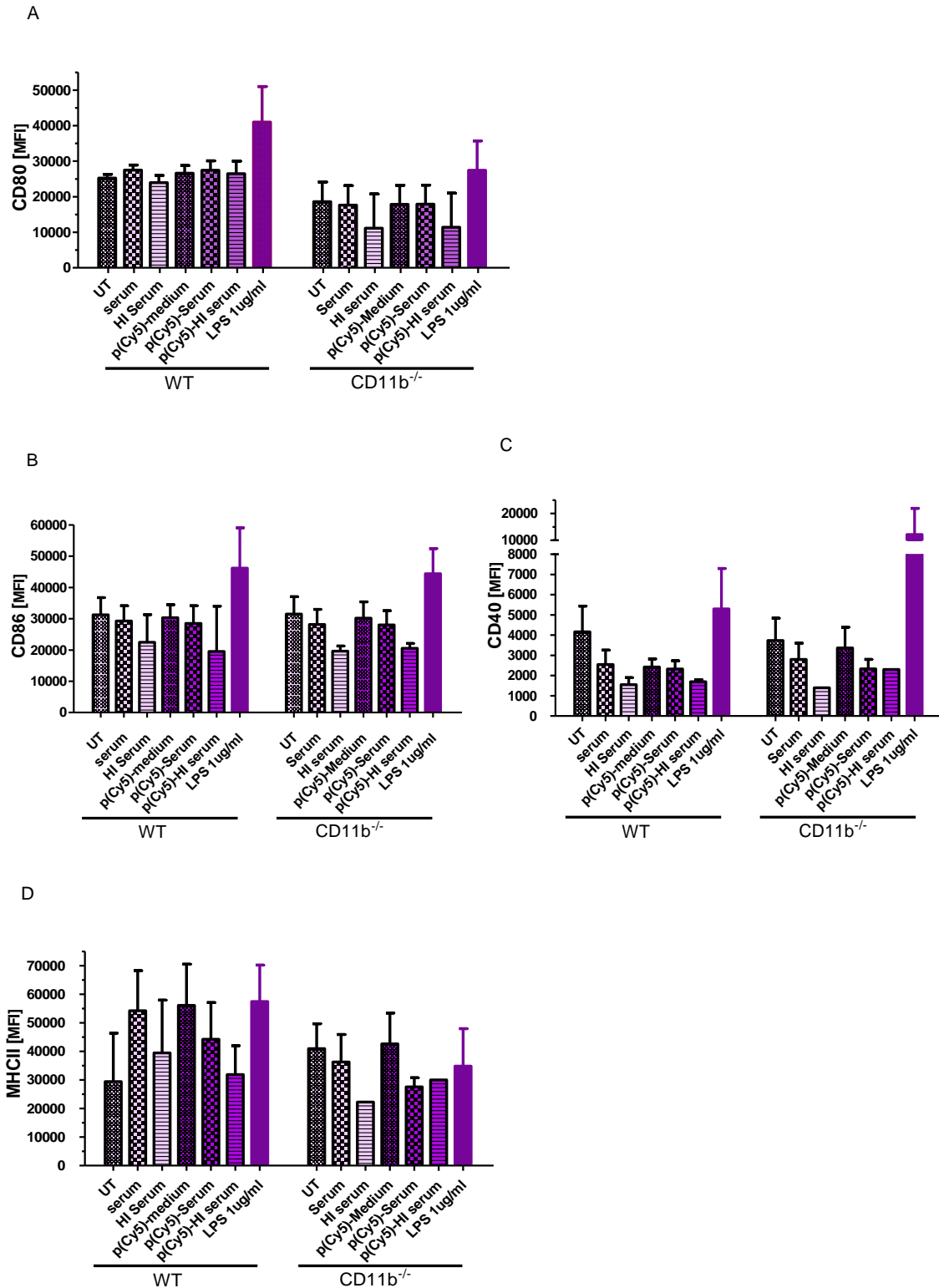


Figure 64. Co-stimulatory molecule expression on the surface of the CD11b<sup>-/-</sup> BM-DC upon treatment with p(Cy5).

BM-DC from the WT and CD11b<sup>-/-</sup> mice were co-incubated with pre-treated p(Cy5) ( standard medium condition, native or HI-native serum) and subsequently analysed via flow cytometry. Mean fluorescence intensity ( MFI, a read-out parameter) was evaluated for the expression of

*CD80 (A), CD86 (B), CD40 (C) and MHC-II (D) on the surface of the CD11c<sup>+</sup> DC. Control treatments: untreated (UT), native serum only and LPS incubation. Bars represent mean values with SEM (n=2-4).*

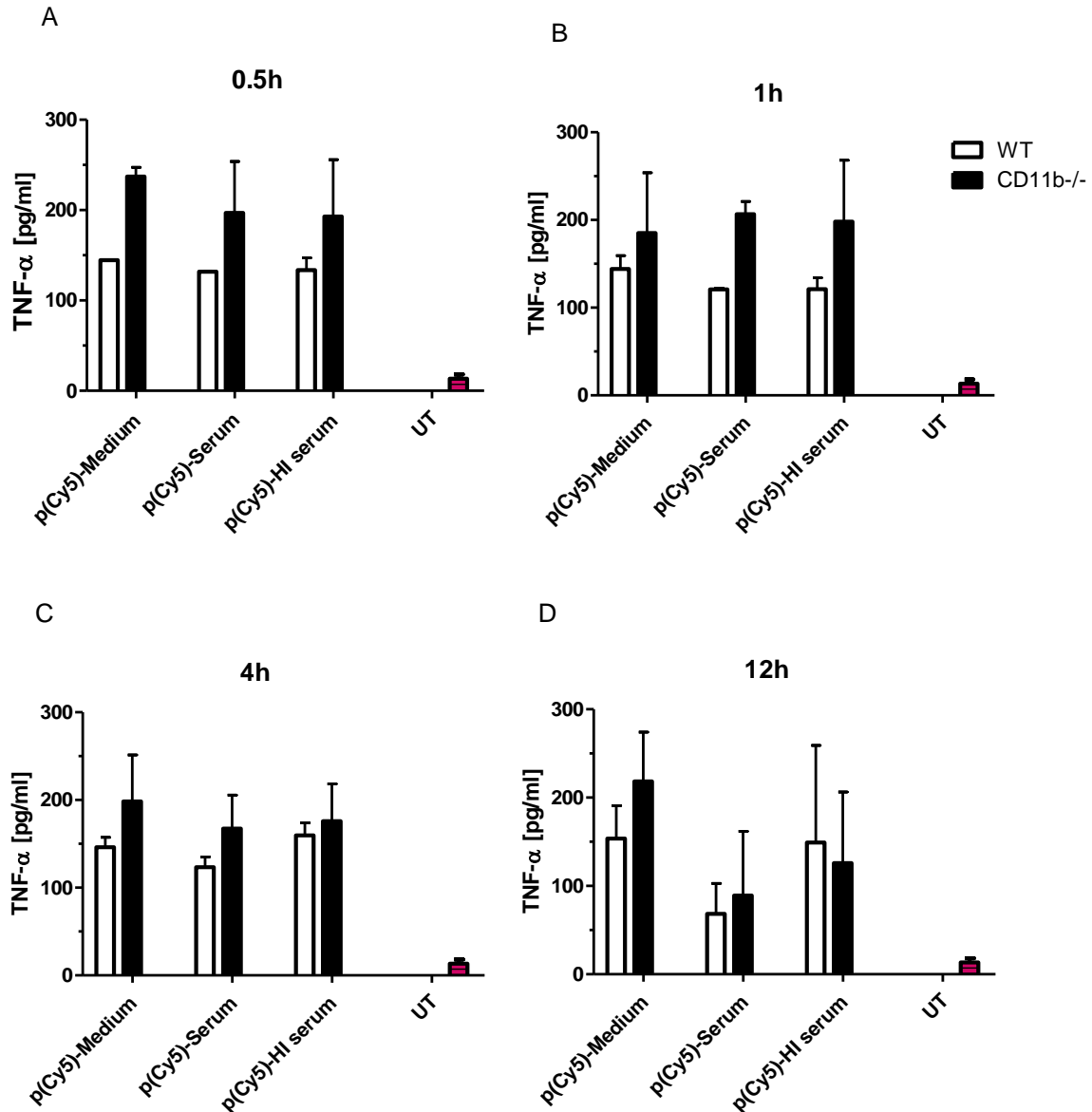


Figure 65. TNF- $\alpha$  secretion by CD11b<sup>-/-</sup> BM-DC exposed to the p(Cy5).

BM-DC derived from the WT and CD11b<sup>-/-</sup> were incubated with p(Cy5) that has been coated with FCS (standard medium condition), native or HI-native mouse serum. After 0.5h (A), 1h (B), 4h (C) and 12h (D) supernatant from the culture was collected and TNF- $\alpha$  concentration was measured (CBA assay). Bars represent mean values with SEM (n=2).

### 2.4.1.2. Engulfment of p(Cy5) by $CD11b^{-/-}$ splenic DC

To analyse the p(Cy5) uptake capacity of primary DC, splenic cells were *ex vivo* exposed to differentially pre-treated p(Cy5) beads and particle binding was examined after 1h and 4h via flow cytometry (Fig. 66). The nano-beads were pre-incubated with standard medium, and native or HI-mouse serum. No genotype-specific differences were observed in p(Cy5) recruitment (Fig. 67).

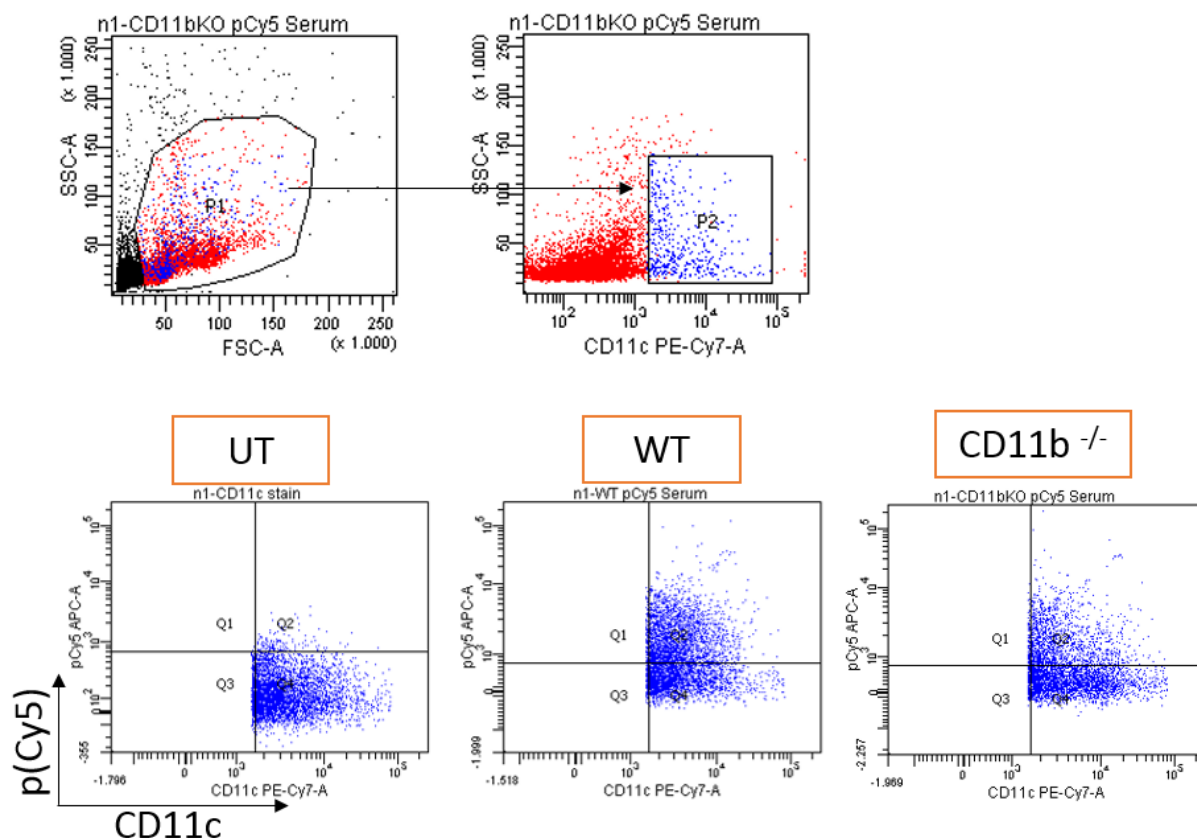


Figure 66. Gating strategy for the uptake of p(Cy5) by  $CD11b^{-/-}$  splenic DC.

Spleens from WT and  $CD11b^{-/-}$  mice were isolated and the whole splenocyte population was exposed to pre-treated p(Cy5) beads (beads were pre-incubated with either FCS-containing standard medium, with native or HI-native murine serum). After 1h and 4h of co-incubation splenocytes were stained with CD11c antibody and the positive fraction was further sub-gated against APC channel detecting p(Cy5).

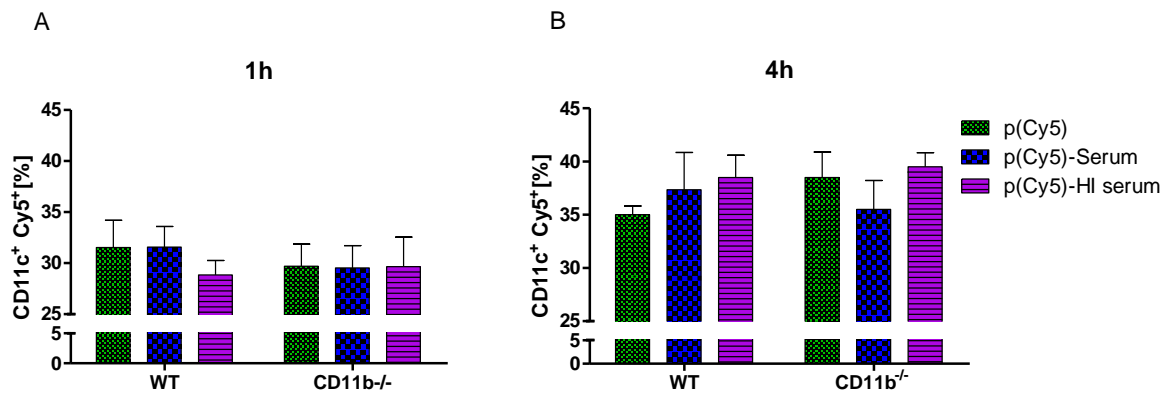


Figure 67. Uptake of p(Cy5) by CD11b<sup>-/-</sup> splenic DC.

Spleens from WT and CD11b<sup>-/-</sup> mice were isolated and the whole splenocyte population was exposed to pre-treated p(Cy5) beads (beads were pre-incubated with either FCS-containing standard medium, with native or HI-native murine serum). After 1h (A) and 4h (B) of co-incubation splenocytes were stained against CD11c. DC that bound p(Cy5) were analysed as the percentage of the whole CD11c<sup>+</sup> population. Bars represent mean values with SEM (n=4).

#### 2.4.2. Role of Mac-1 on DC for the uptake of Dextran

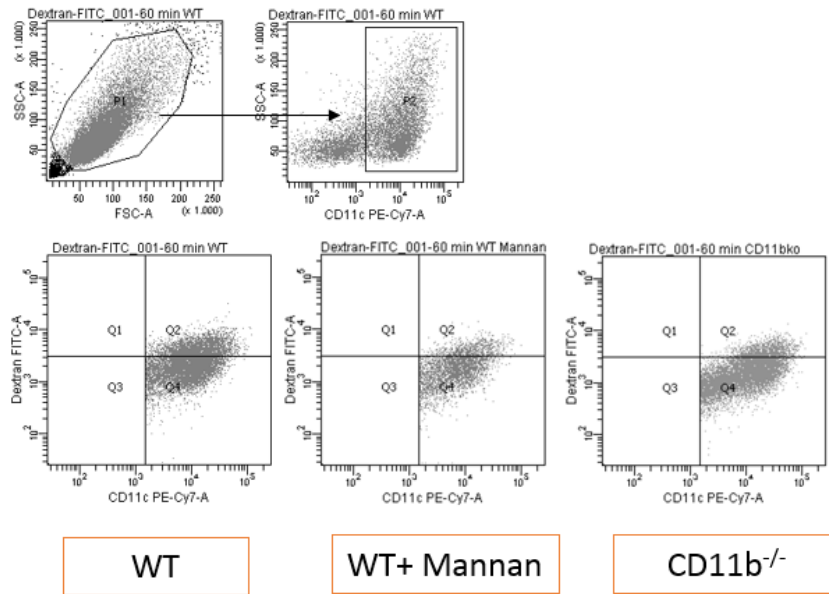
In order to analyse the role of Mac-1 for dextran-uptake CD11b<sup>-/-</sup> DC (both BM-DC as well as splenic DC) were co-incubated with FITC-dextran (1µg/ml) and its engulfment was assessed at different time points (10, 30 and 60 min at 37°C) (Fig.68A). Co-incubation at 4°C in parallel assays and blockade of the mannose-receptor with mannan (0.2µg/ml) were performed as controls.

Analysis showed that CD11b<sup>-/-</sup> BM-DC had a reduced dextran-uptake capacity at the latest time point (60 min). About 25% of CD11c<sup>+</sup> WT BM-DC engulfed dextran in comparison to 11% of CD11c<sup>+</sup> CD11b<sup>-/-</sup> BM-DC (Fig. 68B). After blockade of mannose-receptor with mannan a significant decrease in dextran uptake by 50% was noted only in the WT group. In case of the CD11b<sup>-/-</sup> BM-DC no further decrease occurred in response to blockade of the mannose receptor. The values for dextran binding at 4°C were below the values of any time point at 37°C, which indicates that dextran engulfment was a temperature-dependent active process.

The analysis of the splenic DC *ex vivo*, delivered results that supported the findings obtained for BM-DC. In case of the splenic DC, as in BM-DC, the reduction of the dextran uptake capacity in the CD11b<sup>-/-</sup> was observed after the onset of incubation. A significant 50% drop was noted in the CD11b<sup>-/-</sup> group in comparison to WT splenic DC. No specific uptake was observed

in the early time-points (similarly to the 4°C group) (Fig. 69A, B). No differences in uptake were measured on a per cell level, i.e. both WT and CD11b<sup>-/-</sup> splenic DC engulfed comparable amounts of dextran (mean fluorescence intensity of FITC-dextran was equal in all groups) (Fig. 69C).

**A**



**B**

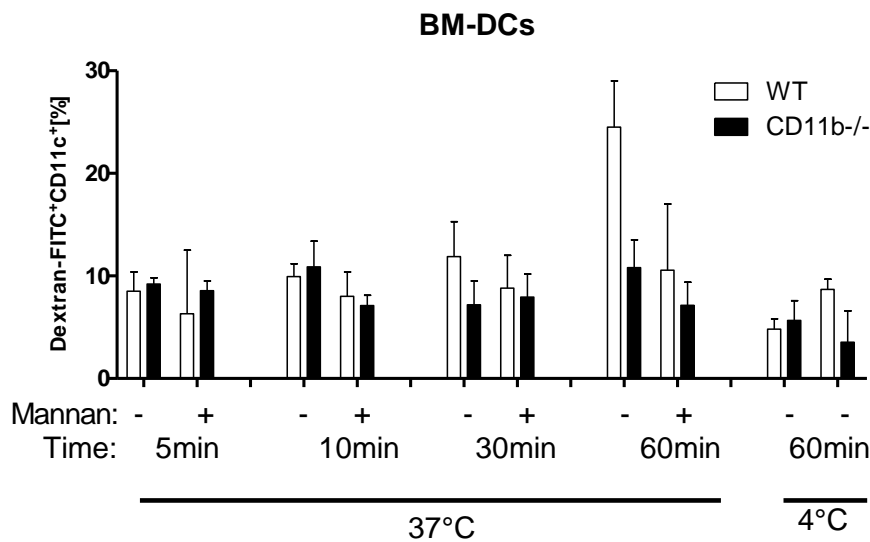


Figure 68. Uptake of dextran by CD11b<sup>-/-</sup> BMDC.

Bone marrow-derived DC from CD11b<sup>-/-</sup> and WT mouse were cultured with FITC-dextran (1µg/ml) for 5min, 10min, 30min and 60min at 37°C (control group was cultured at 4°C for 60 min). In (B) BM-DC were blocked with mannan (0.2µg/ml) prior to co-culture to saturate the mannose receptor. Subsequent to co-incubation cells were stained with α-CD11c Ab and the recruitment of dextran by the BM-DC was evaluated with flow cytometry as double positive FITC-dextran<sup>+</sup>CD11c<sup>+</sup> out of CD11c<sup>+</sup> population (A). Bars represent mean values with SEM (n=2).

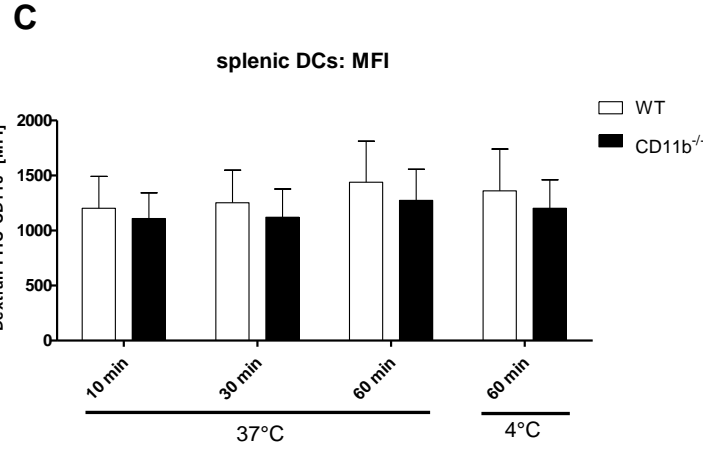
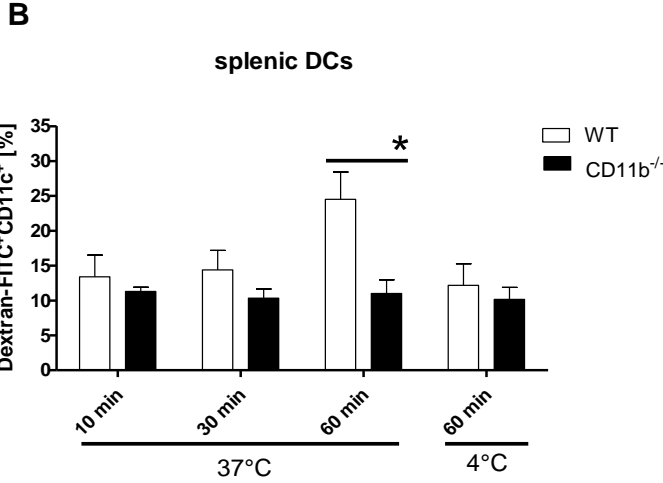
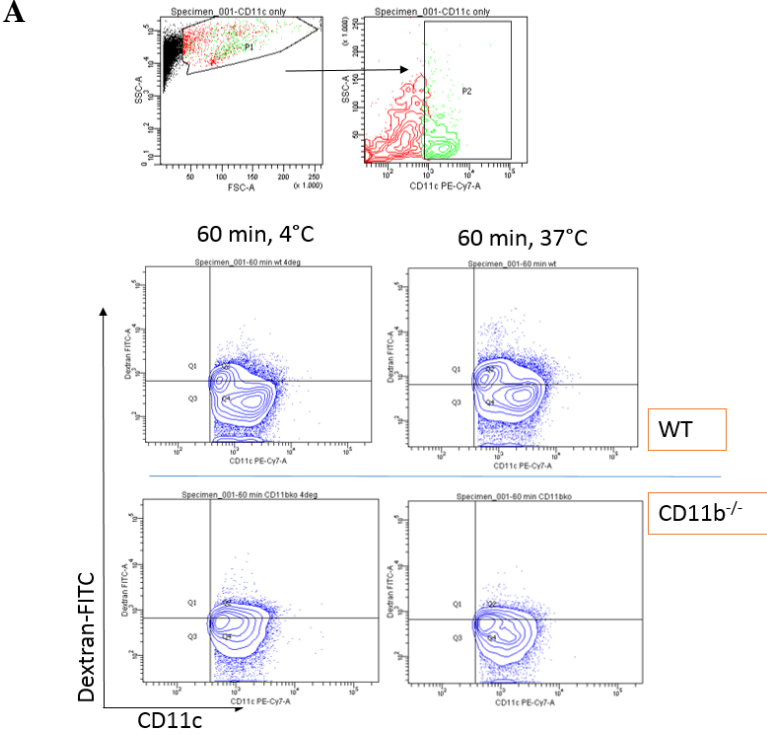


Figure 69. Uptake of dextran by CD11b<sup>-/-</sup> splenic DC.

*The whole splenocyte population from CD11b<sup>-/-</sup> and WT mouse was cultured with dextran (1µg/ml) for 10min, 30min and 60min at 37°C (control group was cultured at 4°C for 60 min). Subsequent to co-incubation cells were stained with α-CD11c Ab and the recruitment of dextran by splenic DC was evaluated with flow cytometry as double positive FITC-dextran<sup>+</sup>CD11c<sup>+</sup> out of CD11c<sup>+</sup> population (A). Bars represent mean values with SEM of the CD11c<sup>+</sup> fraction that took up dextran (B), as well as MFI values of analysed cells (C)(n=4).*

### 2.4.3. Uptake of an antigen (Ovalbumin) by Mac-1 and its intracellular processing

To evaluate the role of Mac-1 for the engulfment and intracellular processing of a model antigen (Ovalbumin), BM-DC and splenic DC were co-incubated with OVA-AlexaFluor647 and OVA-DQ (50µg/ml), respectively, followed by subsequent flow cytometric analysis. In case of OVA-DQ the fluorogenic substrate is quenched and relieved once intracellular proteases cleave the protein into peptides.

#### 2.4.3.1. Engagement of the OVA-AlexaFluor647 by CD11b<sup>-/-</sup> BM-DC and splenic DC

The analysis of OVA-AlexaFluor647 uptake was carried out at three time points, i.e. 10min, 30min and 60min at 37°C. Negative control culture was carried out at 4°C for 60min. Cells were subsequently examined by flow cytometry (Fig. 70A).

We found that as compared to the WT control, the OVA-Alexa647 uptake in the CD11b<sup>-/-</sup> BM-DC was significantly reduced at earlier time points of incubation, namely at 10 and 30 min. The values were, however, below significance after 60min of co-incubation. As expected, the basal level of OVA-binding at 4°C did not exceed 15%, whereas the binding with active uptake at 37°C raised from 32% at 10min to about 52% at 60min (measured as percentage of CD11c<sup>+</sup> BM-DC, Fig. 70B). A similar reduction in the OVA-AlexaFluor647 uptake was observed when WT and CD11b<sup>-/-</sup> BM-DC were cultured together, a drop in uptake by CD11b<sup>-/-</sup> BM-DC was measured at all time points (Appendix F). Blockade of CD11b with an α-CD11b Ab reduced OVA uptake, as compared to the BM-DC treated with a corresponding isotype Ab (Fig. 70C).

Further tests carried out with splenic DC confirmed our initial findings. At all time-points tested uptake of OVA-AF647 was diminished in case of the CD11b<sup>-/-</sup> DC. However, the effect was less pronounced as in BM-DC (Fig. 71A). No difference was observed at an MFI level, i.e. on a per cell basis (Fig. 71B).

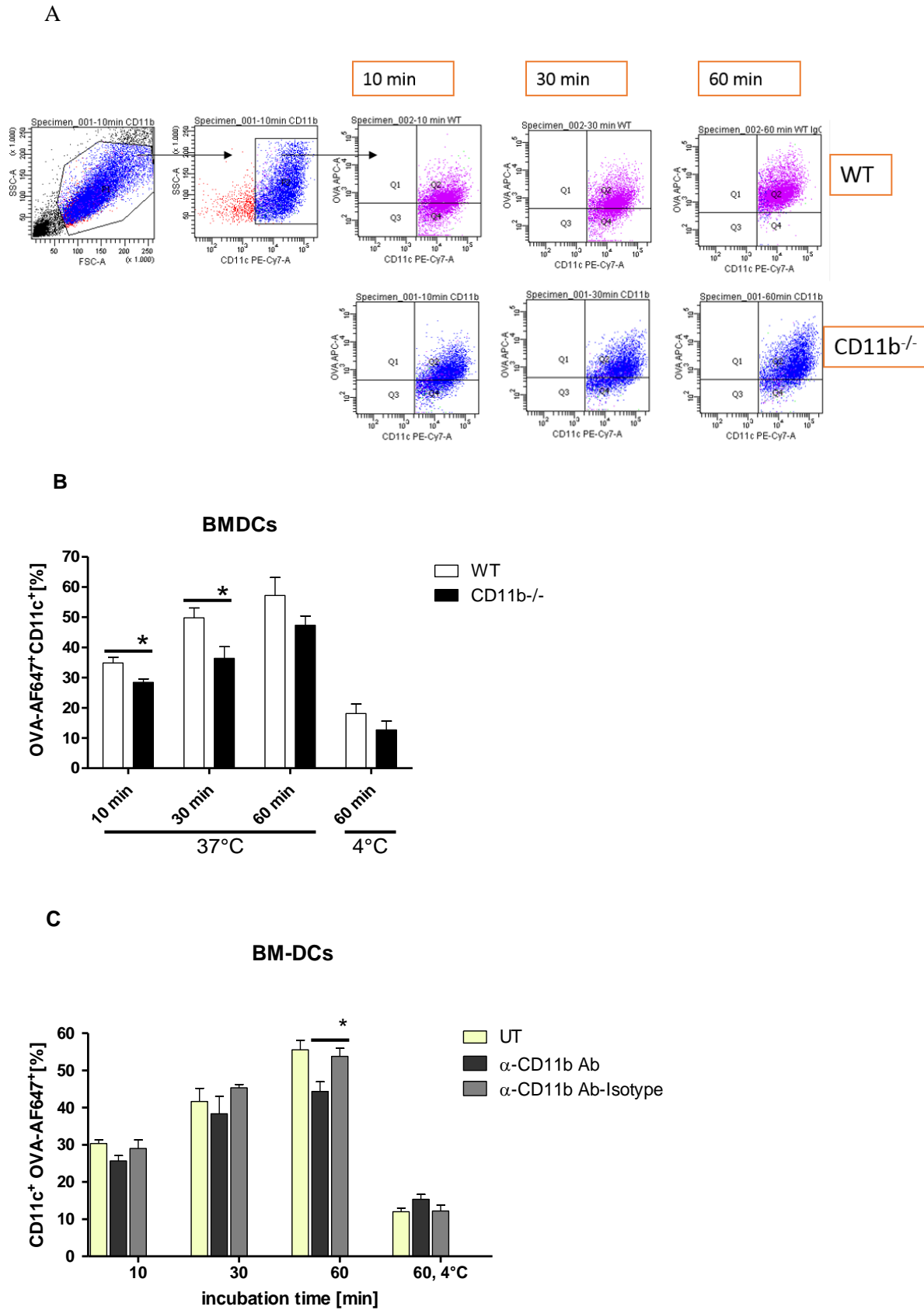


Figure 70. Uptake of OVA-AlexaFluor647 by CD11b<sup>-/-</sup> BM-DC.

BM-DC from WT and CD11b<sup>-/-</sup> mice were isolated and incubated with OVA-AlexaFluor647 (50 $\mu$ g/ml) for 10, 30 and 60min at 37°C (control was incubated at 4°C) (B). Cells from both

genotypes were cultured separately. Additionally, WT BM-DC were either left untreated or pre-blocked with  $\alpha$ -CD11b (10 $\mu$ g/ml for 30min) or treated with the corresponding isotype Ab (C). After incubation time cells were harvested and stained against CD11c. Cells were first gated for CD11c and then sub-gated for CD11c<sup>+</sup>OVA-AF647<sup>+</sup> double positives (A). Bars represent mean values with SEM (n=6 for B, n=3 for C).

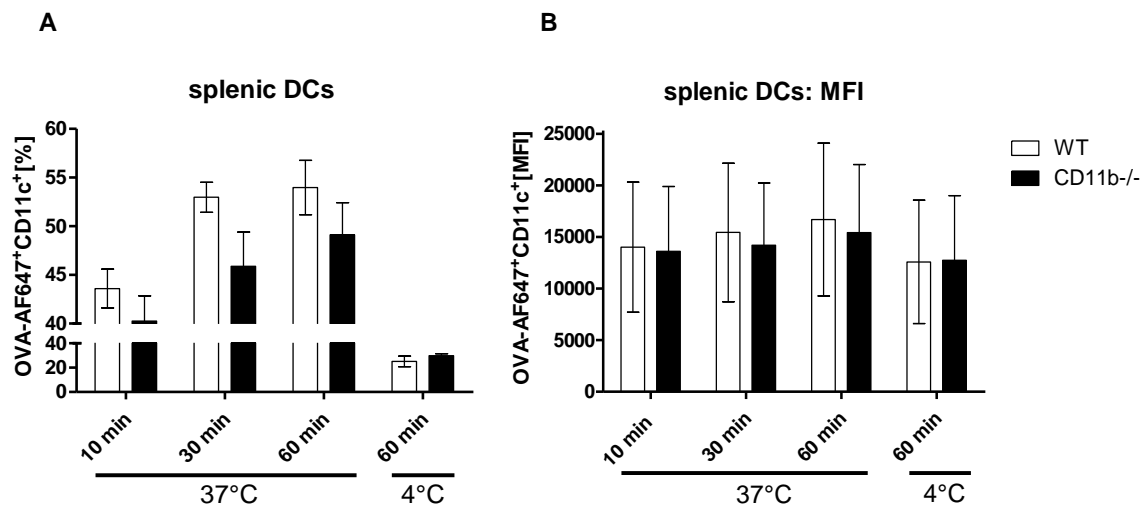


Figure 71. Uptake of OVA-AlexaFluor647 by CD11b<sup>-/-</sup> splenic DC.

Splenocytes from WT and CD11b<sup>-/-</sup> mice were incubated with OVA-AlexaFluor647 (50 $\mu$ g/ml) for 10, 30 and 60min at 37°C (control was incubated at 4°C). After incubation time cells were harvested and stained against CD11c. Cells were first gated for CD11c and then sub-gated for CD11c<sup>+</sup>OVA-AF647<sup>+</sup> double positives. Uptake was evaluated as percentage of the whole DC population (A) and on a per cell level as MFI (B). Bars represent mean values with SEM (n=4).

#### 2.4.3.2. Processing of the OVA-DQ by CD11b<sup>-/-</sup> BM-DC

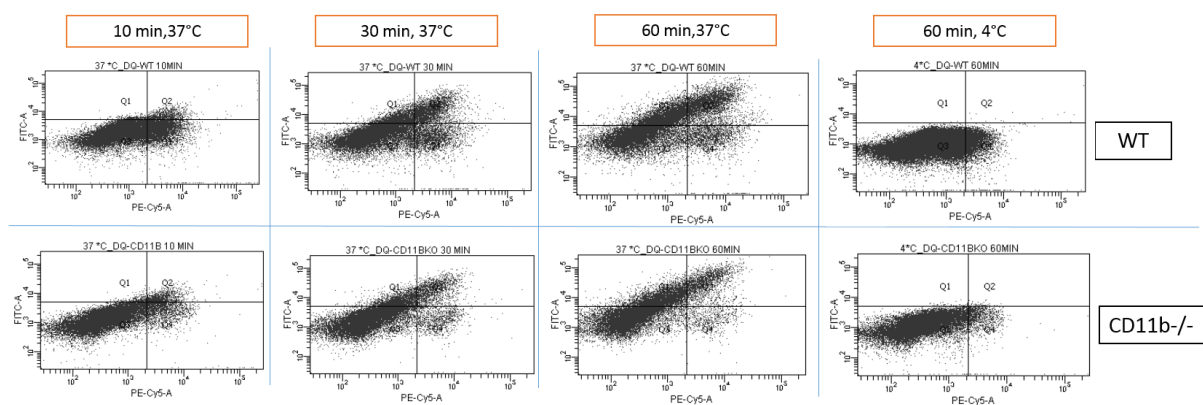
To analyse the potential role of Mac-1 for the intracellular faith of an internalized antigen, CD11b<sup>-/-</sup> and WT BM-DC were incubated with OVA-DQ (50 $\mu$ g/ml) and examined after 10min, 30min, and 60min. Endosomal uptake of an antigen was measured via flow cytometry in the PE-Cy5 channel, whereas antigen processing was assessed as a FITC positive event (Fig. 72A).

We found, as expected, that endosomal uptake of OVA-DQ was reduced in CD11b<sup>-/-</sup> BM-DC by 23% in the first 10 min and by 40% in the later course of incubation in comparison to the WT control. In both WT and CD11b<sup>-/-</sup> BM-DC cultures more than a half of an engulfed antigen left the endosome by the end of the co-incubation (2.5 fold reduction in WT and 2.8 fold reduction in the CD11b<sup>-/-</sup> BM-DC group) (Fig. 72B). When normalized to the initial endosomal antigen load per genotype, slightly more antigen was released from the endosomal compartment

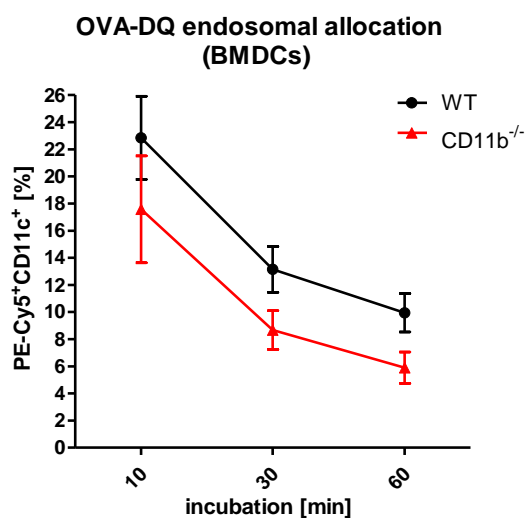
of the CD11b<sup>-/-</sup> BM-DC (44% remained in the WT and 34% remained in the CD11b<sup>-/-</sup> BM-DC) (Fig. 72D). Nevertheless, the values were not statistically significant and thus need to be treated with caution.

Further tests revealed that there was a tendency for a reduced allocation of an antigen to the lysosomal compartment in the CD11b<sup>-/-</sup> BM-DC as compared to the WT. Lysosomal allocation follows endosomal allocation and thus the less antigen first allocates to the endosome the less is then localized within the lysosome. In about 17% of the WT BM-DC and in about 15% of the CD11b<sup>-/-</sup> BM-DC OVA reached the lysosome after 60min (Fig. 72C). When normalized to the initial 10min lysosomal antigen load, in WT BM-DC the amount of antigen enriched 10-fold after 60 min, and in CD11b<sup>-/-</sup> about 7.5-fold, the result is however not significant due to the large error bars (Fig. 72E). We believe therefore, that Mac-1 is not really essential for the processing of the antigen.

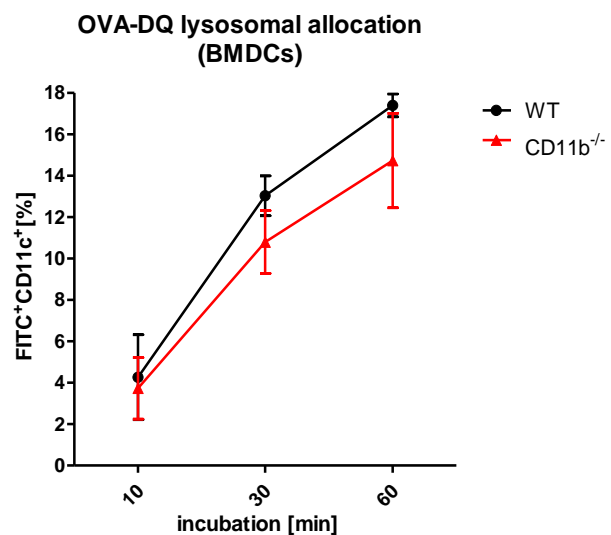
**A**



**B**



**C**



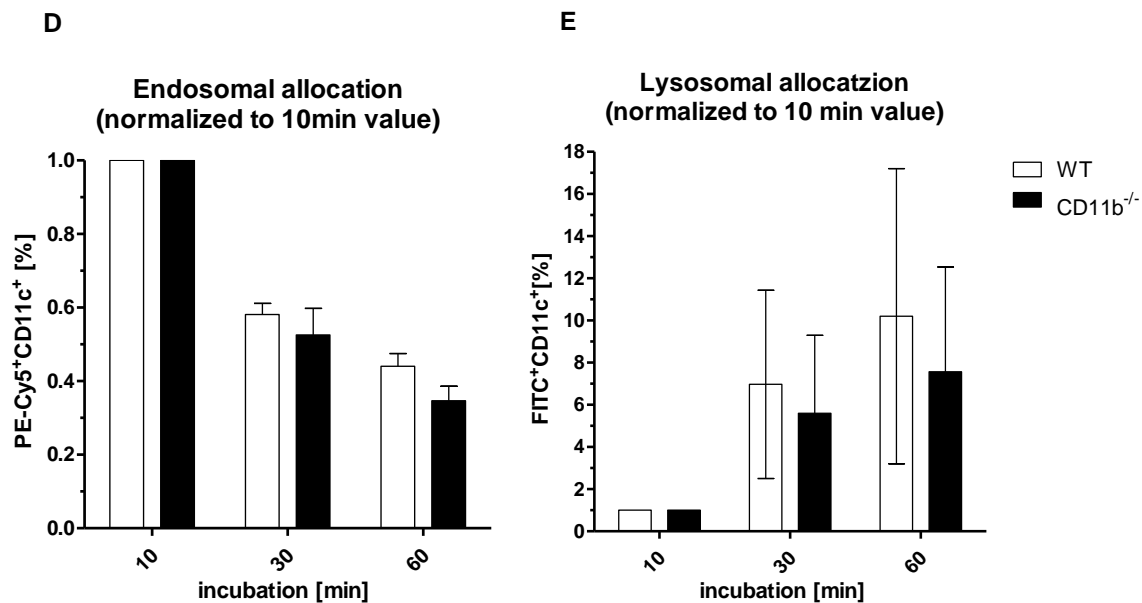


Figure 72. Uptake of OVA-DQ by CD11b<sup>-/-</sup> BM-DC.

BM-DC from WT and CD11b<sup>-/-</sup> mice were incubated with OVA-DQ (50µg/ml) and subsequently cells were analysed after 10min, 30min and 60min by flow cytometry. Cells were then analysed in PE-Cy5 and FITC channel (A). PE-Cy5 indicates the endosomal allocation of OVA and FITC the lysosomal allocation. Results were analysed as the percentage of the BM-DC that allocated OVA to the specified cell compartment, i.e. endosome (B) or lysosome (C). Normalized results (D, E) represent values adjusted the initial 10min measurement. Bars represent mean values with SEM (n=3).

## 3. Discussion

### 3.1. Biological role of $\beta$ 2 integrins

#### 3.1.1. $\beta$ 2 integrins

$\beta$ 2 integrins are critical for leukocyte migration and intercellular interactions. These transmembrane heterodimers consist of a CD18-beta subunit non-covalently associated with one of four different alpha subunits (CD11a, CD11b, CD11c or CD11d).  $\beta$ 2 integrins are expressed exclusively on leukocytes and exert a broad spectrum of biological functions, involving uptake of exogenous material, control of blood coagulation, cell migration and adhesion. Controversially discussed role as pro- and anti-inflammatory signalling modulators makes them interesting therapeutic candidates for cancer or autoimmune diseases.

The role of  $\beta$ 2 integrins in cell migration is essential for the recruitment of immune cells to sites of inflammation or tissue damage. All four  $\beta$ 2 integrins bind extracellular matrix proteins, such as collagen, and proteins involved in intercellular interactions, like intercellular adhesion molecules (ICAMs) (Barczyk et al., 2010). Therefore, they enable a cell to roll along the inflamed endothelium and to extravasate blood vessels towards their target tissue, where they orchestrate an innate (neutrophils) and adaptive (T cells) immune response via cell-to-cell communication.  $\beta$ 2 integrins are, moreover, involved in an immune cell signalling, such as Toll-like receptor (TLR)-signalling. Thus, they can influence TLR-modulated inflammatory responses (Han et al., 2010; Ling et al., 2014; Yee & Hamerman, 2013).

It is well known that integrins are normally expressed in an inactive state on the cell surface, with macrophages being an exception (Varga et al., 2007). Engagement of an agonist leads to an inside-out signalling and a conformational change of the extracellular domain of the integrin toward an open, high affinity state. For the binding of some ligands, like ICAM-1, integrins need to be in an active, high affinity state. The default, inactive state of  $\beta$ 2 integrin allows an undisturbed circulation of the leukocytes in a non-inflamed vessel. CD11b and CD11c, also known as C3- and C4-complement receptors, are essential for binding and phagocytosis of pathogens opsonised with the according complement factors. CD11b is most promiscuous among the  $\beta$ 2 integrins and can bind many distinct soluble or cell-bound ligands, such as fibrinogen, factor Xa, heparin, nucleic acids, ICAMs or VCAMs (J. D. Humphries et al., 2006). Besides, it has been reported that CD11b physically interacts with the human Fc $\gamma$  receptor IIA and IIIB and amplifies its calcium-mediated signalling, which results in an enhanced phagocytosis and release of pro-inflammatory cytokines by neutrophils (Galon

et al., 1996; Kindzelskii et al., 2000; Sehgal et al., 1993; Stockl et al., 1995). Thus, CD11b and CD11c are critical for the phagocytosis of pathogens, which in consequence attributes myeloid cells an essential role for the innate immune response and host defence. Recent findings regarding the role of  $\beta 2$  integrin in the immune system indicate that insufficient activity of these leads to episodes of recurrent infections and impaired wound healing (known as leukocyte adhesion deficiency syndrome), whereas their excessive activity may contribute to loss of the control in the inflammatory response and may cause tissue damage.

### 3.1.2. *Therapeutic usage of $\beta 2$ integrins*

$\beta 2$  integrins have received much attention as therapeutic targets mostly in treatment of autoimmune conditions in the past few decades. Integrin antagonists, such as Efalizumab, a recombinant humanized monoclonal antibody against CD11a, have been developed to treat psoriasis (Berends et al., 2007; Gupta & Cherman, 2006). The drug mainly impaired leukocyte migration and in this way decreased the inflammation. Unfortunately, it had to be withdrawn from the market in 2009 since patients suffered from multifocal leukoencephalopathy in consequence of human polyomavirus 2 (JC virus) reactivation (Major, 2010), most likely caused by an immunodeficiency resulting from deficient leukocyte migration. Similar, although less severe, side effects were reported in patients treated with Natalizunamb, a monoclonal Ab specific for  $\alpha 4$  integrin (Ryschkewitsch, Jensen, Monaco, & Major, 2010). This antibody binds  $\alpha 4\beta 1$  and  $\alpha 4\beta 7$ , and has been successfully used to treat patients suffering from Morbus Crohn or Multiple sclerosis (Akaishi & Nakashima, 2017; Nelson, Nguyen, McDonald, & MacDonald, 2018). Another small molecule, BMS-587101, has been developed to selectively block CD11a and was intended to cause less side effects as monoclonal antibodies. BMS-587101 was reported to effectively reduce lung inflammation and joint destruction in the murine RA model and improved viability of a transplant in a mouse model (Potin et al., 2006; Suchard et al., 2010). However, due to the risk of having similar side effects as the monoclonal antibodies, the substance was not developed further. A recently developed small molecule agonist of CD11b/CD18, leukadherin-1 (LA1), selectively activates Mac-1 and increases cell adhesion to CD11b ligands, such as ICAM-1 (Celik et al., 2013). It has been noted that LA-1 suppresses innate inflammatory signalling in human NK cells. In contrast to CD11a, CD11b not only mediates leukocyte migration, but as well contributes to tolerogenic signalling. LA-1 pre-treated NK cells showed less STAT5 phosphorylation in response to IL-12 and consequently a reduced secretion of  $\text{TNF}\alpha$  and  $\text{IFN}\gamma$  (Roberts, Furnrohr, Vyse, & Rhodes, 2016). In experimental models, LA-1 has been

successfully used to prevent inflammation in hypoxia-induced lung injury in rats (Jagarapu et al., 2015) and in an autoimmune nephritis model in mice (Jagarapu et al., 2015; Khan et al., 2014; Khan, Khan, & Gupta, 2018). Another therapeutic option lies in blockage of ligands that bind to  $\beta$ 2 integrins, like ICAM-1 (CD11a and CD11b ligand). A study on patients with early RA showed benefits of an anti-ICAM-1 mAb. Unfortunately, side effects restricted further testing (Kavanaugh et al., 1996).

Modulating the function of  $\beta$ 2 integrin is currently of great interest and it may bring benefits to patients suffering from inadequate or inefficient immune reactions. Nevertheless, high efficacy is gained mostly on the cost of immunodeficiency and thus side effects are challenging to manage. A progress in development of small molecules and biologicals that block or activate  $\beta$ 2 integrins is long-awaited. Maybe selective, cell-type specific, targeting of  $\beta$ 2 integrins would be suitable to achieve success in therapy without tremendous side effects.

### 3.2. Leukocyte adhesion deficiency syndrome and models to study CD18 ablation

#### 3.2.1. *LAD syndromes*

So far, research has considered  $\beta$ 2 integrins to provide a balance between immune tolerance and immunogenic response. Mice and humans with deficient or defective  $\beta$ 2 integrin suffer from both infections as a consequence of immunocompromising and autoimmune inflammation secondary to deficit in the negative immune system regulation. A deficiency in CD18 activity (ITGB2 mutation) is the primary cause of leukocyte adhesion deficiency syndrome 1 and 3 (LAD1 and LAD3). These are rare autosomal recessive disorders due to complete lack of CD18 or its reduced or aberrant expression or signalling in humans (Harris, Weyrich, & Zimmerman, 2013). In contrast to LAD1 and 3, LAD2 involves malfunction of another class of adhesion molecules, namely selectins (those are involved in the process of leukocyte migration only).

LAD1 syndrome is caused by a complete or partial CD18 deficiency. If LAD1 patients survive the infancy, managed with antibiotics, they suffer from periodontitis, tooth loss, recurrent infection from bacterial and fungal origin, impaired wound-healing and severe bleeding tendency (Kuijpers et al., 2007). In the severe form most patients die before their 5<sup>th</sup> year of life, in a moderate form (with residual 5-15% of CD18 activity) patients have high chance of mortality between 2<sup>nd</sup> and 4<sup>th</sup> life decade due to chronic infections (Kishimoto, O'Conner, & Springer, 1989; Kishimoto & Springer, 1989). CD18 deficiency described in dog and cattle presents with granulocyte dysfunction and recurrent infections of bacterial origin, and thus

resembles LAD symptoms reported for humans, which indicates that  $\beta 2$  integrin-associated pathology is conserved among mammalian species (Giger, Boxer, Simpson, Lucchesi, & Todd, 1987; Kehrli et al., 1990).

LAD2 syndrome, also known as congenital disorder of glycosylation type IIc, is characterized by symptoms similar to those noted in LAD1, i.e. recurrent bacterial infections including pneumonia, periodontitis, and *otitis media* accompanied by leucocytosis, but with another pathomechanism as LAD1 or LAD3 underlying the clinical manifestation. The cause of LAD2 is a deficiency of the GDP-fucose transporter and consequently a defect in the synthesis of Sialyl-LewisX, a P- and E-Selectin binding carbohydrate important for leukocyte tethering and rolling along the endothelium (Sturla et al., 2001; Yakubenia et al., 2008).

LAD3 syndrome, also known as LAD1 variant, is caused by mutation in FERMT3 or KINDLIN3 that are important for the inside-out signalling and activation of  $\beta 2$  integrins on leukocytes. Thus, the adhesive function of leukocytes and platelets in LAD3 patients is impaired and cells cannot effectively bind their ligands to migrate (Stepensky et al., 2015; van de Vijver, van den Berg, & Kuijpers, 2013).

So far, most research has focused on the role of neutrophils in LAD-associated pathologies. Emerging evidence suggests, however, that other leukocytes may play a crucial role in these maladies as well, especially in LAD1 and 3.

### 3.2.2. *Mouse models to study CD18 deficiency*

Even though LAD syndromes are quite rare, investigation of their pathomechanisms provides insight to fundamental immune processes and may serve to develop new immunomodulatory therapies. There are several mouse models available to study LAD maladies. First CD18 knock-out mice have been generated in the laboratory of Prof. Arthur L. Beaudet (Wilson et al., 1993). An insertion mutation was introduced using a homologous recombination in the ES cells, which resulted in a hypomorphic CD18 allele (the targeting vector contained a cryptic promoter that caused a low CD18 gene expression). The pCD18ex3 targeting vector was prepared by ligation of a neomycin resistance cassette with the 5 end of the CD18 exon3 within a pBluescript II KS (+) plasmid. The neomycin cassette disrupted the splice –acceptor site of exon3. The construct introduced an insertion mutation duplicating exon 2 and exon 3, whereas one copy of exon 3 was disrupted by the neomycin cassette. The homozygous offspring displaying 2-16% of the normal CD18 expression was viable and fertile. Mice showed mild granulocytosis, an impaired inflammatory response to chemical peritonitis and a delay in the rejection of cardiac transplants. This CD18 hypomorphic mouse model was widely used to

study psoriasis (Singh et al., 2013; H. Wang, Peters, Sindrilaru, & Scharffetter-Kochanek, 2009).

Few years after generation of the CD18<sup>hypo</sup> mouse, a mouse completely deficient in CD18 was generated also by the means of homologous recombination in the ES cells. The same targeting construct encompassing exon2, exon3 of CD18 and a neomycin resistance cassette was used as for the generation of the CD18<sup>hypo</sup> mice. In contrast to the generation of CD18<sup>hypo</sup>, to obtain a CD18 null knock-out the targeting construct was used to introduce a replacement mutation, instead of a duplication that yielded a hypomorphic allele. Clinical manifestations of the CD18 complete ablation were much more severe as that seen in the CD18<sup>hypo</sup> mice. About one third of the offspring died perinatally and those that survived infancy developed extended facial and submandibular ulcerative dermatitis. Inflamed lesions contained lymphocytes and opportunistic plasma cells, but very few neutrophils, suggesting that migration of these cells was impaired. Affected individuals developed granulocytosis, splenomegaly, and lymphadenopathy. They had about 10-fold increased serum IgG levels, and an elevated IL-3 and IL-6 serum levels as compared with the WT mice. The CD18 knock-out mice were as well not able to clear bacteremia, since all of the *S.pneumnie* inoculated mice died, as compared with a 53% survival by day 10 in WT mice (Scharffetter-Kochanek et al., 1998). The CD18<sup>-/-</sup> mouse model resembles therefore a severe form of the LAD1 syndrome in humans and has been explored in context of various pathologies like psoriasis (Barlow et al., 2003), wound healing disorder (Sisco et al., 2007), diabetes (Glawe et al., 2009; Meakin et al., 2015), carditis (Guerau-de-Arellano, Alroy, & Huber, 2005; Haasken, Auger, & Binstadt, 2011), osteoporosis (Miura et al., 2005), bacterial infections (*Listeria monocytogenes*) (Bose et al., 2013; H. Wu et al., 2003) as well as eukaryotic infections (*Leishmania major*) (Grabbe et al., 2002; Woelbing et al., 2006).

Until now there has been no mouse model available that allowed researchers to study the role of  $\beta$ 2 integrins for a specific cell types *in vivo*. Most of the research that focused on particular CD18<sup>-/-</sup> leukocyte populations was performed employing a bone marrow transplantation, which has got its pitfalls. To contribute to the field and to allow us to address the role of  $\beta$ 2 integrins on selected leukocyte populations *in vivo*, we generated a new mouse strain, in which exon3 of the CD18 gene is flanked by LoxP sites. Crossing of this mouse with a Cre-driver mouse enables a cell type specific deletion of  $\beta$ 2 integrins when cre-transgenic mice express Cre-recombinase under a promotor that is specific for a given cell population (X. Wang, 2009). This system allows us to delineate the contribution of specific types of leukocytes to the immunological consequences of CD18 deficiency.

### 3.3. Conditional deletion of CD18 using a Cre-loxP strategy

Bacterial endonucleases have recently become a powerful tool for mammalian gene editing. Aside from the long-established Cre-loxP system new more time-efficient technologies, like transcription activator-like effector nucleases (TALEN) and clustered regularly interspaced short palindromic repeat-associated nuclease Cas9 (CRISPR/Cas9) found their application in biomedical research (Stoddard, 2011). The main limitation associated with these recently developed technologies, mainly with CRISPR/Cas9, is the unwanted ‘off target’ effect of the endonucleases. A very careful bioinformatical design of the targeting construct is therefore obligatory to successfully edit genes. As the generation of the CD18 conditional knock-out commenced, the other two technologies were not yet well established to generate a conditional deletion and therefore we decided for a more time consuming but a well-approved Cre-LoxP technology.

In brief, the Cre-loxP system involves an enzyme, called Cre-recombinase, and LoxP sites, which contain a 34 bp DNA sequence recognized by the enzyme (both components derived from a bacteriophage P1). Depending on the orientation of the LoxP sites, Cre-recombinase can introduce a deletion, insertion, translocation or an inversion at specific sites in genomic DNA. In order to delete a gene, a transgenic Cre-recombinase expressing mouse has to be crossed with another transgenic mouse that has loxP sites introduced into the genome at the specific site, flanking the exon of a gene of interest. Thus, Cre-recombinase makes a site-specific cut and splices out the DNA sequence between loxP sites oriented in the same direction. A simplified scheme of the Cre-loxP recombination is depicted below (Fig. 73)

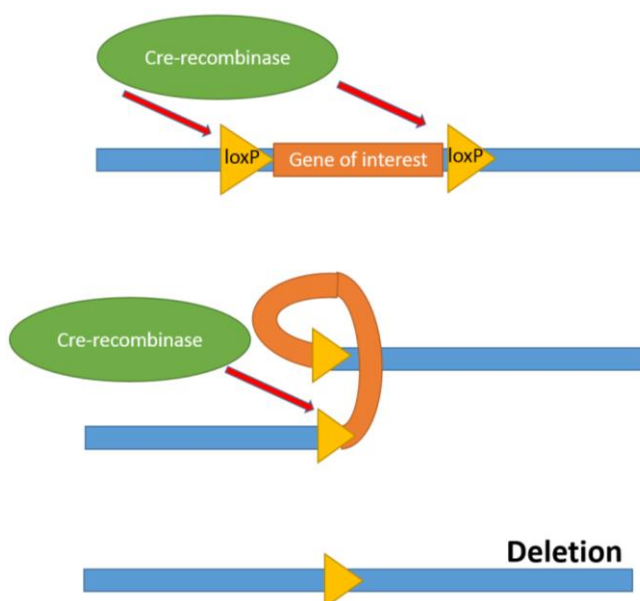


Figure 73. Cre-LoxP recombination scheme.

Just like TALEN or CRISPR/Cas9, the Cre-loxP site specific recombination has as well its pitfalls that one has to be aware of. Firstly, gene ablation may still happen in other cell types and tissues, which creates a difficult to study, complex phenotype. This largely depends on the specificity of the promotor used as the driver for Cre-recombinase expression. A second possible complication is embryonic lethality, which may be a consequence of the gene deletion in the germ line. Thirdly, Cre-associated, dose-dependent toxicity in the cardiac tissue has been reported in several publications (Buerger et al., 2006; Koitabashi et al., 2009; Pugach, Richmond, Azoifeifa, Dowell, & Leinwand, 2015). The mechanism remains, however, poorly defined. Cre-recombinase should be therefore carefully titrated to prevent the onset of myocardial fibrosis resulting from tissue damage.

Despite the outlined pitfalls, we decided that Cre-loxP recombination would still be the best method to generate a mouse that would allow us to study the function of a gene in a cell type-specific manner.

### 3.4. Targeting of CD18 in the murine embryonic stem cells by the means of homologous recombination yielded a CD18 floxed mouse line

The generation of the conditional knock-out using a cre-loxP system is a multi-step process, which involves mating of the floxed, recombined mouse strain (with an essential gene region flanked by loxP sites) with a Cre-driver mouse. There are cell type-specific and/or inducible Cre-expressing mouse lines. The later are mostly needed to study gene deletions in a controlled manner, especially when a null deletion results in an embryonal lethality.

Various strategies have emerged to introduce loxP sites into the genome. Most commonly the gene is targeted in the embryonic stem cell (ES) in order to produce a germline chimeric mice. A well-established homologous recombination in ES is thus a widely used method to introduce the knock-in cassette containing loxP sites into the genome (Capecchi, 1989). We have used it as well in our attempt to generate a CD18 gene-floxed mouse.

Recently, CRISPR/Cas RNA guided nucleases have been as well successfully used to induce gene mutation in the murine zygotes, which is an amazing technological advance. In this system a RNA-guided nuclease induces a double strand break at the target sequence that leads to a mutation subsequently repaired by non-homologous end joining (F. Jiang & Doudna, 2017; Jinek et al., 2012). A co-injection of a donor DNA containing homology to the sequence flanking the double strand breaks can produce a mutation or a DNA insertion, e.g. a loxP site

insertion (Horii et al., 2017). This is a powerful and time efficient method to generate a floxed mouse without the necessity to construct a knock-in vector, nevertheless the method has to be still optimized to gain a high knock-in frequency.

In our approach, a murine CD18 gene targeting construct (BO44.2) based on a loxP-FRT-neo-FRT-LoxP cassette (Fig. 11, Appendix A), was customized by PolyGene. The strategy of targeting is depicted in Fig.10. The CD18 gene was targeted by flanking exon 3, present in all splicing forms of the RNA, with loxP sites. The neomycin phosphotransferase II cloned in the construct provided for resistance against G418 antibiotic and thus served for the selection of recombined ES clone. The Neo cassette was cloned along with the pgk (phosphoglycerate kinase 1) promoter and a poly A. PGK1 is a eukaryotic, non-attenuated promoter and the advantage of it in comparison to viral promoters, such as widely used viral SV40 or CMV promoters, is that it is not that sensitive to silencing. The vector contained two arms of homology. The short arm of homology contained a sequence upstream of the murine CD18 exon3, whereas the long arm of homology consisted of the sequence coding for exons 4-6 of the CD18 gene. The Neo-cassette was inserted between exons 3 and 4, and was flanked by the FRT sites, so that it could be deleted later via Flippase (flp) mediated recombination (Golic, Rong, Petersen, Lindquist, & Golic, 1997). The construct contained two restriction sites, Not1 and Sall1, which could be used for linearization. LoxP sites were inserted as a direct repeat to induce a deletion event.

In order to generate a recombined ES clone, a linearized BO44.2 construct (Fig. 12) was introduced into murine embryonic stem cells (clone JM8) via electroporation. We have obtained a high yield of G418 resistant clones. Over 900 resistant ES clones were expanded individually and the recombination rate was examined using a Southern Blot strategy (Fig. 13-15). Two clones with a recombined allele were identified (Fig.16). After expansion and karyotype analysis (Fig. 17, Appendix B), these were further injected into a blastocyst of a recipient B6 Albino mouse to generate chimeric offspring (Fig. 18). The chimerism rate was assessed according to the coat colour. Most chimeric male offspring was crossed back to the albino background (Fig.19) and new born chimeric litters were screened for the presence of the Neo-cassette in the genome using a PCR approach (Fig. 20). A total of five chimeric Neo<sup>+</sup> mice was acquired. The Neo-cassette was deleted from the genome of the chimeras using an FLP-mediated recombination, i.e. CD18<sup>fl/wt</sup> Neo<sup>+</sup> chimeric mice were crossed to FLP-deleter mice over one generation and the Neo- cassette (flanked by the FRT sites) was entirely excised by the flippase (Fig. 21). Two founder mice, derived from the Transgenetic facility at Polygene, were used to establish a stable, floxed mouse strain.

The genotype of the homozygous CD18<sup>fl/fl</sup> mouse line was tested routinely using a PCR approach (Fig. 22). Moreover, the genomic DNA region containing the floxed allele was sequenced to confirm the orientation and integrity of the insert (Fig. 23-24). The CD18<sup>fl/fl</sup> mice showed, as we expected, no phenotype and the expression of CD18 on leukocytes was undisturbed (Fig. 28-36). They were therefore used in all experiments as a control strain, resembling a WT phenotype.

### 3.5. Deletion of CD18 specifically in murine DC (CD18<sup>ΔCD11c</sup>)

In order to study cell-specific functions of  $\beta 2$  integrins we crossed CD18<sup>fl/fl</sup> mice to CD11c<sup>CRE</sup> (Caton et al., 2007) and thus generated a CD11c-driven CD18 knock-out, i.e. a DC-specific deletion (Fig. 25). CD11c<sup>CRE</sup> harbours a bacterial artificial chromosome (BAC) transgene that expresses Cre-recombinase under the control of CD11c promoter/enhancer. The region coding for Cre-recombinase and a poly A-signal were introduced into the first exon of the Itgax (Integrin alpha X or CD11c) gene embedded in the BAC. The BAC, in turn, was introduced into a donor oocyte to establish a founder mouse line. The strain was subsequently backcrossed to C57/BL/6. CD11c<sup>CRE</sup> mice express Cre-recombinase in most conventional DC and many plasmacytoid DC, a marginal expression has as well been reported in lymphocytes, NK cells and myeloid cells (Abram, Roberge, Hu, & Lowell, 2014; Alves et al., 2015; Ramalingam et al., 2012; Travis et al., 2007).

Analysis of the newly generated CD18<sup>ΔCD11c</sup> mouse revealed a deletion or reduction of  $\beta 2$  integrins in BM-DC (Fig. 33) as well as primary DC derived from various tissues (Fig. 34-36). The major pitfall of the analysis was the lack of CD11c expression on DC surface. CD11c/CD18 belongs to the  $\beta 2$  integrins and therefore deletion of the CD18 beta subunit led to ablation of all alpha chains from the cell surface. The alpha and beta chains dimerize before they get integrated into the cell membrane, i.e. no single alpha or beta chains are expressed on the cell surface (M. J. Humphries, 2000). To solve this problem and to target DC we have applied in our experiments a negative cell selection approach and used alternative markers expressed on the DC surface.

Initially we have investigated the efficiency of Cre-recombination in the BM-DC population, which is a convenient source of a high amount of CD11c-expressing DC. In our WT BM-DC cultures stimulated with GM-CSF we routinely obtained about 80-90% of CD11c<sup>+</sup> cells. The analysis of the CD11c<sup>+</sup> CD18<sup>+</sup> and CD11c<sup>+</sup>CD11b<sup>+</sup> fractions out of the MHC-II<sup>+</sup> BM-DC showed a significant reduction in the expression of the  $\beta 2$  integrins in the CD18<sup>ΔCD11c</sup>

population as compared to the CD18<sup>fl/fl</sup> control. The percentage of aforementioned was decreased by over 70% (Fig. 33).

A similar decrease was observed in primary DC isolated from skin. The expression of CD11c, CD11b and CD18 was detected only in about 30% of the MHC-II<sup>+</sup> cell population derived from skin of the CD18<sup>ΔCD11c</sup> mice, whereas over 80% of MHC-II<sup>+</sup> skin DC from CD18<sup>fl/fl</sup> mice expressed CD11c, CD11b and CD18 (Fig. 34). Expression of CD11c and CD18 on splenic DC was detected only on 11% of the negatively sorted DC derived from CD18<sup>ΔCD11c</sup> mice (Fig. 36), whereas analysis of the lung tissue revealed a complete absence of CD11c expressing DC in the CD18<sup>ΔCD11c</sup> mice (Fig. 35).

Discrepancies between  $\beta 2$  integrin expressions in analysed tissues are most likely due to CD18/CD11c expression kinetics as well as protein turnover. CD11c expression is induced subsequently to CD18, thus CD18 and CD11c accumulate in the cell before CD18 is ablated and with a prolonged CD18 turnover one awaits a time-restricted, residual integrin expression after cre-mediated recombination. Furthermore, various strategies were applied to target DC in the experiments. In the BM-DC and skin, DC were defined as the MHC-II<sup>+</sup> fraction, which in case of the skin sample might have contained traces of other leukocytes, like macrophages or B cells. For the analysis of splenic DC we used a DC negative sorting kit (a fast enrichment kit for untouched isolation of DC) and therefore obtained a DC-enriched starting population (with about 90% of the CD11c<sup>+</sup> cells), which allowed a more precise investigation.

Moreover, the efficiency of the Cre-recombination depends on different factors. Firstly, the conformation of the chromatin (eu- or heterochromatin) plays a role in recombination, since Cre-recombinase requires access to the DNA fragment that contains the loxP sites. If the gene is not actively transcribed and the chromatin is condensed, the floxed allele might not be reached. This, however, should not play a role in our system, as  $\beta 2$  integrins are actively transcribed in DC. Secondly, a loss of Cre-recombinase expression correlating with increasing number of transgenic mouse generations has already been reported and may affect the recombination yield even though Cre is detectable on the genomic level (T. J. Schulz et al., 2007). Hence this is a factor that we may not completely exclude, it is however less likely. A third issue is the compatibility/affinity of the Cre-recombinase to the loxP sequence, there are at least 8 variants of this 34-bp palindromic sequence and they may exert an altered level of recombination (Santoro & Schultz, 2002). Last but not least, it has been reported as well that Cre-recombinase can be toxic to mammalian cells and thus cells with high expression may be prone to apoptosis (Loonstra et al., 2001).

Being aware of the limitations to the Cre-recombination lined out above, we still believe that the incomplete recombination was not really the case. The efficiency of Cre recombination in our model is presumably higher than what our analysis showed, but technical limitations to define a DC in absence of CD11c (and CD11b) made a highly precise analysis difficult to achieve. One solution could be the usage of a Cre-reporter mouse strain, in which a fluorescent protein is expressed along with the Cre-recombinase and so all cells that recombined by default *de novo* express a marker. Successful usage of a CD11c-Cre-GFP mouse line has already been described in the literature and mice are commercially available (Stranges et al., 2007). Hence, future work with CD18<sup>ΔCD11c</sup> mouse should be performed using a Cre-reporter mouse strain.

### 3.6. Ablation of CD18 specifically in CD11c<sup>+</sup> cells has no influence on maturation of other leukocytes

Comprehensive analysis of the mutant mice confirmed the selective deletion of β2 integrin in CD11c expressing DC. Analysis of β2 integrin expression on other leukocytes, including splenic T and B lymphocytes as well as macrophages, revealed no significant differences in expression of CD18, CD11b or CD11a between CD18<sup>ΔCD11c</sup> and CD18<sup>fl/fl</sup> mice (Fig.28-32). A minute decrease in the expression of CD18 was noted only in the F4/80<sup>+</sup>CD68<sup>-</sup> CD18<sup>ΔCD11c</sup> splenic macrophage fraction (Fig. 32). Since DC and macrophages are strongly related subtypes and a fraction of F4/80<sup>+</sup> splenic red pulp macrophages expresses CD11c, the decrease of CD18 expression was expected (Rose, Misharin, & Perlman, 2012). It has been reported as well that splenic monocytes, that may as well express F4/80, can upregulate CD11c without converting towards DC and thus could contaminate the macrophage fraction (Drutman, Kendall, & Trombetta, 2012). The activation state of splenic T and B lymphocytes, measured as the expression of CD25 on T cell (Fig. 30C) and the expression of CD86 and MHC-II on B cell (Fig. 31B), was unaltered. The composition of splenic T lymphocyte populations in the CD18<sup>ΔCD11c</sup>, including CD4<sup>+</sup>, CD8<sup>+</sup> and FoxP3<sup>+</sup> subsets, resembled what has been noted in the control group and stood in line with commonly known cell frequencies in murine spleen (Fig. 30C).

Furthermore, composition of leukocytes found within bone marrow and blood was not influenced by the deletion of CD18 on primary DC. The lymphocytic cell lineages, CD3<sup>+</sup> and CD19<sup>+</sup>, as well as myeloid subsets, including monocytic and granulocytic subsets, were comparable in both tissues of CD18<sup>fl/fl</sup> and CD18<sup>ΔCD11c</sup> mouse (Fig. 28, 29). To sum up, the analysis of non-targeted leukocyte subsets in the CD18<sup>ΔCD11c</sup> mouse showed an

undisturbed expression of  $\beta 2$  integrins and unaltered cell concentrations in the spleen, blood and bone marrow.

### 3.7. CD18 <sup>$\Delta$ CD11c</sup> DC are characterized by elevated production of cytokines in response to stimulation

Initial characterization of splenic DC involved their cell surface marker expression. Co-stimulatory molecules involved in antigen presentation and APC/TC interaction (CD80, CD86, CD40 and MHC-II; see Fig.4) were analysed via flow cytometry after overnight stimulation of cells with various TLR ligands (LPS, CpG, R848, PolyI:C).

Lipopolysaccharides (LPS) originate from gram negative bacteria and stimulate the cell surface receptor TLR4. CpG rich immunostimulatory DNA apparent in bacteria and viruses stimulates the intracellular TLR9 receptor (Akira & Takeda, 2004). Resiquimod (R848) is an imidazoquinoline compound that acts as an agonist for murine TLR7 (Grela et al., 2011), whereas Polyinosinic:polycytidylic acid (PolyI:C) structurally resembles double-stranded RNA and is therefore an intracellular TLR3 stimulant (Natarajan, Yao, & Sriram, 2016). TLR are transmembrane receptors responsible for pathogen sensing. They are located on the cell surface or in the endosome and convey DC maturation as well as antigen-specific adaptive immune response (Vidya et al., 2018). TLR stimulation results in the activation of NF $\kappa$ B (nuclear factor 'kappa-light-chain-enhancer' of activated B-cells) signalling and MAPK (mitogen-activated protein kinases) pathway that recruit co-stimulatory molecules and pro-inflammatory cytokines (Kawasaki & Kawai, 2014; T. Liu, Zhang, Joo, & Sun, 2017). TLR receptor classes and induced signalling are depicted in the Figure 74 below.

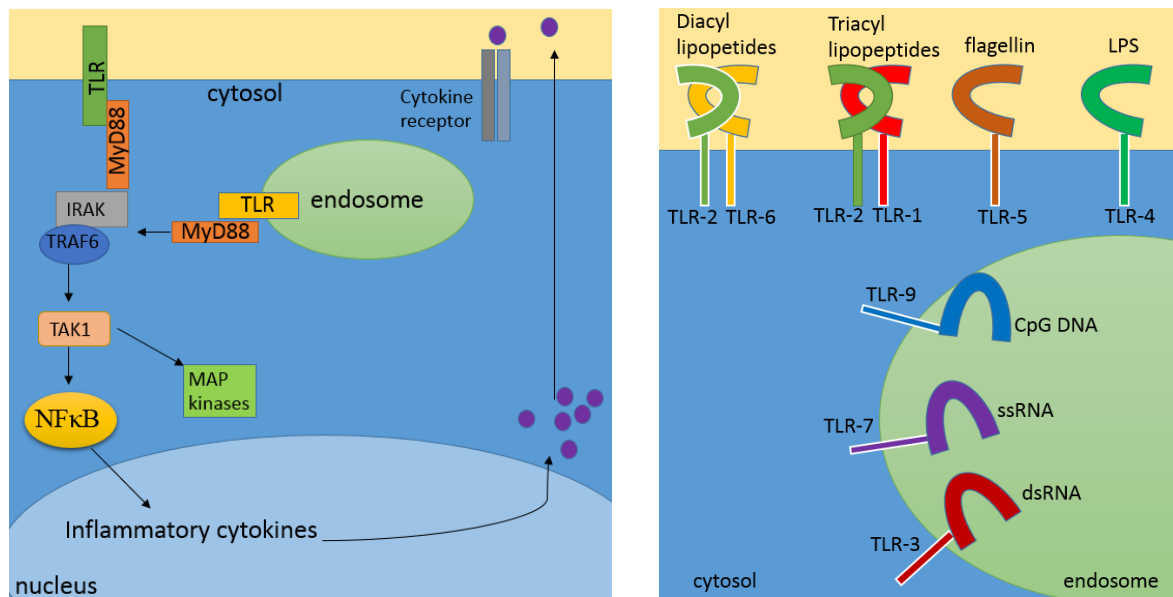


Figure 74. TLR ligands and signalling.

In accordance with analysis of splenic DC derived from a CD18 null mouse carried out by Varga and colleagues (Varga et al., 2007), splenic DC derived from the CD18<sup>ΔCD11c</sup> mouse showed no differences in the expression of activation markers as compared with the CD18<sup>fl/fl</sup> control sample independent of the kind of TLR stimulus applied. An insignificantly lower expression was noted only in case of the MHC-II in both unstimulated (Fig. 37) and stimulated splenic CD18<sup>ΔCD11c</sup> DC (Appendix D).

Similarly, we noted that in case of CD11b<sup>-/-</sup> BM-DC expression of CD80 and MHC-II was insignificantly diminished in the LPS stimulated samples in comparison to the WT control (Fig. 63, 64). We did not monitor CD11a, CD11c or CD11d influence separately in that matter. Since the data we obtained is not statistically valid, it needs to be treated with caution and at the most it suggests that CD11b may influence expression of co-stimulatory molecules on the DC stimulated with MyD88-triggering TLR ligands. Despite of the mild decrease in the MHC-II or CD80 expression we did not observe any defects in the antigen presentation capacity of splenic CD18<sup>ΔCD11c</sup> DC (Fig. 42,44,46), or CD11b<sup>-/-</sup> BM-DC *in vitro* (data not shown). It has been described that only after pharmacological activation of β2 integrin on BM-DC their T cell stimulatory capacity is suppressed, which can be reversed by usage of CD18 or CD11b blocking Ab (Varga et al., 2007). In a physiological condition, however, β2 integrins remain in an inactive state on the DC (Metelitsa et al., 2002). In our setting we did not influence the state of the β2 integrin activation and thus expected it to be mostly in a physiological, i.e. inactive state on the DC. That might be the reason why we did not see any significant changes in the *in vitro* proliferation of CD4<sup>+</sup> (Fig. 42, 44) or CD8<sup>+</sup> T cells (Fig. 46) primed by CD18 or CD11b deficient DC.

The T cell stimulatory and polarizing properties are not only defined by the expression of the surface markers, but also by the secretion of soluble mediators, like cytokines. Thus, we have subsequently investigated secretion of cytokines by splenic CD18<sup>ΔCD11c</sup> DC after stimulation with TLR ligands. We observed that upon stimulation splenic CD18<sup>ΔCD11c</sup> DC secreted higher amounts of assayed cytokine group in comparison to the CD18<sup>fl/fl</sup> control (Fig. 38, 39). Poly I:C turned out to be a weak DC activator in our experiments and led to a low cytokine release at similar concentrations in both studied groups. LPS led to a stronger secretion of TNF- $\alpha$ , IL-10 and IL-1 $\beta$  in the splenic CD18<sup>ΔCD11c</sup> DC as in the CD18<sup>fl/fl</sup> control. CpG and R848 were very potent stimulators and in case of IL-6, TNF- $\alpha$  and IL-10 the concentration of released cytokines was significantly elevated in the cultured CD18<sup>ΔCD11c</sup> splenic DC as compared with CD18<sup>fl/fl</sup> DC (Fig. 38). R848 stimulated CD18<sup>ΔCD11c</sup> DC secreted IL-6, TNF- $\alpha$ , IL-10 and IL-12 in a dose-dependent manner (Fig. 39). Analysis of mRNA derived from the R848-stimulated CD18<sup>ΔCD11c</sup> splenic DC, revealed an elevated expression of IL-6, TNF- $\alpha$  and IL-10 encoding mRNA as compared with the CD18<sup>fl/fl</sup> sample (Fig. 40). All together, these results suggested a cross talk between  $\beta$ 2 integrin and TLR-signalling molecules, which has as well been described by other researchers.

The interaction of  $\beta$ 2 integrin- and TLR4-mediated immune cell signalling remains controversial. On one hand, it has been reported that CD11b positively regulates TLR4-induced endocytosis and subsequent endosomal signalling in DC and that CD11b deficiency leads to a reduced TLR4-induced response and T cell activation *in vivo* (Ling et al., 2014). Another study on murine macrophages demonstrated that synergistic action of CD11b/CD18, CD14 and TLR4 is needed for the responsiveness towards LPS and CD11b deficient macrophages were inhibited in NF $\kappa$ B and MAPK signalling (Perera et al., 2001). These findings suggest that CD11b has a rather pro-inflammatory potential in contrast to what we observed in our research. On the other hand, there is a growing body of literature showing that  $\beta$ 2 integrins, including CD11b/CD18, negatively regulate TLR-triggered inflammatory response and therefore demonstrate a pro-tolerogenic signature preventing the onset of inflammation and subsequent tissue damage. It was shown that CD11b deficient bone-marrow derived macrophages secreted higher levels of IL-6 and TNF- $\alpha$  in response to infection with *Mycobacterium bovis* Bacillus Calmette-Guerin (Q. Zhang, Lee, Kang, Kim, & Kim, 2018). *Mycobacterium bovis* BCG is recognised by DC by TLR2 and TLR4 (Tsuji et al., 2000). Stimulation with other TLR ligands in the absence of  $\beta$ 2 integrin on a DC provided more straightforward results, highlighting the pro-tolerogenic function of the CD18 containing heterodimers. Stimulation of TLR-9 in CD11b deficient DC led to increase in the IL-12p70 production (Bai et al., 2012). As mentioned by

Yee & Hamerman a complete CD18 deficiency in bone-marrow derived murine macrophages and dendritic cells led to hypersensitivity against LPS, CpG and Zymosan (Zymosan directly binds TLR-2 (Sato et al., 2003)). CD18 deficient cells produced more IL-12 and IL-6 in comparison to the WT. These studies underline the contribution of  $\beta 2$  integrins in the negative regulation of TLR-triggered inflammation.

Our data support the hypothesis that  $\beta 2$  integrins negatively regulate TLR-triggered expression of cytokines in DC. Isolated splenic CD18<sup>ΔCD11c</sup> DC were characterized by strongly elevated cytokine production in response to MyD88-triggering TLR ligands as compared with the control group. A complete CD18 or CD11b deficiency had, however, no impact on the expression of the co-stimulatory molecules monitored on the DC or their T cell stimulatory capacity *in vitro* and *in vivo*.

### 3.8. $\beta 2$ integrins may influence the cytokine production in concert with SOCS proteins

TLR-triggered hyperinduction of cytokines in primary CD18<sup>ΔCD11c</sup> DC raised questions about the underlying mechanism. In our analysis we issued the role of SOCS (suppressor of cytokine signalling) proteins, which act as a negative feedback loop in response of immune cells to cytokines and inhibit the Janus kinase/signal transducers and activators of transcription (JAK/STAT) signalling pathway. To address this issue we have used R848-stimulated splenic CD18<sup>ΔCD11c</sup> DC, because stimulation of TLR-7 in these DC demonstrated with a most pronounced phenotype. Moreover, no opposing immunological effects have so far been described for  $\beta 2$  integrins in context of TLR-7/8 stimulation, thus R848 stimulation would create a straightforward immunological scenario.

It is well known that various signalling molecules are involved in the control of the cytokine production and release. An immune cell itself secretes and is controlled by cytokines, which act on the cell via JAK/STAT signalling pathway (Fig. 75). There are seven STAT family members in mammals and they all act as transcription factors involved in immunity, cell proliferation, differentiation and apoptosis. STAT1 and STAT2 were discovered first. They transduce interferon signalling in the cell, and thus are important for anti-viral and anti-bacterial responses, as well as apoptosis and tumour suppression (Au-Yeung, Mandhana, & Horvath, 2013). STAT3 acts in response to IL-6 and epidermal growth factor, and plays an important role in cell survival and oncogenesis (Johnston & Grandis, 2011). STAT4 is stimulated by IL-12 and conveys Th1 responses (Lund, Chen, Scheinin, & Lahesmaa, 2004). STAT5A and STAT5B transduce prolactin and growth hormone signalling, respectively (Lim & Cao, 2006).

STAT6 is activated in response to IL-4 and mediates Th2 immune response (Goenka & Kaplan, 2011). Activation of STATs is very prompt, e.g. phosphorylated STAT1 accumulates in the nucleus only 30min after stimulation and can be dephosphorylated, i.e. deactivated, in less than 15min (Haspel, Salditt-Georgieff, & Darnell, 1996). Therefore, an appropriate control of STAT-induced transcription is required for a safe to the host immune reaction. STATs, on the other hand, can be inactivated by protein inhibitor of activated STAT (PIAS), phosphatases, ubiquitination or by SH2-containing protein (CIS)/suppressor of cytokine signalling (SOCS)/JAK binding protein (Guo et al., 2017; T. K. Kim & Maniatis, 1996).

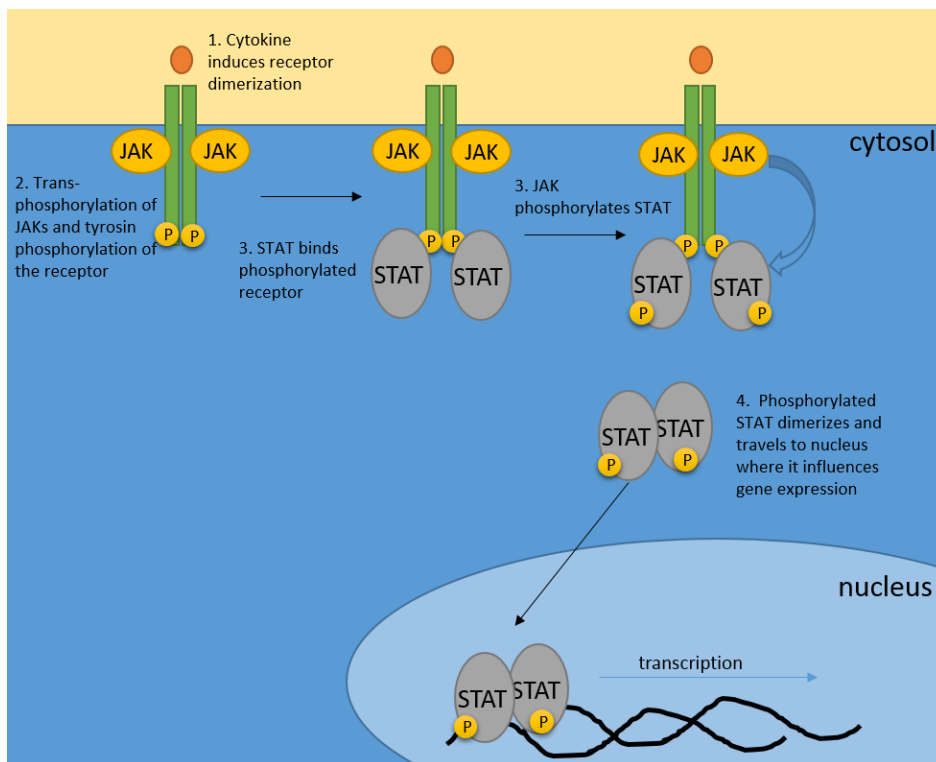


Figure 75. JAK/STAT signalling.

The suppressor of cytokine signalling (SOCS) family of proteins inhibits the activation of JAK/STAT signalling cascades and thus modulates a TLR-induced signalling of cytokines (Duncan, Baganizi, Sahu, Singh, & Dennis, 2017). SOCS proteins suppress signalling via ubiquitin-mediated degradation of the entire cytokine-receptor complex (the SOCS box recruits E2 ubiquitin transferase), or via direct JAK tyrosine kinase inhibition through binding via kinase inhibitory region (KIR), which is apparent exclusively within SOCS1 and SOCS3 (Yoshimura, Naka, & Kubo, 2007). Most SOCS proteins are induced by cytokines and act as a negative-feedback loop, but they may also be stimulated by LPS, cyclic AMP or chemokines (Ilangumaran, Ramanathan, & Rottapel, 2004). The CIS-SOCS family consists of 8 members: CIS and SOCS1-SOCS7 (Hao & Sun, 2016). The function of these CIS-SOCS proteins is briefly summarized in Table 3.

So far, the cross-talk between  $\beta 2$  integrin- and STAT- or SOCS-signalling has not been extensively studied. Using a myeloid cell line, D32, it has been reported though that STAT3 activation leads to  $\beta 2$  integrin activation and resulting cell aggregation could be abrogated by a constitutive SOCS3 expression (Wooten et al., 2000). Moreover, CD11b on human macrophages that bound ICAM inhibited TLR signalling by an indirect expression of IL-10, SOCS3, ABIN-3 and A20 (Savinko et al., 2015). It has as well been shown that pharmacological activation of CD11b on NK cells with leukadherin-1 led to a reduced STAT-5 phosphorylation upon IL-12 stimulation and decrease in secretion of interferon (IFN)- $\gamma$ , tumour necrosis factor (TNF) and macrophage inflammatory protein (MIP)-1 $\beta$  (Roberts et al., 2016).

Table 3. CIS-SOCS protein family.

	CIS	SOCS1	SOCS2	SOCS3	SOCS4 SOCS5 SOCS6	SOCS7
N-terminal aa residues length						
Mode of action	Mainly JAK/STAT pathway inhibition				Mainly through growth factor receptor signaling, but as well via inhibition of JAK/STAT pathway	
Function	<ul style="list-style-type: none"> <li>Negative regulation of cytokines acting over JAK-STAT pathway</li> <li>Inhibition of STAT5 phosphorylation</li> </ul>	<ul style="list-style-type: none"> <li>Inhibition of IFN-<math>\gamma</math>-induced JAK2/STAT1</li> <li>Inhibition of TLR/NF-<math>\kappa</math>B pathway</li> <li>M2 macrophage polarization</li> </ul>	<ul style="list-style-type: none"> <li>M2 macrophage polarization</li> <li>Inhibition of DC activation through TLR</li> </ul>	<ul style="list-style-type: none"> <li>Negative regulation of cytokines acting over JAK-STAT pathway</li> <li>Inhibition of JAK2 kinase activity</li> <li>Regulation of IL-6 signaling</li> </ul>	<ul style="list-style-type: none"> <li>Regulation of epidermal growth factor (EGF) signaling</li> </ul>	<ul style="list-style-type: none"> <li>Inhibition of STAT3 and STAT5 activation</li> </ul>

Our studies showed that upon TLR7 stimulation CD18<sup>ACD11c</sup> splenic DC showed a biphasic change in SOCS2 and SOCS4 mRNA expression. The mRNA level of both SOCS2 and SOCS4 in the CD18<sup>ACD11c</sup> DC was elevated prior and 1h after stimulation and then it drastically dropped 4h after exposure to R848. In the control CD18<sup>fl/fl</sup> samples, on the other hand, the level of SOCS mRNA expression constantly kept rising (Fig. 41). It seems that  $\beta 2$  integrins may positively regulate expression of SOCS2 and SOCS4 mRNA. It has been shown that TLR-triggered phosphatidylinositol 3-OH kinase (PI(3)K) and RapL activate CD11b, which in turn activates tyrosine kinases Src and Syk (Han et al., 2010). Since SYK phosphorylation leads to activation

of various transcription factors, it is likely that  $\beta 2$  integrins activate SOCS transcription factors (such as STATs) via Syk pathway.

It is known that SOCS2 expression can be induced by several cytokines, such as GM-CSF, IL-10, IFN- $\gamma$  or by cytokine receptors, e.g. STATs (B. Sen et al., 2012). As reported by Posselt *et al*, SOCS2 is a feedback inhibitor of TLR-induced activation of a DC, both in human and mouse. Its expression is increased upon stimulation with R848, PolyI:C, Flagellin or CpG ODN. Further reports showed that silencing of SOCS2 led to elevated secretion of IL-10 and IL-1 $\beta$  in human DC, whereas no change was noted in IL-6 or TNF- $\alpha$  expression (Posselt, Schwarz, Duschl, & Horejs-Hoeck, 2011). LPS signalling by SOCS2 remains controversial and is divergent in mouse and human for an unknown reason (Frobose et al., 2006; Hu, Winqvist, Flores-Morales, Wikstrom, & Norstedt, 2009).

The role of SOCS4 in immune functions has not been intensively studied. So far, Kedzierski *et al* has shown that SOCS4 acts protective against a cytokine storm in the course of influenza infection and engages viral clearance. It is, however, not required for an efficient recall response involving CD8<sup>+</sup> T cells (Kedzierski et al., 2015; Kedzierski et al., 2014). In accordance with this study we have shown that SOCS4 may prevent from a cytokine overproduction and that its expression is possibly orchestrated by  $\beta 2$  integrins.

A model of a cross-talk between  $\beta 2$  integrin and SOCS or STAT molecules based on the literature and our findings is depicted in Fig 76 below.

Altogether, there is accumulating evidence that  $\beta 2$  integrins significantly contribute to immunomodulation, not only by mediating cell adhesion and migration, but also affect signalling by degradation of TLR signalling components and modulation of cytokine signalling. A slight disturbance in  $\beta 2$  integrin expression may therefore demonstrate with various immunological effects and contribute to autoimmune conditions or malfunction of the immune system in the context of tumour development or infection. Further work has to be carried out to determine phosphorylation state of STATs and the level of SOCS proteins expression in the CD18 deficient cells, as it may be critical for the subsequent polarization of the cell and therefore influence the immune system function of the host.

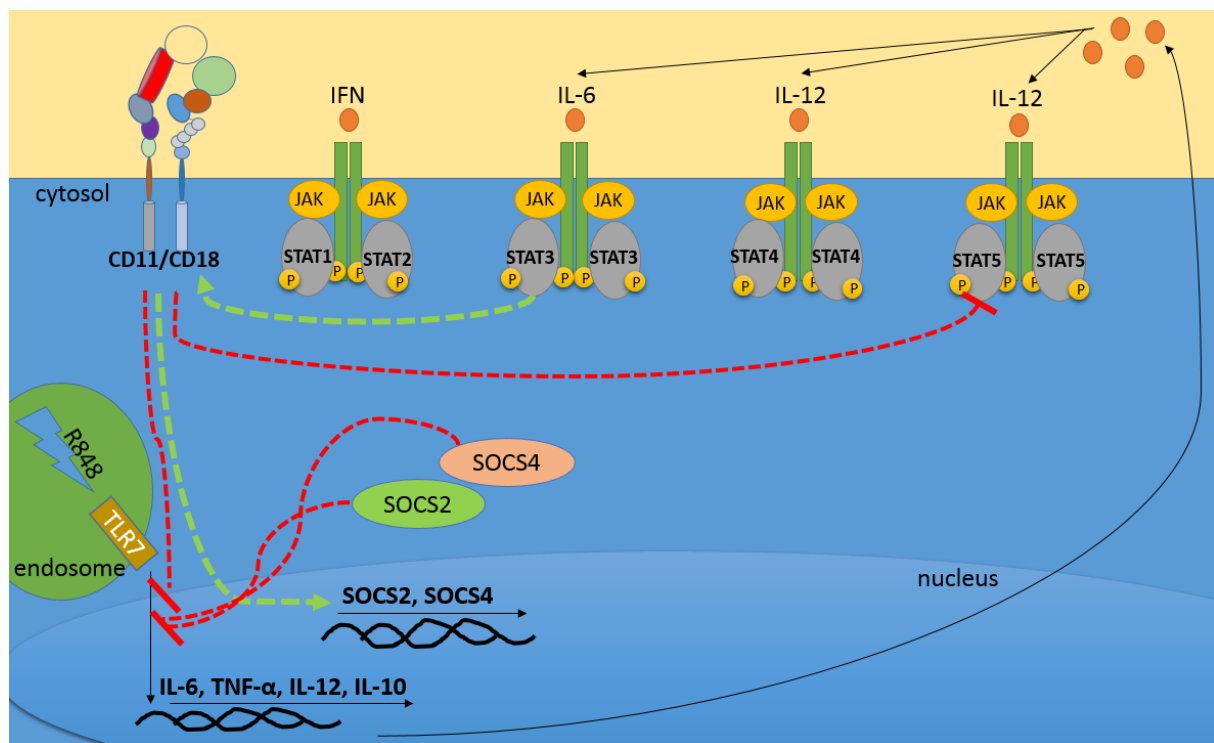


Figure 76. Model of the cross-talk between  $\beta 2$  integrin and SOCS or STAT molecules.

### 3.9. Regulation of tumorigenesis by $\beta 2$ integrin

The observation that CD18-deficient DC demonstrated a pro-inflammatory phenotype with regard to cytokine expression found an implication for research into the field of tumour biology. To address the question whether CD18/CD11b on DC may influence an anti-tumour immune response, we analysed development of melanoma in the CD18<sup>ACD11c</sup> and CD11b null KO mice.

The tumour microenvironment (TME) offers a broad spectrum of antigens and danger signals, such as necrotic debris or cytokines that stimulate immune system to counteract cancer. APCs internalize the antigens and present them to CD8<sup>+</sup> T cells (later CTLs) and CD4<sup>+</sup> naïve T cells (later Th1) in the tumour-draining lymph node. Primed lymphocytes then migrate to TME, to eradicate tumour via secretion of cytokines and cytotoxins (Zamarron & Chen, 2011). Tumours, on the other hand, constantly influence their microenvironment by releasing extracellular signals that induce angiogenesis and immune tolerance, which is a key aspect why tumour evade surveillance and may remain senescent for years before recurrence. In addition, constant cell division and genetic instability leads to a loss of immunogenicity (Swann & Smyth, 2007). In order to achieve tolerance tumours promote regulatory T cells, myeloid derived suppressor cells (MDSCs), and secretion of suppressive mediators (Dunn, Bruce, Ikeda, Old, & Schreiber,

2002). Thus, the cross-talk between immune system and cancer can both inhibit and enhance tumour growth.

Likewise,  $\beta 2$  integrins act as a double-edged sword in tumour immune surveillance. The evidence for their tumour supportive role is however much more extensive. On one hand,  $\beta 2$  integrins act as intercellular adhesion molecules allowing an immunological synapse to form between T cell or NK cell and a tumour cell, which results in a targeted release of cytotoxic granules (Anikeeva et al., 2005). Integrin-mediated migration of leukocytes to infiltrate TEM in early stages of tumour development limits as well its growth and counteracts cancer spreading. On the other hand, as soon as tumour commences the process of immunoediting and reaches equilibrium, integrin-mediated migration of leukocytes turns into a disadvantage, since cells that can induce tolerance localize to the tumour site allowing it to progress (Q. Q. Zhang et al., 2015). CD11a/CD11b expressing PMNs may even bind an ICAM-1 expressing tumour cell and facilitate therefore metastasis (Fu et al., 2011; S. Liang et al., 2005). Apart from conducting intercellular adhesion and transendothelial migration,  $\beta 2$  integrins bind a variety of soluble ligands, many of which can be found within the TME. Interaction of tumour-associated ligands with  $\beta 2$  integrins and the resulting immunoregulation is not well defined yet.

Mechanistically,  $\beta 2$  integrins have been shown to dampen immune responses, to save to host from excessive tissue destruction. They negatively affect cytokine signalling, especially in DC and macrophages, and influence priming of T cells. Activation of CD11b on DC, which normally express  $\beta 2$  integrin in an inactive state, leads to suppression of T cell priming capacity. Likewise, blockage of constitutively active CD11b on macrophages strongly enhances their allo-stimulatory capacity (Balkow et al., 2010; Savinko et al., 2015; Varga et al., 2007). Furthermore, it has been reported that C3b-opsonised apoptotic bodies, which are found within the TME, induce a pro-tolerogenic signal mediated by Mac-1 (Skoberne et al., 2006). Hence,  $\beta 2$  integrins can inhibit immunogenic function of DC and macrophages, which supports tumour progression. As described in the previous chapter, our studies showed that a lack of  $\beta 2$  integrin expression on primary DC derived from the CD18<sup>ACD11c</sup> mouse led to an elevated release of cytokines most likely as a consequence of the reduction in SOCS proteins expression, which act as a negative feedback loop in cytokine signalling. This might potentially influence the immune response against the tumour.

In order to elucidate the role of  $\beta 2$  integrin on the DC in the tumour milieu we have inoculated CD18<sup>ACD11c</sup> mice with B16-OVA melanoma subcutaneously and analysed tumour development. Like many other tumours, melanoma express divergent antigens that can be

recognised by primed T cells. In this case, melanoma cells had been transfected with a model antigen ovalbumin. Using BM-DC and splenic DC derived from CD11b<sup>-/-</sup> mice, we could show that ovalbumin uptake was significantly reduced in CD11b-deficient cells as compared to the WT control (Fig. 70, 71). Subsequent re-allocation of the engulfed antigen from endosome to lysosome was only insignificantly diminished in case of the CD11b<sup>-/-</sup> BM-DC (Fig. 72). Thus, CD11b on DC was important for the engagement of an antigen, not however for its processing. Furthermore, we have investigated the T cell stimulatory capacity of CD18<sup>ΔCD11c</sup> APCs loaded with ovalbumin and an adjuvant. Even though in the *in vitro* co-cultures of ovalbumin-exposed, R848 or CpG stimulated CD18<sup>ΔCD11c</sup> DC with CD4<sup>+</sup> or CD8<sup>+</sup> TC we could measure a significantly higher cytokine level (including TNF- $\alpha$ , IL-2, IL-10 or IFN- $\gamma$ ) (Fig. 43, 45, 47), ablation of CD18 on the primary DC had no functional influence on their stimulatory capacity *in vitro* or *in vivo* (Fig. 42,44,46,49,50). Since we did not manipulate the conformational state of  $\beta$ 2 integrins, which physiologically are expressed on DC in a low affinity conformation (i.e. inactive), our results are consistent with previously reported studies by Balkow *et al.* and Varga *et al.*, supporting the idea that T cell stimulatory capacity of the DC is influenced only once the activation state of the  $\beta$ 2 integrin is altered.

Despite the fact that CD18-deficient DC demonstrated an unaltered T lymphocyte priming ability, we hypothesized that a hyperinduction of cytokines in the CD18<sup>ΔCD11c</sup> DC may nonetheless polarize immune response against a cancer, especially in the later stages when a tumour imprints a tolerogenic signature on infiltrating leukocytes. We speculated that in case of the T lymphocyte proliferation assay, the setting might have been saturated with presented antigen and adjuvants, which would have been a limitation to demonstrate a difference, whereas in case of the TME the amount of molecules activating immune system is moderate, which may emphasize the role of the CD18 deficient DC.

We did, however, not find any difference in the burden, growth or density of the B16-OVA melanoma inoculated in CD18<sup>ΔCD11c</sup> as compared with CD18<sup>fl/fl</sup> control mice (Fig. 51A-C). Analysis of the secondary lymphoid organs revealed that the weight of spleens retrieved from the mice was comparable (Fig. 51D), however we noticed an insignificantly elevated cell count of the tumour draining pelvic lymph node of the CD18<sup>ΔCD11c</sup> mice (Fig. 51E). Restimulation of the lymph node leukocytes *ex vivo* with ovalbumin showed an insignificantly decreased proliferative capacity in the CD18<sup>ΔCD11c</sup> as compared with the CD18<sup>fl/fl</sup> control (Fig. 51F). The reason for this rather contradictory tendency is not entirely clear and does not support our previous findings, where we observed no difference in the T cell stimulatory capacity of the CD18<sup>ΔCD11c</sup> DC.

The apparent lack of correlation between CD18 expression on the DC and melanoma growth can be attributed to the fact that many other cell types infiltrate tumour milieu and may partially fulfil the task of a WT DC and mediate tumour-induced tolerance (Enk, Jonuleit, Saloga, & Knop, 1997). Apart from DC, solid tumours attract MDSC, granulocytes (mostly neutrophils) and other myeloid cell types, such as tumour associated macrophages (TAMs) that support tumour immune evasion (Y. Liu & Cao, 2016; A. A. Wu, Drake, Huang, Chiu, & Zheng, 2015). Our investigation of the role of  $\beta 2$  integrin on immune cells for tumour development was not limited to the CD18 <sup>$\Delta$ CD11c</sup> mouse model. In parallel we have studied the progression of B16-OVA melanoma in CD11b null KO mice. CD11b/CD18 is one of the  $\beta 2$  integrins, also known as Mac-1 or C3 receptor. It is mostly expressed on myeloid cells, predominantly neutrophils, however its expression on the surface of NK cell, some mast cells (Rosenkranz et al., 1998) and lymphocytes has as well been reported (B cell, CD8<sup>+</sup> and  $\gamma\delta$  T cells) (Fiorentini et al., 2001; Ghosn et al., 2008; Graff & Jutila, 2007). Interestingly, we have found that CD11b<sup>-/-</sup> mice inoculated with melanoma cells developed tumours less frequently in comparison to the WT mice (Fig. 54A), and that tumour growth in tumour-burdened CD11b<sup>-/-</sup> mice was significantly lower (Fig. 54B, C). This finding supported results of two separate groups that published their studies at the time as we carried out our experiments. Zhang *et al* (2015) reported on a reduced infiltration of Apc Min/+ spontaneous intestinal adenoma with myeloid cells in the CD11b deficient mice, which resulted in suppression of Wnt/ $\beta$ -catenin pathway apparent in tumour cells and inhibition of tumour growth. In accordance with this Soloviev and colleagues (2014) showed a reduction of tumour growth using two other tumour models, namely B16F10 melanoma and RM1 prostate cancer. The authors proposed that tumour growth in CD11b deficient mice was inhibited due to an impaired infiltration of tumour tissue with PMNs and macrophages, which secrete VEGF and thus neovascularisation of tumours was decreased. Taken together, our results and recent literature evidence suggest that there is a significant positive correlation between CD11b expression and tumour growth. The role of  $\beta 2$  integrin expressed on DC in that regard is however dispensable.

We further analysed leukocytes infiltrating tumour tissue in CD11b-deficient mice and WT controls. Contrary to expectations, flow cytometric analysis of the melanomas did not show any differences in the infiltration of the tissue by CD3<sup>+</sup>, F4/80<sup>+</sup> or CD11c<sup>+</sup> leukocytes (Fig.55B, C). Neither did we see differences in the cellular composition of the tumour draining lymph node, we noted only an insignificant decrease in the CD3<sup>+</sup> cell fraction in CD11b<sup>-/-</sup> mice (Fig. 55 D). Unfortunately, at that time we did not analyse the subsets of the leukocytes outlined above, which might have been a limitation to draw a conclusion about the immunological milieu. A

detailed analysis of the FoxP3<sup>+</sup> or CD8<sup>+</sup> lymphocyte as well as APC polarisation would give a better insight to determine the influence of CD11b in that regard. Since flow cytometric analysis restricted the analysis of different tumour areas (the entire tumour mass was analysed at once), we have performed in addition an immunohistological analysis of the tumour sections derived from CD11b<sup>-/-</sup> and WT mice. Interestingly, these analysis showed a decreased infiltration of F4/80<sup>+</sup>, CD11c<sup>+</sup> and Gr-1<sup>+</sup> cells towards the centre of the tumour mass retrieved from CD11b<sup>-/-</sup> mice and leukocytes were found predominantly within the tumour margin (Fig. 56A-E). Moreover, barely any regulatory CD4<sup>+</sup>FoxP3<sup>+</sup> cells were detected within the tumour mass in case of CD11b<sup>-/-</sup> mouse as compared with the WT control (Fig. 56F), which may partially explain an accelerated tumour growth in the WT mice.

Our analysis of the tumour vasculature did not fully support findings made by Soloviev *et al.*(2014), as we observed that only the rim area of the tumour derived from CD11b<sup>-/-</sup> mice predisposed to a poor vasculature in comparison to WT. No differences were observed in the central tumour mass (Fig. 59G). The difference in the observation may come from a methodological difference, since Soloviev and colleges examined tumours that arouse from 10<sup>6</sup> cells inoculated s.c., whereas we inoculated mice with only 5\*10<sup>4</sup> cells and thus in case of our experiments tumours had more time to establish vasculature. Given that our findings are based on a limited number of tumour sections, they should still be treated with considerable caution.

Our study on the CD11b null KO mouse emphasized the overall tumour-supportive role of  $\beta$ 2 integrin in the TME. Given that CD11b-deficient DC were less efficient in antigen uptake than WT DC and since stimulated primary CD18 <sup>$\Delta$ CD11c</sup> DC secreted more cytokines, we speculated that CD18-deficient DC may therefore be less effective in promoting of tumour-induced tolerance. Our results did not, however, support this hypothesis. Most likely, tumour associated macrophages (TAM) attributed to the induction of tolerance and thus masked any effect CD18 <sup>$\Delta$ CD11c</sup> DC might have exerted.

Further research would therefore need to focus on other CD18 expressing leukocytes, including Foxp3<sup>+</sup> and Ly6G<sup>+</sup> cells. The role of CD18 deficient Foxp3<sup>+</sup> T lymphocytes in the TME would be extremely interesting, as it has already been reported that CD18 is crucial for the development and function of the CD4<sup>+</sup>CD25<sup>+</sup> regulatory T lymphocytes. Furthermore, reduction in the CD18 expression on the T lymphocytes induced their conversion towards pro-inflammatory Th17 cells (Marski *et al.*, 2005; Singh *et al.*, 2013). In accordance with these findings, our primary observation of the newly bred CD18 <sup>$\Delta$ Foxp3</sup> mouse strain, where CD18 was

ablated in the Foxp3 expressing regulatory T cells, was that with increasing age mice developed psoriasis-like skin lesions (with swelling, scaling and lymphocyte infiltration), splenomegaly and lymphadenopathy (Appendix H). Furthermore, preliminary *in vivo* melanoma experiment involving CD18<sup>ΔFoxP3</sup> revealed a tendency to a reduced tumour burden and delayed tumour growth in the conditional knock-out strain as compared with the CD18<sup>fl/fl</sup> mice (Appendix G). This underlines the importance of CD18 expression on regulatory T cells for tolerance induction in TME. The same tendency to reduced tumour burden and growth was noted in case of another, newly bred CD18<sup>ΔLy6G</sup> mouse strain, in which CD18 was deleted in neutrophils and MDSC mainly (Appendix G). Future experimental studies are needed to reveal mechanisms that result in the observed immunological alterations. Our initial findings are already very promising and encouraging for further investigation of the CD18 on lymphocytes and granulocytes in the immunological context, be it TME or an autoimmune disorder.

### 3.10 CD11b modulates engulfment of complex polysaccharides and complement-opsonized polysaccharide coated particles

Experiments preceding the *in vivo* B16-OVA melanoma assay, pointed out the role of CD11b in the engagement of extracellular material. We observed a decrease in the uptake of a model antigen, namely ovalbumin, in the CD11b deficient primary DC as well as BM-DC (Fig. 70A, B and Fig. 71). Despite the fact that the reduction in antigen engulfment had no further functional consequences for the adaptive immune response, such as antigen processing (Fig. 72) and presentation (Fig. 52B, 53A), we decided to study CD11b in the context of extracellular material engagement, because removal of foreign substances is one of the central functions of the innate immune system. We investigated, therefore, the capacity of a CD11b-deficient DC to recruit (serum-opsonised) particulated material or dextran, a water-soluble polysaccharide.

It is well known that cell can engulf an extracellular material by multiple ways. Plasma membrane is a selective barrier that controls the exchange of the substances between the cell and environment. It may either engage the cytoskeleton and actively engulf extracellular material or alternatively let it enter passively. During receptor-mediated endocytosis the exogenous material is engulfed in a vesicle and thus is not directly transported into the cytosol as in case of a passive transport. In general terms, endocytosis may be sub-divided into pinocytosis (cell drinking) and phagocytosis (cell eating). Pinocytosis defines internalization of small molecules along with the surrounding fluid in a vesicle, whereas the term phagocytosis is broadly used for the engulfment of large particulate matter by cells like macrophage, DC or a neutrophil and formation of a phagosome intracellularly. Pinocytosis can be further

subdivided into four categories: clathrin-mediated endocytosis, caveolin-mediated endocytosis, clathrin- and caveolin-independent endocytosis, and macropinocytosis (Treuel, Jiang, & Nienhaus, 2013). Endocytosis mechanisms are specific for different cell types and may define the way an internalized material is processed in the cell (Nam et al., 2009).

Macropinocytosis denotes a non-specific, actin-driven internalization of a larger bulk of fluid containing debris (Commisso et al., 2013). Clathrin-mediated uptake, on the other hand, commences upon specific interaction of a ligand with a receptor on the plasma membrane (Watson, Jones, & Stephens, 2005). Cargo engulfed by clathrin-coated pits and uncoated plasma invaginations is trafficked to the lysosome and is subsequently degraded (L. Jiang, Li, Liu, & Zhang, 2013). Caveolin-dependent uptake involves clustering of the lipid raft domains and formation of an invagination supported by caveolin (dos Santos, Varela, Lynch, Salvati, & Dawson, 2011). Material internalized in the caveolae is further translocated to the Golgi apparatus, to the endoplasmic reticulum or across the cell in a process called transcytosis (L. Jiang et al., 2013). Main routes of cellular cargo uptake are summarized in the Figure 77 below.

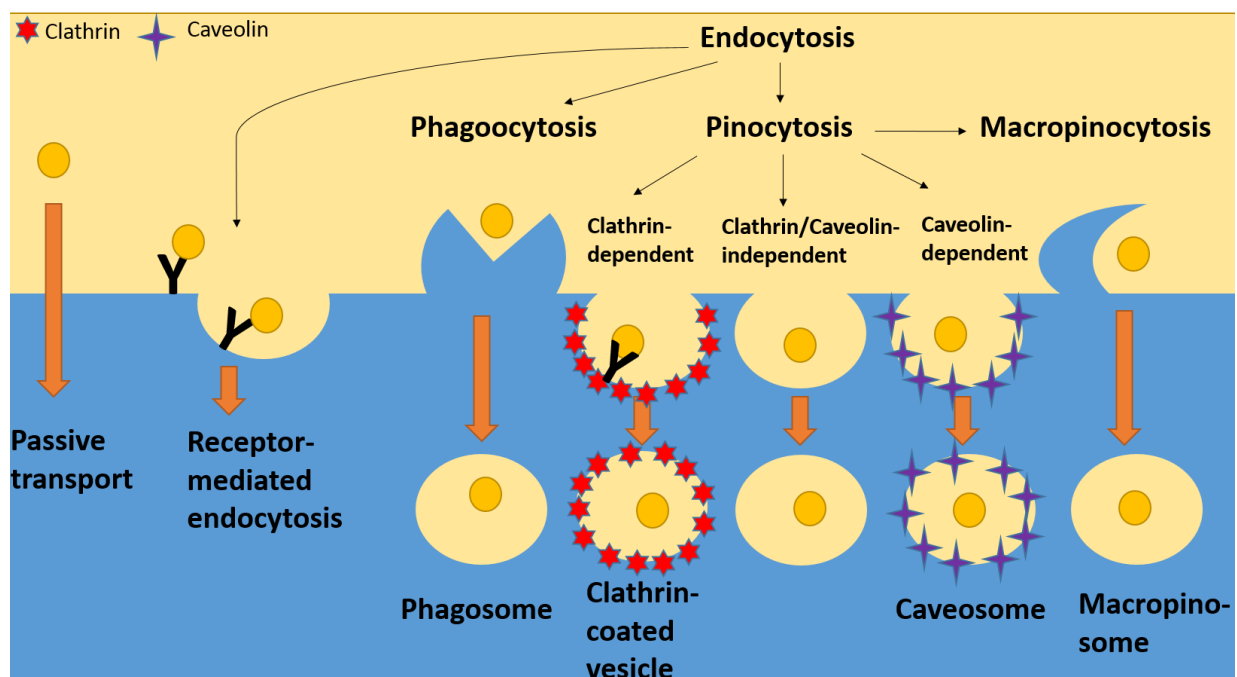


Figure 77. Main routes of cellular uptake of cargo.

Being the most promiscuous ligand binder among  $\beta 2$  integrins, Mac-1 (CD11b/CD18) is a molecule that participates in many immunological process, like leukocyte adhesion or phagocytosis of the extracellular material. Mac-1 was indeed the first integrin to be demonstrated as a phagocytosis mediator (Dupuy & Caron, 2008). As C3 receptor, it plays a crucial role in the clearance of the pathogens, tumour cells, apoptotic cells or cellular debris opsonised by iC3b complement (Hawley, Olson, Carreras-Gonzalez, Navasa, & Anguita,

2015). Beside Fc receptors that bind antibody-opsonised pathogens, CR3 (CD11b/CD18) and CR4 (CD11c/CD18) are most important opsonophagocytic receptors on DC. Notably, the functional interaction between CD11b and Fc-receptor has gained as well attention in the scientific community. It was shown that Fc $\gamma$ RIIIB is constitutively associated with CD11b on human neutrophils (Zhou, Todd, van de Winkel, & Petty, 1993). Even though this physical interaction of receptors was never observed in the murine immune cells, Jongsta-Bilen and colleagues (2003) demonstrated that the phagocytic cup formed in murine leukocytes upon FcR engagement accumulated numerous CD11b molecules. In the model proposed by Jongsta-Bilen *et al.* (2003), recruitment of the FcR led to cytoskeletal rearrangements that in turn released Mac-1 from the cytoskeletal net and allowed its migration to the site of phagocytosis, where it could re-anchor to the cytoskeleton and facilitate phagocytosis and cell migration (Jongstra-Bilen *et al.*, 2003). Spriel *et al.* (2003) reported on an FC receptor-mediated immunity to melanoma and concluded that CD11b is critical for antibody-dependent cellular cytotoxicity against the tumour in the murine model (van Spriel *et al.*, 2003). Thus, there is a body of literature that indicates a cross-talk between integrins and FcRs, and that both act in concert to maximize the efficiency of phagocytosis of serum-opsonized material. Apart from integrins and FcRs, a professional APC expresses in addition other phagocytic receptors like scavenger receptors (Wohner *et al.*, 2018), C-type lectins (J. Tang, Lin, Langdon, Tao, & Zhang, 2018), or CR1g (complement receptor, expressed exclusively on sinusoidal macrophages) (Helmy *et al.*, 2006). There is a limited amount of studies on the role of CD11b in the uptake of particulated, non-biological material. It has been shown though that CD11b participates in the phagocytosis of nanomaterial used in the medicine as drug carrier or a diagnostic tool. Von Zur Muhlen and colleges (2007) found that superparamagnetic iron oxide nanoparticles (SPIONs) coated with dextran are bound by CD11b. Using a recombinant cell line expressing Mac-1 at various activation states, it was shown that binding of SPIONs was increased once Mac-1 was in a high affinity state and that binding could in general be reduced with the usage of  $\alpha$ -CD11b Ab (von Zur Muhlen *et al.*, 2007). It has recently been reported as well that CD11b induces LPS-triggered TLR4 endocytosis exclusively in DC and is important for the endosomal TRIF-dependent pathway. In addition, CD11b deficiency is associated with a reduced T cell stimulatory capacity of LPS triggered DC (Ling *et al.*, 2014). Thus, the endocytosis rate of an APC and the signalling in the endosome can be mediated by the CD11b and the activation of an integrin exerts an additional positive influence on the uptake of extracellular material.

Consistent with the published literature, we demonstrated a positive influence of Mac-1 on the uptake of nanomaterials. It is well established that nanomaterial introduced, into the blood

stream, gets directly coated with serum components such as complement system, antibodies, acetylcholine, laminin, fibronectin, C-reactive protein, or type-I collagen. Most of the aforementioned ligands bind CR3, thus to mimic a physiological conditions in our experiments we have used serum-opsonized nanomaterial. We observed that CD11b<sup>-/-</sup> BM-DC presented with a significantly reduced ability to bind and engulf dextran-coated colloidal superparamagnetic nanoparticles in comparison to the WT control (Fig. 57, 58). Furthermore, we found that particles' protein corona composed of the native mouse serum (including iC3b complement components known to opsonise studied nanomaterial) was a significant factor mediating endocytosis by CD11b (Fig. 58A, B and 60). CD11b-deficient BM-DC were less efficient in binding of serum-opsonised nanoparticles. A similar attenuated uptake was observed when Mac-1 was blocked with an  $\alpha$ -CD11b Ab on the surface of WT BM-DC (Fig. 62), which means that the reduction in nanomaterial binding does not result from the developmental disorder of the cell due to the CD11b ablation. Confocal microscopic analysis revealed that the internalization efficiency of serum-pre-incubated bead formulations is significantly decreased in case of the CD11b<sup>-/-</sup> BM-DC, whereas engulfment of beads opsonized with heat-inactivated serum showed no differences on a per cell base (Fig. 61). As tested, co-incubation of the nanomaterial w/o biocorona did not influence the expression of the co-stimulatory molecules on the BM-DC of either genotype (WT or CD11b<sup>-/-</sup>) (Fig. 63, 64). We observed nevertheless, that CD11b<sup>-/-</sup> BM-DC co-cultured with nanoparticles demonstrated with an elevated secretion of TNF- $\alpha$  in comparison to the WT control (Fig. 65). We, therefore, cannot exclude that a possible CD11b<sup>-/-</sup> DC hyperactivation had an influence on the uptake, since activation of a DC leads inevitable to a subsequent reduction of an endo/phagocytosis (Tirapu et al., 2009). Another factor that might have influenced the analysis is an elevated expression of CD11c on the CD11b<sup>-/-</sup> BM-DC, which can constitute a compensatory mechanism (data not shown). CD11c/CD18 also binds complement components and hence its elevation could positively regulate endocytosis of serum-coated particles. The uptake of serum-coated particles by CD11b<sup>-/-</sup> BM-DC showed, however, no substantial differences as compared to WT BM-DC blocked with  $\alpha$ -CD11b Ab (Fig. 62). Given that, we concluded that CD11c does not compensate for the ablation of CD11b on DC in the uptake of nanomaterial covered by serum corona containing iC3b complement.

We extended our studies with observations on the binding of dextran, a polysaccharide, which is often used to coat medically applied nanomaterials because of its biocompatibility and has as well been applied to coat the nanomaterial we studied earlier. Surprisingly, our analysis revealed a reduction in the binding of FITC-dextran by CD11b<sup>-/-</sup> BM-DC, as compared to the

WT control (Fig. 68). Once we blocked the mannose receptor (CD206; dextran binding receptor) with mannan on the surface of the WT BM-DC, FITC-dextran binding was reduced to same extent as observed in the CD11b-deficient cells. Interestingly, binding of FITC-dextran by CD11b<sup>-/-</sup> was reduced equally devoid of the mannan addition (Fig. 68). Thus, CD11b is either directly involved in dextran binding or regulates uptake via other receptors, such as CD206. The CD206 receptor is C-type lectin that functions in endocytosis of mannan-coated microorganisms, predominantly expressed by myeloid APCs (Azad, Rajaram, & Schlesinger, 2014). It is established that the extracellular region of CD206 binds sugars, like mannose or fucose, with high affinity and various glycoproteins or glycolipids (Martinez-Pomares, Linehan, Taylor, & Gordon, 2001). Recently, it has been as well reported that C-type lectin receptors, including CD209 (DC-SIGN) and CD206, bind dextran (Pustylnikov, Sagar, Jain, & Khan, 2014). Given that, it is likely that the reduction of dextran binding to CD11b deficient BM-DC is caused by the missing cross-talk between CD11b and CD206 or CD11b influences expression of the CD206. As described in the previous chapter, we observed that CD11b also mediates uptake of ovalbumin, which has been used in our tumour studies as a model antigen (Fig. 70). Currently, we cannot exclude a direct interaction between CD11b and ovalbumin, but based on the research of dextran uptake, we speculate that Mac-1 may as well be involved in the regulation of receptors responsible for ovalbumin engulfment, especially since the primary route of ovalbumin uptake is macropinocytosis and clathrin-mediated endocytosis via CD206 (Autenrieth & Autenrieth, 2009). Other potential candidates to study would be the transferrin receptor (TfR), DEC205 and DC-SIGN, all involved in the clathrin-mediated endocytosis, just like mannose or Fc- receptor. The model of CD11b function in endocytosis is depicted below (Fig. 78).

This study is a step towards enhancing our understanding of the  $\beta$ 2 integrin function in context of therapeutic nanocarrier application as well as clearance of bacterial infections or tumour-derived debris. Our future work would focus on the cross-talk between  $\beta$ 2 integrin and receptors involved in endocytosis. It seems that there is a great potential in the analysis of the Mac-1 in particular, as it is not only promiscuous for soluble ligands but possibly may interact with various endocytotic receptors as well.

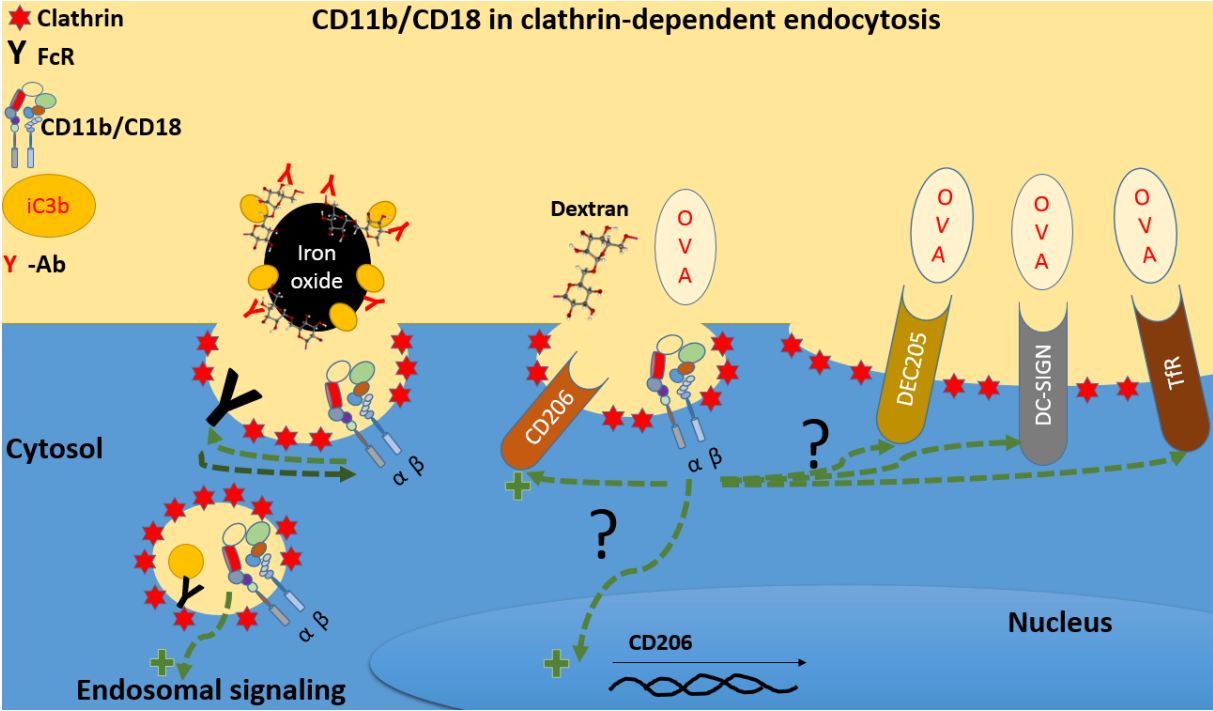


Figure 78. Possible Mac-1 functions in the clathrin-dependent endocytosis.

## 4. Materials and Methods

### 4.1. Materials and equipment

#### 4.1.1. Materials

Table 4. Expendable materials used in the laboratory.

<b>Material</b>	<b>Manufacture</b>
hypodermic needle, 23Gx1¼, 0.6x30 B.	Braun, Melsungen
hypodermic needle, 26Gx1½, 0.45x12	Braun, Melsungen
hypodermic needle, 23Gx1½, 0.3x13	BD, Heidelberg
Cell culture Flask, 25 cm <sup>2</sup>	Greiner Bio-One, Frickenhausen
Cell culture flask, 75 cm <sup>2</sup>	Greiner Bio-One, Frickenhausen
Cell culture plate 6 well, flat bottom	Greiner Bio-One, Frickenhausen
Cell culture plate 24 well, flat bottom	Greiner Bio-One, Frickenhausen
Cell culture plate 48 well, flat bottom	Greiner Bio-One, Frickenhausen
Cell culture plate 96 well, flat bottom	Greiner Bio-One, Frickenhausen
Cell culture plate 96 well, U bottom	Greiner Bio-One, Frickenhausen
Cell strainer, 40µm	Falcon, Fisher Scientific, Schwerte
Greiner Tubes, 15 ml	Greiner-One, Frickenhausen
Greiner Tubes, 50 ml	Greiner-One, Frickenhausen
MACS Cell separation column MS	Miltenyi Biotec, Berg. Gladbach
MACS Cell separation column LS	Miltenyi Biotec, Berg. Gladbach
Petridishes	Greiner Bio-One, Frickenhausen

Pipett tips, 0.1 – 10 µl	Carl Roth, Karlsruhe
Pipett tips, 10 – 200 µl	Carl Roth, Karlsruhe
Pipett tips, 100 – 1000 µl	Carl Roth, Karlsruhe
Plastic pipetts 5ml,10ml,25ml	Cellstar, Germany
Syringe, 0.5 ml	Braun, Melsungen
Syringe injekt-f, 1 ml	Braun, Melsungen

#### 4.1.2. Buffers and solutions

Table 5. Media used for the cell culture.

Medium	Content
Complete medium for splenocytes	500 ml Iscove's Modified Dulbecco's Medium 5% FCS 100U/mL Penicillin/Streptomycin 2mM Glutamine 1mM Sodium Pyruvate 50µM β-mercaptoethanol
Dendritic cell (DC) Medium	500 ml Iscove's Modified Dulbecco's Medium 5% FCS 100U/mL Penicillin/Streptomycin 2mM Glutamine 50µM β-mercaptoethanol

	10ng/mL GM-CSF
Wash medium	500 ml Eagle's Minimum Essential Medium 2% FCS 100U/mL Penicillin/Streptomycin 2mM Glutamine 50µM β-mercaptoethanol
FACS medium	500ml PBS 2% FCS 100U/mL Penicillin/Streptomycin 2mM EDTA
RPMI (for B16-OVA Melanoma cells)	500 ml RPMI 1640 10% FCS 100U/mL Penicillin/Streptomycin 2mM Glutamine, 10mM HEPES, 1mM Sodium Pyruvate, 50µM β-mercaptoethanol G418 (300µg/ml)
Medium for mouse embryo fibroblast (MEF) feeder cells	500 ml DMEM GlutaMAX™ 10% EF-FCS 1x Pen/Strep 1x non-essential amino acids 1mM Sodium Pyruvate
Murine embryonic stem (ES) cell medium	500 ml KnockOut™ DMEM 10% EF-FCS

	<p>1x L-Glutamine</p> <p>1x Pen/Strep</p> <p>1x non-essential amino acids</p> <p>mLIF</p> <p>50µM β-Mercaptoethanol</p> <p>G418 (Geneticin) 200µg/ml</p>
--	--

### 4.1.3. Antibodies

Table 6. List of the antibodies used in the laboratory.

Antibody specificity(clone)	Fluorescence label	Manufacture
CD3e (145-2C11)	PE-Cy5	eBioscience, San Diego, USA
CD4 (GK1.5)	FITC, APC-Cy7 e-Flour450	eBioscience Biolegend, San Diego, USA Biolegend
CD8a (53.6.7)	APC-Cy7 e-Flour450 FITC PE-Cy5	eBioscience eBioscience ImmunoTools eBioscience
CD11a	PE-Cy7	eBioscience
CD11c (N418)	PE-Cy7 APC	eBioscience eBioscience
CD11b (M1/70)	PE-Cy7 PE PE-Cy5	Biolegend BD Pharminogen™ Biolegend

CD18	APC FITC	BD Pharminogen™ BioLegend
CD19 (1D3)	APC-Cy7 APC	Becton Dickinson,USA BD Pharminogen™, CA, USA
CD25 (IL-2 receptor $\alpha$ chain,p55 PC61)	PE	Becton Dickinson
CD40 (1C10)	APC	eBioscience
CD45	FITC	Biolegend
CD45.1 (A20)	PE-Cy5	eBioscience
CD45.1	eFluor40	eBioscience
CD68 (FA-11)	FITC PE	Biolegend Biolegend
CD80	PE	eBioscience
CD86 (GL1)	FITC	eBioscience
CD103	PE	Biolegend
MHC-II (M5/114.15.2)	e-Flour450 PE-Cy5	eBioscience eBioscience
F4/80 (BM8)	e-Flour450	eBioscience
Foxp3 <sup>+</sup> (FJK-16a)	APC	eBioscience
Gr1 (RB6-8C5)	PE	eBioscience
Ly6-C (AL-21)	APC FITC	Becton Dickinson BD Pharminogen™

Ly6-G	e-Flour450	Biolegend
-------	------------	-----------

#### 4.1.4. Reagents and chemicals

*Table 7. Reagents used in the laboratory.*

<b>Substance</b>	<b>Manufacture</b>
Ethanol (70%)	Brüggemann, Heilbronn, Germany
Terralin	Schülke, Norderstedt, Germany
Acetone	Sigma-Aldrich, Taufkirchen, Germany
Collagenase, Clostridiopeptidase A	Sigma-Aldrich
Collagenase type 4	Gibco™, Thermo Fischer Scientific
Hyaluronidase from bovine testes	Sigma-Aldrich
Collagenase type 1a	Sigma-Aldrich
Collagenase from <i>c. histolyticum</i> , type 8	Sigma-Aldrich
Proteinase K	Fermentas, Leon-Rot, Germany
Buffer I	Biotool, Munich, Germany
Gel red	Biotum, Köln, Germany
ScaI-HF	New England Biolabs, Frankfurt, Germany
CpG 1826	Sigma-Aldrich
LPS	Sigma-Aldrich
R848	Sigma-Aldrich
Poly I:C	Sigma-Aldrich
DMEM w/o pyruvate	Merck, Darmstadt, Germany

Dulbecco's phosphate buffered saline	Sigma-Aldrich
Iscove's modified dulbecco's medium	Sigma-Aldrich
EDTA (Ethyldiamintetraacetat)	Sigma-Aldrich
FACS Clean Solution	BD Pharmingen, Heidelberg, Germany
FACS Flow Sheath fluid	BD Pharmingen
FACS Rinse Solution	BD Pharmingen
Ficoll 400	Sigma.-Aldrich
FCS, fetal calf serum	PAA Laboratories, Cölbe, Germany
Forene (Isoflurane)	Abbott, Wiesbaden, Germany
GM-CSF	R&D, Wiesbaden, Germany
L-Glutamin	Gibco, Life Technologies, Germany
Dispase II	Roche, Germany
HEPES buffer, 99.5%	Gibco Life Technologies , Germany
Hydrochloride acid (HCl)	Merck, Darmstadt, Germany
Isopropanol	Hedinger, Stuttgart, Germany
β-mercaptoethanol, 99% p.a.	Carl Roth, Karlsruhe, Germany
Ovalbumin	Sigma-Aldrich
Paraformaldehyde	Sigma-Aldrich
Recombinant murine GM-CSF	Natutec, Germany
RPMI 1640 medium Biochrome, Berlin	Life Technologies , Germany
Sodium azide (NaN <sub>3</sub> )	Sigma-Aldrich

Sodiumchlorid (NaCl)	Sigma-Aldrich
Trypanblau solution	Sigma-Aldrich
Tween 80	Sigma-Aldrich
Tris-Base	Sigma-Aldrich

#### 4.1.5. Cell culture

All tissue/cell culture reagents were from Gibco/BRL (Gaithersburg, Md.). All cells (BM-DC, splenocytes) were cultured at 37°C and 5% CO<sub>2</sub> in RPMI or IMDM media containing heat-inactivated fetal calf serum and supplemented with 2mM glutamine, 100U/mL Penicillin/Streptomycin, 0.5 MEM nonessential amino acids, 1mM sodium pyruvate and 50 µM 2-mercaptoethanol (RPMI Complete media).

#### 4.1.6. B16/OVA Melanoma cell line

B16/OVA is a B16 melanoma cell subline (H2b), which has been stably transfected with an expression construct encoding chicken OVA as a model antigen. This cell line has been kindly provided by Professor Sahin, University Medical Centre Mainz. B16/ OVA cells were grown in T75 flasks (Greiner Bio-One) in 20ml of RPMI medium with 10% FCS, 100U/mL penicillin/streptomycin, 2mM glutamine, 10mM HEPES, 1mM sodium pyruvate, 50µM β-mercaptoethanol and G418 (300µg/ml). OVA expression was analysed by FACS analysis prior of s.c. injection of cells into mice. For injection into mice, the cells were trypsinized with 5 ml trypsin/ EDTA. After 5 min, the cells were collected and washed three times in PBS before counting and diluting them to the appropriate concentration in sterile PBS.

#### 4.1.7. Animals used for breeding and experiments

C57BL/6J and transgenic CD11b<sup>-/-</sup> (Coxon et al., 1996), CD18<sup>low</sup> (Wilson et al., 1993), CD18<sup>fl/fl</sup>, CD18<sup>ΔCD11c</sup>, CD11c-Cre (Caton et al., 2007) (kindly supplied by AG Waisman, Institute for Molecular Medicine, Mainz, Germany), FLP-deleter (kindly supplied by AG Ruf, Centre for Thrombosis and Haemostasis, Mainz) (Schaft, Ashery-Padan, van der Hoeven, Gruss, & Stewart, 2001), OT-I and OT-II (all on C57BL/6 background) (Didierlaurent et al., 2014) as well as OT-I x Ly5.1 and OT-II x Ly5.1 (Janowska-Wieczorek et al., 2001) mouse strains (Table 8) were bred and maintained in the Central Animal Facility of the Johannes

Gutenberg-University Mainz under specific pathogen-free conditions on a standard diet according to the guidelines of the regional animal care committee. All animal experiments were performed in accordance with national and European (86/609/EEC) legislation, and in accordance with the Central Laboratory Animal Facility of the University Medical Centre of Mainz. The protocols were approved by the national investigation office of Rhineland-Palatinate. All *in vivo* experiments were covered by the animal test application: 23 177-07/G14-01-074 (Landesuntersuchungsamt, Koblenz). CD8<sup>+</sup> OT-I T cells derived from OT-I mice recognize OVA257-264 peptide in the context of H-2K<sup>b</sup>, and CD4<sup>+</sup> OT-II T cells derived from OT-II mice are specific for OVA323-339 peptide in the context of H-2 I-A<sup>b</sup> and I-A<sup>d</sup>. OT-I and OT-II mice were crossed with CD45.1<sup>+</sup> C57BL/6J congenic mice. The "Principles of Laboratory Animal Care" (NIH publication no. 85-23, revised 1985) were followed.

Table 8. Mice strains used in the laboratory.

Mouse strain	Source
C57BL/6J	Animal Facility, Johannes Gutenberg University, Mainz
OT-I (C57BL/6J)	Animal Facility, Johannes Gutenberg University, Mainz
OT-II (C57BL/6J)	Animal Facility, Johannes Gutenberg University, Mainz
OT-I x LY5.1	Animal Facility, Johannes Gutenberg University, Mainz
OT-II x LY5.1	Animal Facility, Johannes Gutenberg University, Mainz
CD11b <sup>-/-</sup> (B6.129S4-ITGAM<TM1MYD>/J)	Purchased from Charls River, bred at Animal Facility, Johannes Gutenberg University, Mainz
CD18 <sup>low</sup>	Purchased from Charls River, bred at

(B6.129S7-ITGB2<TM1BAY>/J)	Animal Facility,Johannes Gutenberg University, Mainz
CD11c <sup>CRE</sup> (B6.CG-TG(ITGAX-CRE)1.1REIZ/J)	Mice kindly supplied by Univ.-Prof. Dr. Björn Clausen, Animal Facility,Johannes Gutenberg University, Mainz
FLP-DELETER	Mice kindly supplied by Univ.-Prof. Dr. Wolfram Ruf, Animal Facility,Johannes Gutenberg University, Mainz
CD18 <sup>fl/fl</sup>	Generated in collaboration with Univ.-Prof. Dr. Ari Waisman , Johannes Gutenberg University, Mainz
CD18 <sup>ΔCD11c</sup>	Animal Facility,Johannes Gutenberg University, Mainz

#### 4.1.8. Electrical equipment

Table 9. Electrical equipment.

DEVICE	MANUFAKTURER
CENTRIFUGE HERAEUS MEGAFUGE 40R	Thermo Scientific, Darmstadt, Germany
CENTRIFUGE BIOFUGE PICO	Electron Corporation, Ulm, Germany
CENTRIFUGE MUTLIFUGE 3 L-R	Electron Corporation, Germany
CENTRIFUGE 1-1 <sup>LL</sup>	SIGMA, Darmstadt, Germany
BENCH CENTRIFUGE GALAXY MINISTAR	VWR, Darmstadt, Germany
CO <sub>2</sub> -INCUBATOR	Electron Corporation, Germany

CO <sub>2</sub> - INCUBATOR	BINDER, Tuttlingen, Germany
FACS LSR II, FLOW CYTOMETER	BD, Heidelberg, Germany
ATTUNE® NXT ACOUSTIC FOCUSING CYTOMETER	ThermoFisher Scientific, Germany
LASER SCANNING MICROSCOPY	Zeiss, Jena, Germany
REALTIME PCR 7300	Applied Biosystems, CA,USA
ROBOSEP	STEM CELL Technologie®, Cologne, Germany
SHANDON CYTOSPIN CENTRIFUGE	Thermo Electron, Langenselbold, Germany
VORTEX	Merck Eurolab, Darmstadt, Germany
WATER BATH, TYPE GFL-1003, 14 L	Gesellschaft für Labortechnik, Germany
PTC-200 PELTIER THERMAL CYCLER	MJ Research, Germany
GENE PULSER™, PULSE CONTROLLER, CAPACITANCE EXTENDER	BIO-RAD, Munich, Germany
ELECTROPHORESIS POWER SUPPLY, EPS 3500 XL	Pharmacia Biotech, Munich, Germany
PEQLAB FUSION SL FOR GEL- DOCUMENTATION	PeqLab, Erlangen, Germany
NANODROP 2000C SPECTROPHOTOMETER	Thermo Fisher Scientific, Germany
THERMOMIXER 5436	Eppendorf, Hamburg, Germany
Attune NxT Flow Cytometer	Thermo Fisher Scientific, Germany

## 4.2. Materials and methods for generation of CD18<sup>fl/fl</sup> mouse

### 4.2.1. Amplification of the targeting vector BO44.2

One microliter of the BO44.2 vector solution and 50µl of the SURE competent bacteria (Agilent technologies) were transferred into a chilled cuvette (path length: 1mm) without introducing bubbles. Cells were electroporated with a Bio-Rad Gene Pulser<sup>TM</sup> using the following conditions: 2.1 kV, 200 Ω, and 25µF. Subsequently, electroporated cells were quickly transferred into a glass flask with a pre-warmed recover medium (Neomycin was applied 1h later) and cultured overnight at 37°C shaking. The next day amplified plasmid DNA was isolated using QIAprep®Spin Midiprep Kit and control restriction enzyme digestions were performed using *Not1*+*Sal1*, *Bam*HI and *Kp*N1. Prior to electroporation of the murine embryonic stem cells (ES cells) with the vector DNA, BO44.2 was linearized with *Not1* and *Sal1* (sites were located adjacently and thus restriction digest produced similar DNA fragments). A gel purified (QIAquick® Gel Extraction Kit) vector DNA (25µg) was dissolved in 200µl of PBS and used for the electroporation of the ES cells.

### 4.2.2. Isolation of the genomic DNA

WT genomic DNA served as a negative control for the experiments. WT murine liver, spleen and tail tissue were cut into small pieces using razor blade, transferred into 50 ml tube with 35ml of TENS buffer (50 mM Tris/HCl pH8, 100mM EDTA, 100mM NaCl, 1% SDS) and Proteinase K (10% of the final volume). After an overnight incubation (with shaking) at 56°C digested tissues were mixed with Phenol-Chloroform (1:1) and the emulsion was left for 3-4 min at RT. Subsequently the emulsion was centrifuged (300 RCF) and the upper aqueous phase was collected (this step was repeated once more). The aqueous phase was then mixed with propanol (0.8:1) by inverting and the precipitated, cloudy DNA was rolled around a closed glass stick. DNA along with the glass stick were washed twice with ethanol and air-dried. The glass stick with the air-dried DNA was then placed into an Eppendorf tube with 0.5-1ml water (the glass stick with DNA was gently broken and left in the tube). The tube was incubated at 37°C for an hour to let the DNA detach from the glass stick. Genomic DNA was then stored at 4°C.

### 4.2.3. Genomic Southern Blot

Genomic Southern Blot was established to screen the positive embryonic stem cell (ES) clones, which were successfully electroporated with the linearized vector and recombined through the arms of homology.

#### 4.2.3.1. Buffers for genomic Southern Blot

Table 10. Buffers for the Southern blot.

Buffer name	buffer composition
ES lysis Buffer	20 mM NaCl, 10 mM Tris/HCL pH7.5, 10mM EDTA pH8, 0.5% Sarcosyl  for 100 ml : 400 µl 5M NaCl, 1 ml 1M Tris/HCl, 2 ml 0.5 M EDTA, 5 ml 10% Sarcosyl, 71.6 ml H <sub>2</sub> O
Depurination of the gel	0.25 M HCl (21.6 ml HCl conc. in 1 l H <sub>2</sub> O)
Denaturation of the gel	0.5 M NaOH, 1.5 M NaCl  (20 g NaOH, 87.4 g NaCl in 1 l H <sub>2</sub> O)
Neutralisation of the gel	1.5 M NaCl , 1 M Tris HCl pH 7.2  (87.4 g NaCl, 121 g Tris, ad H <sub>2</sub> O to ~ 800 ml, adjust pH to 7.2, add H <sub>2</sub> O to 1 l)
20x SSC	3 M NaCl, 300 mM sodium citrate pH 7  (175 g NaCl, 88 g sodium citrate in 1 l H <sub>2</sub> O)
Denaturation of the membrane	0,4 M NaOH (8ml 5 M NaOH in 250ml)
Neutralisation of the membrane	0.2 M Tris HCl pH 7.5, 1xSSC  (12.5 ml 20x SSC, 50 ml 1M Tris HCl pH 7.5 in 250 ml )

Pre- and hybridisation solution	0.5 M Sodium phosphate buffer pH 7.2, 7% SDS, 10mM EDTA  (for 1 l: 342 ml 1M Na <sub>2</sub> HPO <sub>4</sub> , 158 ml 1M NaH <sub>2</sub> PO <sub>4</sub> , 350 ml 20% SDS, 20 ml 0.5 M EDTA, 65 ml H <sub>2</sub> O)
Wash-solution 1	2x SSC, 0.1% SDS  (50 ml 20xSSC, 2.5ml 20% SDS for 500 ml)
Wash-solution 2	0.2x SSC, 0.1% SDS  (5 ml 20x SSC, 2.5 ml 20% SDS for 500 ml)
Wash-solution-3	0.1x SSC, 0.1% SDS  (2.5 ml 20xSSC, 2.5ml 20 % SDS for 500 ml)

#### 4.2.3.2. *DNA lysis, precipitation and digestion (gelatine 96-well plates: ES clones) for genomic Southern Blot*

Forty microliters of ES-lysis buffer (Table 10) and 15µl of Proteinase K (2.5mg/ml; final conc. of 0.75 mg/ml) were added pro well and left for an overnight incubation at 56°C (plates were wrapped in a parafilm). The next the day plate was cooled down, briefly spun down and 200 µl of 100% ethanol were added per well. The plate was shaken at RT for 1-2h (DNA would appear as white filaments). The liquid was removed from wells by gentle tapping on the paper towels and the plate was washed twice with 70% Ethanol. Forty microliters of the ScaI-HF digestion mix (New England BioLabs GmbH) were subsequently added to air-dried wells and incubated at 37°C overnight (Table 11).

Table 11. Reaction mix for the ScaI digestion of the ES-clones.

Digestion mix	Per well [µl]	Per 120 wells [µl]
H <sub>2</sub> O	32,8	3936
10x Buffer	4	480
RNase A (10U/µl)	0.4	48
Spermidin (1M)	0.1	12

DTT (1M)	0.1	12
ScaI (20U/ $\mu$ l)	2.5	300
Total volume	40	-

#### 4.2.3.3. Gel preparation for genomic Southern Blot

0.8% agarose gel (3.2g agarose in 400ml 1xTAE; 20 $\mu$ l EtBr) was prepared with 12 rows of wells (8 wells/raw), in order to fit in samples from the complete 96-well plate. Once mixed with the loading dye, samples were applied on the gel and run overnight at 25-30V. Fermentas 1kb plus gene ruler was used as a marker. On the next day a picture of a gel with the ruler on the side was taken and the gel was subsequently shaken in a tray with gel depurination buffer (Table 10) for 5-10min. After a water-rinse the gel was denatured (shaken for 30 min in gel denaturation buffer) and neutralised (shaken for 30 min in gel neutralization buffer).

#### 4.2.3.4. Blotting

A plastic tray was filled with 10x SSC. The gel was placed over the plastic bridge (placed in the tray with 10x SSC) covered with a wet filter paper bridge and 3 wet filter papers (Whatman) of the size of the gel. The wet Hybond N+ Membrane (Amersham) was placed on the gel and covered with 1 wet and 2 dry filter papers. Subsequently many paper towels were placed on the top and 500g weight was applied to allow the optimal buffer flow (Fig. 79). Air bubbles in between the filters/gel and membrane were rolled out using a plastic pipette.

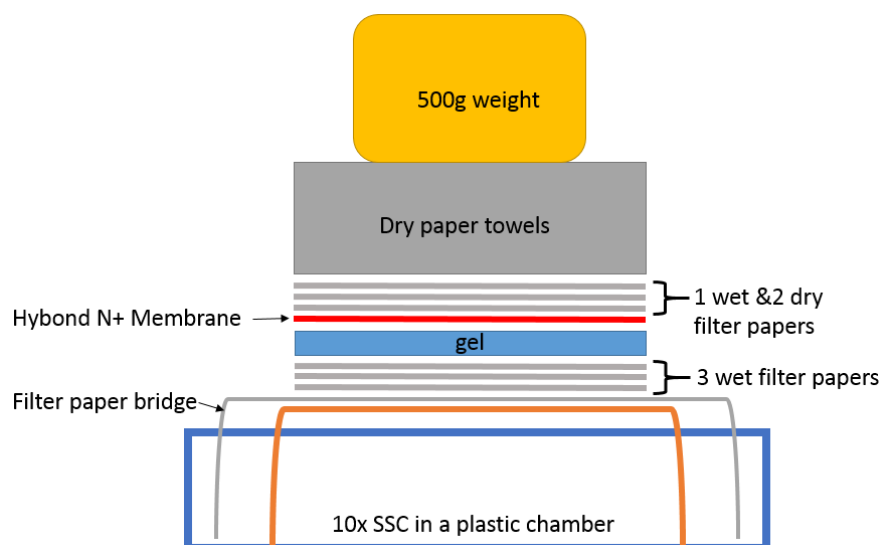


Figure 79. Southern Blot scheme.

The transfer of the DNA from the gel to the membrane was carried out overnight. After the transfer was complete, the gel along with the membrane were removed, turned over, and laid onto a damp Whatman paper; gel slots were marked with a pencil on the membrane. Right upper corner was removed for the orientation.

The membrane was then denatured for 1 min with 0.4M NaOH and neutralized for another minute with 0.2M Tris HCl pH 7.5/1xSSC. Neutralised membrane was placed on the Whatman filter paper and incubated at 80°C for 2h to fix DNA to the membrane. The membrane was then directly hybridised or sealed in a plastic foil and stored in a fridge.

#### 4.2.3.5. Southern Blot probe synthesis

Two Southern Blot probes were generated for the screening of the ES-clones. One overlapped exon1 of CD18 and the other one exon7 of CD18.

Table 12. Primers used for the synthesis of the Southern Blot probes (s-sense, as-antisense).

Southern Blot probe	Primer sequence	PCR product length
1. Overlapping exon 1	s:5'-CAGTCCCCATCTCCACTCAG-3' as: 5'-GGCACTCTTTGAAGCACCAA-3'	569bp
2. Overlapping exon 7	s:5'-ACACATGACAGCTGGGAAGA-3' as: 5'-GTCACCAACAGCGAACAGTT-3'	647bp

Probes were amplified via PCR [3'-95°C, (30s-95°C, 30s-60°C, 45s-72°C) x34, 4°C] (GoTaq® Flexi DNA Polymerase, Promega) using a primer set outlined in table 12 and purified from the gel (QIAquick® Gel Extraction Kit). Sequences of both probes and locations of primers are depicted in Fig. 80.

A)



B)

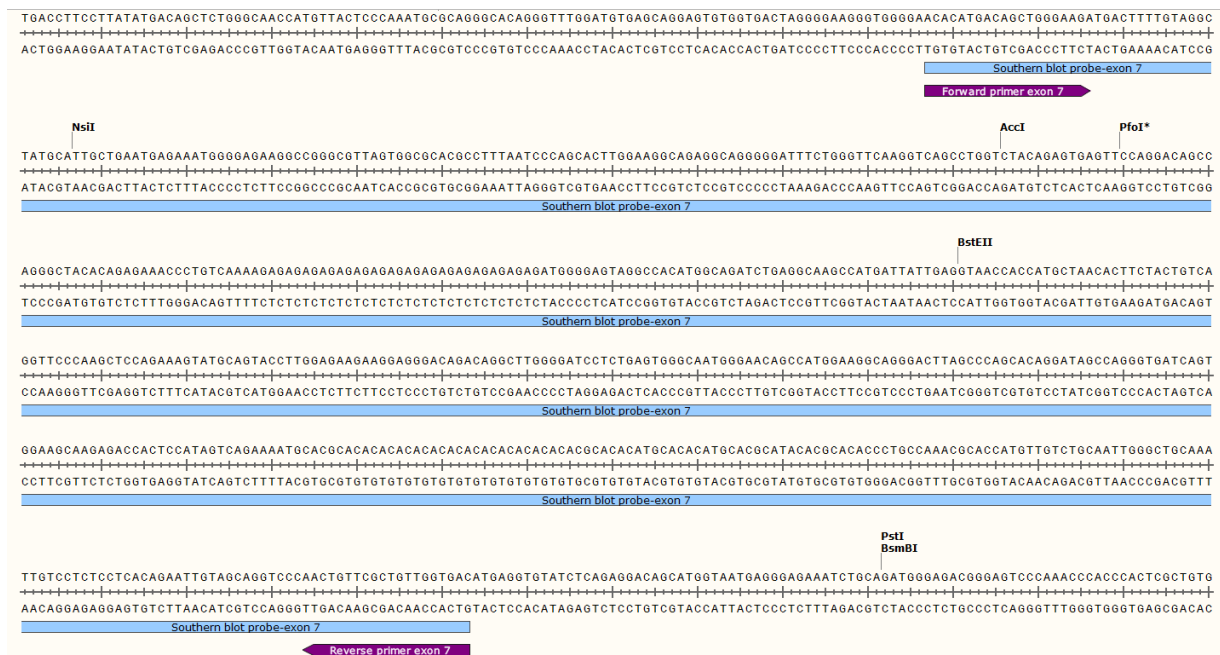


Figure 80. Southern Blot probes overlapping exon 1 (A) and exon 7 (B) of the CD18 gene.

#### 4.2.3.6. Southern Blot probe labelling

The probe was labelled with <sup>32</sup>P using TAKARA Ladderman Labelling Kit. Thirty nanograms of the probe DNA in 12µl volume were added along with 2µl of the random primer to the tube and heated for 3 min at 95°C. After subsequent 5 min incubation on ice further reagents were added: 2.5 µl of the 10x buffer, 2.5µl of dNTPs (without dCTP, 0.2mM each), 5µl of <sup>32</sup>P-dCTP

(3000Ci/mmol, 50  $\mu$ Ci), and 1 $\mu$ l Bca DNA Polymerase. The probe was labelled for 1.5-2h at 55°C and purified with Amersham Illustra MicroSpin G-50 Columns.

#### 4.2.3.7. *Hybridisation*

The membrane (pre-soaked in 2x SSC) was placed on the hybridisation mash, rolled up and put in to the hybridisation flask with 40 ml of the hybridisation buffer (pre-warmed to 65°C; table 10). The membrane was pre-hybridised for 4h in the oven at 65°C. The pre-hybridisation buffer was then exchanged with the fresh hybridisation buffer (20ml) and subsequently a denatured <sup>32</sup>P labelled probe (3 min at 95°C, 5 min on ice) was added to the buffer in the flask (avoiding direct contact of the concentrated probe with membrane before it was diluted in the buffer). The hybridisation was carried out in the oven overnight at 65°C.

The next day the solution with the probe was removed and the membrane was washed off to remove excess of the probe with wash solutions (30 min with wash-solution 1; 5-30 min with wash-solution 2, 5-30 min with wash-solution 3; buffers described in table 10) until the measured radioactivity was lower than 70cps and no less than 20-30 cps (to provide a detectable but not harmful range).

#### 4.2.3.8. *Detection of the Southern Blot Probe*

The membrane was soaked in 2x SSC and sealed in a plastic foil with 1ml of 2xSSC. It was then fixed onto the Biomax cassette with intensifying screens along with a Kodak MS Biomax film. The film was exposed overnight at -80°C and developed the next day.

### 4.2.4. Preparation of the Mouse Embryo Fibroblast (MEF) feeder cells

MEF feeder cells served as a layer on top of which the ES cells were cultured. MEF feeder cells provided a milieu that prevented ES to lose their pluripotency. They were mitotically inactivated with Mitomycin after expansion and used as a stable non-proliferative cell layer.

#### 4.2.4.1. *Thawing EFO*

Two vials of embryonic feeder cells (EFO) were thawed in a water bath at 37°C and directly diluted in 10ml of pre-warmed MEF Medium (DMEM GlutaMAX™, 10% EF-FCS, 1x Pen/Strep, 1x non-essential amino acids, 1mM sodium pyruvate). The cell suspension was pelleted by spinning for 3 min at 1000rpm and resuspended in 5 ml of pre-warmed medium. Then another 35ml of medium were added and cells were plated on Nunc™ Petri dishes, 15cm

diameter (20ml of cells suspension per plate). Cell were cultured at 37°C in a humidified 10% CO<sub>2</sub> incubator with medium being changed daily.

#### *4.2.4.2. Expanding and splitting of the feeder cells*

Once cells were confluent, the dish was washed twice with PBS and incubated for 2 min with 5ml of 1xTrypsin at 37°C. The trypsin reaction was blocked by adding 5ml of MEF Medium. Cells were pelleted by centrifugation (300 RCF), resuspended with MEF medium in a 50ml tube and plated newly at half concentration (cells derived from 1 plate would be resuspended in 40ml of medium and split in two: 20 ml per plate). At that point cells (EF2) can be either frozen or split again.

#### *4.2.4.3. Treatment of active MEF with Mitomycin C (MMC)*

To mitotically inactivate the feeder cells, the normal MEF Medium on confluent cells was replaced with 10ml of inactivation medium (2mg of Mitomycin C from Sigma-Aldrich in 200 ml of MEF feeder medium, end conc. 0.01mg/ml). After 2-4h of incubation at 37°C the inactivation medium was aspirated completely, and the plate was washed twice with a pre-warmed PBS. Cells were subsequently trypsinized and pelleted (incubation with 5ml of trypsin solution for 4 min and inactivation of the enzyme with 5ml of medium). Cells from about 20 plates were resuspended in 40 ml-50 ml of medium and counted using Neubauer chamber. Mitotically inactivated cells were then frozen at a density of  $4 \times 10^6$  cells per vial (1ml).

#### *4.2.4.4. Freezing of MMC-treated feeder cells*

MMC-treated feeder cells were resuspended at  $8 \times 10^6$  cells/ml and placed in a cryovial. One millilitre of ice cold 2x freezing medium (40% EF Medium, 40% EF FCS, 20% DMSO) was added dropwise to 1ml of the cell suspension in the cryovials in an isopropanol-cryobox precooled to -20°C. The cryovials were subsequently stored for 24h in an isopropanol-cryobox at -80°C and transferred afterwards to liquid nitrogen for long term storage.

#### *4.2.4.5. Plating of the mitotically inactive MEF feeder cells*

One vial of the mitotically inactive MEF feeder cells (approximately  $3.5 \times 10^6$  cells were viable) was thawed in a water bath at 37°C and directly diluted within 10ml of pre-warmed MEF feeder cell medium. Cells were pelleted (4 min, 300 RCF, 4°C). The medium was then completely aspirated and the cell pellet was reconstituted with 5ml of pre-warmed ES medium (1x KnockOut™ DMEM, 1x L-Glutamine, 10% EF-FCS, 1x Pen/Strep, 1x non-essential amino acids, 1000 units/ml mLIF, and 50µM β-Mercaptoethanol). Cells were then plated on a 10cm

diameter NUNC Petri dish and incubated at 37°C in a humidified incubator with 10% CO<sub>2</sub>. MMC-treated feeder cells may be used after 6-12h and be maintained in the incubator for a maximum of 8-10 days.

#### 4.2.5. Preparation of the Embryonic Stem cells (ES-cells) JM8

Embryonic Stem Cells JM8 (Sub-cloned from JM8 parental cell line, derived from C57BL/6N mice) were used for the electroporation with the linearized vector carrying the LoxP sites. Positive ES clones were subsequently prepared for the blastocyst injection into a recipient mouse, whose offspring carried the construct.

##### 4.2.5.1. Thawing and splitting of ES-cells

One cryovial of ES cells (highly germline competent C57BL/6N mouse embryonic stem cell line, JM8) was thawed at 37°C in a water bath and transferred into a 15ml tube containing 7ml of a pre-warmed ES medium (1x KnockOut™ DMEM, 1x L-Glutamin, 10% EF-FCS, 1x Pen/Strep, 1x non-essential amino acids, 1000units/ml mLIF, 50µM β-Mercaptoethanol) in 15ml tube. Cells were then pelleted ( 3min, 300 RCF, 4°C) and resuspended in 2ml of ES medium using a fire-polished Pasteur pipette to single out the cell suspension (the opening of the Pasteur pipette had its edges smoothen and was reduced in diameter using a flame). Another 8 ml of ES medium was added to the cell suspension and cells were then plated on the MMC-treated feeder layer (the cell culture supernatant was removed from the feeder cell culture beforehand). The medium was changed every day. After 2-4 days ES were confluent. Two hours before splitting medium was changed. Subsequently the ES plate was washed twice with pre-warmed PBS and incubated with trypsin for 4 min at 37°C. The trypsin reaction was stopped with ES medium, cells were collected from the plate using a fire-polished Pasteur pipette and spun down in a falcon tube for 3 minutes (300 RCF, 4°C).

##### 4.2.5.2. Electroporation of the ES-cells

ES cells were trypsinized, harvested, and resuspended in PBS at a concentration of  $13 \times 10^6$  cells/ml ( $1 \times 10^7$  cells in 800µl). The cells suspension was then combined with 25µg of gel-purified, linearized BO44.2 vector DNA (dissolved in 200µl of PBS) in a 1.5ml sterile Eppendorf tube and placed on ice for 10min. The Cell-DNA suspension was then applied into a pre-cooled cuvette and pulsed at 240V and 500µF. Directly after electroporation cells were placed again on ice for 10min and subsequently resuspended in 50ml of ES-medium and plated on 5 MMC-treated 10cm Feeder-plates (Nunc™). For the generation of the CD18<sup>fl/fl</sup> mouse 2 rounds of electroporation were carried out, generating 10 plates, where clones grew initially.

Non-electroporated cells served as a survival control group. After two days of culture Neo-resistance selection was introduced by adding G418 (Geneticin) at a concentration of 200µg/ml. Cells were selected with this antibiotic for 8-12 days prior to clone picking.

#### 4.2.6. Picking of the ES cell colonies resistant to Neomycin

After selection in G418 containing ES-Medium for 8-12 days many colonies arose, which were about 0.5-2mm in diameter. Separate colonies were picked and plated separately onto a 96-well plate with a MMC-treated Feeder cell layer. To generate the latter, MMC-treated feeders, cells were plated onto a flat-bottom 96-well plate the night before clones were picked; one vial containing approx.  $4 \times 10^6$  cells was used to seed two 96-well plates (50µl of the cell suspension per well; a total of ten 96-well plates was prepared). Two hours before picking clones, the medium of the ES cultures was changed. Directly before the procedure an ES-clone dish was washed twice with pre-warmed PBS and 8ml of a pre-warmed PBS/Pen-Strep was added. Then, an ES-clone dish was placed under a microscope (under the hood) and each clone was scraped using a pipette with a filter-tip (in a maximum volume of 50µl). The selected clone was transferred into a well of a round-bottom 96-well plate coated with trypsin/PBS (1:1) (50µl/well). Each clone was pipetted up and down 20 times within the trypsin solution to single-out colony cells. Each clone was picked with a fresh filter-tip. After transferring of 8 clones (one column of the plate), trypsinized and single-celled clones were added 100µl of ES-Medium to inactivate trypsin, pipetted up and down using a multi-channel pipette and transferred for further culture onto a 96-well plate coated with MMC-treated feeder cell layer. A total of nine 96-well plates were seeded with Neo-resistant single ES-clones. The medium (containing G418) was changed first on the following day and then every other day.

#### 4.2.7. Coating of 96-well plates with gelatine

The gelatine was warmed up in a water bath and diluted in PBS (0.1% solution). Sixty microliters of gelatine solution was then added per well into a 96-well flat-bottom plate and incubated at 37°C for 30min. Subsequently, gelatine solution was aspirated and left over gelatine coating was left under the hood with an open lid to dry for 10-20min. Gelatine plates were stored at 4°C, wrapped in a parafilm. They served as culture-bed for the ES clones that were used for Southern Blot screening (to avoid DNA contamination derived from the feeder cells).

#### 4.2.8. Splitting of the ES cells on 96-well plates (Feeder cell & gelatine coated)

When most of the clones on the plate were confluent (around 5th day after clone picking) clones cultured on the 96-well plates were split. MMC-treated feeder cells were plated onto 96-well plates for further ES culture one day before. Medium in the ES culture was changed 2h prior to splitting. Then cell were washed twice with 100µl of PBS per well. Subsequently 50µl of 1x trypsin was added per well and incubated for 4 min at 37°C. The trypsin digest was stopped by applying 100µl of ES medium per well. Cells were singled out via pipetting up and down for at least 20 times. Initially, cells were split in two onto MMC-treated feeder cell (MEF) plates and in the course of next splitting one plate was split again onto MEF plates and the other onto gelatine plates.

#### 4.2.9. Freezing of the ES clones cultured on Feeder cells & gelatine

Once ES cultures were confluent (around 3 days after splitting) plates were frozen in duplicates. Clones cultured on gelatine were washed twice with PBS, which was then aspirated and the plates were stored at -20°C until the Southern Blot analysis commenced. Clones that were cultured on the MEF plates were changed medium and 2h later they were detached with 50µl of trypsin per well. The reaction was stopped with 50µl of ES medium, cells were singled-out and plates were stored on ice before addition of 2x freezing medium ( 2ml DMSO, 4ml FBS, 4ml ES-medium), 100µl/well. Plates were wrapped with parafilm and immediately placed in the freezer at -20°C. After 30min, plates were transferred into a Styrofoam box and stored in the freezer at -80°C.

#### 4.2.10. Expansion of positive clones

Clones that turned out positive in the Southern Blot screening were further expanded to create a stock, which was used for the blastocyst injection. Positive clones were thawed from the 96-well MEF-plates in 2ml of pre-warmed ES medium, spun down (only 1.5ml of the medium would be aspirated to prevent cell loss) and cultured on 24-well MEF-plates. Once clones were confluent they were transferred to 6-well plates and subsequently the culture format would be scaled up to a 10cm dish. The clones adjacent to the positive ones on the 96-well plate were cultured as well up to a 6-well format and then were frozen, to prevent loss of a clone in case of a mistaken location (a given plate could be thawed once only). The expanded positive clones were re-screened by Southern Blot, mycoplasma-tested and stored in liquid nitrogen, at least

10 vials per clone ( $10^6$  cells in 1ml of freezing medium per vial), until used for the blastocyst injection.

#### 4.2.11. Blastocyst injection

The blastocyst injections were carried out at two sites: at Polygene Transgenetics in Rümlang, Switzerland and at the Transgenic Facility Mainz (TFM). Clones were karyotyped prior to injections (10 cells per clone were randomly picked and analysed according to their nuclei integrity and presence of all 40 chromosomes). Each two ES clones (P1-9F and P3-10G) were used for the blastocyst injection, which was subsequently transferred into the uterus of a recipient B6 Albino female mouse in order to generate chimeric mice (Fig. 81 A).

#### 4.2.12. CD18<sup>fl/fl</sup> screening and breeding strategy.

##### 4.2.12.1. Screening of chimeras

The F1 generation of mice generated after blastocyst injection was screened with primers specific for the Neo-cassette to identify mice with a CD18<sup>fl/fl</sup> genotype. The PCR conditions were established by the Polygene Transgenetics and are described in Table 13 below. The PCR was performed using GoTaq®Flexi DNA Polymerase (Promega).

Table 13. Neo Cassette detection PCR protocol.

Neo-Cassette detection PCR	Primer sequence	PCR product length(bp)
1. Neo forward primer	5'-CAAGCTCTTCAGCAATATCACGGG-3'	542
2. Neo reverse primer	5'-CCTGTCCGGTGCCCTGAATGAACT-3'	
Cycling protocol	1 x (95°C/180s) 35 x (95°C/30s - 56°C/30s - 72°C/45s) 1 x (72°C/120s)	

The FLP-recombined mice were screened by PCR in order to distinguish between the floxed homozygous, floxed heterozygous and wild type genotype. The PCR conditions are described in detail in Table 14 below.

Table 14. CD18 homo- and heterozygote PCR screening protocol (s-sense, as-antisense).

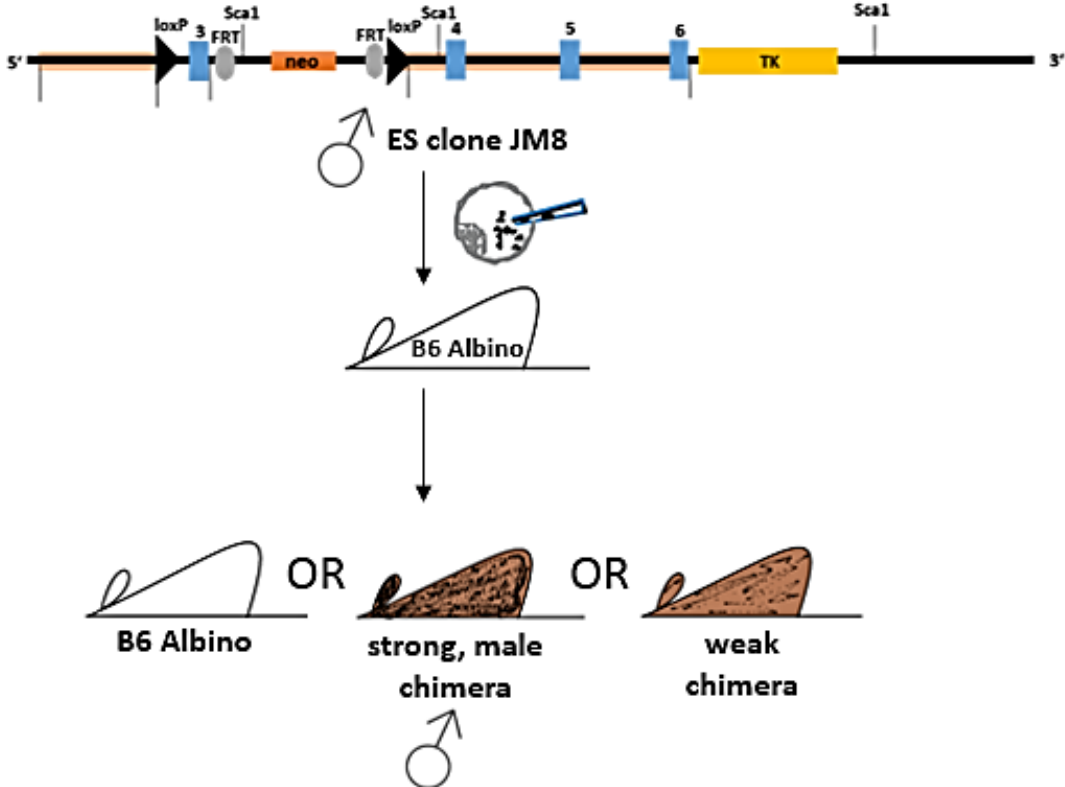
Homozygote and Heterozygote screening PCR for FLP-recombined CD18 <sup>fl/fl</sup>	Primer sequence	PCR product length (bp)		
		BO44.2	CD18 <sup>fl/fl</sup> after FLP-recombination	WT
<b>1. Primers B1+B4</b>	B1(s):5'-GGCAACGGAAACAGCTATCT-3' B4(as):5'-ATAGAACCACCAACCTCGCA-3'	2728	802	547
<b>2. Primers B2+B3</b>	B2(s): 5'-GTGACACTTTACTTGCGACCA-3' B3(as):5'TGCCAATAAAGAATTCAGAGCC-3'	2413	487	233
<b>Cycling protocol</b>	1 x (95°C/180s) 35 x (95°C/30s - 58°C/30s - 72°C/45s) 1 x (72°C/120s)			

#### 4.2.12.2. Breeding of chimeras

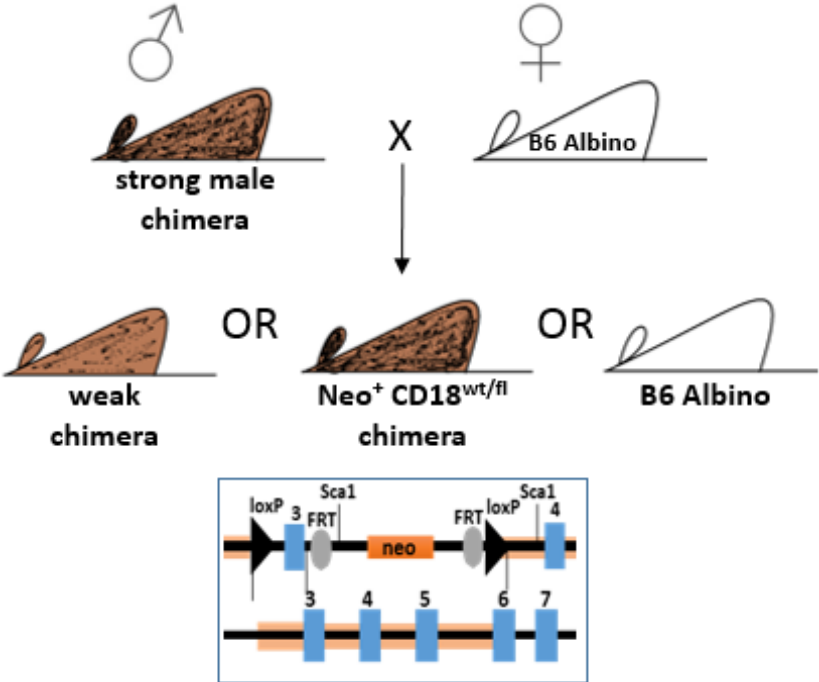
Chimeric mice born after blastocyst injection were identified according to their coat colour. ES cells encoded black coat, whereas blastocyst-recipient albino mice would have white coat. Highly chimeric mice with strongest BL/6 background were crossed back to BL/6 Albino mice and among their offspring (F1 generation) mice with agouti coat would have the CD18<sup>fl/fl</sup> genotype (Fig. 81 B). The F1 generation with an agouti coat was screened for genomic presence of the Neo-cassette (encoded by the BO44.2 vector) by PCR and Neo<sup>+</sup> mice were further bred with Flp Deleter mice (C57BL/6 background; kindly supplied by the lab of Professor Ruf, University Medical Centre, Centre for Thrombosis and Haemostasis Mainz (CTH), Mainz) in order to delete the Neo-resistance gene using FRT– recombination sites (Fig. 81 C).

The offspring of Flp Deleter x CD18<sup>fl/wt</sup> mice was screened to determine FLP-recombined heterozygous CD18<sup>fl/wt</sup> mice, which were then crossed (CD18<sup>fl/wt</sup> x CD18<sup>fl/wt</sup>) in order to generate a homozygous CD18<sup>fl/fl</sup> offspring (Fig. 81 D).

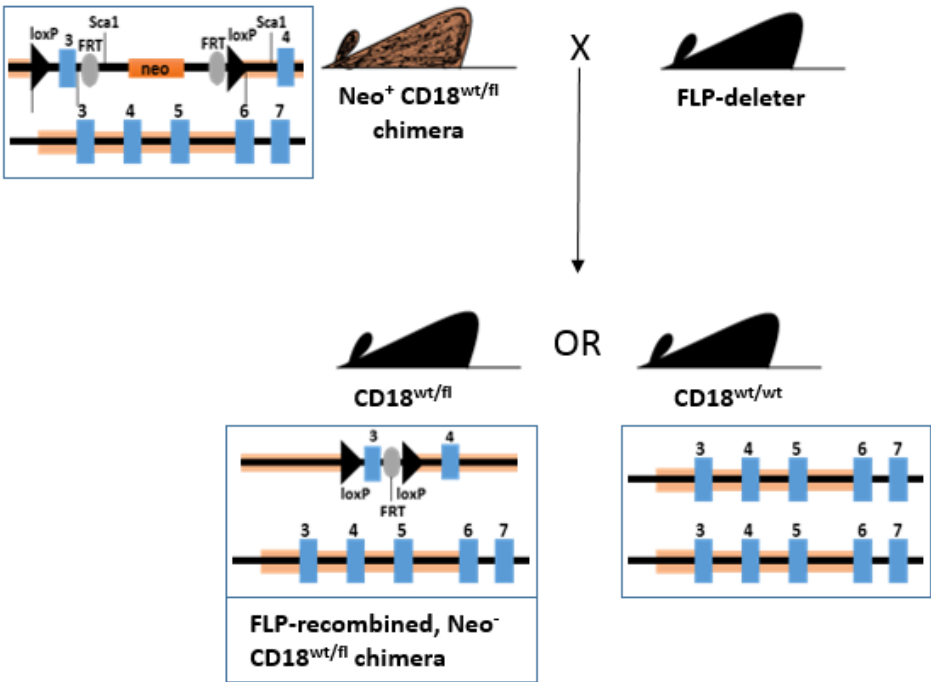
A)



B)



C)



D)

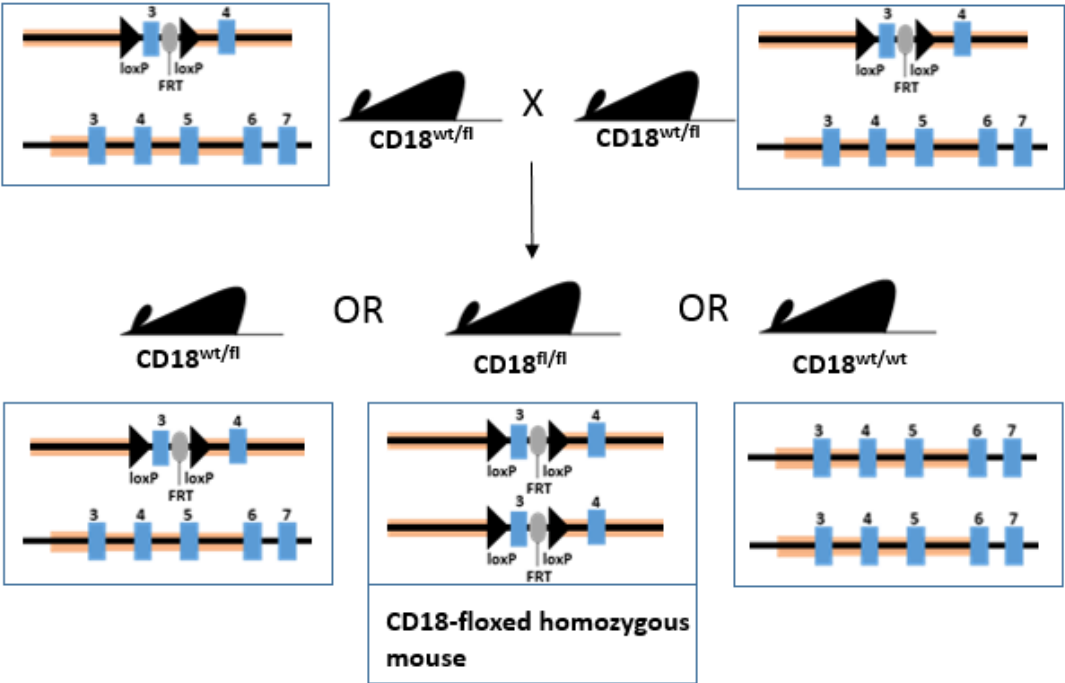


Figure 81 . Breeding strategy of the chimera mice acquired after blastocyst injection. Positive JM8 ES clone was injected into a blastocyst of a B6-Albino recipient mouse (A). The strongest male chimeric mice among the offspring were selected and crossed back to B6-Albino mice (B). Mice with strongest chimeric background were screened for Neo-cassette and positive

*ones were crossed with Flp Deleter mice. The offspring of CD18<sup>wt/fl</sup> Neo<sup>+</sup> and Flp Deleter was in 50% WT and in 50% CD18<sup>wt/fl</sup> Neo<sup>-</sup> (C). The CD18<sup>wt/fl</sup> Neo<sup>-</sup> mice were further crossed with each other in order to generate a homozygous CD18<sup>fl/fl</sup> mice strain. The offspring was in 25% homozygous, in 25% wild type and in 50% heterozygous (D).*

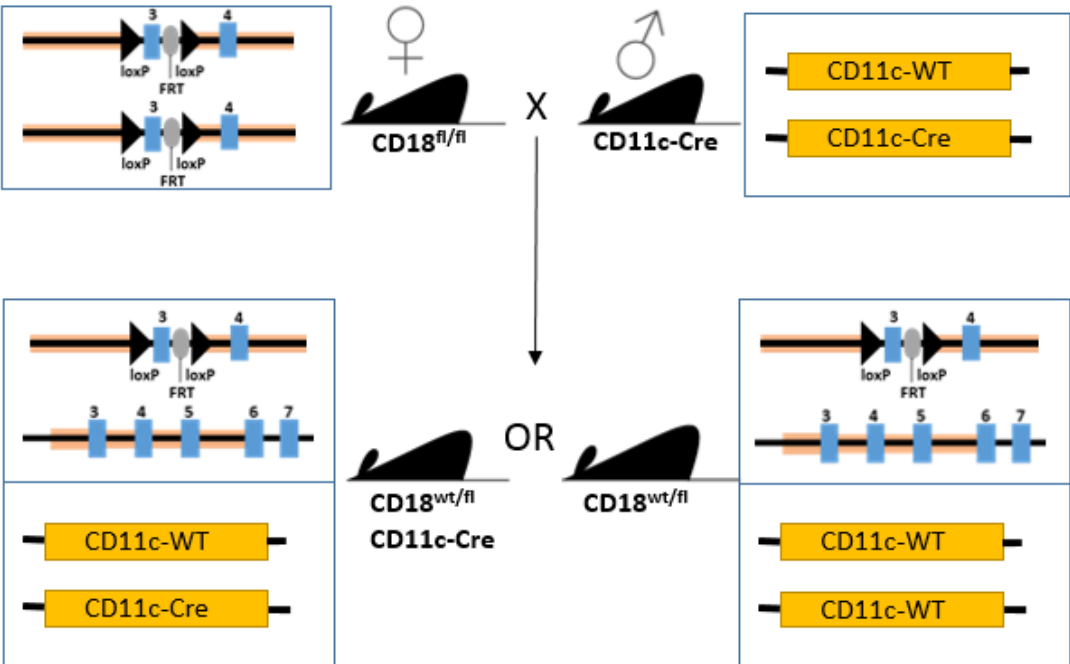
#### 4.2.13. DNA sequencing of the CD18<sup>fl/fl</sup> mice

Tail biopsies from mice positively screened for CD18<sup>fl/fl</sup> were used as a source of genomic DNA. This DNA was amplified using primers A1 ('GACCCCTAGATCTTCCCTGC') and B4 ('ATAGAACCACCAACCTCGCA'), which yielded a 1367bp fragment containing Exon 3 of the CD18 along with the overlapping loxP sites. The PCR was performed using GoTaq® Flexi DNA Polymerase (Promega). Gel purified (QIAquick® Gel Extraction Kit) DNA fragment was then sequenced by StarSEQ® GmbH, Mainz.

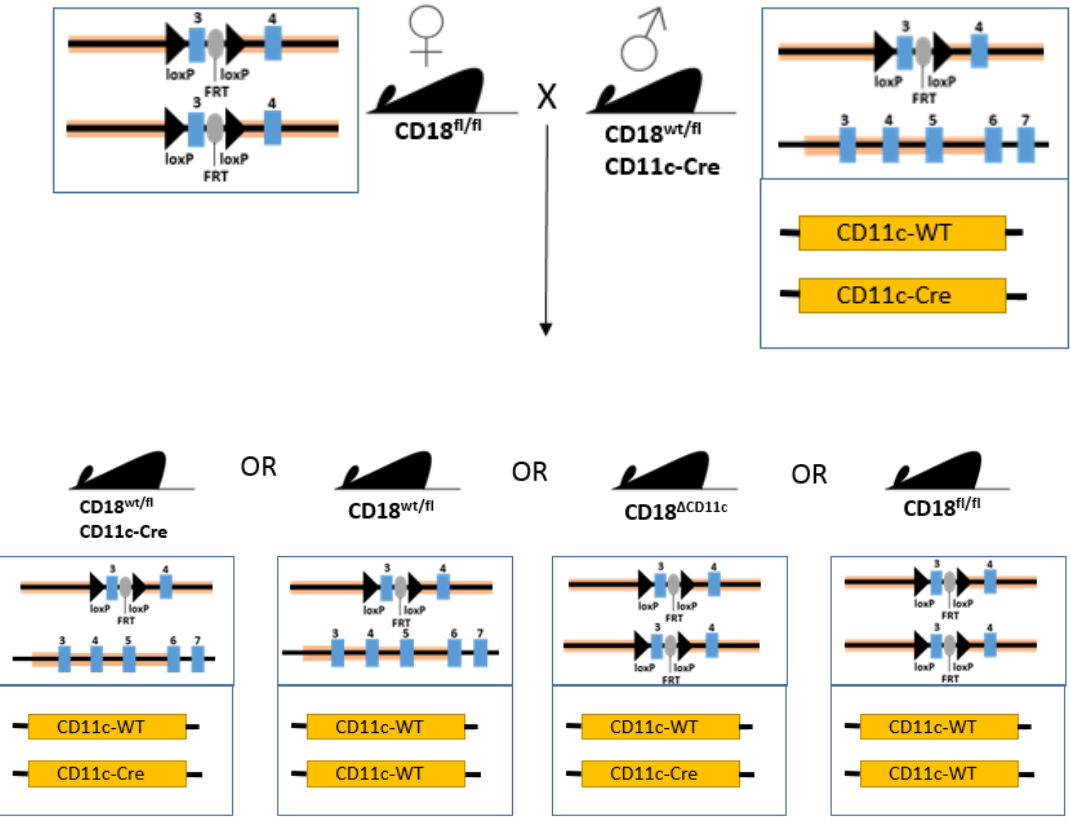
#### 4.2.14. Breeding scheme of the CD18<sup>ΔCD11c</sup>

Since the generation of the transgenic mice at the Transgenic Facility Mainz (TFM) took more time than expected, those mice were bred only until a CD18<sup>fl/fl</sup> homozygous genotype was acquired and then sperm of 4 breeding males was cryopreserved at the Translational Animal Research Center (TARC) Biotechnik in Mainz. Only mice derived from blastocyst injections carried out at Polygene Transgenetics in Rümlang were used for further crossing with mice expressing CRE recombinase in a cell type-specific manner. For this, CD18<sup>fl/fl</sup> female mice were crossed with CD11c<sup>CRE</sup> male mice (Fig. 82 A) (B6.Cg-Tg(Itgax-cre)1-1Reiz/J) (Caton et al., 2007), which were kindly supplied by the group of Professor Björn Clausen in Mainz. The CD18<sup>fl/wt</sup> CRE<sup>+</sup> male offspring was then crossed with CD18<sup>fl/fl</sup> females (Fig. 82 B). In the next generation CD18<sup>fl/fl</sup> CD11c-CRE<sup>+</sup> males were acquired and those were paired with CD18<sup>fl/fl</sup> females (Fig. 82 C). Subsequent offspring had to be screened only for presence of CRE recombinase insert, since all mice were homozygous for the floxed CD18 gene locus (CD18<sup>fl/fl</sup>).

A)



B)



C)

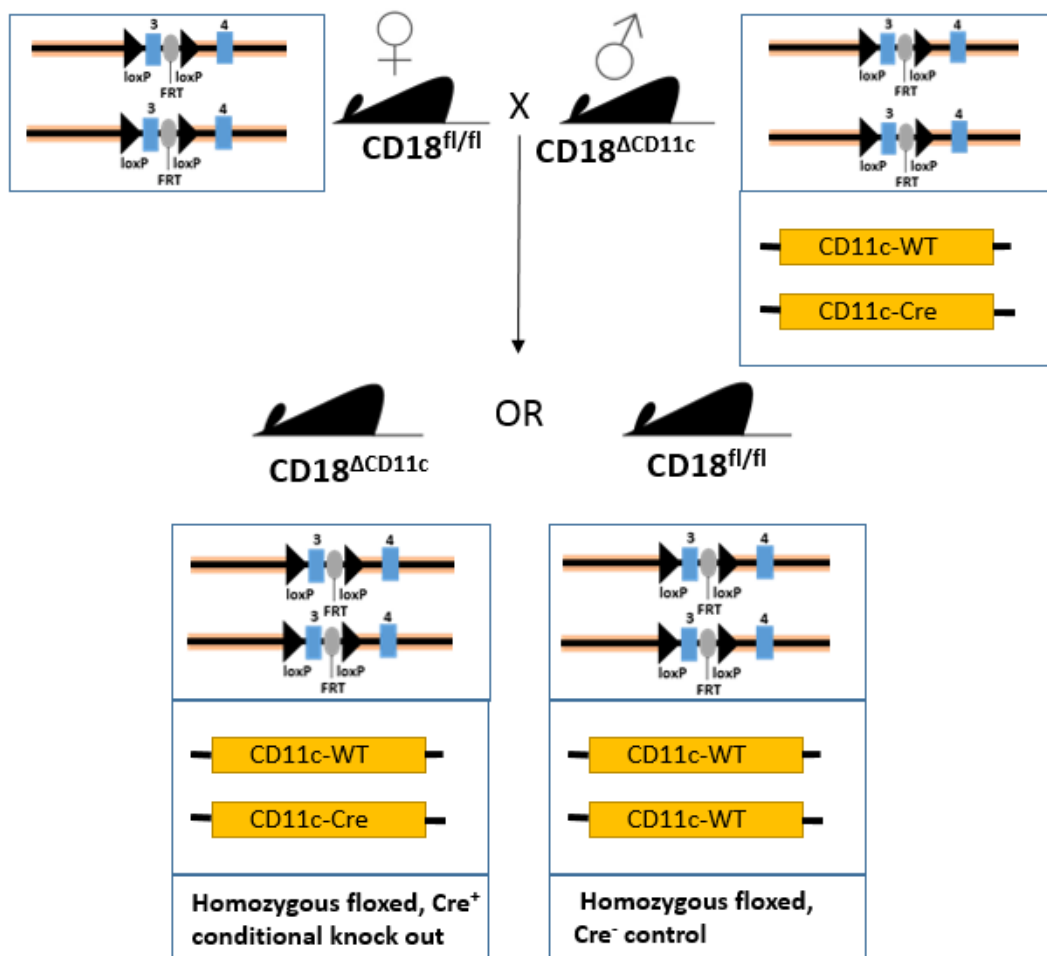


Figure 82. *CD18<sup>ΔCD11c</sup> breeding strategy.*

The *CD18<sup>fl/fl</sup>* FLP-recombined mice were crossed with *CD11c<sup>CRE</sup>*. Fifty percent of the heterozygous offspring was positive for Cre (A). The *CD18<sup>wt/fl</sup>* Cre<sup>+</sup> mice were crossed back to *CD18<sup>fl/fl</sup>* in order to generate a homozygous *CD18<sup>fl/fl</sup>* Cre<sup>+</sup> mouse (B). Male *CD18<sup>ΔCD11c</sup>* mice were crossed with *CD18<sup>fl/fl</sup>* females to maintain the strain. Half of the offspring was conditionally knock-out and the other half was used as control mice (C).

#### 4.2.15. *CD18<sup>ΔCD11c</sup>* mouse screening

The *CD18<sup>fl/fl</sup>* genotype was analysed as described before (table 14). The presence of CRE recombinase was analysed using 4 primers: one primer-pair detected the integrated CRE recombinase gene and the second primer-pair actin (serving as an internal DNA quality control). The PCR was performed using GoTaq®Flexi DNA Polymerase (Promega), conditions and primer sequences are summarized in table 15 below.

Table 15. PCR protocol for the detection of *CD11c<sup>CRE</sup>* genotype.

<b>CRE-recombinase detection PCR</b>	<b>Primer sequence</b>	<b>PCR product length(bp)</b>
1. Cre-primers	oIMR7841: ACT TGG CAG CTG TCT CCA AG oIMR7842: GCG AAC ATC TTC AGG TTC TG	313
2. Actin-primers	Forward: 'TGT TAC CAA CTG GGA CGA CA' Reverse: 'GAC ATG CAA GGA GTG CAA GA'	510
Cycling protocol	1 x (95°C/300s) 35 x (95°C/30s - 63°C/40s - 72°C/45s) 1 x (72°C/600s)	

### 4.3. Cell biology methods

#### 4.3.1. Generation and analysis of Murine Bone Marrow-Derived Dendritic Cells (BMDC)

##### 4.3.1.1. Generation of BMDC

BMDC were generated as previously described (Balkow et al., 2007) with some modifications. In brief,  $5 \times 10^6$  BM cells derived from femurs were resuspended in 5 ml of RPMI 1640 medium (PAA Laboratories, Pasing, Austria), supplemented with 5% FCS, 2mM L-Glutamine, 0.1mM nonessential amino acids, 50µg/ml Penn/Strep (all from PAA), 50 µM β-mercaptoethanol (Sigma-Aldrich, Deisenhofen, Germany), and 4 ng/ml recombinant murine GM-CSF (R&D, Wiesbaden, Germany), and were seeded into 6-well cell culture plates (BD, Franklin Lakes, NJ). On day 3 and 6, fresh medium (5 ml) was added. On day 7, non-adherent and loosely adherent BMDC were harvested, washed and used for experiments.

The following antibodies were used for analysis of untreated BMDC of different genotypes using flow cytometry: eFluor450-conjugated-anti-MHC-II, PE-Cy7-conjugated-anti-CD11c, PE-conjugated-anti-CD11b, and FITC-conjugated-anti-CD18.

#### 4.3.1.2. *BMDC activation assay*

Untouched (not reseeded prior to the experiment) BMDC ( $0.5 \times 10^6/0.5\text{ml}$ ) differentiated in 48-well plates (CELLSTAR®, Greiner bio-one) were stimulated overnight with various agents at different concentrations: CpG ( $0.005 < 0.05 < 0.5 \mu\text{g/ml}$ ), LPS ( $0.01 < 0.1 < 1 \mu\text{g/ml}$ ), Poly I:C ( $0.1 < 1 < 10 \mu\text{g/ml}$ ) and R848 ( $0.01 < 0.1 < 1 \mu\text{g/ml}$ ). On the following day the supernatants of the cultures were frozen for the subsequent cytokine analysis and cells were harvested for flow cytometric analysis.

The following antibodies were used for the cell staining: eFluor450-conjugated-anti-MHC-II, PE-Cy7-conjugated-anti-CD11c, APC-conjugated-anti-CD40, FITC-conjugated-anti-CD86, PE-conjugated-anti-CD80, APC-conjugated-anti-CD18, and PE-conjugated-anti-CD11b.

#### 4.3.2. Isolation and analysis of splenocytes

Various splenic immune cell populations derived from  $\text{CD18}^{\text{ACD11c}}$  and the corresponding CRE-negative mice were analysed for their co-stimulatory molecules expression and activation capacity.

##### 4.3.2.1. *Isolation of splenic dendritic cells*

Murine spleens were isolated and mashed with a sterile syringe plunger (Braun) on a PBS-pre-soaked  $40 \mu\text{m}$  cell strainer (EASYstrainer™, greiner bio-one). Mashed tissue was washed through the strainer using 10ml of FACS buffer (PBS 2%FCS, Pen/Strep, 2mM EDTA) and spun down (1200 rpm, 10min, 4°C). The cell pellet was resuspended in 1ml of a Geys lysis buffer and after a minute erythrocyte-depletion was stopped with FACS buffer. The cell suspension was spun down, resuspended in MACS buffer and subsequently DC were isolated using a Pan Dendritic Cell Isolation Kit, mouse as recommended by the manufacturer (Miltenyi Biotec).

The following antibodies were used for analysis of untreated splenic DC using flow cytometry: eFluor450-conjugated-anti-MHC-II, PE-Cy7-conjugated-anti-CD11c, PE-conjugated-anti-CD11b, PE-conjugated-anti-CD68, APC-conjugated-anti-CD19, and APC-conjugated-anti-CD18.

#### 4.3.2.2. *Activation of splenic dendritic cells*

Splenic dendritic cells ( $2 \times 10^5/200\mu\text{l}$ ) were seeded on a 96-well flat bottom plate (CELLSTAR®, greiner bio-one) in RPMI medium supplemented with 5% FCS, 2mM L-Glutamine, 0.1mM nonessential amino acids, 50 $\mu\text{g/ml}$  Penn/Strep (all from PAA) and 50  $\mu\text{M}$   $\beta$ -mercaptoethanol (Sigma-Aldrich, Deisenhofen, Germany). DC were stimulated overnight with various agents: CpG (0.5 $\mu\text{g/ml}$ ), LPS (1 $\mu\text{g/ml}$ ), Poly I:C (10 $\mu\text{g/ml}$ ) and R848 (1 $\mu\text{g/ml}$ ). The following day cell culture supernatants were harvested and frozen for cytokine analysis and cells were harvested and stained for the flow cytometric analysis or qPCR. For the former the following antibodies were used: eFluor450-conjugated-anti-MHC-II, PE-Cy7-conjugated-anti-CD11c, APC-conjugated-anti-CD40, FITC-conjugated-anti-CD86, PE-conjugated-anti-CD80, APC-conjugated-anti-CD18, and PE-conjugated-anti-CD11b.

#### 4.3.2.3. *Isolation and analysis of splenic lymphocytes*

Murine spleens were prepared as in 4.3.2.1 “Isolation of splenic dendritic cells “. Splenic cell suspension was spun down, resuspended in FACS buffer and subsequently stained.

The following antibodies were used for the analysis of TC: PE-Cy5-conjugates-anti-CD3, PE-Cy7-conjugates-anti-CD11a, APC-conjugates-anti-CD18, conjugated-anti-CD4, conjugated-anti-CD8, conjugated-anti-CD25, and conjugated-anti-FoxP3.

The following antibodies were used for the analysis of BC: FITC-conjugated-anti-CD19, PE-Cy7-conjugates-anti-CD11a, APC-conjugates-anti-CD18, eFluor450-conjugated-anti-MHC-II, FITC-conjugated-anti-CD86.

#### 4.3.3. Isolation and analysis of murine blood and bone marrow cells

Bone marrow cells derived from femurs were first resuspended in 10 ml of RPMI 1640 medium (PAA Laboratories, Pasing, Austria), supplemented with 5% FCS, 2mM L-Glutamine, 0.1mM nonessential amino acids, 50 $\mu\text{g/ml}$  Penn/Strep (all from PAA), 50  $\mu\text{M}$   $\beta$ -mercaptoethanol (Sigma-Aldrich, Deisenhofen, Germany), spun down and resuspended in 1ml of a Geys lysis buffer and after a minute erythrocyte-depletion was stopped with FACS buffer. The cell suspension was spun down (10min, 300 RCF, 4°C), resuspended in FACS buffer and subsequently stained.

The following antibodies were used for the analysis of bone marrow: PE-Cy5-conjugated-anti-CD3, eFluor450-conjugated-anti-CD4, FITC-conjugated-anti-CD8a, APC-conjugated-anti-

CD19, PE-Cy5-conjugated-anti-CD11b, eFluor-conjugated-anti-Ly6G, FITC-conjugated-anti-Ly6C.

#### 4.3.4. Antigen uptake and processing analysis

Endocytosis and antigen processing was analysed using OVA-Alexa 647 (Invitrogen, #O34784) and OVA-DQ (Invitrogen #D-1203), respectively. OVA-DQ emits red fluorescence once it accumulated in the endosome, and with green fluorescence (FITC channel) once it's processed in acidified lysosomes. In this manner one can distinguish between uptake and intracellular processing using flow cytometry analysis after incubation.

Hundred microliters of the cell suspension ( $3 \times 10^6$ /ml; BMDC or splenic DC) were added directly to the FACS tube and subsequently OVA antigen was applied, either OVA-Alexa647 or OVA-DQ (both at an end conc. of 50 $\mu$ g/ml). Three periods of incubation were analysed: 10, 30 and 60min. At the end of each incubation samples were directly placed on ice and further processed for FACS analysis. Incubations were performed in parallel at 37°C and 4°C.

#### 4.3.5. Preparation and staining of lung cells

In order to examine the surface marker expression on the lung dendritic cells, one lung (left or right) was cut into small pieces on a Petri dish using scissors and scalpel. The chopped tissue was then transferred into a 50ml tube and the Petri dish was washed with 2.5ml PBS to collect the rest, which was then added into the same 50ml tube. Collagenase from *Clostridium histolyticum* Type IA (Sigma-Aldrich) dissolved in PBS (2.5ml, 1mg/ml) was applied to the tissue suspension (final volume: 5ml, Collagenase end conc.: 0.5mg/ml), which was subsequently incubated for 45min at 37°C (shaken every 5-10min). After the incubation, the tissue was further homogenized by pulling the cell suspension up and blowing out three times using a 10ml syringe with a needle (G 20 x 1 1/2" /  $\varnothing$  0,90 x 40 mm). The cell suspension was run through a 70 $\mu$ m strainer and centrifuged (1400rpm, 4°C, 8min). Cell pellet was resuspended with Geys lysing buffer and after 1min of incubation, erythrocyte-depleted cell suspension was washed twice with PBS-1%FCS. Cells were then resuspended in 5ml of FACS buffer (PBS, 2%FCS, 2mM EDTA), counted and stained for FACS analysis.

The following antibodies were used for surface marker detection of the erythrocyte-depleted lung cell suspension ( $2 \times 10^7$  cells/ml): FITC-conjugated anti- Ly6C, PE-conjugated-anti-CD103, eFluor450-conjugated-anti-MHC-II, PE-Cy7-conjugated-anti- CD11c, PE-Cy5-conjugated-anti-CD11b. One free channel (APC) was left out to gate out the autofluorescent macrophages. Cells were stained at room temperature for 15 min and washed using FACS

buffer (PBS, 2%FCS, 2mMEDTA). Cell pellets were resuspended in FACS -fixation buffer (PBS, 4% PFA) and analysed on LSRII, BD (BD FACSDIVA™ Software).

#### 4.3.6. Preparation and staining of a single-cell suspensions from a murine skin

To assess surface marker expression of the skin dendritic cells, ears of mice were cut off and washed in PBS. The tissue was transferred into a 2ml Eppendorf tube along with 300µl of a digestion mix (400U/ml Collagenase IV, Dispase 1.25mg/ml, 100U/ml, Hyaluronidase, 0.5U/ml DNase, in RPMI). The tissue was further cut into smaller pieces using scissors, filled up to 2ml with the digestion mix and incubated in thermoshaker for 60min at 37°C. Subsequently, 40µl of 500mM EDTA were added to the digestion solution (final concentration 10mM) and incubated for additional 5min at 37°C. Finally the sample was pipetted up and down, passed through a 70µm strainer (the strainer was then flashed with 10ml of PBS/2mM EDTA to collect the remaining cells) and spun down at 400g for 7min. The supernatant was discarded and cells were resuspended in 1ml of ice cold PBS for further analysis.

The following antibodies were used for the analysis of the skin cell suspension: FITC-conjugated-anti-CD45, PE-conjugated-anti-CD103, PE-Cy5-conjugated-anti-MHC-II, APC-conjugated-anti-CD11c, PE-Cy7-conjugated-anti-CD11b. Cells were stained at RT for 15 min and washed using FACS buffer (PBS, 2%FCS, 2mMEDTA). Cell pellet was resuspended in FACS -fixation buffer (PBS, 4% PFA) and analysed on LSRII, BD (BD FACSDIVA™ Software).

#### 4.3.7. *In vitro* T Cell Proliferation

Incorporation of tritium-labelled thymidine (3H-TdR) into cellular DNA was used to monitor rates of DNA synthesis and thereby proliferation of T cells. Splenic T cells derived from an OT-II or OT-I (C57BL/6) mouse were isolated using a CD4<sup>+</sup> or CD8a<sup>+</sup> T cell Isolation Kit (Miltenyi Biotec) and added (5x10<sup>4</sup> cells/well in 100µl) to serial dilutions (in triplicates, starting with 10<sup>4</sup> cells/well) of dendritic cells derived from BMDC culture ( WT C57BL/6 and CD11b<sup>-/-</sup>) or isolated from the spleen of CD18<sup>ΔCD11c</sup> and CD18<sup>fl/fl</sup> mice (Pan Dendritic Cell Isolation Kit, mouse ; Miltenyi Biotec) in a total of 200µl/well. DC were loaded with antigen prior to harvest/co-culture with T cells adjuvants (0.1µg/ml OVA peptide for OT-II cultures or SIINFEKL for OT-I cultures). DC-TC co-cultures were stimulated with 0.1µg/ml CpG or 0.1µg/ml R848 in an end volume of 200µl. Control co-cultures contained DC only, TC only, DC-TC or DC-TC with OVA peptide. Cells were co-cultured in RPMI 1640 medium (PAA

Laboratories, Pasing, Austria), supplemented with 5% FCS, 2mM L-Glutamine, 0.1mM nonessential amino acids, 50µg/ml Penn/Strep (all from PAA), 50 µM β-mercaptoethanol (Sigma-Aldrich, Deisenhofen, Germany). On the third day of co-culture 3H-Thymidine was added (0.5µCi/well) and after an overnight culture (max. 16h) plates were frozen at -20°C prior to analysis. For this cellular DNA was transferred onto a filter membrane that enriched solely intact genomic DNA (Tomtec Harvester 96 Mach II Cell Harvester with AutoTrap 24). The filter membrane was dried and the amount of membrane-bound radioactivity was counted using a Beta-counter.

#### 4.3.8. Cell apoptosis/necrosis detection

To distinguish between apoptotic and necrotic cells within a sample, a set of two reagents was applied. 7-AAD (7-Actinoaminomycin D) is a dye that detects necrotic/late apoptotic cells, as it enters cells with a damaged cell membrane and intercalates DNA resulting in a highly fluorescent adduct. AnnexinV is used to detect apoptotic cells since it binds to phosphatidylserine, a marker of apoptosis exposed on the outer side of the cellular membrane.

Samples were first stained according to the cellular markers (e.g. CD11c) and then washed with FACS buffer. Subsequently 7-AAD (2.5 µl / 50 µl HBSS) and AnnexinV (0.3 µl / 50µl HBSS) were added and samples were incubated for 15min at RT in the dark. Then, samples were washed with HBSS buffer and placed on ice prior to measurement (samples had to be analysed within 60min after staining).

Alternatively, samples were treated with another live/dead agent, namely fixable viability dye (Thermo Fisher Scientific), which irreversibly stains dead cells. Fluorescently reactive dye reacts with amines of a dead cell intracellularly and thus allows its detection by the means of flow cytometry.

#### 4.3.9. Cytotoxicity test

To assay metabolic activity of the cell, tetrazolium substrate was added, which is reduced to a chromogenic formazan product by mitochondrial NADPH-dependent oxidoreductase, correlating with the metabolic activity of the cells. The reaction was stopped by addition of an organic solvent, and the concentration of solubilized formazan was detected spectrophotometrically in an ELISA reader according to the protocol provided by manufacturer (Promega, Madison, WI, USA).

## 4.4. Nanoparticle experiments

Several nanoparticle formulations were used for the uptake experiments employing dendritic cells.

### 4.4.1. Adsorption of mouse native serum onto Dextran-Coated Colloidal Superparamagnetic Nanoparticles

Blood from mice was obtained using the orbital sinus blood collection procedure. Blood samples were collected in 1.1ml Z Gel micro tubes (Sarstedt) and spun down at 10000xg for 5 min, in order to isolate the serum, which was afterwards stored at -20°C until use. Prior to co-incubation with cells, NPs were incubated with medium, native serum or heat-inactivated native serum ( $5 \times 10^{11}$  NP in the volume of 2  $\mu$ l + 18  $\mu$ l medium/serum) for 30 min at 37°C. After 30min of incubation at 37°C, beads were applied to the culture without prior washing to prevent disruption of corona (especially the soft biocorona), so that our setting resemble the physiological scenario.

### 4.4.2. Cellular Binding and Uptake of Dextran-Coated Colloidal Superparamagnetic Nanoparticles

BM-DC ( $3 \times 10^5$ / 180 $\mu$ l) derived from C57BL/6 or CD11b<sup>-/-</sup> (B6.129S4-Itgamtm1Myd/J) mice were added NP-suspension (20  $\mu$ l;  $5 \times 10^{11}$  NP per samples) in a 96-well plate, flat bottom plate and incubated for the indicated periods of time at 37°C. Control co-cultures were carried out at 4°C. For the blocking experiments, CD11b was blocked on the surface of the BMDC using anti-mouse CD11b Ab (clone M1/70, BioLegend). Afterwards, cells were stained for surface lineage markers, and were analysed by either flow cytometry or confocal laser scanning microscopy (see 4.4.4. and 4.4.5.).

### 4.4.3. Cellular Binding and Uptake of FITC-Dextran

BM-DC or splenic DC ( $3 \times 10^5$ / 180 $\mu$ l) derived from C57BL/6 or CD11b<sup>-/-</sup> (B6.129S4-Itgamtm1Myd/J) mice were co-incubated with FITC-dextran (1 $\mu$ g/ml, SIGMA-ALDRICH) in a 96-well plate, flat bottom plate and its engulfment was assessed at different time points (10, 30 and 60 min at 37°C). Control co-cultures were carried out at 4°C. For the blocking experiments, mannose receptor was blocked on the surface of the DC using mannan (0.2 $\mu$ g/ml). Afterwards, cells were stained for surface lineage markers, and were analysed by either flow cytometry (see 4.4.4.).

#### 4.4.4. Flow Cytometric analysis of NP uptake

BM-DC were washed in FACS buffer (PBS, 1% FCS, 0.5mM EDTA), and were stained with anti-mouse CD11c antibodies (labelled with PE-Cy7 or APC, clone N418, eBioscience, SanDiego, CA), PE-labelled anti-CD11b (M1/70, eBioscience), FITC-labelled anti-CD86 (GL1, eBioscience). Cy5- labelled NPs were detected in the APC channel. Expression intensities were assessed by flow cytometry (LSR II) and analysed using FACS Diva (both from BD Biosciences).

#### 4.4.5. Confocal Laser Scanning Microscopy (CLSM)

NPs were pre-incubated in parallel assays with medium, native or native-heat-inactivated serum (7 $\mu$ l NPs + 63 $\mu$ l medium/ native serum or HI native serum, 30min pre-incubation at 37°C). The mixture was added to BM-DC (2.5\*10<sup>5</sup>/500 $\mu$ L) derived from C57BL/6 or CD11b<sup>-/-</sup> (B6.129S4-Itgamtm1Myd/J) mice and samples were cultured for 4h in 24-well plates. Subsequently cells were transferred onto 8-chamber slides (Lab-Tek® Chambered # 1.0 Borosilicate Cover glass System, Nunc™) and nuclei were stained with Hoechst 33342 for 1 h under gentle shaking in the dark. After two washing steps with PBS, the plasma membrane was counter-stained with Cell Mask Orange (Life Technologies, Carlsbad, CA) as recommended by the manufacturer, and samples were immediately analysed using a TCS SP5 Confocal Microscope equipped with 40x/1.3oil objective at the Microscopy Core Facility of the IMB, Mainz, Germany. Hoechst dye was excited at 405 nm, NP at 635 nm, and Cell Mask Orange at 543 nm.

#### 4.4.6. *In vitro* T cell-proliferation assays

BM-DC or splenic DC (seeded in triplicates in serial dilutions, starting with 5\*10<sup>4</sup> cells/100 $\mu$ l) were treated with soluble OVA peptide or SIINFEKL at a final concentration of 0.1 $\mu$ g/ml. The incubation with an antigen was finalized with a set of two washes. Next, cells were stimulated with CpG (0.1 $\mu$ g/ml) overnight in a volume of 100 $\mu$ l. The day after CD4<sup>+</sup> or CD8<sup>+</sup> T cells were isolated from a spleen of an OT-II or an OT-I mouse (CD4<sup>+</sup>/CD8<sup>+</sup> T cell isolation kit, Miltanyi Biotec) and CFSE-stained. T cells (10<sup>5</sup> /100 $\mu$ l) were added to pre-treated BM-DC or splenic DC. After 4-5 days of co-culture cells were harvested, stained with anti-mouse-CD4-PE (Clone GK1.5, Biolegend) and T cells proliferation was analysed by flow cytometry (LSR II).

Alternatively to CFSE staining, after three days of co-culture supernatants were collected for the CBA analysis and cells were added 3H-Thymidine (0.5 $\mu$ Ci/well). After an overnight culture (max. 16h) plates were frozen at -20°C prior to analysis of the genomically integrated radioactivity on a Beta-counter.

## 4.5. Immunological methods.

### 4.5.1. Magnetic cell sorting

Specific target cells can be isolated from a mixture of different cell populations by immunomagnetic sorting, using e.g. the MACS technique. For this, target cells are incubated with ferromagnetic microbeads that are labelled with antibodies specific for molecules on the surface of the cells. The heterogeneous cell suspension is loaded onto a magnetic column, and bead-negative cells were washed off. After removing the column from the magnetic field, the purified fraction of target cells was eluted. The MACS method was used in accordance with the manufactures guidelines for isolation of CD4<sup>+</sup>/CD8<sup>+</sup> T cells, and for DC negative isolation.

### 4.5.2. Fluorescence activated cell sorting (FACS)

Flow cytometry is a technique to count and characterize single cells within a cell suspension in a stream of fluid that passes an electronic detection unit. A beam of laser light of a single wavelength is directed onto the hydro dynamically-focussed stream of the cell suspension often stained with fluorescence-labelled antibodies. Each cell with a diameter of 0.2-150 µm passes through the beam and scatters the light. Fluorescent dyes attached to or within the cell due to detection of proteins with fluorescence-labelled antibodies may be excited to emit light at a longer wavelength than the original light source. The combination of scattered and fluorescent light is analysed by detectors. The forward scatter (FSC) correlates with the cell volume and the sideward scatter (SSC) with the granularity of the cell.

For FACS analysis, cells were washed with FACS buffer (0.5% FCS, Pen/Step, 2mM EDTA in PBS), and free Fc-receptors were blocked with anti-mouse Fc-blocking antibody 2.4G2 (anti-CD16/32; ≤1.0 µg per 10<sup>6</sup> cells in 100 µl volume) for 15 min at RT. Then cells were incubated in a volume of 100µl with fluorescently labelled antibodies (0.5-10 µg/ml final conc., depending on the antibody) for an additional 15 min at RT. Afterwards cells were washed with FACS buffer and fixed with PFA (Paraformaldehyde, 0.5-4% final dilution in PBS)

For intracellular detection of Foxp3<sup>+</sup>, spleen cells were first stained with Cy5-PE-conjugated anti-CD8a, FITC-conjugated anti-CD25, and APC-conjugated anti-CD4. Subsequently, cells were washed with ice-cold FACS buffer and fixed/permeabilized with fixation / permeabilization buffer (FoxP3 staining buffer set, Miltenyi Biotec). Permeabilized cells were then intracellularly stained with anti-FoxP3-PE conjugated Ab (clone 3G3, Miltenyi Biotec) or the corresponding IgG1-PE conjugated control Ab (Miltenyi Biotec). After 30min of incubation

at 4°C cells were washed with permeabilization buffer and fixed with PFA (paraformaldehyde, 0.5-4% final dilution in PBS) prior to FACS analysis.

### 4.5.3. Cytokine measurement

The cytokine production by BMDC was determined in cell culture supernatants derived from CD11c<sup>+</sup> DC or co-cultures of BM-DC and CD4<sup>+</sup> T cells using a cytometric bead array (CBA Inflammation; BD Pharmingen). One or more bead populations (bead) with discrete and distinct fluorescence intensities are used to simultaneously detect multiple cytokines in a small sample volume. The beads were captured and cytokines quantified. Each capture bead in the array has a unique fluorescence intensity and is coated with a capture antibody specific for a single cytokine. A combination of different beads is mixed with a sample or standard and afterwards with detection antibodies that are conjugated to a reporter molecule (PE). Following incubation and subsequent washing, the samples are acquired on a flow cytometer.

### 4.5.4. Immunohistochemical staining

The preparation of the frozen tissue sections was kindly carried out by Claudia Braun at the Histology Unit of the Department of Dermatology (University Medical Centre of the Johannes Gutenberg University Mainz) and the immunohistological staining were performed by Alexei Niloalev (Institute for Molecular Medicine, Mainz)

Frozen section slides, stored at -80°C, were thawed for 15 min at RT and then placed into a humidity chamber. Tissue sections were fixed with 4% PFA fixative (added dropwise onto the slide and incubated for 20 min at RT) and after fixation were washed with water and placed into a glass chamber with PBS. To block endogenous peroxidase activity, tissue slides were subsequently incubated in 3% H<sub>2</sub>O<sub>2</sub> solution in methanol (100%) at RT for 20 min under shaking. Slides were rinsed with 1xPBS and left to dry briefly (the back of the slides was rinsed with water; it is important that the section does not dry out). The tissue section was circled with a marker (VWR lab marker fine tip, permanent, and alcohol/waterproof) so that the solutions used for further incubations would stay within the area of the section. Slides were rinsed once with 1xPBS, placed into the humidity chamber. For intracellular staining slides were incubated with permeabilization buffer for 10 min and then rinsed with 1xPBS. Slides were then rinsed in TBST (Tris Buffer Saline, 0.1% Tween-20), dried briefly and placed in the humidity chamber, where Avidin-blocking solution (Vector Kit SP-2001) was added dropwise onto the sections and incubated for 15 min. Slides were washed with aqua dest., rinsed in the glass chamber with TBST, dried briefly and placed back in the humidity chamber, where 2% BSA-TBST solution

was applied dropwise onto the section. After removal of the 2% BSA-TBST solution, Biotin-blocking solution (Vector Kit SP-2001) was added and the section was washed with TBST+2% BSA after 15 min of incubation. Subsequently, third blocking agent, Roti-ImmunoBlock (ROTH Art. T144.1 ; 1:10 in TBST+2% BSA), was applied and after 15 min 1° Antibody was applied and left for an overnight incubation at 4°C. After overnight incubation slides were washed with 3xTBST for 5 min shaking and 2° Antibody (Biotin-conjugated) was applied (1:1000 in TBST). After 30 min of incubation at RT in the humidity chamber, slides were washed three times in TBS for 5 min and Streptavidin-HRP (1:100 in TBS) was added for a 30 min incubation (25-100 µl solution per section). Afterwards fluorochrome (e.i. Cyanine 3 Tyramide Reagent FP1046, PerkinElmer 1:50 or Fluorescein Tyramide Reagent FP1098-FITC 1:50 PerkinElmer; double the concentration of the Streptavidin-HRP) was added and washed briefly first with water and then 3x/2 min with TBS after 5 min of incubation. After slides dried, they were further stained with DAPI or Höchst (1: 10 000) for 5 min. Finally, the slides were covered with a cover slip (25x50 mm #1 Menzel-Gläser) with Mounting Medium (Vector H-1000). Alternatively, a slip cover solution with DAPI was used (Vectrashield with DAPI, H-1200 Vector Laboratories).

If the section was stained with another antibody using amplification kit, after the fluorochrome was coupled during the first staining, all the blocking steps were repeated and the slide was subsequently stained with another antibody as described above. While staining without the amplification kit for the second time, the other antibody was added directly to the slide, without prior blocking steps and incubated for 2 h at RT. Antibodies used for the staining are listed in table 16 below. Stained sections were visualized using a fluorescence microscope (Olympus IX81).

*Table 16. List of antibodies used for the immunohistochemical staining of the frozen B16-OVA melanoma sections.*

1° Antibody	2° Antibody
Rat anti-mouse CD4 (RM4-5) BD Pharminogen CAT-553043 (1:50)	Biotin Goat anti-Rat Ig, BD Pharminogen #554014 (1:1000)
Rabbit anti-mouse CD8 (Ep115OY), Abcam #52854 (1:300)	Biotinylated anti-Rabbit IgG (H+L), affinity purified made in goat (VECTOR, BA-100) (1:1000)

Rat anti-mouse FoxP3 (FJK-16s), eBioscience #14-5773-82 (1:20)	Biotin Goat anti-Rat Ig, BD Pharminogen #554014 (1:1000)
Rat anti-mouse F4/80 (BM8.), eBioscience #14-4801-81 (1:1000)	Biotin Goat anti-Rat Ig, BD Pharminogen #554014 (1:1000)
Rat anti-mouse Panendothelial Cell Antigen-Alexa Fluor 488 (MECA-32), Biolegend #120502 (1:200)	-
Rat anti-mouse Gr-1 (RB6-8C5) Alexa Fluor 488, Biolegend #108417 (1:100)	-
Hamster anti-mouse CD3e, eBioscience #14-0031-82 (1:100)	Goat anti-Hamster-Cy3, Jackson #127-165-099 (1:200)
Hamster anti-mouse CD11c, BD Pharminogen #550283 (1:200)	Goat anti-Hamster-Cy3, Jackson #127-165-099 (1:200)
Rat anti-mouse I-A/I-E (MHC-II) (M5/114.15.2) Alexa Fluor 647, Biolegend (1:100)	-
Rat anti-mouse CD206- Biotin, AbD Serotec, MCA2235B	-

## 4.6. Real time quantitative PCR (qPCR)

Real time PCR analysis was applied to analyse the expression of the candidate genes on the mRNA level. This PCR based method, monitors amplification of the target DNA, after it was reverse transcribed from RNA, using a non-specific fluorescent dye (SYBRgreen) that intercalates within the double-stranded DNA.

The RNA was purified from the samples (cultured cells, e.g. splenic DC) using RNasy Plus Mini Kit (QIAGEN) containing gDNA Eliminator Spin Columns according to the manufacturer's protocol. Purified RNA was then reverse transcribed into cDNA using the iScript™ cDNA Synthesis Kit (BIO-RAD) (remaining RNA was stored at -80°C). Synthesised cDNA was stored at -20°C prior to qPCR analysis. The real time PCR reactions were prepared using Absolute SYBR Green ROX MIX and run in a 7300 Real Time PCR System qPCR cycler

(for details see Table 17). Subsequently, the results were evaluated using 7300 System Software. The results were analysed according to the Schmittgen&Livak method (Livak & Schmittgen, 2001; Schmittgen & Livak, 2008).

Primers used for the detection of given mRNA are listed in Table 18 below.

*Table 17. Reverse transcription and qPCR reaction protocol.*

<b>Reaction</b>	<b>Protocol</b>
<b>Reverse transcription</b>	1 x (25°C/300s) 1 x (42°C/1:00h) 1 x (85°C/300s)
<b>qPCR</b>	1 x (95°C/600s) 40 x (95°C/15s - 60°C/60s - 95°C/15s- 60°C/60s - 95°C/15s- 60°C/60s - 95°C/15s )

*Table 18. Primers used for the qPCR reactions (s-sense, as-antisense).*

<b>Target gene</b>	<b>Primer sequence</b>
<b>mSOCS2</b>	s: 5'-AACCTGCGGATTGAGTAC-3' as: 5'-GGTACAGGTGAACAGTC-3'
<b>mSOCS4</b>	s: 5'-TTCCCACCTCGCTCAGAT-3' as: 5'-GCTGGCCATTGGTATGT-3'
<b>IL-6</b>	s: 5'-CCGGAGAGGAGACTTCACAG-3' as: 5'-CAGAATTGCCATTGCACAAC-3'
<b>IL-10</b>	s: 5'-CCAAGCCTTATCGGAAATGA-3' as: 5'-TTTTCACAGGGGAGAAATCG-3'
<b>IL-12</b>	s: 5'-CATCTGCTCCACAAGAA-3' as: 5'-CATCTGCTGCTCCACAAGAA-3'

<b>TNF-<math>\alpha</math></b>	s: 5'-CCACCACGCTCTTCTGTCTA-3' as: 5'-AGGGTCTGGGCCATAGAACT-3'
<b>mSTAT1</b>	s: 5'-TGGTGAAATTGCAAGAGCTG-3' as: 5'-TGTGTGCGTACCCAAGATGT-3'
<b>B2M</b>	s: 5'-CGGCCTGTATGCTATCCAGA-3' as: 5'-GGGTGAATTCAGTGTGAGCC-3'
<b>UBC</b>	s: 5'-GTCTGCTGTGTGAGGACTGC-3' as: 5'-CAGGGTGGACTCTTTCTGGA-3'

#### 4.7. In vivo tumour model (B16-OVA Melanoma)

B16-OVA cells were grown in T75 flasks (Greiner Bio-One) with 20ml of RPMI medium with 10% FCS, 100U/mL penicillin/streptomycin, 2mM glutamine, 10mM HEPES, 1mM sodium pyruvate, 50 $\mu$ M  $\beta$ -mercaptoethanol and G418 (300 $\mu$ g/ml). OVA expression was analysed by FACS before injection.

Mice (C57BL/6 and CD11b<sup>-/-</sup> on C57BL/6 background) were injected s.c. with B16/OVA cells (Kedl et al., 2001); 5x10<sup>4</sup> in 50  $\mu$ l PBS. Tumour growth was monitored every other day with a caliper, and the tumour size was calculated as the product of three orthogonal diameters (a: longest diameter, b: orthogonal width, c: depth). The following formula was used to calculate tumour volume: a\*b\*c\*3.14/6. Mice were sacrificed when the tumour size exceeded 800 mm<sup>3</sup> or when ulceration of the tumours was observed. Tumours and spleens were removed for subsequent analysis. Isolated tumours were directly used for FACS analysis or placed in a tube in liquid nitrogen (afterwards stored at -80°C) prior to subsequent immunofluorescence staining and confocal microscopy of the frozen tumour sections.

#### 4.8. In vivo T Cell Proliferation

Carboxyfluorescein diacetate succinimidyl ester (CFSE) is an amine-reactive reagent, which diffuses through the cell membrane. CFSE becomes fluorescent upon cleavage of its acetate groups by esterase in the cytoplasm. Due to its amine-reactivity, the succinimidyl ester group binds to amine-containing residues of intracellular proteins, which are passed over to daughter

cells. As CFSE is halved between daughter cells during cellular division, CFSE labelling can be used to monitor proliferation of lymphocytes in vitro and in vivo by FACS (Lyons, 2000).

To assess the T cell proliferation in vivo, splenocytes derived from mice with transgenic T cell receptor (OT-IxCD45.1, OT-IIxCD45.1) were labelled with 0.5  $\mu$ M CFSE for 10 min. CFSE-labelled splenocytes ( $10^7$  in 200  $\mu$ l PBS) were transferred i.v. (tail vein) into , CD11b<sup>-/-</sup>, C57BL/6, CD18 <sup>$\Delta$ CD11c</sup> or CD18<sup>fl/fl</sup> mice. After 48 h, 4 $\mu$ g of OVA and 4 $\mu$ g of CpG ODN1826 were injected i.v. as indicated. Control groups of mice were injected with PBS or 4 $\mu$ g of OVA protein only. Four days later, spleens and peripheral LN were removed, and cell suspensions were analysed for proliferation of CFSE-labelled T cells by flow cytometry.

Part of the splenic cell suspension was used for the T cell restimulation assay. Isolated splenocytes, derived from the treated mice, were seeded in triplicates onto the 96-well F-bottom plate ( $5 \times 10^5$  cells/200 $\mu$ l complete medium) and added antigen in serial dilutions ( $10 > 5 > 2.5 > 0$   $\mu$ M; SIINFEKL or OVA-peptide). Three days later culture supernatants were collected for the CBA analysis and cells were added 3H-Thymidine (0.5 $\mu$ Ci/well). After an overnight culture (max. 16h) plates were frozen at -20°C prior to analysis of the genomically integrated radioactivity on a Beta-counter.

## 4.9. Statistical analysis

Statistical significance was determined using the unpaired Students-t-test with GraphPad Prism 5 Software. Results are expressed as mean $\pm$ SEM; statistically significant differences are designated as \* $p \leq 0.05$ , \*\* $p \leq 0.005$ , and \*\*\* $p \leq 0.001$ .

## References

- Abram, C. L., Roberge, G. L., Hu, Y., & Lowell, C. A. (2014). Comparative analysis of the efficiency and specificity of myeloid-Cre deleting strains using ROSA-EYFP reporter mice. *J Immunol Methods*, *408*, 89-100. doi:10.1016/j.jim.2014.05.009
- Acuto, O. (2003). T cell-dendritic cell interaction in vivo: random encounters favor development of long-lasting ties. *Sci STKE*, *2003*(192), PE28. doi:10.1126/stke.2003.192.pe28
- Ahn, G. O., Tseng, D., Liao, C. H., Dorie, M. J., Czechowicz, A., & Brown, J. M. (2010). Inhibition of Mac-1 (CD11b/CD18) enhances tumor response to radiation by reducing myeloid cell recruitment. *Proc Natl Acad Sci U S A*, *107*(18), 8363-8368. doi:10.1073/pnas.0911378107
- Akaishi, T., & Nakashima, I. (2017). Efficiency of antibody therapy in demyelinating diseases. *Int Immunol*, *29*(7), 327-335. doi:10.1093/intimm/dxx037
- Akira, S., & Takeda, K. (2004). Toll-like receptor signalling. *Nat Rev Immunol*, *4*(7), 499-511. doi:10.1038/nri1391
- Alloatti, A., Rookhuizen, D. C., Joannas, L., Carpier, J. M., Iborra, S., Magalhaes, J. G., . . . Amigorena, S. (2017). Critical role for Sec22b-dependent antigen cross-presentation in antitumor immunity. *J Exp Med*, *214*(8), 2231-2241. doi:10.1084/jem.20170229
- Alves, C. H., Ober-Blobaum, J. L., Brouwers-Haspels, I., Asmawidjaja, P. S., Mus, A. M., Razawy, W., . . . Lubberts, E. (2015). Dendritic Cell-Specific Deletion of beta-Catenin Results in Fewer Regulatory T-Cells without Exacerbating Autoimmune Collagen-Induced Arthritis. *PLoS One*, *10*(11), e0142972. doi:10.1371/journal.pone.0142972
- Anderson, M. E., & Siahahaan, T. J. (2003). Targeting ICAM-1/LFA-1 interaction for controlling autoimmune diseases: designing peptide and small molecule inhibitors. *Peptides*, *24*(3), 487-501.
- Anikeeva, N., Somersalo, K., Sims, T. N., Thomas, V. K., Dustin, M. L., & Sykulev, Y. (2005). Distinct role of lymphocyte function-associated antigen-1 in mediating effective cytolytic activity by cytotoxic T lymphocytes. *Proc Natl Acad Sci U S A*, *102*(18), 6437-6442. doi:10.1073/pnas.0502467102
- Au-Yeung, N., Mandhana, R., & Horvath, C. M. (2013). Transcriptional regulation by STAT1 and STAT2 in the interferon JAK-STAT pathway. *JAKSTAT*, *2*(3), e23931. doi:10.4161/jkst.23931
- Autenrieth, S. E., & Autenrieth, I. B. (2009). Variable antigen uptake due to different expression of the macrophage mannose receptor by dendritic cells in various inbred mouse strains. *Immunology*, *127*(4), 523-529. doi:10.1111/j.1365-2567.2008.02960.x
- Azad, A. K., Rajaram, M. V., & Schlesinger, L. S. (2014). Exploitation of the Macrophage Mannose Receptor (CD206) in Infectious Disease Diagnostics and Therapeutics. *J Cytol Mol Biol*, *1*(1). doi:10.13188/2325-4653.1000003
- Aziz, M. H., Cui, K., Das, M., Brown, K. E., Ardell, C. L., Febbraio, M., . . . Yakubenko, V. P. (2017). The Upregulation of Integrin alphaDbeta2 (CD11d/CD18) on Inflammatory Macrophages Promotes Macrophage Retention in Vascular Lesions and Development of Atherosclerosis. *J Immunol*, *198*(12), 4855-4867. doi:10.4049/jimmunol.1602175

- Bai, Y., Qian, C., Qian, L., Ma, F., Hou, J., Chen, Y., . . . Cao, X. (2012). Integrin CD11b negatively regulates TLR9-triggered dendritic cell cross-priming by upregulating microRNA-146a. *J Immunol*, *188*(11), 5293-5302. doi:10.4049/jimmunol.1102371
- Balkow, S., Heinz, S., Schmidbauer, P., Kolanus, W., Holzmann, B., Grabbe, S., & Laschinger, M. (2010). LFA-1 activity state on dendritic cells regulates contact duration with T cells and promotes T-cell priming. *Blood*, *116*(11), 1885-1894. doi:10.1182/blood-2009-05-224428
- Balkow, S., Krux, F., Loser, K., Becker, J. U., Grabbe, S., & Dittmer, U. (2007). Friend retrovirus infection of myeloid dendritic cells impairs maturation, prolongs contact to naive T cells, and favors expansion of regulatory T cells. *Blood*, *110*(12), 3949-3958. doi:10.1182/blood-2007-05-092189
- Barczyk, M., Carracedo, S., & Gullberg, D. (2010). Integrins. *Cell Tissue Res*, *339*(1), 269-280. doi:10.1007/s00441-009-0834-6
- Barlow, S. C., Collins, R. G., Ball, N. J., Weaver, C. T., Schoeb, T. R., & Bullard, D. C. (2003). Psoriasisform dermatitis susceptibility in Itgb2(tm1Bay) PL/J mice requires low-level CD18 expression and at least two additional loci for progression to severe disease. *Am J Pathol*, *163*(1), 197-202. doi:10.1016/S0002-9440(10)63643-7
- Bechard, D., Scherpereel, A., Hammad, H., Gentina, T., Tsicopoulos, A., Aumercier, M., . . . Lassalle, P. (2001). Human endothelial-cell specific molecule-1 binds directly to the integrin CD11a/CD18 (LFA-1) and blocks binding to intercellular adhesion molecule-1. *J Immunol*, *167*(6), 3099-3106.
- Bedoui, S., Whitney, P. G., Waithman, J., Eidsmo, L., Wakim, L., Caminschi, I., . . . Heath, W. R. (2009). Cross-presentation of viral and self antigens by skin-derived CD103+ dendritic cells. *Nat Immunol*, *10*(5), 488-495. doi:10.1038/ni.1724
- Berends, M. A., Driessen, R. J., Langewouters, A. M., Boezeman, J. B., Van De Kerkhof, P. C., & De Jong, E. M. (2007). Etanercept and efalizumab treatment for high-need psoriasis. Effects and side effects in a prospective cohort study in outpatient clinical practice. *J Dermatolog Treat*, *18*(2), 76-83. doi:10.1080/09546630601121086
- Bian, J., Liu, R., Fan, T., Liao, L., Wang, S., Geng, W., . . . Ruan, Q. (2018). miR-340 Alleviates Psoriasis in Mice through Direct Targeting of IL-17A. *J Immunol*. doi:10.4049/jimmunol.1800189
- Bose, T. O., Pham, Q. M., Jellison, E. R., Mouries, J., Ballantyne, C. M., & Lefrancois, L. (2013). CD11a regulates effector CD8 T cell differentiation and central memory development in response to infection with *Listeria monocytogenes*. *Infect Immun*, *81*(4), 1140-1151. doi:10.1128/IAI.00749-12
- Buerger, A., Rozhitskaya, O., Sherwood, M. C., Dorfman, A. L., Bisping, E., Abel, E. D., . . . Jay, P. Y. (2006). Dilated cardiomyopathy resulting from high-level myocardial expression of Cre-recombinase. *J Card Fail*, *12*(5), 392-398. doi:10.1016/j.cardfail.2006.03.002
- Bullard, D. C., Hu, X., Schoeb, T. R., Axtell, R. C., Raman, C., & Barnum, S. R. (2005). Critical requirement of CD11b (Mac-1) on T cells and accessory cells for development of experimental autoimmune encephalomyelitis. *J Immunol*, *175*(10), 6327-6333.
- Cao, L. Y., Soler, D. C., Debanne, S. M., Grozdev, I., Rodriguez, M. E., Feig, R. L., . . . Korman, N. J. (2013). Psoriasis and cardiovascular risk factors: increased serum myeloperoxidase and corresponding immunocellular overexpression by Cd11b(+) CD68(+) macrophages in skin lesions. *Am J Transl Res*, *6*(1), 16-27.

- Capecchi, M. R. (1989). Altering the genome by homologous recombination. *Science*, 244(4910), 1288-1292.
- Caton, M. L., Smith-Raska, M. R., & Reizis, B. (2007). Notch-RBP-J signaling controls the homeostasis of CD8- dendritic cells in the spleen. *J Exp Med*, 204(7), 1653-1664. doi:10.1084/jem.20062648
- Celik, E., Faridi, M. H., Kumar, V., Deep, S., Moy, V. T., & Gupta, V. (2013). Agonist leukadherin-1 increases CD11b/CD18-dependent adhesion via membrane tethers. *Biophys J*, 105(11), 2517-2527. doi:10.1016/j.bpj.2013.10.020
- Chang, J. T., Wherry, E. J., & Goldrath, A. W. (2014). Molecular regulation of effector and memory T cell differentiation. *Nat Immunol*, 15(12), 1104-1115. doi:10.1038/ni.3031
- Chen, J., Salas, A., & Springer, T. A. (2003). Bistable regulation of integrin adhesiveness by a bipolar metal ion cluster. *Nat Struct Biol*, 10(12), 995-1001. doi:10.1038/nsb1011
- Chen, L., & Flies, D. B. (2013). Molecular mechanisms of T cell co-stimulation and co-inhibition. *Nat Rev Immunol*, 13(4), 227-242. doi:10.1038/nri3405
- Choi, J., Leyton, L., & Nham, S. U. (2005). Characterization of alphaX I-domain binding to Thy-1. *Biochem Biophys Res Commun*, 331(2), 557-561. doi:10.1016/j.bbrc.2005.04.006
- Choi, J. W., Ku, Y., Yoo, B. W., Kim, J. A., Lee, D. S., Chai, Y. J., . . . Kim, H. C. (2017). White blood cell differential count of maturation stages in bone marrow smear using dual-stage convolutional neural networks. *PLoS One*, 12(12), e0189259. doi:10.1371/journal.pone.0189259
- Chouhan, B. S., Kapyla, J., Denessiouk, K., Denesyuk, A., Heino, J., & Johnson, M. S. (2014). Early chordate origin of the vertebrate integrin alphaI domains. *PLoS One*, 9(11), e112064. doi:10.1371/journal.pone.0112064
- Comi, M., Amodio, G., & Gregori, S. (2018). Interleukin-10-Producing DC-10 Is a Unique Tool to Promote Tolerance Via Antigen-Specific T Regulatory Type 1 Cells. *Front Immunol*, 9, 682. doi:10.3389/fimmu.2018.00682
- Commisso, C., Davidson, S. M., Soydaner-Azeloglu, R. G., Parker, S. J., Kamphorst, J. J., Hackett, S., . . . Bar-Sagi, D. (2013). Macropinocytosis of protein is an amino acid supply route in Ras-transformed cells. *Nature*, 497(7451), 633-637. doi:10.1038/nature12138
- Cooper, M. D., & Alder, M. N. (2006). The evolution of adaptive immune systems. *Cell*, 124(4), 815-822. doi:10.1016/j.cell.2006.02.001
- Coxon, A., Rieu, P., Barkalow, F. J., Askari, S., Sharpe, A. H., von Andrian, U. H., . . . Mayadas, T. N. (1996). A novel role for the beta 2 integrin CD11b/CD18 in neutrophil apoptosis: a homeostatic mechanism in inflammation. *Immunity*, 5(6), 653-666.
- D'Agata, I. D., Paradis, K., Chad, Z., Bonny, Y., & Seidman, E. (1996). Leucocyte adhesion deficiency presenting as a chronic ileocolitis. *Gut*, 39(4), 605-608.
- Davies, L. C., Jenkins, S. J., Allen, J. E., & Taylor, P. R. (2013). Tissue-resident macrophages. *Nat Immunol*, 14(10), 986-995. doi:10.1038/ni.2705
- De Rose, D. U., Giliani, S., Notarangelo, L. D., Lougaris, V., Lanfranchi, A., Moratto, D., . . . Badolato, R. (2018). Long term outcome of eight patients with type 1 Leukocyte Adhesion Deficiency (LAD-1): Not only infections, but high risk of autoimmune complications. *Clin Immunol*, 191, 75-80. doi:10.1016/j.clim.2018.03.005

- Didierlaurent, A. M., Collignon, C., Bourguignon, P., Wouters, S., Fierens, K., Fochesato, M., . . . Morel, S. (2014). Enhancement of adaptive immunity by the human vaccine adjuvant AS01 depends on activated dendritic cells. *J Immunol*, *193*(4), 1920-1930. doi:10.4049/jimmunol.1400948
- Dinarello, C. A. (2011). Interleukin-1 in the pathogenesis and treatment of inflammatory diseases. *Blood*, *117*(14), 3720-3732. doi:10.1182/blood-2010-07-273417
- Ding, C., Ma, Y., Chen, X., Liu, M., Cai, Y., Hu, X., . . . Yan, J. (2013). Integrin CD11b negatively regulates BCR signalling to maintain autoreactive B cell tolerance. *Nat Commun*, *4*, 2813. doi:10.1038/ncomms3813
- dos Santos, T., Varela, J., Lynch, I., Salvati, A., & Dawson, K. A. (2011). Effects of transport inhibitors on the cellular uptake of carboxylated polystyrene nanoparticles in different cell lines. *PLoS One*, *6*(9), e24438. doi:10.1371/journal.pone.0024438
- Drutman, S. B., Kendall, J. C., & Trombetta, E. S. (2012). Inflammatory spleen monocytes can upregulate CD11c expression without converting into dendritic cells. *J Immunol*, *188*(8), 3603-3610. doi:10.4049/jimmunol.1102741
- Dudziak, D., Kamphorst, A. O., Heidkamp, G. F., Buchholz, V. R., Trumpheller, C., Yamazaki, S., . . . Nussenzweig, M. C. (2007). Differential antigen processing by dendritic cell subsets in vivo. *Science*, *315*(5808), 107-111. doi:10.1126/science.1136080
- Dugger, K. J., Zinn, K. R., Weaver, C., Bullard, D. C., & Barnum, S. R. (2009). Effector and suppressor roles for LFA-1 during the development of experimental autoimmune encephalomyelitis. *J Neuroimmunol*, *206*(1-2), 22-27. doi:10.1016/j.jneuroim.2008.10.006
- Duncan, S. A., Baganizi, D. R., Sahu, R., Singh, S. R., & Dennis, V. A. (2017). SOCS Proteins as Regulators of Inflammatory Responses Induced by Bacterial Infections: A Review. *Front Microbiol*, *8*, 2431. doi:10.3389/fmicb.2017.02431
- Dunn, G. P., Bruce, A. T., Ikeda, H., Old, L. J., & Schreiber, R. D. (2002). Cancer immunoediting: from immunosurveillance to tumor escape. *Nat Immunol*, *3*(11), 991-998. doi:10.1038/ni1102-991
- Dupuy, A. G., & Caron, E. (2008). Integrin-dependent phagocytosis: spreading from microadhesion to new concepts. *J Cell Sci*, *121*(11), 1773-1783. doi:10.1242/jcs.018036
- Edwards, A. D., Diebold, S. S., Slack, E. M., Tomizawa, H., Hemmi, H., Kaisho, T., . . . Reis e Sousa, C. (2003). Toll-like receptor expression in murine DC subsets: lack of TLR7 expression by CD8 alpha+ DC correlates with unresponsiveness to imidazoquinolines. *Eur J Immunol*, *33*(4), 827-833. doi:10.1002/eji.200323797
- Ehreichiou, D., Xiong, Y., Xu, G., Chen, W., Shi, Y., & Zhang, L. (2007). CD11b facilitates the development of peripheral tolerance by suppressing Th17 differentiation. *J Exp Med*, *204*(7), 1519-1524. doi:10.1084/jem.20062292
- Engelhardt, B. (2008). Adhesion and Signalling Molecules Controlling the Extravasation of Leukocytes across the Endothelium. *Transfus Med Hemother*, *35*(2), 73-75. doi:10.1159/000119115
- Enk, A. H., Jonuleit, H., Saloga, J., & Knop, J. (1997). Dendritic cells as mediators of tumor-induced tolerance in metastatic melanoma. *Int J Cancer*, *73*(3), 309-316.

- Fagerholm, S. C., MacPherson, M., James, M. J., Sevier-Guy, C., & Lau, C. S. (2013). The CD11b-integrin (ITGAM) and systemic lupus erythematosus. *Lupus*, 22(7), 657-663. doi:10.1177/0961203313491851
- Fan, Y., Li, L. H., Pan, H. F., Tao, J. H., Sun, Z. Q., & Ye, D. Q. (2011). Association of ITGAM polymorphism with systemic lupus erythematosus: a meta-analysis. *J Eur Acad Dermatol Venereol*, 25(3), 271-275. doi:10.1111/j.1468-3083.2010.03776.x
- Faridi, M. H., Khan, S. Q., Zhao, W., Lee, H. W., Altintas, M. M., Zhang, K., . . . Gupta, V. (2017). CD11b activation suppresses TLR-dependent inflammation and autoimmunity in systemic lupus erythematosus. *J Clin Invest*, 127(4), 1271-1283. doi:10.1172/JCI88442
- Fiorentini, S., Licenziati, S., Alessandri, G., Castelli, F., Caligaris, S., Bonafede, M., . . . Caruso, A. (2001). CD11b expression identifies CD8+CD28+ T lymphocytes with phenotype and function of both naive/memory and effector cells. *J Immunol*, 166(2), 900-907.
- Frobose, H., Ronn, S. G., Heding, P. E., Mendoza, H., Cohen, P., Mandrup-Poulsen, T., & Billestrup, N. (2006). Suppressor of cytokine Signaling-3 inhibits interleukin-1 signaling by targeting the TRAF-6/TAK1 complex. *Mol Endocrinol*, 20(7), 1587-1596. doi:10.1210/me.2005-0301
- Fu, C., Tong, C., Wang, M., Gao, Y., Zhang, Y., Lu, S., . . . Long, M. (2011). Determining beta2-integrin and intercellular adhesion molecule 1 binding kinetics in tumor cell adhesion to leukocytes and endothelial cells by a gas-driven micropipette assay. *J Biol Chem*, 286(40), 34777-34787. doi:10.1074/jbc.M111.281642
- Galon, J., Gauchat, J. F., Mazieres, N., Spagnoli, R., Storkus, W., Lotze, M., . . . Sautes, C. (1996). Soluble Fcgamma receptor type III (FcgammaRIII, CD16) triggers cell activation through interaction with complement receptors. *J Immunol*, 157(3), 1184-1192.
- Garbers, C., & Rose-John, S. (2017). The balance between Treg and TH17 cells: CD11b and interleukin-6. *Eur J Immunol*, 47(4), 629-632. doi:10.1002/eji.201746988
- Ghosh, H. S., Cisse, B., Bunin, A., Lewis, K. L., & Reizis, B. (2010). Continuous expression of the transcription factor e2-2 maintains the cell fate of mature plasmacytoid dendritic cells. *Immunity*, 33(6), 905-916. doi:10.1016/j.immuni.2010.11.023
- Ghosh, S., Chackerian, A. A., Parker, C. M., Ballantyne, C. M., & Behar, S. M. (2006). The LFA-1 adhesion molecule is required for protective immunity during pulmonary Mycobacterium tuberculosis infection. *J Immunol*, 176(8), 4914-4922.
- Ghosn, E. E., Yang, Y., Tung, J., Herzenberg, L. A., & Herzenberg, L. A. (2008). CD11b expression distinguishes sequential stages of peritoneal B-1 development. *Proc Natl Acad Sci U S A*, 105(13), 5195-5200. doi:10.1073/pnas.0712350105
- Giger, U., Boxer, L. A., Simpson, P. J., Lucchesi, B. R., & Todd, R. F., 3rd. (1987). Deficiency of leukocyte surface glycoproteins Mo1, LFA-1, and Leu M5 in a dog with recurrent bacterial infections: an animal model. *Blood*, 69(6), 1622-1630.
- Ginhoux, F., Liu, K., Helft, J., Bogunovic, M., Greter, M., Hashimoto, D., . . . Merad, M. (2009). The origin and development of nonlymphoid tissue CD103+ DCs. *J Exp Med*, 206(13), 3115-3130. doi:10.1084/jem.20091756
- Glawe, J. D., Patrick, D. R., Huang, M., Sharp, C. D., Barlow, S. C., & Kevil, C. G. (2009). Genetic deficiency of Itgb2 or ItgaL prevents autoimmune diabetes through distinctly different mechanisms in NOD/LtJ mice. *Diabetes*, 58(6), 1292-1301. doi:10.2337/db08-0804

- Goenka, S., & Kaplan, M. H. (2011). Transcriptional regulation by STAT6. *Immunol Res*, 50(1), 87-96. doi:10.1007/s12026-011-8205-2
- Goldin, L. R., McMaster, M. L., Rotunno, M., Herman, S. E., Jones, K., Zhu, B., . . . Caporaso, N. E. (2016). Whole exome sequencing in families with CLL detects a variant in Integrin beta 2 associated with disease susceptibility. *Blood*, 128(18), 2261-2263. doi:10.1182/blood-2016-02-697771
- Golic, M. M., Rong, Y. S., Petersen, R. B., Lindquist, S. L., & Golic, K. G. (1997). FLP-mediated DNA mobilization to specific target sites in Drosophila chromosomes. *Nucleic Acids Res*, 25(18), 3665-3671.
- Gower, R. M., Wu, H., Foster, G. A., Devaraj, S., Jialal, I., Ballantyne, C. M., . . . Simon, S. I. (2011). CD11c/CD18 expression is upregulated on blood monocytes during hypertriglyceridemia and enhances adhesion to vascular cell adhesion molecule-1. *Arterioscler Thromb Vasc Biol*, 31(1), 160-166. doi:10.1161/ATVBAHA.110.215434
- Grabbe, S., Varga, G., Beissert, S., Steinert, M., Pendl, G., Seeliger, S., . . . Scharffetter-Kochanek, K. (2002). Beta2 integrins are required for skin homing of primed T cells but not for priming naive T cells. *J Clin Invest*, 109(2), 183-192. doi:10.1172/JCI11703
- Graff, J. C., & Jutila, M. A. (2007). Differential regulation of CD11b on gammadelta T cells and monocytes in response to unripe apple polyphenols. *J Leukoc Biol*, 82(3), 603-607. doi:10.1189/jlb.0207125
- Grela, F., Aumeunier, A., Bardel, E., Van, L. P., Bourgeois, E., Vanoirbeek, J., . . . Thieblemont, N. (2011). The TLR7 agonist R848 alleviates allergic inflammation by targeting invariant NKT cells to produce IFN-gamma. *J Immunol*, 186(1), 284-290. doi:10.4049/jimmunol.1001348
- Guerau-de-Arellano, M., Alroy, J., Bullard, D., & Huber, B. T. (2005). Aggravated Lyme carditis in CD11a<sup>-/-</sup> and CD11c<sup>-/-</sup> mice. *Infect Immun*, 73(11), 7637-7643. doi:10.1128/IAI.73.11.7637-7643.2005
- Guerau-de-Arellano, M., Alroy, J., & Huber, B. T. (2005). Beta2 integrins control the severity of murine Lyme carditis. *Infect Immun*, 73(6), 3242-3250. doi:10.1128/IAI.73.6.3242-3250.2005
- Guerriero, A., Langmuir, P. B., Spain, L. M., & Scott, E. W. (2000). PU.1 is required for myeloid-derived but not lymphoid-derived dendritic cells. *Blood*, 95(3), 879-885.
- Guilliams, M., Ginhoux, F., Jakubzick, C., Naik, S. H., Onai, N., Schraml, B. U., . . . Yona, S. (2014). Dendritic cells, monocytes and macrophages: a unified nomenclature based on ontogeny. *Nat Rev Immunol*, 14(8), 571-578. doi:10.1038/nri3712
- Gultner, S., Kuhlmann, T., Hesse, A., Weber, J. P., Riemer, C., Baier, M., & Hutloff, A. (2010). Reduced Treg frequency in LFA-1-deficient mice allows enhanced T effector differentiation and pathology in EAE. *Eur J Immunol*, 40(12), 3403-3412. doi:10.1002/eji.201040576
- Guo, J., Chen, D., Gao, X., Hu, X., Zhou, Y., Wu, C., . . . Chen, X. (2017). Protein Inhibitor of Activated STAT2 Restricts HCV Replication by Modulating Viral Proteins Degradation. *Viruses*, 9(10). doi:10.3390/v9100285
- Gupta, A. K., & Cherman, A. M. (2006). Efalizumab in the treatment of psoriasis. *J Cutan Med Surg*, 10(2), 57-68. doi:10.2310/7750.2006.00014
- Gutierrez-Martinez, E., Planes, R., Anselmi, G., Reynolds, M., Menezes, S., Adiko, A. C., . . . Guermonprez, P. (2015). Cross-Presentation of Cell-Associated Antigens by MHC

- Class I in Dendritic Cell Subsets. *Front Immunol*, 6, 363. doi:10.3389/fimmu.2015.00363
- Guttman-Yassky, E., Vugmeyster, Y., Lowes, M. A., Chamian, F., Kikuchi, T., Kagen, M., . . . Krueger, J. G. (2008). Blockade of CD11a by efalizumab in psoriasis patients induces a unique state of T-cell hyporesponsiveness. *J Invest Dermatol*, 128(5), 1182-1191. doi:10.1038/jid.2008.4
- Haasken, S., Auger, J. L., & Binstadt, B. A. (2011). Absence of beta2 integrins impairs regulatory T cells and exacerbates CD4+ T cell-dependent autoimmune carditis. *J Immunol*, 187(5), 2702-2710. doi:10.4049/jimmunol.1000967
- Hajishengallis, G., & Moutsopoulos, N. M. (2016). Role of bacteria in leukocyte adhesion deficiency-associated periodontitis. *Microb Pathog*, 94, 21-26. doi:10.1016/j.micpath.2015.09.003
- Halle, S., Halle, O., & Forster, R. (2017). Mechanisms and Dynamics of T Cell-Mediated Cytotoxicity In Vivo. *Trends Immunol*, 38(6), 432-443. doi:10.1016/j.it.2017.04.002
- Hamalainen, S., Solovieva, S., Vehmas, T., Leino-Arjas, P., & Hirvonen, A. (2014). Variations in the TNFalpha gene and their interactions with the IL4R and IL10 genes in relation to hand osteoarthritis. *BMC Musculoskelet Disord*, 15, 311. doi:10.1186/1471-2474-15-311
- Han, C., Jin, J., Xu, S., Liu, H., Li, N., & Cao, X. (2010). Integrin CD11b negatively regulates TLR-triggered inflammatory responses by activating Syk and promoting degradation of MyD88 and TRIF via Cbl-b. *Nat Immunol*, 11(8), 734-742. doi:10.1038/ni.1908
- Hao, L. X., & Sun, L. (2016). Comparative analysis of the expression patterns of eight suppressors of cytokine signaling in tongue sole, *Cynoglossus semilaevis*. *Fish Shellfish Immunol*, 55, 595-601. doi:10.1016/j.fsi.2016.06.034
- Harris, E. S., Weyrich, A. S., & Zimmerman, G. A. (2013). Lessons from rare maladies: leukocyte adhesion deficiency syndromes. *Curr Opin Hematol*, 20(1), 16-25. doi:10.1097/MOH.0b013e32835a0091
- Hartmann, T. N., Grabovsky, V., Wang, W., Desch, P., Rubenzer, G., Wollner, S., . . . Alon, R. (2009). Circulating B-cell chronic lymphocytic leukemia cells display impaired migration to lymph nodes and bone marrow. *Cancer Res*, 69(7), 3121-3130. doi:10.1158/0008-5472.CAN-08-4136
- Haspel, R. L., Salditt-Georgieff, M., & Darnell, J. E., Jr. (1996). The rapid inactivation of nuclear tyrosine phosphorylated Stat1 depends upon a protein tyrosine phosphatase. *EMBO J*, 15(22), 6262-6268.
- Hawley, K. L., Olson, C. M., Jr., Carreras-Gonzalez, A., Navasa, N., & Anguita, J. (2015). Serum C3 Enhances Complement Receptor 3-Mediated Phagocytosis of *Borrelia burgdorferi*. *Int J Biol Sci*, 11(11), 1269-1271. doi:10.7150/ijbs.13395
- Helmy, K. Y., Katschke, K. J., Jr., Gorgani, N. N., Kljavin, N. M., Elliott, J. M., Diehl, L., . . . van Lookeren Campagne, M. (2006). CR1g: a macrophage complement receptor required for phagocytosis of circulating pathogens. *Cell*, 124(5), 915-927. doi:10.1016/j.cell.2005.12.039
- Hewitt, E. W. (2003). The MHC class I antigen presentation pathway: strategies for viral immune evasion. *Immunology*, 110(2), 163-169.
- Hildner, K., Edelson, B. T., Purtha, W. E., Diamond, M., Matsushita, H., Kohyama, M., . . . Murphy, K. M. (2008). Batf3 deficiency reveals a critical role for CD8alpha+ dendritic

- cells in cytotoxic T cell immunity. *Science*, 322(5904), 1097-1100. doi:10.1126/science.1164206
- Hirota, K., Hashimoto, M., Ito, Y., Matsuura, M., Ito, H., Tanaka, M., . . . Sakaguchi, S. (2018). Autoimmune Th17 Cells Induced Synovial Stromal and Innate Lymphoid Cell Secretion of the Cytokine GM-CSF to Initiate and Augment Autoimmune Arthritis. *Immunity*, 48(6), 1220-1232 e1225. doi:10.1016/j.immuni.2018.04.009
- Hochrein, H., Shortman, K., Vremec, D., Scott, B., Hertzog, P., & O'Keeffe, M. (2001). Differential production of IL-12, IFN- $\alpha$ , and IFN- $\gamma$  by mouse dendritic cell subsets. *J Immunol*, 166(9), 5448-5455.
- Hoefig, K. P., & Heissmeyer, V. (2018). Posttranscriptional regulation of T helper cell fate decisions. *J Cell Biol*. doi:10.1083/jcb.201708075
- Horii, T., Morita, S., Kimura, M., Terawaki, N., Shibutani, M., & Hatada, I. (2017). Efficient generation of conditional knockout mice via sequential introduction of lox sites. *Sci Rep*, 7(1), 7891. doi:10.1038/s41598-017-08496-8
- Hu, J., Winqvist, O., Flores-Morales, A., Wikstrom, A. C., & Norstedt, G. (2009). SOCS2 influences LPS induced human monocyte-derived dendritic cell maturation. *PLoS One*, 4(9), e7178. doi:10.1371/journal.pone.0007178
- Huang, L., & Appleton, J. A. (2016). Eosinophils in Helminth Infection: Defenders and Dupes. *Trends Parasitol*, 32(10), 798-807. doi:10.1016/j.pt.2016.05.004
- Huang, W. D., Guo, J. T., Liu, X., Hong, X. O., Xu, J. J., Huang, S. W., & Huang, Y. S. (2009). [CD11b expression in neutrophils and lymphocytes of children with systemic inflammatory response syndrome]. *Zhongguo Dang Dai Er Ke Za Zhi*, 11(7), 540-542.
- Humphries, J. D., Byron, A., & Humphries, M. J. (2006). Integrin ligands at a glance. *J Cell Sci*, 119(Pt 19), 3901-3903. doi:10.1242/jcs.03098
- Humphries, M. J. (2000). Integrin structure. *Biochem Soc Trans*, 28(4), 311-339.
- Humphries, M. J., Symonds, E. J., & Mould, A. P. (2003). Mapping functional residues onto integrin crystal structures. *Curr Opin Struct Biol*, 13(2), 236-243.
- Hynes, R. O. (2002). Integrins: bidirectional, allosteric signaling machines. *Cell*, 110(6), 673-687.
- Hyun, Y. M., Lefort, C. T., & Kim, M. (2009). Leukocyte integrins and their ligand interactions. *Immunol Res*, 45(2-3), 195-208. doi:10.1007/s12026-009-8101-1
- Ilangumaran, S., Ramanathan, S., & Rottapel, R. (2004). Regulation of the immune system by SOCS family adaptor proteins. *Semin Immunol*, 16(6), 351-365. doi:10.1016/j.smim.2004.08.015
- Ito, A., Hong, C., Oka, K., Salazar, J. V., Diehl, C., Witztum, J. L., . . . Tontonoz, P. (2016). Cholesterol Accumulation in CD11c(+) Immune Cells Is a Causal and Targetable Factor in Autoimmune Disease. *Immunity*, 45(6), 1311-1326. doi:10.1016/j.immuni.2016.11.008
- Jagarapu, J., Kelchtermans, J., Rong, M., Chen, S., Hehre, D., Hummler, S., . . . Wu, S. (2015). Efficacy of Leukadherin-1 in the Prevention of Hyperoxia-Induced Lung Injury in Neonatal Rats. *Am J Respir Cell Mol Biol*, 53(6), 793-801. doi:10.1165/rcmb.2014-0422OC

- Janowska-Wieczorek, A., Majka, M., Kijowski, J., Baj-Krzyworzeka, M., Reca, R., Turner, A. R., . . . Ratajczak, M. Z. (2001). Platelet-derived microparticles bind to hematopoietic stem/progenitor cells and enhance their engraftment. *Blood*, *98*(10), 3143-3149.
- Jiang, F., & Doudna, J. A. (2017). CRISPR-Cas9 Structures and Mechanisms. *Annu Rev Biophys*, *46*, 505-529. doi:10.1146/annurev-biophys-062215-010822
- Jiang, L., Li, X., Liu, L., & Zhang, Q. (2013). Cellular uptake mechanism and intracellular fate of hydrophobically modified pullulan nanoparticles. *Int J Nanomedicine*, *8*, 1825-1834. doi:10.2147/IJN.S44342
- Jin, R., Yu, S., Song, Z., Zhu, X., Wang, C., Yan, J., . . . Li, G. (2013). Soluble CD40 ligand stimulates CD40-dependent activation of the beta2 integrin Mac-1 and protein kinase C zeta (PKCzeta) in neutrophils: implications for neutrophil-platelet interactions and neutrophil oxidative burst. *PLoS One*, *8*(6), e64631. doi:10.1371/journal.pone.0064631
- Jinek, M., Chylinski, K., Fonfara, I., Hauer, M., Doudna, J. A., & Charpentier, E. (2012). A programmable dual-RNA-guided DNA endonuclease in adaptive bacterial immunity. *Science*, *337*(6096), 816-821. doi:10.1126/science.1225829
- Johnson, M. S., Lu, N., Denessiouk, K., Heino, J., & Gullberg, D. (2009). Integrins during evolution: evolutionary trees and model organisms. *Biochim Biophys Acta*, *1788*(4), 779-789. doi:10.1016/j.bbamem.2008.12.013
- Johnston, P. A., & Grandis, J. R. (2011). STAT3 signaling: anticancer strategies and challenges. *Mol Interv*, *11*(1), 18-26. doi:10.1124/mi.11.1.4
- Jongstra-Bilen, J., Harrison, R., & Grinstein, S. (2003). Fcgamma-receptors induce Mac-1 (CD11b/CD18) mobilization and accumulation in the phagocytic cup for optimal phagocytosis. *J Biol Chem*, *278*(46), 45720-45729. doi:10.1074/jbc.M303704200
- Kamphorst, A. O., Guermonprez, P., Dudziak, D., & Nussenzweig, M. C. (2010). Route of antigen uptake differentially impacts presentation by dendritic cells and activated monocytes. *J Immunol*, *185*(6), 3426-3435. doi:10.4049/jimmunol.1001205
- Kaplan, M. J., & Radic, M. (2012). Neutrophil extracellular traps: double-edged swords of innate immunity. *J Immunol*, *189*(6), 2689-2695. doi:10.4049/jimmunol.1201719
- Karnell, J. L., Kumar, V., Wang, J., Wang, S., Voynova, E., & Ettinger, R. (2017). Role of CD11c(+) T-bet(+) B cells in human health and disease. *Cell Immunol*, *321*, 40-45. doi:10.1016/j.cellimm.2017.05.008
- Kashiwada, M., Pham, N. L., Pewe, L. L., Harty, J. T., & Rothman, P. B. (2011). NFIL3/E4BP4 is a key transcription factor for CD8alpha(+) dendritic cell development. *Blood*, *117*(23), 6193-6197. doi:10.1182/blood-2010-07-295873
- Kaufman, J. (2002). The origins of the adaptive immune system: whatever next? *Nat Immunol*, *3*(12), 1124-1125. doi:10.1038/ni1202-1124
- Kavanaugh, A. F., Davis, L. S., Jain, R. I., Nichols, L. A., Norris, S. H., & Lipsky, P. E. (1996). A phase I/II open label study of the safety and efficacy of an anti-ICAM-1 (intercellular adhesion molecule-1; CD54) monoclonal antibody in early rheumatoid arthritis. *J Rheumatol*, *23*(8), 1338-1344.
- Kawasaki, T., & Kawai, T. (2014). Toll-like receptor signaling pathways. *Front Immunol*, *5*, 461. doi:10.3389/fimmu.2014.00461
- Kedl, R. M., Jordan, M., Potter, T., Kappler, J., Marrack, P., & Dow, S. (2001). CD40 stimulation accelerates deletion of tumor-specific CD8(+) T cells in the absence of

- tumor-antigen vaccination. *Proc Natl Acad Sci U S A*, 98(19), 10811-10816. doi:10.1073/pnas.191371898
- Kedzierski, L., Clemens, E. B., Bird, N. L., Kile, B. T., Belz, G. T., Nicola, N. A., . . . Nicholson, S. E. (2015). SOCS4 is dispensable for an efficient recall response to influenza despite being required for primary immunity. *Immunol Cell Biol*, 93(10), 909-913. doi:10.1038/icb.2015.55
- Kedzierski, L., Linossi, E. M., Kolesnik, T. B., Day, E. B., Bird, N. L., Kile, B. T., . . . Nicholson, S. E. (2014). Suppressor of cytokine signaling 4 (SOCS4) protects against severe cytokine storm and enhances viral clearance during influenza infection. *PLoS Pathog*, 10(5), e1004134. doi:10.1371/journal.ppat.1004134
- Kehrli, M. E., Jr., Schmalstieg, F. C., Anderson, D. C., Van der Maaten, M. J., Hughes, B. J., Ackermann, M. R., . . . Whetstone, C. A. (1990). Molecular definition of the bovine granulocytopeny syndrome: identification of deficiency of the Mac-1 (CD11b/CD18) glycoprotein. *Am J Vet Res*, 51(11), 1826-1836.
- Khan, S. Q., Guo, L., Cimbaluk, D. J., Elshabrawy, H., Faridi, M. H., Jolly, M., . . . Gupta, V. (2014). A Small Molecule beta2 Integrin Agonist Improves Chronic Kidney Allograft Survival by Reducing Leukocyte Recruitment and Accompanying Vasculopathy. *Front Med (Lausanne)*, 1, 45. doi:10.3389/fmed.2014.00045
- Khan, S. Q., Khan, I., & Gupta, V. (2018). CD11b Activity Modulates Pathogenesis of Lupus Nephritis. *Front Med (Lausanne)*, 5, 52. doi:10.3389/fmed.2018.00052
- Kim, H. Y., Kim, S. K., Seo, H. S., Jeong, S., Ahn, K. B., Yun, C. H., & Han, S. H. (2018). Th17 activation by dendritic cells stimulated with gamma-irradiated *Streptococcus pneumoniae*. *Mol Immunol*, 101, 344-352. doi:10.1016/j.molimm.2018.07.023
- Kim, T. K., & Maniatis, T. (1996). Regulation of interferon-gamma-activated STAT1 by the ubiquitin-proteasome pathway. *Science*, 273(5282), 1717-1719.
- Kim, W. S., Shin, M. K., & Shin, S. J. (2018). MAP1981c, a Putative Nucleic Acid-Binding Protein, Produced by *Mycobacterium avium* subsp. *paratuberculosis*, Induces Maturation of Dendritic Cells and Th1-Polarization. *Front Cell Infect Microbiol*, 8, 206. doi:10.3389/fcimb.2018.00206
- Kindzelskii, A. L., Yang, Z., Nabel, G. J., Todd, R. F., 3rd, & Petty, H. R. (2000). Ebola virus secretory glycoprotein (sGP) diminishes Fc gamma RIIIB-to-CR3 proximity on neutrophils. *J Immunol*, 164(2), 953-958.
- Kishimoto, T. K., O'Conner, K., & Springer, T. A. (1989). Leukocyte adhesion deficiency. Aberrant splicing of a conserved integrin sequence causes a moderate deficiency phenotype. *J Biol Chem*, 264(6), 3588-3595.
- Kishimoto, T. K., & Springer, T. A. (1989). Human leukocyte adhesion deficiency: molecular basis for a defective immune response to infections of the skin. *Curr Probl Dermatol*, 18, 106-115.
- Koitaishi, N., Bedja, D., Zaiman, A. L., Pinto, Y. M., Zhang, M., Gabrielson, K. L., . . . Kass, D. A. (2009). Avoidance of transient cardiomyopathy in cardiomyocyte-targeted tamoxifen-induced MerCreMer gene deletion models. *Circ Res*, 105(1), 12-15. doi:10.1161/CIRCRESAHA.109.198416
- Kondo, M. (2010). Lymphoid and myeloid lineage commitment in multipotent hematopoietic progenitors. *Immunol Rev*, 238(1), 37-46. doi:10.1111/j.1600-065X.2010.00963.x

- Krauss, J. C., PooH, Xue, W., Mayo-Bond, L., Todd, R. F., 3rd, & Petty, H. R. (1994). Reconstitution of antibody-dependent phagocytosis in fibroblasts expressing Fc gamma receptor IIIB and the complement receptor type 3. *J Immunol*, *153*(4), 1769-1777.
- Krystel-Whittemore, M., Dileepan, K. N., & Wood, J. G. (2015). Mast Cell: A Multi-Functional Master Cell. *Front Immunol*, *6*, 620. doi:10.3389/fimmu.2015.00620
- Kuijpers, T. W., van Bruggen, R., Kamerbeek, N., Tool, A. T., Hicsonmez, G., Gurgey, A., . . . Roos, D. (2007). Natural history and early diagnosis of LAD-1/variant syndrome. *Blood*, *109*(8), 3529-3537. doi:10.1182/blood-2006-05-021402
- Kummer, D., & Ebneth, K. (2018). Junctional Adhesion Molecules (JAMs): The JAM-Integrin Connection. *Cells*, *7*(4). doi:10.3390/cells7040025
- Le Cabec, V., Carreno, S., Moisan, A., Bordier, C., & Maridonneau-Parini, I. (2002). Complement receptor 3 (CD11b/CD18) mediates type I and type II phagocytosis during nonopsonic and opsonic phagocytosis, respectively. *J Immunol*, *169*(4), 2003-2009.
- Lee, Y. H., & Bae, S. C. (2015). Association between the functional ITGAM rs1143679 G/A polymorphism and systemic lupus erythematosus/lupus nephritis or rheumatoid arthritis: an update meta-analysis. *Rheumatol Int*, *35*(5), 815-823. doi:10.1007/s00296-014-3156-2
- Li, H., Zhang, G. X., Chen, Y., Xu, H., Fitzgerald, D. C., Zhao, Z., & Rostami, A. (2008). CD11c+CD11b+ dendritic cells play an important role in intravenous tolerance and the suppression of experimental autoimmune encephalomyelitis. *J Immunol*, *181*(4), 2483-2493.
- Li, N., Yang, H., Wang, M., Lu, S., Zhang, Y., & Long, M. (2018). Ligand-specific binding forces of LFA-1 and Mac-1 in neutrophil adhesion and crawling. *Mol Biol Cell*, *29*(4), 408-418. doi:10.1091/mbc.E16-12-0827
- Li, W., Okuda, A., Yamamoto, H., Yamanishi, K., Terada, N., Yamanishi, H., . . . Okamura, H. (2013). Regulation of development of CD56 bright CD11c + NK-like cells with helper function by IL-18. *PLoS One*, *8*(12), e82586. doi:10.1371/journal.pone.0082586
- Li, Y., Wei, C., Xu, H., Jia, J., Wei, Z., Guo, R., . . . Gao, X. (2018). The Immunoregulation of Th17 in Host against Intracellular Bacterial Infection. *Mediators Inflamm*, *2018*, 6587296. doi:10.1155/2018/6587296
- Liang, M., Liwen, Z., Yun, Z., Yanbo, D., & Jianping, C. (2018). The Imbalance between Foxp3(+)Tregs and Th1/Th17/Th22 Cells in Patients with Newly Diagnosed Autoimmune Hepatitis. *J Immunol Res*, *2018*, 3753081. doi:10.1155/2018/3753081
- Liang, S., Slattery, M. J., & Dong, C. (2005). Shear stress and shear rate differentially affect the multi-step process of leukocyte-facilitated melanoma adhesion. *Exp Cell Res*, *310*(2), 282-292. doi:10.1016/j.yexcr.2005.07.028
- Lim, C. P., & Cao, X. (2006). Structure, function, and regulation of STAT proteins. *Mol Biosyst*, *2*(11), 536-550. doi:10.1039/b606246f
- Ling, G. S., Bennett, J., Woollard, K. J., Szajna, M., Fossati-Jimack, L., Taylor, P. R., . . . Botto, M. (2014). Integrin CD11b positively regulates TLR4-induced signalling pathways in dendritic cells but not in macrophages. *Nat Commun*, *5*, 3039. doi:10.1038/ncomms4039
- Liu, K., & Nussenzweig, M. C. (2010). Origin and development of dendritic cells. *Immunol Rev*, *234*(1), 45-54. doi:10.1111/j.0105-2896.2009.00879.x

- Liu, T., Zhang, L., Joo, D., & Sun, S. C. (2017). NF-kappaB signaling in inflammation. *Signal Transduct Target Ther*, 2. doi:10.1038/sigtrans.2017.23
- Liu, X., Jiang, X., Liu, R., Wang, L., Qian, T., Zheng, Y., . . . Chu, Y. (2015). B cells expressing CD11b effectively inhibit CD4+ T-cell responses and ameliorate experimental autoimmune hepatitis in mice. *Hepatology*, 62(5), 1563-1575. doi:10.1002/hep.28001
- Liu, Y., & Cao, X. (2016). Immunosuppressive cells in tumor immune escape and metastasis. *J Mol Med (Berl)*, 94(5), 509-522. doi:10.1007/s00109-015-1376-x
- Liu, Y. X., Zhang, F., Yao, Q. M., Yuan, T., Xu, J., & Zhu, X. J. (2015). Expression of CD11a in lymphocyte subpopulation in immune thrombocytopenia. *Int J Clin Exp Pathol*, 8(12), 15642-15651.
- Liu, Z., Zhao, M., Li, N., Diaz, L. A., & Mayadas, T. N. (2006). Differential roles for beta2 integrins in experimental autoimmune bullous pemphigoid. *Blood*, 107(3), 1063-1069. doi:10.1182/blood-2005-08-3123
- Livak, K. J., & Schmittgen, T. D. (2001). Analysis of relative gene expression data using real-time quantitative PCR and the 2(-Delta Delta C(T)) Method. *Methods*, 25(4), 402-408. doi:10.1006/meth.2001.1262
- Lo, S. K., Van Seventer, G. A., Levin, S. M., & Wright, S. D. (1989). Two leukocyte receptors (CD11a/CD18 and CD11b/CD18) mediate transient adhesion to endothelium by binding to different ligands. *J Immunol*, 143(10), 3325-3329.
- Loonstra, A., Vooijs, M., Beverloo, H. B., Allak, B. A., van Drunen, E., Kanaar, R., . . . Jonkers, J. (2001). Growth inhibition and DNA damage induced by Cre recombinase in mammalian cells. *Proc Natl Acad Sci U S A*, 98(16), 9209-9214. doi:10.1073/pnas.161269798
- Loretsen, K. J., Cho, J. J., Luo, X., Zuniga, A. N., Urban, J. F., Jr., Zhou, L., . . . Avram, D. (2018). Bcl11b is essential for licensing Th2 differentiation during helminth infection and allergic asthma. *Nat Commun*, 9(1), 1679. doi:10.1038/s41467-018-04111-0
- Lu, Y., Wang, W., Liu, G., Zhang, J., Gao, Y., Jia, Y., . . . Xu, J. (2016). [The number of peripheral blood CD11c+ antigen presenting cells increases and their function strengthens in the patients with active pulmonary tuberculosis]. *Xi Bao Yu Fen Zi Mian Yi Xue Za Zhi*, 32(3), 378-381.
- Luber, C. A., Cox, J., Lauterbach, H., Fancke, B., Selbach, M., Tschopp, J., . . . Mann, M. (2010). Quantitative proteomics reveals subset-specific viral recognition in dendritic cells. *Immunity*, 32(2), 279-289. doi:10.1016/j.immuni.2010.01.013
- Lund, R. J., Chen, Z., Scheinin, J., & Lahesmaa, R. (2004). Early target genes of IL-12 and STAT4 signaling in th cells. *J Immunol*, 172(11), 6775-6782.
- Luo, B. H., Carman, C. V., & Springer, T. A. (2007). Structural basis of integrin regulation and signaling. *Annu Rev Immunol*, 25, 619-647. doi:10.1146/annurev.immunol.25.022106.141618
- Major, E. O. (2010). Progressive multifocal leukoencephalopathy in patients on immunomodulatory therapies. *Annu Rev Med*, 61, 35-47. doi:10.1146/annurev.med.080708.082655
- Marski, M., Kandula, S., Turner, J. R., & Abraham, C. (2005). CD18 is required for optimal development and function of CD4+CD25+ T regulatory cells. *J Immunol*, 175(12), 7889-7897.

- Martinez-Pomares, L., Linehan, S. A., Taylor, P. R., & Gordon, S. (2001). Binding properties of the mannose receptor. *Immunobiology*, *204*(5), 527-535. doi:10.1078/0171-2985-00089
- McHeyzer-Williams, M., Okitsu, S., Wang, N., & McHeyzer-Williams, L. (2011). Molecular programming of B cell memory. *Nat Rev Immunol*, *12*(1), 24-34. doi:10.1038/nri3128
- McKenna, H. J., Stocking, K. L., Miller, R. E., Brasel, K., De Smedt, T., Maraskovsky, E., . . . Peschon, J. J. (2000). Mice lacking flt3 ligand have deficient hematopoiesis affecting hematopoietic progenitor cells, dendritic cells, and natural killer cells. *Blood*, *95*(11), 3489-3497.
- Meakin, P. J., Morrison, V. L., Sneddon, C. C., Savinko, T., Uotila, L., Jalicy, S. M., . . . Fagerholm, S. C. (2015). Mice Lacking beta2-Integrin Function Remain Glucose Tolerant in Spite of Insulin Resistance, Neutrophil Infiltration and Inflammation. *PLoS One*, *10*(9), e0138872. doi:10.1371/journal.pone.0138872
- Metelitsa, L. S., Gillies, S. D., Super, M., Shimada, H., Reynolds, C. P., & Seeger, R. C. (2002). Antidisialoganglioside/granulocyte macrophage-colony-stimulating factor fusion protein facilitates neutrophil antibody-dependent cellular cytotoxicity and depends on FcgammaRII (CD32) and Mac-1 (CD11b/CD18) for enhanced effector cell adhesion and azurophil granule exocytosis. *Blood*, *99*(11), 4166-4173.
- Mitroulis, I., Alexaki, V. I., Kourtzelis, I., Ziogas, A., Hajishengallis, G., & Chavakis, T. (2015). Leukocyte integrins: role in leukocyte recruitment and as therapeutic targets in inflammatory disease. *Pharmacol Ther*, *147*, 123-135. doi:10.1016/j.pharmthera.2014.11.008
- Miura, Y., Miura, M., Gronthos, S., Allen, M. R., Cao, C., Uveges, T. E., . . . Zhang, L. (2005). Defective osteogenesis of the stromal stem cells predisposes CD18-null mice to osteoporosis. *Proc Natl Acad Sci U S A*, *102*(39), 14022-14027. doi:10.1073/pnas.0409397102
- Miyazaki, Y., Vieira-de-Abreu, A., Harris, E. S., Shah, A. M., Weyrich, A. S., Castro-Faria-Neto, H. C., & Zimmerman, G. A. (2014). Integrin alphaDbeta2 (CD11d/CD18) is expressed by human circulating and tissue myeloid leukocytes and mediates inflammatory signaling. *PLoS One*, *9*(11), e112770. doi:10.1371/journal.pone.0112770
- Nam, H. Y., Kwon, S. M., Chung, H., Lee, S. Y., Kwon, S. H., Jeon, H., . . . Jeong, S. Y. (2009). Cellular uptake mechanism and intracellular fate of hydrophobically modified glycol chitosan nanoparticles. *J Control Release*, *135*(3), 259-267. doi:10.1016/j.jconrel.2009.01.018
- Natarajan, C., Yao, S. Y., & Sriram, S. (2016). TLR3 Agonist Poly-IC Induces IL-33 and Promotes Myelin Repair. *PLoS One*, *11*(3), e0152163. doi:10.1371/journal.pone.0152163
- Nelson, S. M., Nguyen, T. M., McDonald, J. W., & MacDonald, J. K. (2018). Natalizumab for induction of remission in Crohn's disease. *Cochrane Database Syst Rev*, *8*, CD006097. doi:10.1002/14651858.CD006097.pub3
- Okita, Y., Tanaka, H., Ohira, M., Muguruma, K., Kubo, N., Watanabe, M., . . . Hirakawa, K. (2014). Role of tumor-infiltrating CD11b+ antigen-presenting cells in the progression of gastric cancer. *J Surg Res*, *186*(1), 192-200. doi:10.1016/j.jss.2013.08.024
- Onai, N., Obata-Onai, A., Schmid, M. A., Ohteki, T., Jarrossay, D., & Manz, M. G. (2007). Identification of clonogenic common Flt3+M-CSFR+ plasmacytoid and conventional

- dendritic cell progenitors in mouse bone marrow. *Nat Immunol*, 8(11), 1207-1216. doi:10.1038/ni1518
- Orange, J. S., & Ballas, Z. K. (2006). Natural killer cells in human health and disease. *Clin Immunol*, 118(1), 1-10. doi:10.1016/j.clim.2005.10.011
- Ortiz-Stern, A., & Rosales, C. (2003). Cross-talk between Fc receptors and integrins. *Immunol Lett*, 90(2-3), 137-143.
- Palmblad, J. (1984). The role of granulocytes in inflammation. *Scand J Rheumatol*, 13(2), 163-172.
- Perera, P. Y., Mayadas, T. N., Takeuchi, O., Akira, S., Zaks-Zilberman, M., Goyert, S. M., & Vogel, S. N. (2001). CD11b/CD18 acts in concert with CD14 and Toll-like receptor (TLR) 4 to elicit full lipopolysaccharide and taxol-inducible gene expression. *J Immunol*, 166(1), 574-581.
- Podolnikova, N. P., Podolnikov, A. V., Haas, T. A., Lishko, V. K., & Ugarova, T. P. (2015). Ligand recognition specificity of leukocyte integrin alphaMbeta2 (Mac-1, CD11b/CD18) and its functional consequences. *Biochemistry*, 54(6), 1408-1420. doi:10.1021/bi5013782
- Posselt, G., Schwarz, H., Duschl, A., & Horejs-Hoeck, J. (2011). Suppressor of cytokine signaling 2 is a feedback inhibitor of TLR-induced activation in human monocyte-derived dendritic cells. *J Immunol*, 187(6), 2875-2884. doi:10.4049/jimmunol.1003348
- Potin, D., Launay, M., Monatlik, F., Malabre, P., Fabreguettes, M., Fouquet, A., . . . Dhar, T. G. (2006). Discovery and development of 5-[(5S,9R)-9-(4-cyanophenyl)-3-(3,5-dichlorophenyl)-1-methyl-2,4-dioxo-1,3,7-triazaspiro[4.4]non-7-yl-methyl]-3-thiophenecarboxylic acid (BMS-587101)--a small molecule antagonist of leukocyte function associated antigen-1. *J Med Chem*, 49(24), 6946-6949. doi:10.1021/jm0610806
- Pugach, E. K., Richmond, P. A., Azofeifa, J. G., Dowell, R. D., & Leinwand, L. A. (2015). Prolonged Cre expression driven by the alpha-myosin heavy chain promoter can be cardiotoxic. *J Mol Cell Cardiol*, 86, 54-61. doi:10.1016/j.yjmcc.2015.06.019
- Pustynnikov, S., Sagar, D., Jain, P., & Khan, Z. K. (2014). Targeting the C-type lectins-mediated host-pathogen interactions with dextran. *J Pharm Pharm Sci*, 17(3), 371-392.
- Ramalingam, R., Larmonier, C. B., Thurston, R. D., Midura-Kiela, M. T., Zheng, S. G., Ghishan, F. K., & Kiela, P. R. (2012). Dendritic cell-specific disruption of TGF-beta receptor II leads to altered regulatory T cell phenotype and spontaneous multiorgan autoimmunity. *J Immunol*, 189(8), 3878-3893. doi:10.4049/jimmunol.1201029
- Raphael, I., Nalawade, S., Eagar, T. N., & Forsthuber, T. G. (2015). T cell subsets and their signature cytokines in autoimmune and inflammatory diseases. *Cytokine*, 74(1), 5-17. doi:10.1016/j.cyto.2014.09.011
- Rizzitelli, A., Hawkins, E., Todd, H., Hodgkin, P. D., & Shortman, K. (2006). The proliferative response of CD4 T cells to steady-state CD8+ dendritic cells is restricted by post-activation death. *Int Immunol*, 18(3), 415-423. doi:10.1093/intimm/dxh382
- Roberts, A. L., Furnrohr, B. G., Vyse, T. J., & Rhodes, B. (2016). The complement receptor 3 (CD11b/CD18) agonist Leukadherin-1 suppresses human innate inflammatory signalling. *Clin Exp Immunol*, 185(3), 361-371. doi:10.1111/cei.12803

- Rose, S., Misharin, A., & Perlman, H. (2012). A novel Ly6C/Ly6G-based strategy to analyze the mouse splenic myeloid compartment. *Cytometry A*, 81(4), 343-350. doi:10.1002/cyto.a.22012
- Rosenkranz, A. R., Coxon, A., Maurer, M., Gurish, M. F., Austen, K. F., Friend, D. S., . . . Mayadas, T. N. (1998). Impaired mast cell development and innate immunity in Mac-1 (CD11b/CD18, CR3)-deficient mice. *J Immunol*, 161(12), 6463-6467.
- Rosetti, F., Tsuboi, N., Chen, K., Nishi, H., Hernandez, T., Sethi, S., . . . Mayadas, T. N. (2012). Human lupus serum induces neutrophil-mediated organ damage in mice that is enabled by Mac-1 deficiency. *J Immunol*, 189(7), 3714-3723. doi:10.4049/jimmunol.1201594
- Rui, X., Mehrbod, M., Van Agthoven, J. F., Anand, S., Xiong, J. P., Mofrad, M. R., & Arnaout, M. A. (2014). The alpha-subunit regulates stability of the metal ion at the ligand-associated metal ion-binding site in beta3 integrins. *J Biol Chem*, 289(33), 23256-23263. doi:10.1074/jbc.M114.581470
- Ryschkewitsch, C. F., Jensen, P. N., Monaco, M. C., & Major, E. O. (2010). JC virus persistence following progressive multifocal leukoencephalopathy in multiple sclerosis patients treated with natalizumab. *Ann Neurol*, 68(3), 384-391. doi:10.1002/ana.22137
- Sadhu, C., Ting, H. J., Lipsky, B., Hensley, K., Garcia-Martinez, L. F., Simon, S. I., & Staunton, D. E. (2007). CD11c/CD18: novel ligands and a role in delayed-type hypersensitivity. *J Leukoc Biol*, 81(6), 1395-1403. doi:10.1189/jlb.1106680
- Saed, G. M., Fletcher, N. M., Diamond, M. P., Morris, R. T., Gomez-Lopez, N., & Memaj, I. (2018). Novel expression of CD11b in epithelial ovarian cancer: Potential therapeutic target. *Gynecol Oncol*, 148(3), 567-575. doi:10.1016/j.ygyno.2017.12.018
- Santala, P., & Heino, J. (1991). Regulation of integrin-type cell adhesion receptors by cytokines. *J Biol Chem*, 266(34), 23505-23509.
- Santoni, G., Cardinali, C., Morelli, M. B., Santoni, M., Nabissi, M., & Amantini, C. (2015). Danger- and pathogen-associated molecular patterns recognition by pattern-recognition receptors and ion channels of the transient receptor potential family triggers the inflammasome activation in immune cells and sensory neurons. *J Neuroinflammation*, 12, 21. doi:10.1186/s12974-015-0239-2
- Santoro, S. W., & Schultz, P. G. (2002). Directed evolution of the site specificity of Cre recombinase. *Proc Natl Acad Sci U S A*, 99(7), 4185-4190. doi:10.1073/pnas.022039799
- Sato, M., Sano, H., Iwaki, D., Kudo, K., Konishi, M., Takahashi, H., . . . Kuroki, Y. (2003). Direct binding of Toll-like receptor 2 to zymosan, and zymosan-induced NF-kappa B activation and TNF-alpha secretion are down-regulated by lung collectin surfactant protein A. *J Immunol*, 171(1), 417-425.
- Savina, A., & Amigorena, S. (2007). Phagocytosis and antigen presentation in dendritic cells. *Immunol Rev*, 219, 143-156. doi:10.1111/j.1600-065X.2007.00552.x
- Savinko, T. S., Morrison, V. L., Uotila, L. M., Wolff, C. H. J., Alenius, H. T., & Fagerholm, S. C. (2015). Functional Beta2-Integrins Restrict Skin Inflammation In Vivo. *J Invest Dermatol*, 135(9), 2249-2257. doi:10.1038/jid.2015.164
- Schaft, J., Ashery-Padan, R., van der Hoeven, F., Gruss, P., & Stewart, A. F. (2001). Efficient FLP recombination in mouse ES cells and oocytes. *Genesis*, 31(1), 6-10.

- Scharffetter-Kochanek, K., Lu, H., Norman, K., van Nood, N., Munoz, F., Grabbe, S., . . . Beaudet, A. L. (1998). Spontaneous skin ulceration and defective T cell function in CD18 null mice. *J Exp Med*, *188*(1), 119-131.
- Schiavoni, G., Mattei, F., & Gabriele, L. (2013). Type I Interferons as Stimulators of DC-Mediated Cross-Priming: Impact on Anti-Tumor Response. *Front Immunol*, *4*, 483. doi:10.3389/fimmu.2013.00483
- Schiavoni, G., Mattei, F., Sestili, P., Borghi, P., Venditti, M., Morse, H. C., 3rd, . . . Gabriele, L. (2002). ICSBP is essential for the development of mouse type I interferon-producing cells and for the generation and activation of CD8alpha(+) dendritic cells. *J Exp Med*, *196*(11), 1415-1425.
- Schlitzer, A., McGovern, N., Teo, P., Zelante, T., Atarashi, K., Low, D., . . . Ginhoux, F. (2013). IRF4 transcription factor-dependent CD11b+ dendritic cells in human and mouse control mucosal IL-17 cytokine responses. *Immunity*, *38*(5), 970-983. doi:10.1016/j.immuni.2013.04.011
- Schmittgen, T. D., & Livak, K. J. (2008). Analyzing real-time PCR data by the comparative C(T) method. *Nat Protoc*, *3*(6), 1101-1108.
- Schubert, K., Polte, T., Bonisch, U., Schader, S., Holtappels, R., Hildebrandt, G., . . . Saalbach, A. (2011). Thy-1 (CD90) regulates the extravasation of leukocytes during inflammation. *Eur J Immunol*, *41*(3), 645-656. doi:10.1002/eji.201041117
- Schulz, O., Edwards, A. D., Schito, M., Aliberti, J., Manickasingham, S., Sher, A., & Reis e Sousa, C. (2000). CD40 triggering of heterodimeric IL-12 p70 production by dendritic cells in vivo requires a microbial priming signal. *Immunity*, *13*(4), 453-462.
- Schulz, T. J., Glaubitz, M., Kuhlowl, D., Thierbach, R., Birringer, M., Steinberg, P., . . . Ristow, M. (2007). Variable expression of Cre recombinase transgenes precludes reliable prediction of tissue-specific gene disruption by tail-biopsy genotyping. *PLoS One*, *2*(10), e1013. doi:10.1371/journal.pone.0001013
- Scott, C. L., Soen, B., Martens, L., Skrypek, N., Saelens, W., Taminau, J., . . . Berx, G. (2016). The transcription factor *Zeb2* regulates development of conventional and plasmacytoid DCs by repressing *Id2*. *J Exp Med*, *213*(6), 897-911. doi:10.1084/jem.20151715
- Sehgal, G., Zhang, K., Todd, R. F., 3rd, Boxer, L. A., & Petty, H. R. (1993). Lectin-like inhibition of immune complex receptor-mediated stimulation of neutrophils. Effects on cytosolic calcium release and superoxide production. *J Immunol*, *150*(10), 4571-4580.
- Sen, B., Peng, S., Woods, D. M., Wistuba, I., Bell, D., El-Naggar, A. K., . . . Johnson, F. M. (2012). STAT5A-mediated SOCS2 expression regulates Jak2 and STAT3 activity following c-*Src* inhibition in head and neck squamous carcinoma. *Clin Cancer Res*, *18*(1), 127-139. doi:10.1158/1078-0432.CCR-11-1889
- Sen, M., Yuki, K., & Springer, T. A. (2013). An internal ligand-bound, metastable state of a leukocyte integrin, alphaXbeta2. *J Cell Biol*, *203*(4), 629-642. doi:10.1083/jcb.201308083
- Shaw, S. K., Ma, S., Kim, M. B., Rao, R. M., Hartman, C. U., Froio, R. M., . . . Lusinskas, F. W. (2004). Coordinated redistribution of leukocyte LFA-1 and endothelial cell ICAM-1 accompany neutrophil transmigration. *J Exp Med*, *200*(12), 1571-1580. doi:10.1084/jem.20040965
- Shier, P., Otulakowski, G., Ngo, K., Panakos, J., Chourmouzis, E., Christjansen, L., . . . Fung-Leung, W. P. (1996). Impaired immune responses toward alloantigens and tumor cells

- but normal thymic selection in mice deficient in the beta2 integrin leukocyte function-associated antigen-1. *J Immunol*, 157(12), 5375-5386.
- Shimaoka, M., Salas, A., Yang, W., Weitz-Schmidt, G., & Springer, T. A. (2003). Small molecule integrin antagonists that bind to the beta2 subunit I-like domain and activate signals in one direction and block them in the other. *Immunity*, 19(3), 391-402.
- Shimaoka, M., Xiao, T., Liu, J. H., Yang, Y., Dong, Y., Jun, C. D., . . . Springer, T. A. (2003). Structures of the alpha L I domain and its complex with ICAM-1 reveal a shape-shifting pathway for integrin regulation. *Cell*, 112(1), 99-111.
- Siegers, G. M., Barreira, C. R., Postovit, L. M., & Dekaban, G. A. (2017). CD11d beta2 integrin expression on human NK, B, and gammadelta T cells. *J Leukoc Biol*, 101(4), 1029-1035. doi:10.1189/jlb.3AB0716-326RR
- Singh, K., Colmegna, I., He, X., Weyand, C. M., & Goronzy, J. J. (2008). Synoviocyte stimulation by the LFA-1-intercellular adhesion molecule-2-Ezrin-Akt pathway in rheumatoid arthritis. *J Immunol*, 180(3), 1971-1978.
- Singh, K., Gatzka, M., Peters, T., Borkner, L., Hainzl, A., Wang, H., . . . Scharffetter-Kochanek, K. (2013). Reduced CD18 levels drive regulatory T cell conversion into Th17 cells in the CD18hypo PL/J mouse model of psoriasis. *J Immunol*, 190(6), 2544-2553. doi:10.4049/jimmunol.1202399
- Sisco, M., Chao, J. D., Kim, I., Mogford, J. E., Mayadas, T. N., & Mustoe, T. A. (2007). Delayed wound healing in Mac-1-deficient mice is associated with normal monocyte recruitment. *Wound Repair Regen*, 15(4), 566-571. doi:10.1111/j.1524-475X.2007.00264.x
- Sjogren, F., Ljunghusen, O., Baas, A., Coble, B. I., & Stendahl, O. (1999). Expression and function of beta 2 integrin CD11B/CD18 on leukocytes from patients with psoriasis. *Acta Derm Venereol*, 79(2), 105-110.
- Skoberne, M., Somersan, S., Almodovar, W., Truong, T., Petrova, K., Henson, P. M., & Bhardwaj, N. (2006). The apoptotic-cell receptor CR3, but not alphavbeta5, is a regulator of human dendritic-cell immunostimulatory function. *Blood*, 108(3), 947-955. doi:10.1182/blood-2005-12-4812
- Soloviev, D. A., Hazen, S. L., Szpak, D., Bledzka, K. M., Ballantyne, C. M., Plow, E. F., & Pluskota, E. (2014). Dual role of the leukocyte integrin alphaMbeta2 in angiogenesis. *J Immunol*, 193(9), 4712-4721. doi:10.4049/jimmunol.1400202
- Somoza, C., & Lanier, L. L. (1995). T-cell costimulation via CD28-CD80/CD86 and CD40-CD40 ligand interactions. *Res Immunol*, 146(3), 171-176.
- Steinman, R. M., Kaplan, G., Witmer, M. D., & Cohn, Z. A. (1979). Identification of a novel cell type in peripheral lymphoid organs of mice. V. Purification of spleen dendritic cells, new surface markers, and maintenance in vitro. *J Exp Med*, 149(1), 1-16.
- Steinman, R. M., & Witmer, M. D. (1978). Lymphoid dendritic cells are potent stimulators of the primary mixed leukocyte reaction in mice. *Proc Natl Acad Sci U S A*, 75(10), 5132-5136.
- Stepensky, P. Y., Wolach, B., Gavrieli, R., Rousso, S., Ben Ami, T., Goldman, V., . . . Weintraub, M. (2015). Leukocyte adhesion deficiency type III: clinical features and treatment with stem cell transplantation. *J Pediatr Hematol Oncol*, 37(4), 264-268. doi:10.1097/MPH.0000000000000228

- Stevanin, M., Busso, N., Chobaz, V., Pigni, M., Ghassem-Zadeh, S., Zhang, L., . . . Ehrchiou, D. (2017). CD11b regulates the Treg/Th17 balance in murine arthritis via IL-6. *Eur J Immunol*, *47*(4), 637-645. doi:10.1002/eji.201646565
- Stockl, J., Majdic, O., Pickl, W. F., Rosenkranz, A., Prager, E., Gschwantler, E., & Knapp, W. (1995). Granulocyte activation via a binding site near the C-terminal region of complement receptor type 3 alpha-chain (CD11b) potentially involved in intramembrane complex formation with glycosylphosphatidylinositol-anchored Fc gamma RIIIB (CD16) molecules. *J Immunol*, *154*(10), 5452-5463.
- Stoddard, B. L. (2011). Homing endonucleases: from microbial genetic invaders to reagents for targeted DNA modification. *Structure*, *19*(1), 7-15. doi:10.1016/j.str.2010.12.003
- Stranges, P. B., Watson, J., Cooper, C. J., Choisy-Rossi, C. M., Stonebraker, A. C., Beighton, R. A., . . . Chervonsky, A. V. (2007). Elimination of antigen-presenting cells and autoreactive T cells by Fas contributes to prevention of autoimmunity. *Immunity*, *26*(5), 629-641. doi:10.1016/j.immuni.2007.03.016
- Sturla, L., Puglielli, L., Tonetti, M., Berninsone, P., Hirschberg, C. B., De Flora, A., & Etzioni, A. (2001). Impairment of the Golgi GDP-L-fucose transport and unresponsiveness to fucose replacement therapy in LAD II patients. *Pediatr Res*, *49*(4), 537-542. doi:10.1203/00006450-200104000-00016
- Stutman, O. (1977). Two main features of T-cell development: thymus traffic and postthymic maturation. *Contemp Top Immunobiol*, *7*, 1-46.
- Suchard, S. J., Stetsko, D. K., Davis, P. M., Skala, S., Potin, D., Launay, M., . . . Salter-Cid, L. (2010). An LFA-1 (alphaLbeta2) small-molecule antagonist reduces inflammation and joint destruction in murine models of arthritis. *J Immunol*, *184*(7), 3917-3926. doi:10.4049/jimmunol.0901095
- Swann, J. B., & Smyth, M. J. (2007). Immune surveillance of tumors. *J Clin Invest*, *117*(5), 1137-1146. doi:10.1172/JCI31405
- Takada, Y., Ye, X., & Simon, S. (2007). The integrins. *Genome Biol*, *8*(5), 215. doi:10.1186/gb-2007-8-5-215
- Tanaka, T., Yamamoto, Y., Muromoto, R., Ikeda, O., Sekine, Y., Grusby, M. J., . . . Matsuda, T. (2011). PDLIM2 inhibits T helper 17 cell development and granulomatous inflammation through degradation of STAT3. *Sci Signal*, *4*(202), ra85. doi:10.1126/scisignal.2001637
- Tang, J., Lin, G., Langdon, W. Y., Tao, L., & Zhang, J. (2018). Regulation of C-Type Lectin Receptor-Mediated Antifungal Immunity. *Front Immunol*, *9*, 123. doi:10.3389/fimmu.2018.00123
- Tang, T., Rosenkranz, A., Assmann, K. J., Goodman, M. J., Gutierrez-Ramos, J. C., Carroll, M. C., . . . Mayadas, T. N. (1997). A role for Mac-1 (CD11b/CD18) in immune complex-stimulated neutrophil function in vivo: Mac-1 deficiency abrogates sustained Fc gamma receptor-dependent neutrophil adhesion and complement-dependent proteinuria in acute glomerulonephritis. *J Exp Med*, *186*(11), 1853-1863.
- ten Broeke, T., Wubbolts, R., & Stoorvogel, W. (2013). MHC class II antigen presentation by dendritic cells regulated through endosomal sorting. *Cold Spring Harb Perspect Biol*, *5*(12), a016873. doi:10.1101/cshperspect.a016873
- Thery, C., & Amigorena, S. (2001). The cell biology of antigen presentation in dendritic cells. *Curr Opin Immunol*, *13*(1), 45-51.

- Thomas, A. P., Dunn, T. N., Oort, P. J., Grino, M., & Adams, S. H. (2011). Inflammatory phenotyping identifies CD11d as a gene markedly induced in white adipose tissue in obese rodents and women. *J Nutr*, *141*(6), 1172-1180. doi:10.3945/jn.110.127068
- Till, K. J., Harris, R. J., Linford, A., Spiller, D. G., Zuzel, M., & Cawley, J. C. (2008). Cell motility in chronic lymphocytic leukemia: defective Rap1 and alphaLbeta2 activation by chemokine. *Cancer Res*, *68*(20), 8429-8436. doi:10.1158/0008-5472.CAN-08-1758
- Tirapu, I., Giquel, B., Alexopoulou, L., Uematsu, S., Flavell, R., Akira, S., & Diebold, S. S. (2009). PolyI:C-induced reduction in uptake of soluble antigen is independent of dendritic cell activation. *Int Immunol*, *21*(7), 871-879. doi:10.1093/intimm/dxp053
- Toller-Kawahisa, J. E., Vigato-Ferreira, I. C., Pancoto, J. A., Mendes-Junior, C. T., Martinez, E. Z., Palomino, G. M., . . . Marzocchi-Machado, C. M. (2014). The variant of CD11b, rs1143679 within ITGAM, is associated with systemic lupus erythematosus and clinical manifestations in Brazilian patients. *Hum Immunol*, *75*(2), 119-123. doi:10.1016/j.humimm.2013.11.013
- Travis, M. A., Reizis, B., Melton, A. C., Masteller, E., Tang, Q., Proctor, J. M., . . . Sheppard, D. (2007). Loss of integrin alpha(v)beta8 on dendritic cells causes autoimmunity and colitis in mice. *Nature*, *449*(7160), 361-365. doi:10.1038/nature06110
- Treanor, B. (2012). B-cell receptor: from resting state to activate. *Immunology*, *136*(1), 21-27. doi:10.1111/j.1365-2567.2012.03564.x
- Treuel, L., Jiang, X., & Nienhaus, G. U. (2013). New views on cellular uptake and trafficking of manufactured nanoparticles. *J R Soc Interface*, *10*(82), 20120939. doi:10.1098/rsif.2012.0939
- Tsuji, S., Matsumoto, M., Takeuchi, O., Akira, S., Azuma, I., Hayashi, A., . . . Seya, T. (2000). Maturation of human dendritic cells by cell wall skeleton of Mycobacterium bovis bacillus Calmette-Guerin: involvement of toll-like receptors. *Infect Immun*, *68*(12), 6883-6890.
- Uzel, G., Kleiner, D. E., Kuhns, D. B., & Holland, S. M. (2001). Dysfunctional LAD-1 neutrophils and colitis. *Gastroenterology*, *121*(4), 958-964.
- van de Vijver, E., van den Berg, T. K., & Kuijpers, T. W. (2013). Leukocyte adhesion deficiencies. *Hematol Oncol Clin North Am*, *27*(1), 101-116, viii. doi:10.1016/j.hoc.2012.10.001
- van Pelt, J. P., Kuijpers, S. H., van de Kerkhof, P. C., & de Jong, E. M. (1998). The CD11b/CD18-integrin in the pathogenesis of psoriasis. *J Dermatol Sci*, *16*(2), 135-143.
- Van Seventer, G. A., Shimizu, Y., Horgan, K. J., & Shaw, S. (1990). The LFA-1 ligand ICAM-1 provides an important costimulatory signal for T cell receptor-mediated activation of resting T cells. *J Immunol*, *144*(12), 4579-4586.
- van Spriël, A. B., van Ojik, H. H., Bakker, A., Jansen, M. J., & van de Winkel, J. G. (2003). Mac-1 (CD11b/CD18) is crucial for effective Fc receptor-mediated immunity to melanoma. *Blood*, *101*(1), 253-258. doi:10.1182/blood.V101.1.253
- Varga, G., Balkow, S., Wild, M. K., Stadtbaeumer, A., Krummen, M., Rothoef, T., . . . Grabbe, S. (2007). Active MAC-1 (CD11b/CD18) on DCs inhibits full T-cell activation. *Blood*, *109*(2), 661-669. doi:10.1182/blood-2005-12-023044
- Varga, G., Nippe, N., Balkow, S., Peters, T., Wild, M. K., Seeliger, S., . . . Grabbe, S. (2010). LFA-1 contributes to signal I of T-cell activation and to the production of T(h)1 cytokines. *J Invest Dermatol*, *130*(4), 1005-1012. doi:10.1038/jid.2009.398

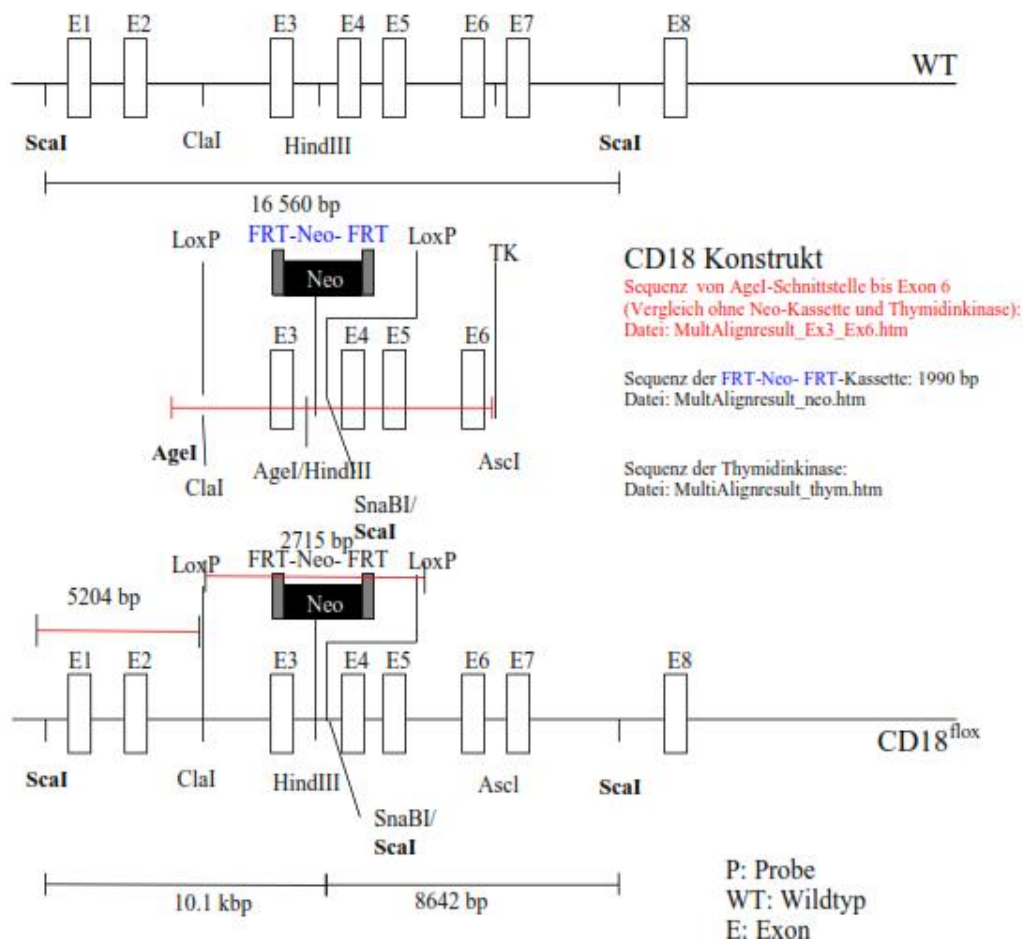
- Vicente, A., Varas, A., Acedon, R. S., Jimenez, E., Munoz, J. J., & Zapata, A. G. (1998). Appearance and maturation of T-cell subsets during rat thymus ontogeny. *Dev Immunol*, 5(4), 319-331.
- Vidya, M. K., Kumar, V. G., Sejian, V., Bagath, M., Krishnan, G., & Bhatta, R. (2018). Toll-like receptors: Significance, ligands, signaling pathways, and functions in mammals. *Int Rev Immunol*, 37(1), 20-36. doi:10.1080/08830185.2017.1380200
- Vinay, D. S., & Kwon, B. S. (2010). CD11c+CD8+ T cells: two-faced adaptive immune regulators. *Cell Immunol*, 264(1), 18-22. doi:10.1016/j.cellimm.2010.05.010
- Vivier, E., Tomasello, E., Baratin, M., Walzer, T., & Ugolini, S. (2008). Functions of natural killer cells. *Nat Immunol*, 9(5), 503-510. doi:10.1038/ni1582
- von Zur Muhlen, C., von Elverfeldt, D., Bassler, N., Neudorfer, I., Steitz, B., Petri-Fink, A., . . . Peter, K. (2007). Superparamagnetic iron oxide binding and uptake as imaged by magnetic resonance is mediated by the integrin receptor Mac-1 (CD11b/CD18): implications on imaging of atherosclerotic plaques. *Atherosclerosis*, 193(1), 102-111. doi:10.1016/j.atherosclerosis.2006.08.048
- Walling, B. L., & Kim, M. (2018). LFA-1 in T Cell Migration and Differentiation. *Front Immunol*, 9, 952. doi:10.3389/fimmu.2018.00952
- Wang, H., Peters, T., Sindrilaru, A., & Scharffetter-Kochanek, K. (2009). Key role of macrophages in the pathogenesis of CD18 hypomorphic murine model of psoriasis. *J Invest Dermatol*, 129(5), 1100-1114. doi:10.1038/jid.2009.43
- Wang, X. (2009). Cre transgenic mouse lines. *Methods Mol Biol*, 561, 265-273. doi:10.1007/978-1-60327-019-9\_17
- Wang, Y., Gao, H., Shi, C., Erhardt, P. W., Pavlovsky, A., D, A. S., . . . Simon, D. I. (2017). Leukocyte integrin Mac-1 regulates thrombosis via interaction with platelet GPIIb/IIIa. *Nat Commun*, 8, 15559. doi:10.1038/ncomms15559
- Wang, Y., Shu, Y., Xiao, Y., Wang, Q., Kanekura, T., Li, Y., . . . Xiao, R. (2014). Hypomethylation and overexpression of ITGAL (CD11a) in CD4(+) T cells in systemic sclerosis. *Clin Epigenetics*, 6(1), 25. doi:10.1186/1868-7083-6-25
- Watson, P., Jones, A. T., & Stephens, D. J. (2005). Intracellular trafficking pathways and drug delivery: fluorescence imaging of living and fixed cells. *Adv Drug Deliv Rev*, 57(1), 43-61. doi:10.1016/j.addr.2004.05.003
- Watts, G. M., Beurskens, F. J., Martin-Padura, I., Ballantyne, C. M., Klickstein, L. B., Brenner, M. B., & Lee, D. M. (2005). Manifestations of inflammatory arthritis are critically dependent on LFA-1. *J Immunol*, 174(6), 3668-3675.
- Weiskopf, K., Schnorr, P. J., Pang, W. W., Chao, M. P., Chhabra, A., Seita, J., . . . Weissman, I. L. (2016). Myeloid Cell Origins, Differentiation, and Clinical Implications. *Microbiol Spectr*, 4(5). doi:10.1128/microbiolspec.MCHD-0031-2016
- West, M. A., Wallin, R. P., Matthews, S. P., Svensson, H. G., Zaru, R., Ljunggren, H. G., . . . Watts, C. (2004). Enhanced dendritic cell antigen capture via toll-like receptor-induced actin remodeling. *Science*, 305(5687), 1153-1157. doi:10.1126/science.1099153
- Wilson, R. W., Ballantyne, C. M., Smith, C. W., Montgomery, C., Bradley, A., O'Brien, W. E., & Beaudet, A. L. (1993). Gene targeting yields a CD18-mutant mouse for study of inflammation. *J Immunol*, 151(3), 1571-1578.
- Woelbing, F., Kostka, S. L., Moelle, K., Belkaid, Y., Sunderkoetter, C., Verbeek, S., . . . von Stebut, E. (2006). Uptake of *Leishmania major* by dendritic cells is mediated by

- Fcgamma receptors and facilitates acquisition of protective immunity. *J Exp Med*, 203(1), 177-188. doi:10.1084/jem.20052288
- Wohner, N., Muczynski, V., Mohamadi, A., Legendre, P., Proulle, V., Ayme, G., . . . Casari, C. (2018). Macrophage scavenger receptor SR-AI contributes to the clearance of von Willebrand factor. *Haematologica*, 103(4), 728-737. doi:10.3324/haematol.2017.175216
- Wooten, D. K., Xie, X., Bartos, D., Busche, R. A., Longmore, G. D., & Watowich, S. S. (2000). Cytokine signaling through Stat3 activates integrins, promotes adhesion, and induces growth arrest in the myeloid cell line 32D. *J Biol Chem*, 275(34), 26566-26575. doi:10.1074/jbc.M003495200
- Wu, A. A., Drake, V., Huang, H. S., Chiu, S., & Zheng, L. (2015). Reprogramming the tumor microenvironment: tumor-induced immunosuppressive factors paralyze T cells. *Oncoimmunology*, 4(7), e1016700. doi:10.1080/2162402X.2015.1016700
- Wu, H., Prince, J. E., Brayton, C. F., Shah, C., Zeve, D., Gregory, S. H., . . . Ballantyne, C. M. (2003). Host resistance of CD18 knockout mice against systemic infection with *Listeria monocytogenes*. *Infect Immun*, 71(10), 5986-5993.
- Wu, H., Rodgers, J. R., Perrard, X. Y., Perrard, J. L., Prince, J. E., Abe, Y., . . . Ballantyne, C. M. (2004). Deficiency of CD11b or CD11d results in reduced staphylococcal enterotoxin-induced T cell response and T cell phenotypic changes. *J Immunol*, 173(1), 297-306.
- Wu, L., D'Amico, A., Winkel, K. D., Suter, M., Lo, D., & Shortman, K. (1998). RelB is essential for the development of myeloid-related CD8alpha- dendritic cells but not of lymphoid-related CD8alpha+ dendritic cells. *Immunity*, 9(6), 839-847.
- Xiao, T., Takagi, J., Collier, B. S., Wang, J. H., & Springer, T. A. (2004). Structural basis for allostery in integrins and binding to fibrinogen-mimetic therapeutics. *Nature*, 432(7013), 59-67. doi:10.1038/nature02976
- Yakubenia, S., Frommhold, D., Scholch, D., Hellbusch, C. C., Korner, C., Petri, B., . . . Wild, M. K. (2008). Leukocyte trafficking in a mouse model for leukocyte adhesion deficiency II/congenital disorder of glycosylation IIc. *Blood*, 112(4), 1472-1481. doi:10.1182/blood-2008-01-132035
- Yakubenko, V. P., Yadav, S. P., & Ugarova, T. P. (2006). Integrin alphaDbeta2, an adhesion receptor up-regulated on macrophage foam cells, exhibits multiligand-binding properties. *Blood*, 107(4), 1643-1650. doi:10.1182/blood-2005-06-2509
- Yang, J., Zhang, L., Yu, C., Yang, X. F., & Wang, H. (2014). Monocyte and macrophage differentiation: circulation inflammatory monocyte as biomarker for inflammatory diseases. *Biomark Res*, 2(1), 1. doi:10.1186/2050-7771-2-1
- Yang, W., Shimaoka, M., Salas, A., Takagi, J., & Springer, T. A. (2004). Intersubunit signal transmission in integrins by a receptor-like interaction with a pull spring. *Proc Natl Acad Sci U S A*, 101(9), 2906-2911. doi:10.1073/pnas.0307340101
- Yee, N. K., & Hamerman, J. A. (2013). beta(2) integrins inhibit TLR responses by regulating NF-kappaB pathway and p38 MAPK activation. *Eur J Immunol*, 43(3), 779-792. doi:10.1002/eji.201242550
- Yoshimura, A., Naka, T., & Kubo, M. (2007). SOCS proteins, cytokine signalling and immune regulation. *Nat Rev Immunol*, 7(6), 454-465. doi:10.1038/nri2093

- Zamarron, B. F., & Chen, W. (2011). Dual roles of immune cells and their factors in cancer development and progression. *Int J Biol Sci*, 7(5), 651-658.
- Zhang, K., & Chen, J. (2012). The regulation of integrin function by divalent cations. *Cell Adh Migr*, 6(1), 20-29. doi:10.4161/cam.18702
- Zhang, M., March, M. E., Lane, W. S., & Long, E. O. (2014). A signaling network stimulated by beta2 integrin promotes the polarization of lytic granules in cytotoxic cells. *Sci Signal*, 7(346), ra96. doi:10.1126/scisignal.2005629
- Zhang, Q., Lee, W. B., Kang, J. S., Kim, L. K., & Kim, Y. J. (2018). Integrin CD11b negatively regulates Mincle-induced signaling via the Lyn-SIRPalpha-SHP1 complex. *Exp Mol Med*, 50(2), e439. doi:10.1038/emm.2017.256
- Zhang, Q. Q., Hu, X. W., Liu, Y. L., Ye, Z. J., Gui, Y. H., Zhou, D. L., . . . Wang, L. J. (2015). CD11b deficiency suppresses intestinal tumor growth by reducing myeloid cell recruitment. *Sci Rep*, 5, 15948. doi:10.1038/srep15948
- Zhang, Y., Zhang, Y., Gu, W., & Sun, B. (2014). TH1/TH2 cell differentiation and molecular signals. *Adv Exp Med Biol*, 841, 15-44. doi:10.1007/978-94-017-9487-9\_2
- Zhao, M., Sun, Y., Gao, F., Wu, X., Tang, J., Yin, H., . . . Lu, Q. (2010). Epigenetics and SLE: RFX1 downregulation causes CD11a and CD70 overexpression by altering epigenetic modifications in lupus CD4+ T cells. *J Autoimmun*, 35(1), 58-69. doi:10.1016/j.jaut.2010.02.002
- Zhou, M., Todd, R. F., 3rd, van de Winkel, J. G., & Petty, H. R. (1993). Cocapping of the leukoadhesin molecules complement receptor type 3 and lymphocyte function-associated antigen-1 with Fc gamma receptor III on human neutrophils. Possible role of lectin-like interactions. *J Immunol*, 150(7), 3030-3041.
- Zhu, J., Luo, B. H., Xiao, T., Zhang, C., Nishida, N., & Springer, T. A. (2008). Structure of a complete integrin ectodomain in a physiologic resting state and activation and deactivation by applied forces. *Mol Cell*, 32(6), 849-861. doi:10.1016/j.molcel.2008.11.018

## Appendices

### Appendix A. BO44.2 Vector



**CD18 K110:** ca. 10,4 kb

**Plasmid:** pGEM-T Easy Vector 3015 bp (Promega).

**Insert:** CD 18 Exon 3-6 stammt von RP23-95M21 (BAC Klon-BACPAC Resources)  
[www.chori.org/bacpac](http://www.chori.org/bacpac).

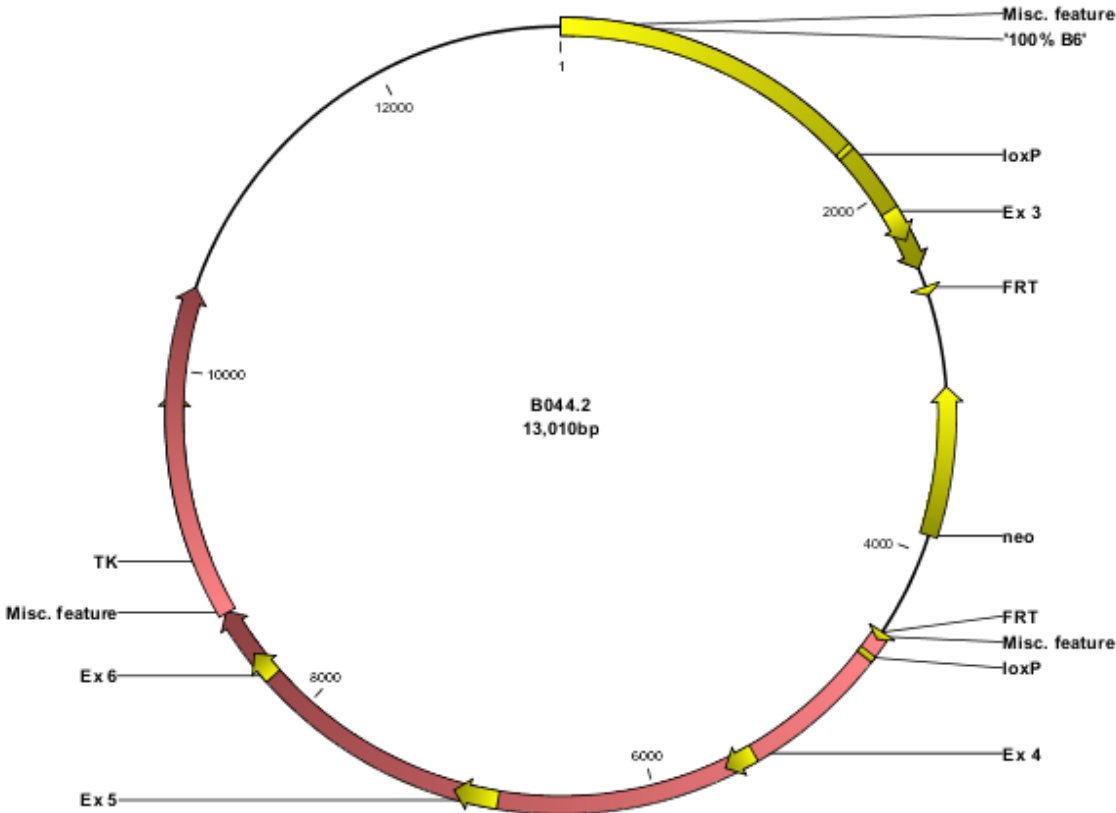
**Teil des Introns und Exon 3** wurden in AgeI-Schnittstellen ligiert.

**FRT-Neo-SV40-FRT** liegt hinter Exon 3 ( Dr. Martin Hafner-Braunschweig), 2,8 kb, wurde in AgeI- und HindIII/SnaBI- Schnittstellen ligiert

**Exon 4-6** : 3,2 Kb wurde in SnaBI-Schnittstelle ligiert; vor Exon 4 liegt ScaI-Schnittstelle für Southernblot-Strategie.

**T.K.** : Thymidin Kinase-Kassette liegt am Ende von Exon 6 (Dr. Jutta Wenk, Bonn), 1,7 kb, in Ascl-Schnittstelle ligiert.

**LoxP-Site:** erste liegt vor Exon 3 und zweite liegt nach FRT-NEO-SV40-FRT vor Exon (LoxP primer- biomers.net).



ORIGIN

1 CCGGTGTCCC TCTGCTAGTG GTGTTTCCGG AGGTGCCACC TTCCAGATTT CTCCTCACTT  
61 CCTATGTCAC CTTATAGTGA GTGACAGGCC ATCAGTGAGG CTCTATCAAG CTGGCTGTCT  
121 CCACTAAACT ATATCTGTGC CCTTGCAGTC TGTCTACTGA AGACTCAGGC AGGATCCATT  
181 ACCAATGTAG TGGTTATTAA ATGGCTCTCT GCCTCTCTCT CTCTCTGTCT CTCTCTGTCT  
241 TTCTGTCTCT CTGTCTCTCG TGTGTGTGTG TGTGTGTGTG TGTGTGTGTG TGTGTGTCTC  
301 CAGACTTCTA CCTCCATTGG TAAATCTGGA GATCTTAATT CTGGTCAGTA GTTTATAACC  
361 ATTATTTTTT CAATCTGATG TTCAAGCTGT CCACATCTGG CCGCTGGACC CCTCTAAGCT  
421 GTTCTGGTGT TCTGGGTGCT GTTCATATGA GCTTTCTTGT CATTTTATTT TGTCCCTCAA  
481 TTTTTCTTAC TCTAGACTGA CTAGCTGTGC TGA CTGTACT CTGGCCTCCC CTCCCCTCGC  
541 CCAAGAGTTA GAGTTAAAGA CCACTCCTAG TATTGTGTTT TATAAAACGA TAGGGAGAAA  
601 AGAAGTGTGT TTGCTGGATG TACAGTCAGG TGTGGGAAGG GGGTGCCTCT GCAGGCCCAG  
661 GCTGAGGCAT CCCTTCCCC TGAGGGACCA GCCACACGAT GGTATAGTAT AGAATAAAGT  
721 TTGTTTCAGG CATGGGGAGG GGGTTTAAGG GAGCAGAGGT GGATAAGGGC AGAGAGAGAG  
781 AGGGAGAGAG AGAGAGAGAG GGAGAGAGAG AGAGAGAGAG AGAGAGAGAG AGAGAGAGAG  
841 AGAGAGAATA TGAATAGTAG TAGAGGTCAG CTATGAGCAC ATGGAGCATG GTTAAGGAG  
901 CAGGAGCAAG GGCAAGAGAG AGGAAGGAGT AAGCAGCCTC CTTCGTAGTG AGTCAGGCAC  
961 ACCTGGCTAT TGCCAGGTAA CTGTGGGGTG GAGCCTAGAC TAAATGCCAA CTTCTAGGCC  
1021 TTCGCATTCT GTGCTACTTT TCTCATCTTC TCCATCCCAC AAGGCTTCTG GCTTCCATCT  
1081 CCAGCAAACA CCCCACCGT AGGCAGAGCT CCAGAGCAGA AAGGCCTGAT GTTGTAACCT  
1141 CTATCCTGTG ACTGAGGGCT GTGGTCCAAG CCTTGGACGA GCCATTCTCA GATGAGCTGG  
1201 CGTTTCTCTC TTCCTCTTGA GTCATTTGGC TCATCTGAAA TGAACAGCCA GATGGCTAGT  
1261 TCTGCATGGA TTACCAGTTA GCTTCTCTTC TCTCTGTTCT CTCTGGTTGC TTGTGTTTCT  
1321 TGAGGACTTA ACACGGGGCT CTGAAGGCCA ATGCAGAACA GAGGGACTCT GGAGGTGATG  
1381 TCTACTGCAT TTCTGGGTTG GTGTTCTTCT GGGTTTACTT TCTGTGAGCA AGCAGGCAAT  
1441 CCCTGGTGCT TTCCAGTACC TTGCAGTTGA GCCAGACCTG CTTTGGATGC AATGGGTTCC  
1501 AGTTCAGGAC CAAGAACAAC CAAATACTTC CATGTCAGAT CCATGGGACC TTTGAAGGGA  
1561 GATGGTGGTC AAGATGGAGG TGCCCTGAGC TCTCCAGTCT CCTCACCAAC TCCATTCCCT  
1621 ATGAACCGAG AGAGACTTGA CCCCTAGATC TTCCCTGCAT CTCAGCAAGA GCTGTCACAT  
1681 AAGCCTAAAG AGATAACTTC GTATAATGTA TGCTATACGA AGTTATACGC GTCACCTTTG  
1741 GAGATGGCAT CTCCCCGGCA TCTCAACAGA CAAAGGCTCT GTTGAGAAAT GGTAAAGAG

## The role of CD18/CD11b on Dendritic cells and Generation of the CD18 fl/fl mouse

1801 TTCTTCTGGT CAACACTGAA ACTCAAGGAT GCTGATTAGC CTTTTGATTG GAGGTAGAGG  
1861 ACCCCATGTC TTTGCTGATG AAGTCAGTGC CCAAATGATA GAGAAAGGTC TATATAGTCT  
1921 ATGCTTTTGG TAACACAGAG CTCTCGGGGA GACCTAGACT CTCTGGGAGT CCGGTCTTCC  
1981 TTAGATGACT ACCGCATCCC ACAGAGATGT CTAAGTGAAC TTTCAAGGGC AGGTAAGAAG  
2041 GAAACAGGGC TGGATCCCAC TATTCTAGCC TATGCCCTCT GCCTGACCTC AGATCCCTCC  
2101 TCTAGAACTT CACTGGACCA GGAGAACCTG ACTCCTTGCG CTGTGACACA CGAGCACAGC  
2161 TGCTGCTGAA GGGTTGTCCA GCCGATGATA TCATGGACCC CAGGAGCATC GCTAATCCTG  
2221 AGTTCGACCA ACGGGGGCAA CGGAAACAGC TATCTCCACA AAAAGTGACA CTTTACTTGC  
2281 GACCAGGTAG GTATGGAACC TGGTTGGAAT GTGTGTGTGT GTGTGGCGGG GGGGGGGGGG  
2341 GGTGGAACAT CCCAGAGGGT AGGGAGAAGA ACCATGGCCA TTGACATGAA CCCGCATGGC  
2401 AATTACCAGC CACAAGTTGC TATGATTTCA TAAGGTTAGA AATATTGGGT TGTAATACGA  
2461 CTCACTAGTG GGCAGATCTT CGAATGCATC GCGCGCACCG TACGTCTCGA GGAATTCCTG  
2521 CAGGATTTAA GGCCTTGACT AGAGGGTACC TCGAGAAGTT CCTATTCCGA AGTTCCTATT  
2581 CTCTAGAAAG TATAGGAACT TCGGATAAATT CTAGAGTCAG CTTCTGATGG AATTAGAACT  
2641 TGGCAAAACA ATACTGAGAA TGAAGTGTAT GTGGAACAGA GGCTGCTGAT CTCGTTCTTC  
2701 AGGCTATGAA ACTGACACAT TTGGAAACCA CAGTACTTAG AACCACAAAG TGGGAATCAA  
2761 GAGAAAAACA ATGATCCCAC GAGAGATCTA TAGATCTATA GATCATGAGT GGGAGGAATG  
2821 AGCTGGCCCT TAATTTGGTT TTGCTTGTTT AAATTATGAT ATCCAACAT GAAACATTAT  
2881 CATAAAGCAA TAGTAAAGAG CCTTCAGTAA AGAGCAGGCA TTTATCTAAT CCCACCCAC  
2941 CCCCACCCCC GTAGCTCCAA TCCTTCCATT CAAAATGTAG GTRACTCTGTT CTCACCCCTC  
3001 TTAACAAAGT ATGACAGGAA AACTTCCAT TTTAGTGGAC ATCTTTATTG TTAAATAGAT  
3061 CATCAATTTT TGCAGACTTA CAGCGGATCG ATCCCCTCAG AAGAACTCGT CAAGAAGGCG  
3121 ATAGAAGGCG ATGCGCTGCG AATCGGGAGC GCGGATACCG TAAAGCACGA GGAAGCGGTC  
3181 AGCCCATTCG CCGCCAAGCT CTTCAGCAAT ATCACGGGTA GCCAACGCTA TGTCTGATA  
3241 GCGGTCCGCC ACACCCAGCC GGCCACAGTC GATGAATCCA GAAAAGCGGC CATTTTCCAC  
3301 CATGATATTC GGCAAGCAGG CATCGCCATG GGTACGACG AGATCATCGC CGTCGGGCAT  
3361 GCGCGCCTTG AGCCTGGCGA ACAGTTCGGC TGGCGGAGC CCCTGATGCT CTTCGTCCAG  
3421 ATCATCCTGA TCGACAAGAC CGGCTTCCAT CCGAGTACGT GCTCGCTCGA TCGATGTTT  
3481 CGCTTGGTGG TCGAATGGGC AGGTAGCCGG ATCAAGCGTA TGCAGCCGCC GCATTGCATC  
3541 AGCCATGATG GATACTTTCT CGGCAGGAGC AAGGTGAGAT GACAGGAGAT CCTGCCCCGG  
3601 CACTTCGCCC AATAGCAGCC AGTCCCTTCC CGCTTCAGTG ACAACGTCGA GCACAGCTGC

## The role of CD18/CD11b on Dendritic cells and Generation of the CD18 fl/fl mouse

3661 GCAAGGAACG CCCGTCGTGG CCAGCCACGA TAGCCGCGCT GCCTCGTCCT GCAGTTCATT  
3721 CAGGGCACCG GACAGGTCGG TCTTGACAAA AAGAACC GGGG CGCCCCTGCG CTGACAGCCG  
3781 GAACACGGCG GCATCAGAGC AGCCGATTGT CTGTTGTGCC CAGTCATAGC CGAATAGCCT  
3841 CTCCACCCAA GCGGCCGGAG AACCTGCGTG CAATCCATCT TGTTC AATGG CCGATCCCAT  
3901 ATTGGCTGCA GGTTCGAAAGG CCCGGAGATG AGGAAGAGGA GAACAGCGCG GCAGACGTGC  
3961 GCTTTTGAAG CGTGCAGAAT GCCGGGCCTC CGGAGGACCT TCGGGCGCCC GCCCCGCCCC  
4021 TGAGCCCGCC CCTGAGCCCG CCCCCGGACC CACCCCTTCC CAGCCTCTGA GCCCAGAAAAG  
4081 CGAAGGAGCA AAGCTGCTAT TGGCCGCTGC CCCAAAGGCC TACCCGCTTC CATTGCTCAG  
4141 CGGTGCTGTC CATCTGCACG AGACTAGTGA GACGTGCTAC TTCCATTTGT CACGTCTCGC  
4201 ACGACGCGAG CTGCGGGGCG GGGGGGAACT TCCTGACTAG GGGAGGAGTA GAAGGTGGCG  
4261 CGAAGGGGCC ACCAAAGAAC GGAGCCGGTT GCGCCTACC GGTGGATGTG GAATGTGTGC  
4321 GAGGCCAGAG GCCACTTGTG TAGCGCCAAG TGCCCAGCGG GGCTGCTAAA GCGCATGCTC  
4381 CAGACTGCCT TGGGAAAAGC GCCTCCCCTA CCCGGTAGAA TTGACCTGCA GGGGCCCTCG  
4441 ATATCAAGCT CCTTGACTAG AGGGTACCTC GAGAAGTTCC TATTCCGAAG TTCCTATTCT  
4501 CTAGAAAGTA TAGGAACTTC AGATCTGGCC TCGTGGGGCA GGTAGTGGGG AGAGCCTGAT  
4561 AGTTTTCTTT ACTGTGTGCA ATGTTTTCCC ACAGGACAAC ATA ACTTCGT ATAATGTATG  
4621 CTATACGAAG TTATAAGCTT TATCATTATC AACTGGCTCT GAAATTC TTT ATTGGCATCT  
4681 TGTA AATTGT TATTTTATTG ATACATAAAT CTAATTGGTT AACTTTAAGA TTAAGAGTCT  
4741 AATTTTGCTT GGCAGTGGTG GCACATGCCT TTAATCCCAG CACTTAGGAG GCAGAGGCAG  
4801 ATGGATTTCT GAGTTCAAGG CCAGCCTGGT CTACAGAGTG AGTTCCAGGA CAGCCTGGGC  
4861 TATACAGAGA AACCTATTT CAAAAAGCCA AAAAAAAAAA AAAGTCTGAT TTTACCAGAG  
4921 TATTGGGTGT TGTGAGATGC AACTGCGAGG TTGGTGGTTC TATTTGGCCA CTGGAGTGTG  
4981 GGATCTCTGG TTACAGGGGA TTATAGCAGA AAGGGA ACTA GTGGTTCCTT GGACAAGCAA  
5041 GCCAGATGCT GCAGGTGGGG GGGGGGCAGG TAGCTGCAGA GAGTTGACAG GTTCATTTTT  
5101 TAATATTTCC ACAATAGATG GCACCCAATG TGGGGCACCT GACTATTTCT AGCACCATAA  
5161 TCTGGGTGTC TAGGCTTCCA ACTCATGAAT CTGCACCTTA CAGAAACCCT CCACCATCCA  
5221 GGCATTCTTG TACCTGGGGT GAGCCTACTT ATCTGAGTTC AAACCTACCC TTAAGAAGCT  
5281 TTACGTAAGT ACTTGTCTTG TGTCTGGTC ACAACCCCTT CCAGGTCATA GGAAATGGGG  
5341 GAGACAATAG GAATCTGGGG ACTGGGTGAG AGCCAAGACT CCAGCCAGGC TCAGAGTGTC  
5401 CCTTGCTTTT CTCTGACACG CAGGACAGGC TGCCGCATTC AATGTGACTT TCCGGCGGGC  
5461 CAAGGGATAC CCCATTGATC TGTACTACCT CATGGATCTC TCCTACTCCA TGCTTGATGA

## The role of CD18/CD11b on Dendritic cells and Generation of the CD18 fl/fl mouse

5521 CCTCAACAAC GTCAAGAAGC TGGGCGGGGA CTTGCTGCAG GCCCTCAACG AGATCACCGA  
5581 GTCTGGCCGC ATCGGTGAGA CCTGCAGTGC ACACACTCCT TTCAACCTTG GGAACTCCCT  
5641 GCCGCCCCAC ACCTCCATGT ACGGTGGATC CGCAGAGGCA GAAGCTGGGA GCTGCATAGG  
5701 CAATGTTTCGT GGGGCCAGAG TTCATCCTGA ATCCTTACCA GGGGCTGTCC TTGGTCACAG  
5761 GCTGCTAAGA CCTCTCTCTC TCTCTCTCTA GTTTATATTT TAATGTTTAA AAGGCAAAAAG  
5821 TCCTACAATG CTAATTACTA AAAAGTATAT CTACCTTAAC ACAGCAACCA TGCATTAACA  
5881 GAATAGTGGA AGTAAACTAC AGGGCAGGGG TCACAGGGCT AGGGCCACTG GGCAAGGGTC  
5941 ACAGGGCAGG AGTCATAGGG TGAGAATTAC AACACTGACC AATACCACCA AGCATGTGGG  
6001 ACAAGGGAAC AGGGTACACC TACTCACTCC AGAACATCCC TCTGCCTCAT CGTCTATGTT  
6061 TAAGGATGCC CACATGAACA CGAACACTGG ATGCAAGCTC ATATATTCTT CTTTTTTTTT  
6121 TTTAAGACTT TTTAATTTCA TTTATATGAG TACACTGTAG CTGTCTTCAG ACACACCCGA  
6181 AGAGGGCATC AAATCCCATG ACAGATGGTT GTGAGCCACC ATGTGGTTGC TGGGAATTGA  
6241 ACTCAGAACC TCTGAAAGAG CAGTCAGTGC TCTTACCCGC TGAGCCATCT CTCCAGCCCC  
6301 CATATATTCT TGTGTGTTCA TACATTCACA TGTGTACATT CGTGTTTACA CATGTCCAAG  
6361 ATCCCATACA CAAGCACATT TGCACATGTG CAAGCAAGCA CATGTACAAA TGCCTAGTCA  
6421 TACCTGTGTG CCTGTATGCC TGCATACACA AGACCACATG TATATATACA GGTACTCGCA  
6481 TGCCACCCA CACTCATGGT CACACCTGTC CATGACCCCA TACATATACA TGCTCTGTCA  
6541 CATGCACACA CATGTTTGTA CATGGCCTCA CATATACTCA GCCGCACATG GCTACACACA  
6601 TGCTTGACC ACACGCTCAG CTATCATGTT CACACAACCA TCATCTTGCT TTCTCCCTTG  
6661 TTTGAGAAAC TGAGGCTTGG TCCTTAGTCC ACTGGAAGGT TCACTGTTCAT GCCTGGAGCC  
6721 CTGCCTGCTG CCTTGTCCCT GTGCCCTCCA GCCTCTGTTG TATATCCCTT GGACTIONCAGG  
6781 TCTTCCAGT CCTGGTGTCT GCTTCTGTCT GCTGTCCCC TGCCATACAT CATGTACCCT  
6841 TAGGCTTTGG GTCGTTTGTG GACAAGACGG TGCTGCCTTT TGTTAACACC CATCCTGAGA  
6901 AGCTGAGGAA CCCATGTCCC AACAAGGAGA AGGCCTGCCA GCCCCCATTG GCCTTTCGGC  
6961 ACGTGCTCAA GTTAACCGAC AACTCCAACC AGTTTCAGAC AGAGGTCGGC AAGCAACTGA  
7021 TTTCCGAAA CCTGGACGCC CCTGAGGGTG GGCTGGATGC CATAATGCAA GTTGCTGCAT  
7081 GTCCGGTGAG GCCATTGTCC CTGTTTCTGAT TTCCCAACTT CCTCAAATC AGGGCCTTCA  
7141 CCAGTGCCGT GGTGGTGGGT CTGTTTCTGAC ACTCACCCCA TCTGGTCCCA TGCTGTACC  
7201 CCGGGTCTCA GAAGGGCAGC CTCCGTGGGC CACATCACTC CCAGGCATAG AGAAGGAAGA  
7261 GCCCTGAAAA CACCCACCCA TGCCCGTGCT AACTGACAGC CTTCATAGCT CTCTGTGAG  
7321 CCAGGCTACC CAGCAGCAGG TCTTCTGGTT CCTAAAGCCT TTTCCCTCTC AGATCAAGAG

## The role of CD18/CD11b on Dendritic cells and Generation of the CD18 fl/fl mouse

7381 TGTGAGAACT GTTGTGGGAC AAAGGAACAG GGGCCCATGT CACCTCAATC ACATCCTGCC  
7441 TGTCGGCTCC AGATTGTGTT TATCAAGTGG TCACTGCAGC AAGCCAATCC CACCCCAGCC  
7501 TGGCTCTCAG CTCTCTCACT TTGCTGGGTT CACGCAGTGG GCACACACAC TCTACATGTG  
7561 TGTTGGACTA GGGTAGGATA CATGGGTGCA GCAAGTGTAT GCTACTTCAA TGGTTCCAGG  
7621 CCCTCGGCTC TCCTGTGGAT GTCCCTTGGT CCCTTCTTTT GTGGCTGGGA GGTGTTTGCA  
7681 TTTTAACATA CAAGGCCATA CTCTTTTCCT TTCATGACTG TGTGCTGGA ATCTAGTTTC  
7741 AGGTCTGAAG AGGGTTGCAA AGACATTTCT CTTTAGATTC AGATGTGTTT CTGTTCTTAC  
7801 CTCATACTGC TGCAGGGCAT GCTGGGAGTT GACGGCTTTG GCACTTCCTT GGCCTGGAT  
7861 TGGGGCTCTA TCTTCCTCTG TCTGTCTGTC TGTCTGTCTG TCTGTCTGTC TGTCTGTCTG  
7921 TCGTATCTGG GGGGTGTCTG TTTGTTTCCA TGTTTCTGTC TCTCTTTATA TATATATATC  
7981 TGTCTCTCTC TTTATCTCTA TCTGTTTTTA TGTCTTGTTG TCTCTGTCTC TATGTCTCTG  
8041 TGTCTCTATC ACTCTGTGTG TGTGTGTCTC TTTGTATGTA TGTCTCTGTC TGTGTTGTCTG  
8101 TCTCTTTCTC TGTCTTTCTA TCTCTCTGTG TCTCTCTTTC TGTCTCTGTC TCTCTCACTC  
8161 TCCCTCACAC ACACACAACCT CTTCTCCCCT GAGGGCCCCA GGGGGAAACC AAGGCAGGTA  
8221 ACCCCTGGAT GCCTTCTTCC CAGGAGGAAA TTGGCTGGCG CAATGTCACG AGGCTGCTGG  
8281 TGTTTGCCAC AGACGATGGC TTCCACTTTG CTGGTGATGG CAAACTGGGT GCCATCCTGA  
8341 CCCCCAATGA TGGCCGCTGC CACCTGGAGG ATAACATGTA CAAGAGGAGC AATGAGTTCG  
8401 TGAGTGCTCT GCCTGCCTTG GCACGCCCCG GTACCAAGGC TGGTTACATA AACATAAAGG  
8461 TTACAGGAGT GACAACGGGA CAGGCTGAGA GCAGAGTCAC ATTGCCCAAT CACACAAACA  
8521 GAACCCAGAC TCCTCCTAAC ACGAATAACA AATCACAGAT GCAGTCCCAG AGACCCTGGT  
8581 GATAACATGA GACTCCCAGC ACCCACATCA GCCTGCAGGG CAGTCTCTAC CCTGATCCTC  
8641 ATGGCAGAGG GCCTCACACA GGCGCGCCTC GAGCAGTGTG GTTTTGCAAG AGGAAGCAAA  
8701 AAGCCTCTCC ACCCAGGCCT GGAATGTTTC CACCCAATGT CGAGCAAACC CCGCCAGCG  
8761 TCTTGTCATT GCGAATTCG AACACGCAGA TGCAGTCGGG GCGGCGCGGT CCGAGGTCCA  
8821 CTTCGCATAT TAAGGTGACG CGTGTGGCCT CGAACACCGA GCGACCCTGC AGCGACCCGC  
8881 TTAACAGCGT CAACAGCGTG CCGCAGATCT TGGTGGCGTG AAACCTCCCGC ACCTCTTCGG  
8941 CCAGCGCCTT GTAGAAGCGC GTATGGCTTC GTACCCCGGC CATCAACACG CGTCTGCGTT  
9001 CGACCAGGCT GCGCGTTCTC GCGGCCATAG CAACCGACGT ACGGCGTTGC GCCCTCGCCG  
9061 GCAGCAAGAA GCCACGGAAG TCCGCCCGGA GCAGAAAATG CCCACGCTAC TCGGGGTTTA  
9121 TATAGACGGT CCCCACGGGA TGGGGAAAAC CACCACCACG CAACTGCTGG TGGCCCTGGG  
9181 TTCGCGCGAC GATATCGTCT ACGTACCCGA GCCGATGACT TACTGGCGGG TGCTGGGGGG

## The role of CD18/CD11b on Dendritic cells and Generation of the CD18 fl/fl mouse

9241 TTCCGAGACA ATCGCGAACA TCTACACCAC ACAACACCGC CTCGACCAGG GTGAGATATC  
9301 GGCCGGGGAC GCGGCGGTGG TAATGACAAG CGCCCAGATA ACAATGGGCA TGCCTTATGC  
9361 CGTGACCGAC GCCGTTCTGG CTCCTCATAT CGGGGGGGAG GCTGGGAGCT CACATGCCCC  
9421 GCCCCGGGCC CTCGCCCTCA TCTTCGACCG CCATCCCATC GCCGCCCTCC TGTGCTACCC  
9481 GGCCGCGCGG TACCTTATGG GCAGCATGAC CCCCAGGCC GTGCTGGCGT TCGTGGCCCT  
9541 CATCCCGCCG ACCTTGCCCG GCACCAACAT CGTGCTTGGG GCCCTTCCGG AGGACAGACA  
9601 CATCGACCGC CTGGCCAAAC GCCAGCGCCC CGGCGAGCGG CTGGACCTGG CTATGCTGGC  
9661 TGCGATTTCG CGCGTTTACG GGCTACTTGC CAATACGGTG CGGTATCTGC AGTGCGGCGG  
9721 GTCGTGGCGG GAGGACTGGG GACAGCTTTC GGGGACGGCC GTGCCGCCCC AGGGTGCCGA  
9781 GCCCCAGAGC AACGCGGGCC CACGACCCCA TATCGGGGAC ACGTTATTTA CCCTGTTTCG  
9841 GGCCCCGAG TTGCTGGCCC CCAACGGCGA CCTGTATAAC GTGTTTGCCT GAGCCTTGA  
9901 CGTCTTGCC AAACGCCTCC GTTCCATGCA CGTCTTTATC CTGGATTACG ACCAATCGCC  
9961 CGCCGGCTGC CGGGACGCC TGCTGCAACT TACCTCCGGG ATGGTCCAGA CCCACGTCAC  
10021 CACCCCCGGC TCCATAACCGA CGATATGCGA CCTGGCGCGC ACGTTTGCCC GGGAGATGGG  
10081 GGAGGCTAAC TGAAACACGG AAGGAGACAA TACCGGAAGG AACCCGCGCT ATGACGGCAA  
10141 TAAAAAGACA GAATAAAACG CACGGGTGTT GGGTCGTTT TCCATAAACG CGGGGTTTCG  
10201 TCCCAGGGCT GGCACCTCTGT CGATACCCCA CCGAGACCCC ATTGGGGCCA ATACGCCCGC  
10261 GTTTCTTCTT TTTCCCCACC CCACCCCCA AGTTCCGGTG AAGGCCCAGG GCTCGCAGCC  
10321 AACGTCGGGG CGGCAGGCC TGCCATAGCC ACTGGCCCCG TGGGTTAGGG ACGGGTCCC  
10381 CCATGGGGAA TGGTTTATGG TTCGTGGGGG TTATTATTTT GGGCGTTGCG TGGGGTCAGG  
10441 TCCACGACCC AAGCTGGCGC GCCTACGTAA TCTTGAATCG AATTCCCGCA ACTACGTCAG  
10501 GTGGCACTTT TCGGGGAAAT GTGCGCGGAA CCCCTATTTG TTTATTTTTTC TAAATACATT  
10561 CAAATATGTA TCCGCTCATG AGACAATAAC CCTGATAAAT GCTTCAATAA TATTGAAAAA  
10621 GGAAGAGTAT GAGTATTCAA CATTTCCGTG TCGCCCTTAT TCCCTTTTTT GCGGCATTTT  
10681 GCCTTCCTGT TTTTGCTCAC CCAGAAACGC TGGTGAAAAGT AAAAGATGCT GAAGATCAGT  
10741 TGGGTGCACG AGTGGGTTAC ATCGAACTGG ATCTCAACAG CGGTAAGATC CTTGAGAGTT  
10801 TTCGCCCCGA AGAACGTTCT CCAATGATGA GCACTTTTAA AGTTCTGCTA TGTGGCGCGG  
10861 TATTATCCCG TGTTGACGCC GGGCAAGAGC AACTCGGTG CCGCATAAC TATTCTCAGA  
10921 ATGACTTGGT TGAGTACTCA CCAGTCACAG AAAAGCATCT TACGGATGGC ATGACAGTAA  
10981 GAGAATTATG CAGTGCTGCC ATAACCATGA GTGATAACAC TGCGGCCAAC TTACTIONCTGA  
11041 CAACGATCGG AGGACCGAAG GAGCTAACCG CTTTTTTTGCA CAACATGGGG GATCATGTAA

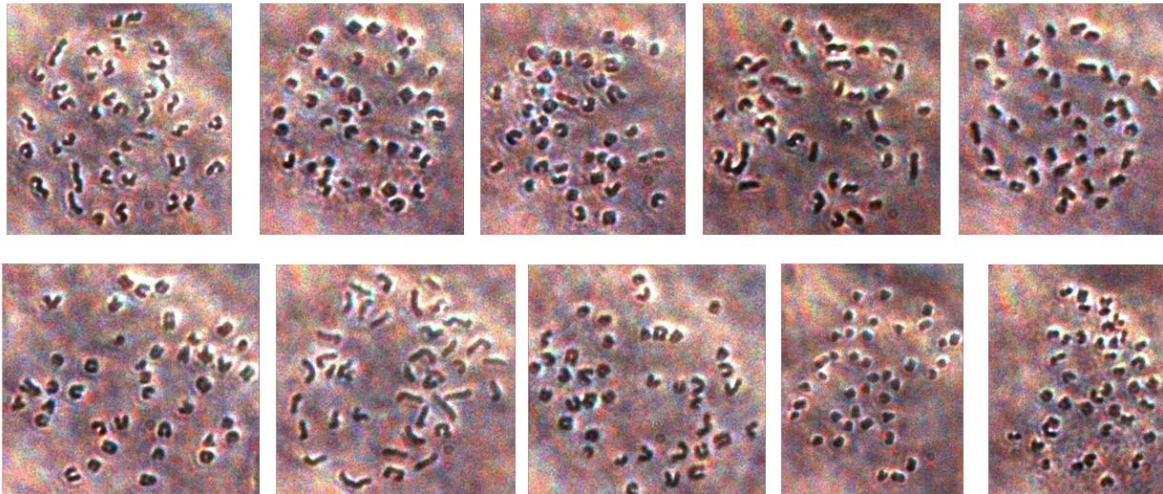
## The role of CD18/CD11b on Dendritic cells and Generation of the CD18 fl/fl mouse

11101 CTCGCCTTGA TCGTTGGGAA CCGGAGCTGA ATGAAGCCAT ACCAAACGAC GAGCGTGACA  
11161 CCACGATGCC TGTAGCAATG GCAACAACGT TGCGCAAACCT ATTAACCTGGC GAACTACTTA  
11221 CTCTAGCTTC CCGGCAACAA TTAATAGACT GGATGGAGGC GGATAAAGTTF GCAGGACCAC  
11281 TTCTGCGCTC GGCCCTTCCG GCTGGCTGGT TTATTGCTGA TAAATCTGGA GCCGGTGAGC  
11341 GTGGGTCTCG CGGTATCATT GCAGCACTGG GGCCAGATGG TAAGCCCTCC CGTATCGTAG  
11401 TTATCTACAC GACGGGGAGT CAGGCAACTA TGGATGAACG AAATAGACAG ATCGCTGAGA  
11461 TAGGTGCCTC ACTGATTAAG CATTGGTAAC TGTCAGACCA AGTTTACTCA TATATACTTT  
11521 AGATTGATTT ACCCCGGTTG ATAATCAGAA AAGCCCCAAA AACAGGAAGA TTGTATAAGC  
11581 AAATATTTAA ATTGTAAACG TTAATATTTT GTTAAAATTC GCGTTAAATF TTTGTAAAT  
11641 CAGCTCATTT TTTAACCAAT AGGCCGAAAT CGGCAAAATC CCTTATAAAT CAAAAGAATA  
11701 GCCCGAGATA GGGTTGAGTG TTGTTCCAGT TTGGAACAAG AGTCCACTAT TAAAGAACGT  
11761 GGACTIONAAC GTCAAAGGGC GAAAAACCGT CTATCAGGGC GATGGCCAC TACGTGAACC  
11821 ATCACCCAAA TCAAGTTTTT TGGGGTCGAG GTGCCGTAAA GCACTAAATC GGAACCCTAA  
11881 AGGGAGCCCC CGATTTAGAG CTTGACGGGG AAAGCGAACG TGGCGAGAAA GGAAGGGGAA  
11941 AAAGCGAAAG GAGCGGGCGC TAGGGCGCTG GCAAGTGTAG CCGTCACGCT GCGCGTAACC  
12001 ACCACACCCG CCGCGCTTAA TGCGCCGCTA CAGGGCGCGT AAAAGGATCT AGGTGAAGAT  
12061 CCTTTTTGAT AATCTCATGA CCAAATCCC TTAACGTGAG TTTTCGTTCC ACTGAGCGTC  
12121 AGACCCCGTA GAAAAGATCA AAGGATCTTC TTGAGATCCT TTTTTTCTGC GCGTAATCTG  
12181 CTGCTTGCAA ACAAAAAAAC CACCGCTACC AGCGGTGGTT TGTTTGCCGG ATCAAGAGCT  
12241 ACCAACTCTT TTTCCGAAGG TAACTGGCTT CAGCAGAGCG CAGATACCAA ATACTGTTCT  
12301 TCTAGTGTAG CCGTAGTTAG GCCACCACTT CAAGAACTCT GTAGCACCGC CTACATACCT  
12361 CGCTCTGCTA ATCCTGTTAC CAGTGGCTGC TGCCAGTGGC GATAAGTCGT GTCTTACCGG  
12421 GTTGACTCA AGACGATAGT TACCGGATAA GGCGCAGCGG TCGGGCTGAA CGGGGGGTTT  
12481 GTGCACACAG CCCAGCTTGG AGCGAACGAC CTACACCGAA CTGAGATACC TACAGCGTGA  
12541 GCTATGAGAA AGCGCCACGC TTCCCGAAGG GAGAAAAGCG GACAGGTATC CGGTAAGCGG  
12601 CAGGGTCGGA ACAGGAGAGC GCACGAGGGA GCTTCCAGGG GGAAACGCCT GGTATCTTTA  
12661 TAGTCTGTC GGGTTTCGCC ACCTCTGACT TGAGCGTCGA TTTTTGTGAT GCTCGTCAGG  
12721 GGGGCGGAGC CTATGGAAAA ACGCCAGCAA CGCGGCCTTT TTACGGTTCC TGGCCTTTTG  
12781 CTGGCCTTTT GCTCACATGT AATGTGAGTT AGCTCACTCA TTAGGCACCC CAGGCTTTAC  
12841 ACTTTATGCT TCCGGCTCGT ATGTTGTGTG GAATTGTGAG CGGATAACAA TTTACACAG  
12901 GAAACAGCTA TGACCATGAT TACGCCAAGC TACTCCAACG CGTTGGGAGC TCTCCCATAT

12961 GGTCGACCTG CAGGCGGCCG CGAATTCACT AGTGATTGAC CGTGACGTCA

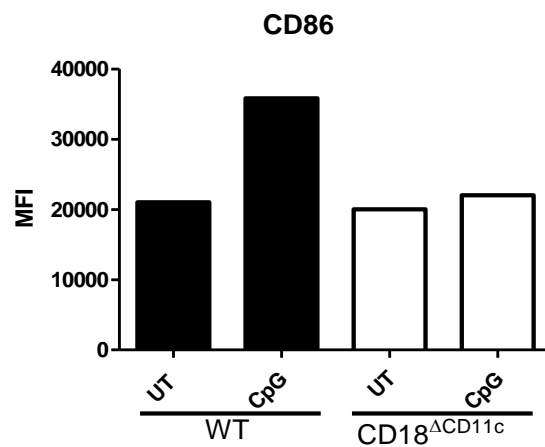
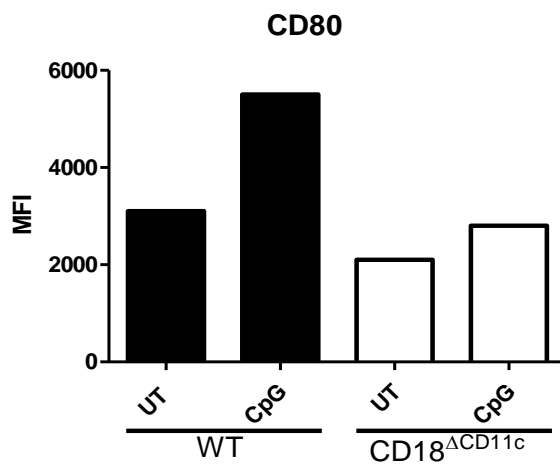
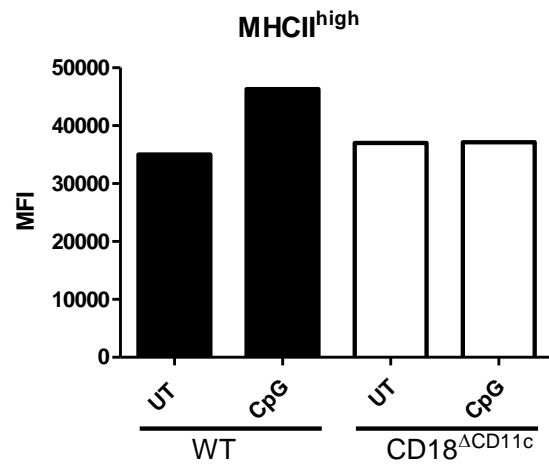
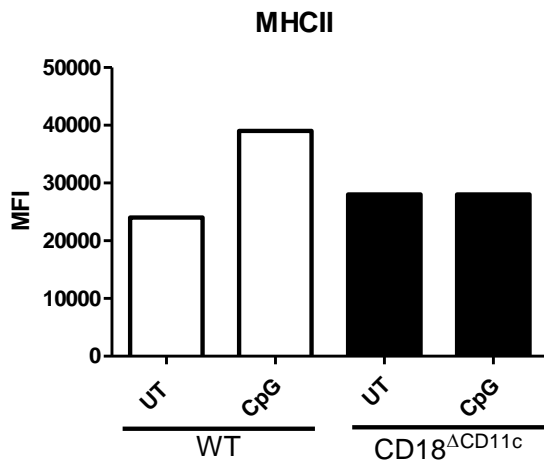
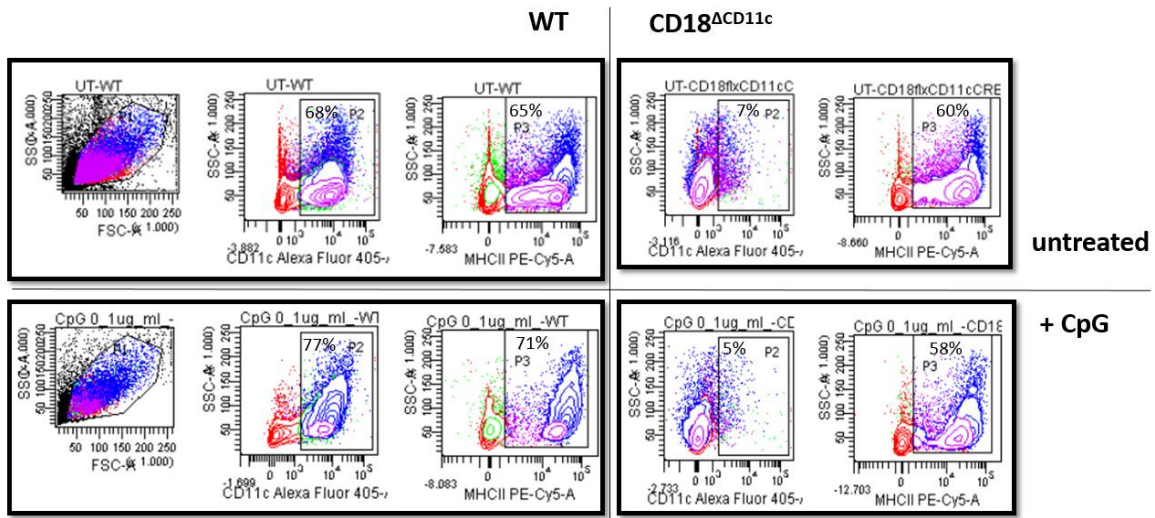
//

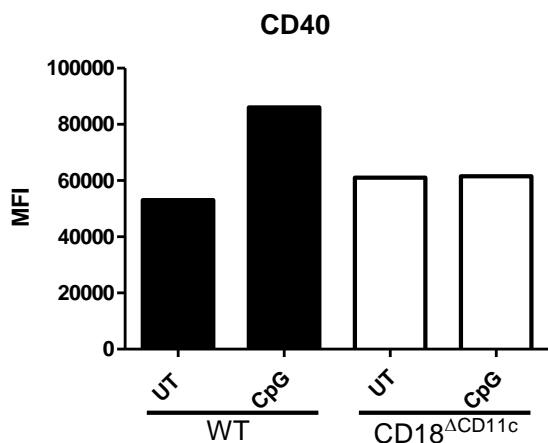
## Appendix B. Karyotyping of recombinant ES.



Appendix B. Karyotyping of the recombined P3-10G ES clone. Karyotypes were counted for both clones (P.1, 9F and P.3,10G), 10 cells per clone ( here only karyotypes for the P3-10G shown as an example). Hundred percent of the nuclei (10 out of 10) showed the expected karyotype of 40 chromosomes.

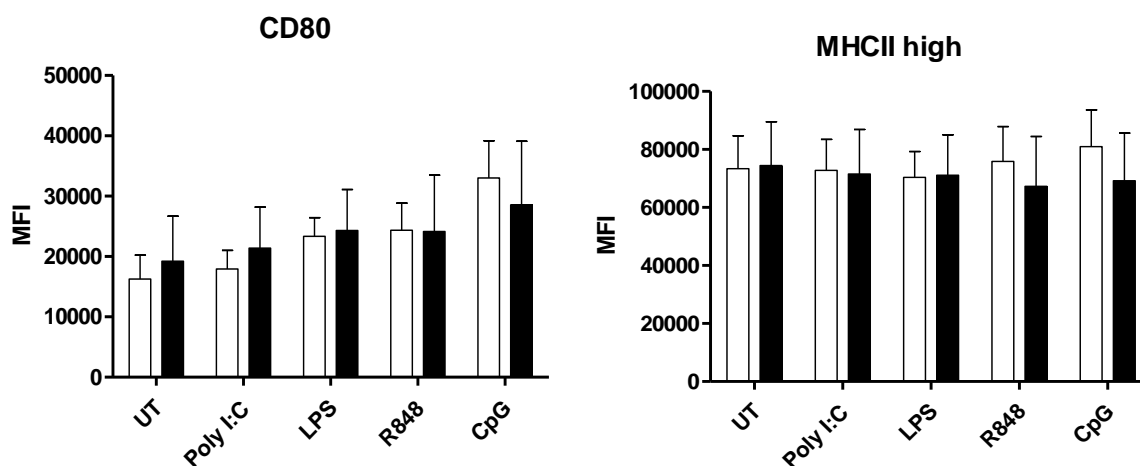
## Appendix C. CD18<sup>ΔCD11c</sup> BM-DC activation.

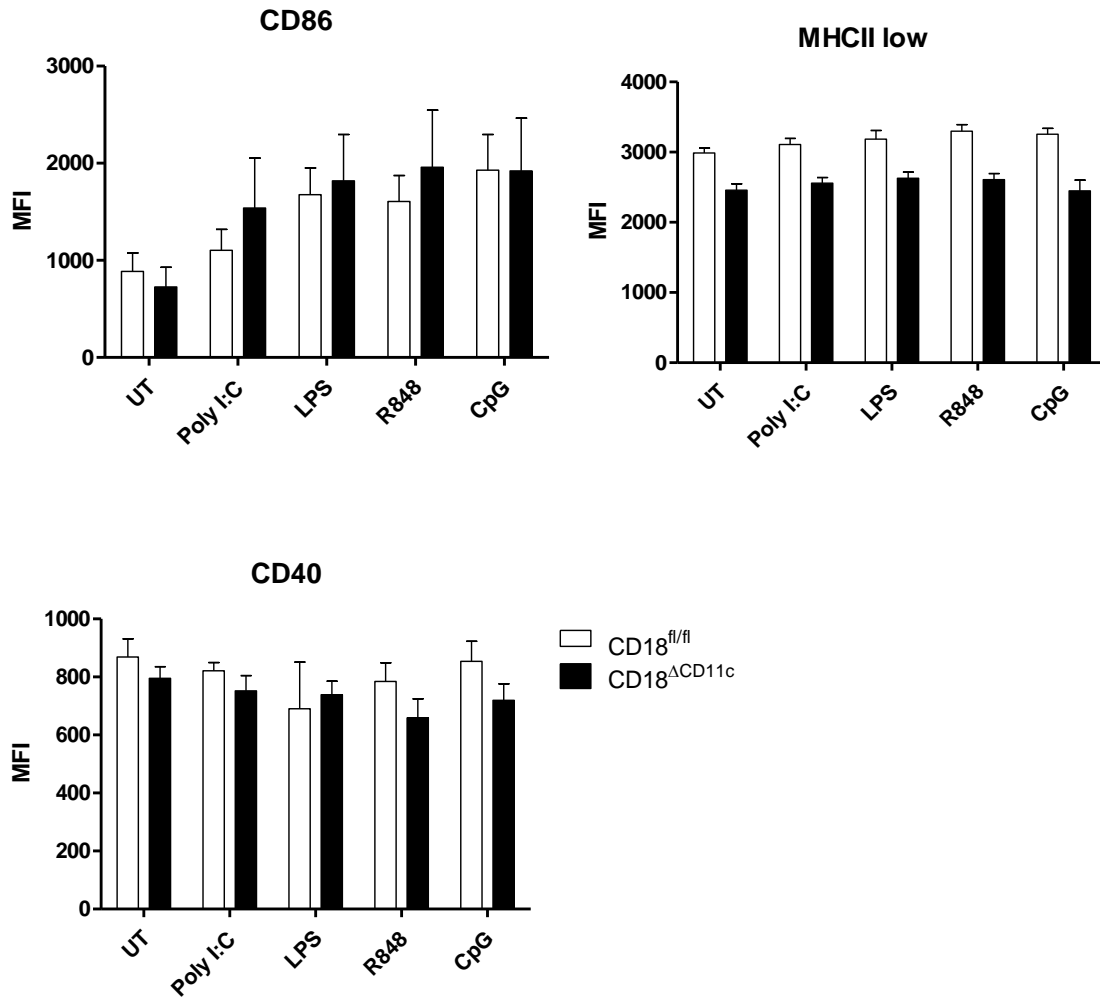




Appendix C. CD18<sup>ΔCD11c</sup> BM-DC stimulated overnight with CpG lost the capacity to upregulate activation markers. GM-SCF cultured BM-DC derived from the CD18<sup>ΔCD11c</sup> and CD18<sup>fl/fl</sup> control mice were exposed overnight to CpG (100ng/ml) and subsequently analysed by flow cytometry for the expression of MHC-II, CD80, CD86 and CD40. A representative dot blot shows the expression of CD11c and MHC-II in WT vs CD18<sup>ΔCD11c</sup> BM-DC with or without the stimulus. The marker expression was validated as mean fluorescent intensity (MFI) and presented in the 5 separate graphs (n=1).

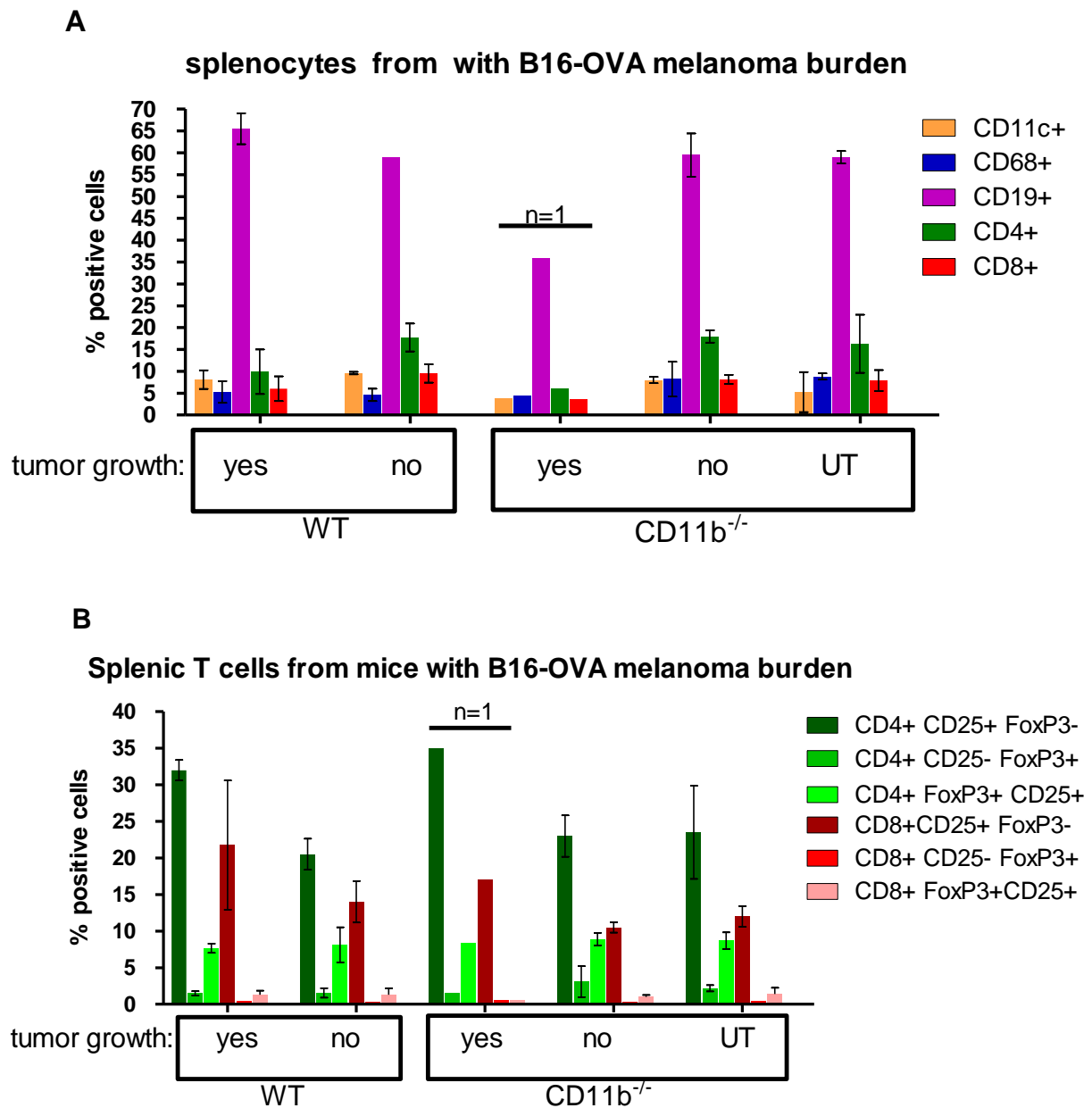
### Appendix D. CD18<sup>ΔCD11c</sup> splenic DC activation.





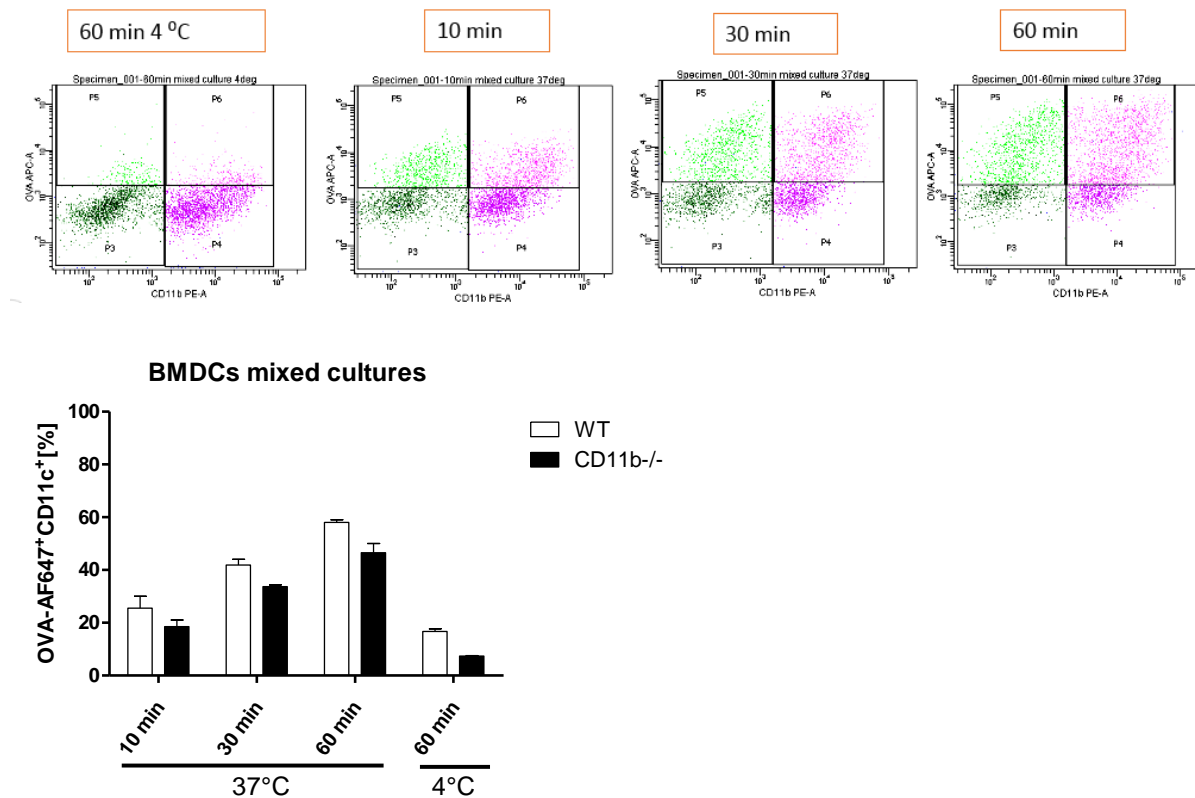
Appendix C. CD18<sup>ΔCD11c</sup> splenic dendritic cells change the expression of activation markers upon TLR-ligand stimulation to the same extent as the control CD18<sup>fl/fl</sup> except for MHC-II. Pan Dendritic Cell Kit (Miltenyi Biotec) isolated DC from the spleen were stimulated overnight with various TLR ligands (PolyI:C, LPS, R848, CpG) and subsequently the expression of the activation markers was evaluated as mean fluorescent intensity. Following markers were investigated: MHC-II<sup>low</sup>, MHC-II<sup>high</sup>, CD80, CD86, and CD40. Depicted bars represent mean with SEM (n=5).

## Appendix E. Analysis of the splenocytes from the CD11b<sup>-/-</sup> mice with B16-OVA Melanoma burden.



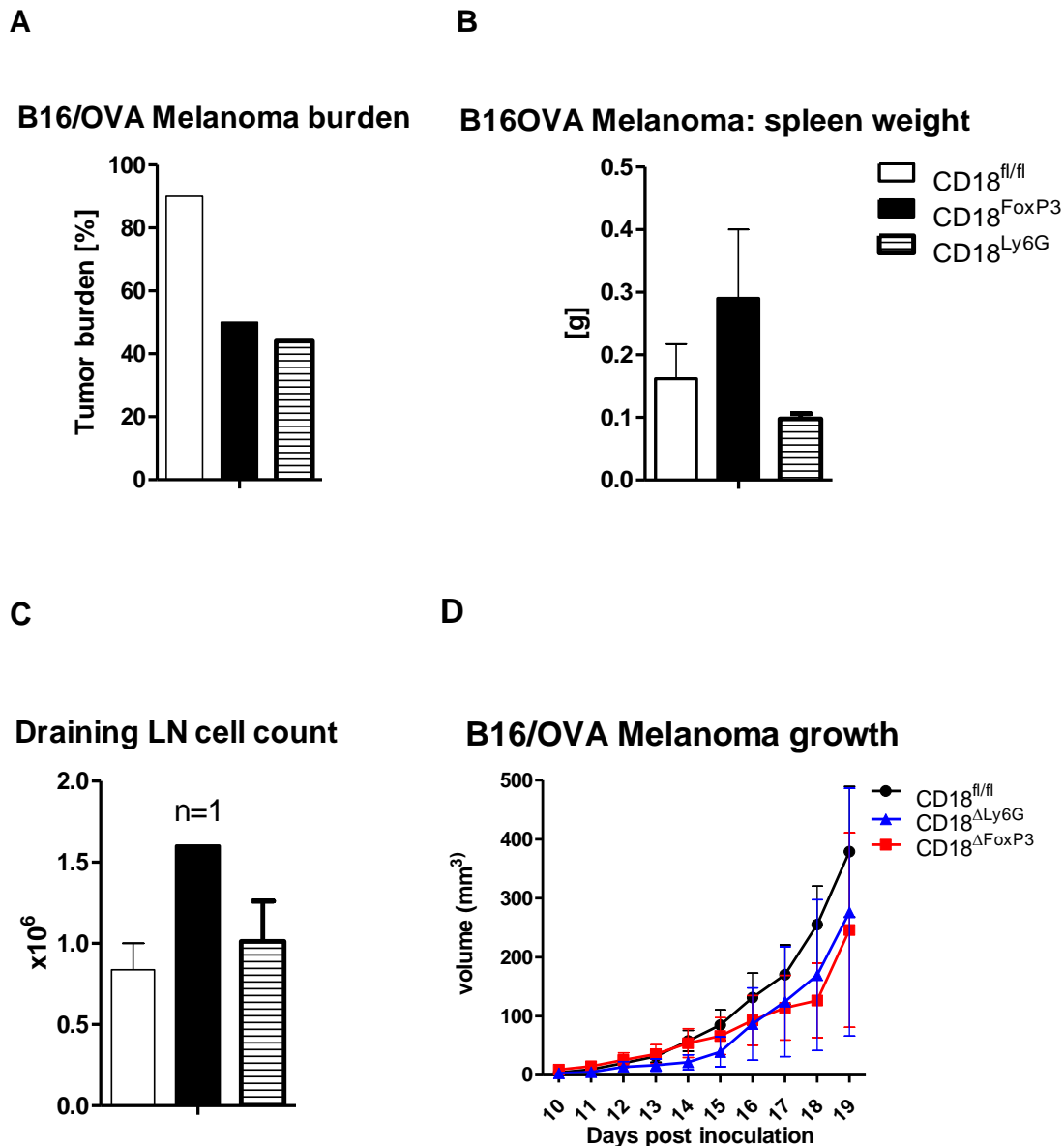
Appendix E. Analysis of the splenocytes from the CD11b<sup>-/-</sup> mice with B16-OVA melanoma burden. Splens from mice with/without tumour growth as well as non-inoculated(UT) mice (CD11b<sup>-/-</sup> only), were isolated and stained against CD11c, CD68, CD19, CD4, CD8 in general panel (A) as well as for CD4, CD8, FoxP3 and CD25 in T lymphocyte panel (B). Bars represent mean with SEM (n=2).

## Appendix F. Uptake of OVA-AlexaFluor647 by CD11b<sup>-/-</sup> and WT BM-DC in mixed cultures.



Appendix F. Uptake of OVA-AlexaFluor647 by CD11b<sup>-/-</sup> and WT BM-DC in mixed cultures. BM-DC from WT and CD11b<sup>-/-</sup> mice were isolated and incubated with OVA-AlexaFluor647 (50µg/ml) for 10, 30 and 60min at 37°C ( control was incubated at 4°C). After incubation time cells were harvested and stained against CD11c and against CD11b. Cells were first gated for CD11c and then sub-gated for CD11b<sup>+</sup>OVA-AF647<sup>+</sup> /CD11b<sup>-</sup> OVA-AF647<sup>+</sup>. Bars represent mean values with SEM (n=2).

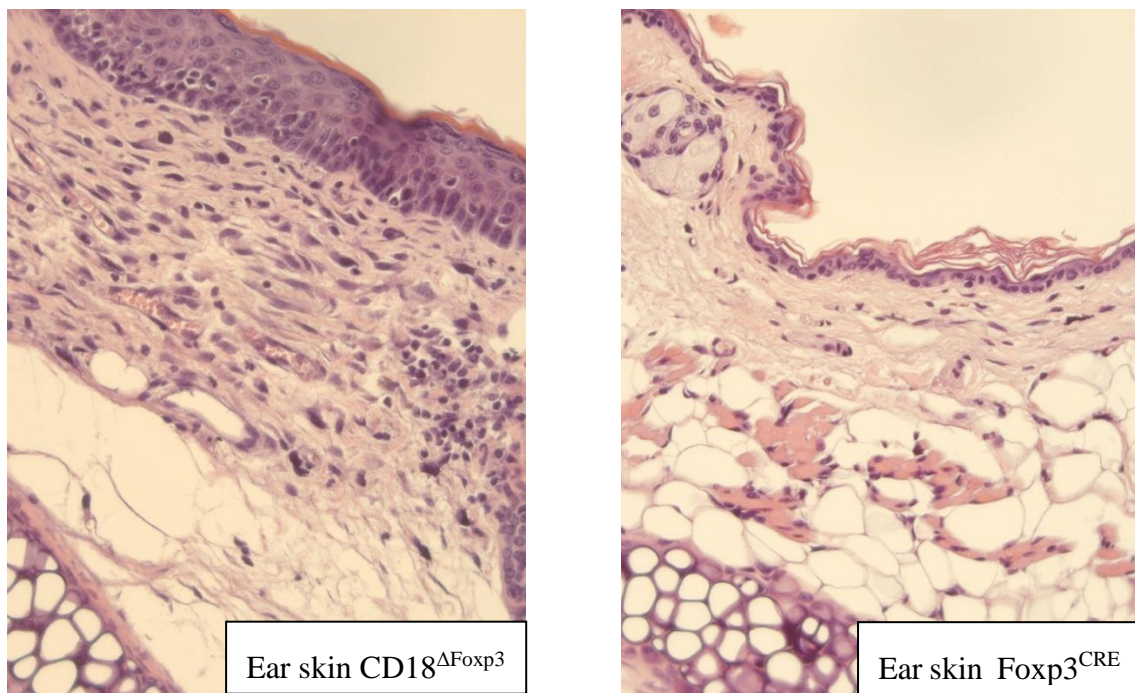
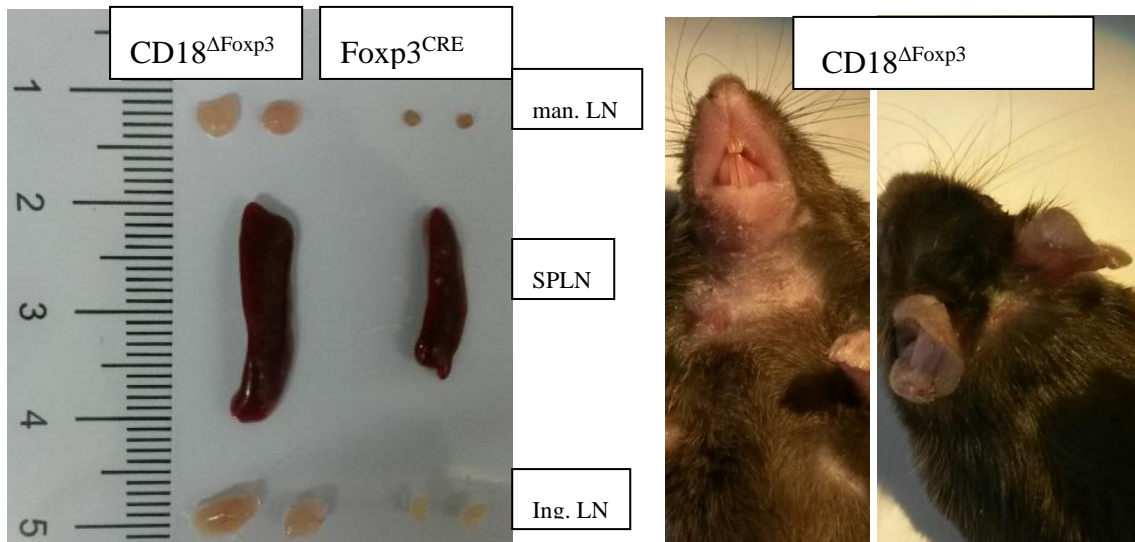
## Appendix G. Ablation of CD18 in FoxP3<sup>+</sup> and Ly6G<sup>+</sup> cells prevents tumour development



Appendix G. Ablation of CD18 in FoxP3<sup>+</sup> and Ly6G<sup>+</sup> cells prevents tumour development.

B16/OVA Melanoma was inoculated s.c. in the flank (ventral) of 10 CD18<sup>fl/fl</sup>, 7 CD18<sup>ΔFoxP3</sup> and 9 CD18<sup>ΔLy6G</sup> mice. Tumour burden (A) and growth (D) were determined during the course of experiment. Post mortem spleen weight (B) and draining lymph node cell count (C) were measured. Bars represent mean values with SEM.

## Appendix H. CD18<sup>ΔFoxp3</sup> phenotype



Appendix G. CD18<sup>ΔFoxp3</sup> phenotype. At about week 14, CD18<sup>ΔFoxp3</sup> mice developed psoriasis-like lesion and skin of the tail and ears scaled. Mandibular and inguinal lymph nodes, as well as spleen were enlarged. H&E staining of the ear sections derived from CD18<sup>ΔFoxp3</sup> revealed swelling and a strong infiltration of the skin with lymphocytes as compared with the control Foxp3<sup>CRE</sup> mice.

## Publications

1.  $\beta$ 2 Integrins- Multi-Functional Leukocyte Receptors in Health and Disease. Monika Bednarczyk, Henner Stege, Stephan Grabbe and Matthias Bros. *Int. J. Mol. Sci.* **2020**, 21(4), 1402.
2. Toward anticancer immunotherapeutics: well-defined polymer-antibody conjugates for selective dendritic cell targeting. Tappertzhofen K, Bednarczyk M, Koynov K, Bros M, Grabbe S, Zentel R. *Macromol Biosci.* **2014** Oct;14(10):1444-57.

## List of presentations and conferences attended

**September 2019-** II Joint Meeting of the German Society for Immunology (DGfI) and the Italian Society of Immunology, Clinical Immunology and Allergology (SIICA)

Talk: "Ablation of  $\beta 2$  Integrins (CD18/CD11) in Foxp3 expressing T regulatory lymphocytes results in generalized inflammation accompanied by psoriasis-like skin lesions"

**September 2018-** Frankfurt Cancer Conference 2018, Poster Presentation: "The role of beta 2 Integrins in tumor development"

**September 2016-** 46<sup>th</sup> Annual Meeting of the German Society for Immunology (DGfI), Hamburg, Poster Presentation: "The role of Mac-1 in binding and uptake of the dextran-coated colloidal superparamagnetic nanoparticles"

**September 2014-** 44<sup>th</sup> Annual Meeting of the German Society for Immunology (DGfI), Bonn  
Poster Presentation: "Well-defined Polymer-Antibody Conjugates for selective dendritic cell (DC) targeting"